




Universitetet  
i Stavanger

FACULTY OF SCIENCE AND TECHNOLOGY

## MASTER'S THESIS

Study programme/specialisation: Engineering Structures and Materials - Civil engineering structures	Spring / Autumn semester, 2019  Open
Author: Johan Mikaelsson	 (signature of author)
Programme coordinator: Sudath C. Siriwardane Supervisor(s): Sudath C. Siriwardane (UiS), Bjørn Reidar Nygård (Rambøll)	
Title of master's thesis: Design optimization in building projects by using composite steel/concrete columns	
Credits: 30	
Keywords: Composite steel/concrete construction Eurocodes Column Span length Fire load bearing resistance Environmental footprint	Number of pages: 104  + supplemental material/other: 88  Stavanger, 13.06.2019 date/year

## Abstract

While being relatively common in other parts of Europe, the construction of steel-concrete composite buildings in Norway is rare. As an introduction the constituent materials, examples of different composite building elements and examples of the usage of composite elements in building constructions of different parts of the world are given.

The main part of this thesis investigates the structural and environmental benefits of using composite instead of steel columns when they are designed according to the Eurocode rules. To introduce the reader to composite column analysis, ultimate limit state and fire calculations of an HE-300B steel column are given both for a reference pure steel column and for one fully encased in concrete. Significant improvements in resistance are shown for the fully encased column for all types of loads except shear force.

Parametric comparisons between composite and steel columns are given for:

- The maximum span length which can be achieved in similarly dimensioned pinned and rigid rectangular frames. By only considering the resistance of the columns and by encasing a steel column fully or partially in concrete, the span length is increased between 30% and 100%.
- The minimum column depth required for a number of different load cases and fire load-bearing resistances. While the results varied, the composite columns in general allowed for a depth reduction towards the steel column.
- The load-bearing resistance achieved per steel cross-sectional area. This study shows that concrete filled tubular columns can achieve the same load bearing resistance as a steel column by using less than half the amount of steel. Partially encased steel composite columns require approximately 75% of the steel amount on average. These results are however dependent on factors such as end moments and the column buckling length. Adding reinforcement to partially encased or concrete filled tubular composite columns is not an efficient way to increase the strength or stiffness.
- The environmental footprint by determining the CO<sub>2</sub> mass equivalents and the energy use associated with production of the column building materials. The composite columns are better than those made of steel on both accounts, except for concrete filled tubular columns where larger amounts of CO<sub>2</sub> are emitted in production.

Two software tools were specifically written in MATLAB for the parametric studies. One for analysing the maximum span length of steel and composite columns in a rigid frame by using an element method, another for doing member verifications of reinforced concrete filled tubular columns according to Eurocode 4.

The final part of this thesis is a case study of a single storey in-door sports hall with a no-sway steel frame. The HE-300B steel columns are replaced by partially encased composite columns to investigate whether the columns can be made thinner that way. For normal temperature conditions a partially encased HE-240A is sufficient. When fire load-bearing resistances are considered, the columns cannot be calculated according to the simplified calculation rules of Eurocode 4 due to length restrictions. However, R15 resistance can be achieved with by calculating an encased HE-240B for fire loads in accordance to Eurocode 3. Based on indicative calculations using the simplified calculation rules of Eurocode 4; it is also likely that R30 resistance is achievable with a HE-240B section, while R60 resistance is unlikely.

## Acknowledgements

This master's degree thesis is submitted to finalize my studies of engineering structures and materials at the University of Stavanger. It is written in cooperation with the civil engineering department at Rambøll in Kristiansand.

To my supervisor at the University of Stavanger Sudath C. Siriwardane I like to express appreciation for continuous support and input to the thesis.

Gratitude also goes towards my supervisor at Rambøll, Bjørn-Reidar Nygård and also to structural engineer Edvin Duka, who were vital in defining the topic of the thesis as well as providing assistance with the case study and additionally contributing with general knowledge of the Norwegian building industry at large.

Finally my wife deserves a huge personal thanks for encouraging me to undertake these studies and for taking a lion's share in the raising of our three lovely children during the last two years.

Lyngdal, 13 June 2019

Johan Mikaelsson

## Table of Contents

Abstract .....	i
Acknowledgements .....	ii
1 Introduction .....	1
1.1 Background.....	1
1.2 Objective.....	1
1.3 Scope / thesis structure.....	2
1.4 Limitations .....	2
1.5 Abbreviations.....	3
1.6 Symbols .....	4
1.7 Definitions .....	7
2 Composite steel/concrete structures .....	8
2.1 Overview.....	8
2.2 A brief history of steel/concrete composite construction .....	8
2.3 Constituent materials.....	9
2.3.1 Structural steel .....	9
2.3.2 Concrete.....	10
2.3.3 Reinforcement steel .....	13
2.4 Composite members .....	13
2.4.1 Shear connection.....	13
2.4.2 Composite beam .....	15
2.4.3 Composite slab.....	16
2.4.4 Composite column.....	17
2.4.5 Beam to column joint .....	19
2.4.6 Composite shear wall .....	20
2.5 Usage of composite structural elements .....	20
2.5.1 Norway/Sweden.....	21
2.5.2 Australia.....	21
2.5.3 Europe.....	22
2.6 Previous research – composite columns.....	23
3 Column design according to Eurocodes.....	24
3.1 The column .....	24
3.2 Worked examples - comparison of steel and composite column.....	24
3.3 Ultimate limit state (ULS) .....	27
3.3.1 Yield resistance of a cross-section towards compression (N).....	28
3.3.2 Yield resistance of a cross-section towards compression (N) + uniaxial bending (M) .	29

3.3.3	Yield resistance of a cross-section towards compression (N)+ bi-axial bending ( $M_y$ & $M_z$ )	35
3.3.4	Yield resistance of a cross-section towards transverse shear force (V)	37
3.3.5	Buckling resistance of a column towards compression	39
3.3.6	Buckling resistance of column towards compression + bending about major axis	42
3.3.7	Global structural behaviour	47
3.4	Fire loads	49
3.4.1	Structural behaviour of a column subjected to fire	49
3.4.2	The Eurocode approach to fire design	50
3.4.3	Global structural response in fire	51
3.4.4	Member fire resistance	52
3.5	Impact loads	55
3.6	Blast loads	56
3.7	Seismic loads	57
4	Parametric studies of composite and steel columns	58
4.1	Software	59
4.1.1	A3C	59
4.1.2	MATLAB model – ULS and fire verification of CFT column	60
4.1.3	CALFEM	61
4.2	Maximum span	63
4.2.1	Study set-up	63
4.2.2	Study results	68
4.3	Column depth reduction	70
4.3.1	Study set-up	70
4.3.2	Study results	73
4.4	Steel efficiency	74
4.4.1	Study set-up	75
4.4.2	Study results	76
4.5	Environmental foot-print	77
4.5.1	Study set-up	79
4.5.2	Study results	79
5	Case study	80
5.1	Case selection	80
5.2	Case description	80
5.3	Case calculations	82
5.4	Case results	83

6	Discussion/Conclusions.....	86
6.1	Discussion .....	86
6.2	Conclusions.....	89
6.3	Further work .....	90
7	References.....	91
	<i>Appendix A. Worked example – ULS verification of HE-300B steel column .....</i>	<i>96</i>
	<i>Appendix B. Worked example – ULS verification of FEC, HE300B column .....</i>	<i>102</i>
	<i>Appendix C. Worked example – fire resistance verification of HE-300B steel column .....</i>	<i>114</i>
	<i>Appendix D. Cross-sections and reinforcement sizes used in parametric studies.....</i>	<i>118</i>
	<i>Appendix E. Maximum span study supporting calculations.....</i>	<i>120</i>
	<i>Appendix F. Minimum depth of fire protected column supporting calculations.....</i>	<i>126</i>
	<i>Appendix G. Steel efficiency study .....</i>	<i>135</i>
	<i>Appendix H. Environmental foot-print study .....</i>	<i>138</i>
	<i>Appendix I. MATLAB/CALFEM Codes for span study .....</i>	<i>140</i>
	<i>Appendix J. MATLAB codes for ULS and fire verification of a CFT column .....</i>	<i>149</i>
	<i>Appendix K. Calculations for the case study.....</i>	<i>168</i>

## List of Figures

Figure 2-1: Typical stress-strain curve for structural steel [10].	9
Figure 2-2: Typical stress-strain curve for reinforced concrete [15]	11
Figure 2-3: Simply supported composite beam with a) full shear connection; b) no shear connection.	14
Figure 2-4: Steel I-beam connected to a concrete slab by shear connectors.	15
Figure 2-5: Partially encased composite beam.	16
Figure 2-6: Composite slab steel profiles; trapezoidal (left) and dove-tail (right).	16
Figure 2-7: Slim-floor composite slab.	17
Figure 2-8: Examples of composite column cross-sections using standard steel sections, inspired by [3].	18
Figure 2-9: ISRC column, basic principle.	19
Figure 3-1: Illustration of load cases resulting in column moments	24
Figure 3-2: HE-300B profile with measurements in mm, according DIN 1025-5 [38].	26
Figure 3-3: Fully encased composite HE-300B section. Measurements in mm.	26
Figure 3-4: Stress blocks for plastic moment cross-sectional resistance in the presence of axial force	30
Figure 3-5: Stress blocks for polygonal curve points A to D for a fully encased composite section. Inspired by [24].	32
Figure 3-6: M-N polygonal interaction diagram for the fully encased HE300B section	33
Figure 3-7: M-N interaction curves for HE300B. Comparison steel and FEC HE-300B cross-sections.	34
Figure 3-8: Reduced moment resistance about y-axis due to axial force, biaxial bending for three different ratios $M_y/M_z$ . Comparison steel and FEC HE-300B cross-sections.	37
Figure 3-9: Load scenarios for buckling due to combined axial force and uniaxial bending.	43
Figure 3-10: Typical 1st and 2nd order BMD for double/single curvature bending. Visually inspired by [25].	46
Figure 3-11: Reduced design moment resistance about the major axis due to buckling and axial force, comparison steel and FEC HE-300B columns.	47
Figure 3-12: ISO 834 fire curve	52
Figure 4-1: 2-dimensional Euler beam element with axial and distributed loads	61
Figure 4-2: Idealized pinned plane frame for span study, with design load distribution and the calculated reaction forces of the beams	64
Figure 4-3: Idealization of rigid frame, plus example of the first order elastic rigid steel frame analysis results.	66
Figure 4-4: Pinned frame maximum span study results.	68
Figure 4-5: Composite to steel ratio of steel efficiency for a column in compression	76
Figure 4-6 Composite to steel ratio of steel efficiency for a column in combined compression+ bending	77
Figure 5-1: Case study - In-door sports hall	80
Figure 5-2: Column spacing, case study (measurements in mm)	81
Figure E-1: Relation between span length and axial force on column B1/E1.	121
Figure F-1: Example of H-profile boxed in by 50mm of fire protection board.	127
Figure F-2: Depth reduction for columns with no loadbearing fire criteria (R0)	131
Figure F-3: Depth reduction for columns with 30 min. loadbearing fire criteria (R30)	132
Figure F-4: Depth reduction for columns with 60 min. loadbearing fire criteria (R60)	132
Figure F-5: Depth reduction for columns with 90 min. loadbearing fire criteria (R90)	133
Figure F-6: Depth reduction for columns with 120 min. loadbearing fire criteria (R120)	133

Figure F-7: Depth reduction for columns with 180 min. loadbearing fire criteria (R180) .....	134
Figure G-1: PEC section dimensions (typical).....	135
Figure H-1: CO2 mass equivalents per m of column length for each load case.....	139
Figure H-2: Energy use per m of column length for each load case.....	139
Figure J-1: CFT cross-section without rebars, area determination .....	150
Figure J-2: PNA positions on CFT cross-section with 4 rebars .....	151
Figure J-3: Comparison of MN interaction diagrams, worked example C2 [39] and the developed MATLAB model.....	153
Figure K-1: Self-weight of lattice girders, calculation [76].....	172
Figure K-2: PEC HE-240B cross-section according EC4, part 1-2 Annex G [4]. .....	175

## List of Tables

Table 3-1: Specifications of the worked example steel and FEC columns in chapter 3 .....	25
Table 3-2: Point locations on the A to E polygonal curve suggested by EC4, part 1-1[3].....	31
Table 4-1: Maximum span frame input data .....	63
Table 4-2: Concrete and reinforcement specification for maximum span study.....	65
Table 4-3: Selected beam sections for the rigid span study .....	68
Table 4-4: Average differences between pinned and rigid frames. ....	69
Table 4-5: Cross-sectional area due to fire protection study - constant parameters .....	71
Table 4-6: Column depth reduction – structural load cases. ....	72
Table 4-7: Results, column depth reduction study. Average and minimum reductions. ....	73
Table 4-8: Price comparison of steel profiles.....	74
Table 4-9: Key EPD factors for 1 kg of building material .....	78
Table 4-10: EPD values for production of building materials for one meter of column, average values for all load cases.....	79
Table 5-1: Design actions, case study.....	83
Table 5-2: Case study results .....	84
Table 5-3: Indicative calculation of the utilization of the case study column in a fire scenario, using EC4 part 1-2 Annex G [4] .....	85
Table A-1: HEB-300 steel section geometrical and material properties: .....	96
Table C-1: Example calculation of the critical steel temperature .....	115
Table C-2: Temperature development in steel member exerted to ISO 834 fire curve.....	117
Table D-1: Cross-section sizes used in studies .....	118
Table D-2: Reinforcement bar sizes used in studies.....	119
Table E-1: Steel equivalent area and second moment of area for the maximum span study cross-sections.....	122
Table E-2: Pinned frame study, effect of using C25/30 or C50/60 concrete strength .....	123
Table E-3: Pinned frame study, effect of using 4xØ12mm or 4xØ25mm longitudinal reinforcement .....	123
Table E-4: Pinned and rigid frame span length comparison .....	124
Table E-5: Pinned and rigid frame beam maximum moment comparison.....	125
Table F-1: Steel cross-sections and passive fire protection thickness, column depth study.....	129
Table F-2: FEC steel sections and concrete cover thickness, column depth study .....	130
Table F-3: Partially encased steel sections, column depth study.....	130
Table F-4: CFT steel CHS cross-section diameter (D) and thickness (t), column depth study .....	131
Table G-1: Design moments for steel amount study.....	136
Table G-2: Steel efficiency for steel, PEC and CFT columns with axial load.....	137



Table G-3: Steel efficiency for steel and PEC columns with axially load + bending moment .....	137
Table G-4: Steel efficiency for PEC and CFT columns with varying degrees of reinforcement.....	137
Table H-1: CFT cross-sections for the environmental foot-print study .....	138
Table J-1: Calculation, worked example of column C2 from [39] - input data. ....	152

# 1 Introduction

## 1.1 Background

Composite steel/concrete structures have existed since the early 1900s [1] and they are commonly used throughout the world today. Composite structural elements are utilized in many different applications, usually in large scale projects such as industrial buildings, high-rise buildings and bridges. A well-designed composite structure utilizes the strengths and reduces the weaknesses of the constituent materials (here structural steel and reinforced concrete). The possible benefits of using composite building elements obviously depends on which type of element is considered and which type of element it is evaluated against, but composite structures can in general allow for:

- Higher strengths and stiffnesses of the structural elements.
- Larger architectural freedom due to many possible cross-sectional configurations.
- Good resistance towards seismic and other dynamic actions, due to energy dissipation.
- Better resistance towards thermal strength/stiffness reductions in a fire scenario, when compared to a steel structure due to the insulating properties of concrete.
- Shorter construction time due to a large initial strength in the elements, when compared to site cast reinforced concrete structures.
- Lighter total weight, when compared to reinforced concrete structures.
- Less negative environmental impact, due to a better utilization of the materials.

There are potential disadvantages of using composite structural elements, related to the increased complexity of the design and manufacturing of composite members. Element joining methods which work well on a steel structure may not be suitable and more complex detailing may be required for composite structures. There is also less experience and fewer suppliers of composite structural elements in the Norwegian construction industry.

Economy often dictates the choice of construction and the total cost for a composite construction (when compared to a steel or concrete) is complex to determine, since it is not only due to a difference in material costs. The costs will also differ due to for instance differences in foundation work, engineering, manufacturing, construction time and methods and future demands on building maintenance and renovation.

This thesis is written together with the Rambøll department in Kristiansand. Rambøll is a multinational consulting engineering company with 1500 employees in Norway and 15000 world-wide. According to their website, their consulting expertise encompasses construction, infrastructure, transport, energy, health and safety and management [2].

Constructions using composite elements are rare in Norway when compared to other European countries. Norwegian research output and academic work on steel/concrete composite structures is also very low when compared to that of other European countries. It is of interest to Rambøll and arguably the Norwegian construction industry at large to learn more about composite structures and when/if it may be beneficial to utilize them.

## 1.2 Objective

The objective of this thesis is to:

- Familiarize the reader to steel/concrete composite structures as they are defined by Eurocode 4 [3,4]. The reader is not expected to know anything of such structures, although a basic understanding of structural and fire theory is necessary for a full understanding of the thesis.

- Describe the differences in structural performance between steel and composite columns, when they are designed to the relevant Eurocodes.
- Determine the difference in environmental footprint between steel and composite columns.
- Demonstrate the impact of these differences with a case study, where a typical steel structure proposed by Rambøll is redesigned and optimized using composite columns.

### 1.3 Scope / thesis structure

This thesis is divided in three principal parts.

- The first part, chapter 2 describes the history, development and typical usage of composite steel/concrete elements in building constructions. Different types of structural elements, e.g. beams, slabs and columns are discussed as well as the properties of the constituent materials.
- The second part consists of two chapters:  
Chapter 3 provides worked examples of the resistances of a steel and a composite column, when calculated in accordance to the relevant Eurocodes, alongside relevant structural theory.  
Chapter 4 contains comparative parametric studies between steel and composite columns, where differences in structural behaviour and environmental footprint are demonstrated by using the following criteria:
  - o The maximum span between columns in a rectangular frame construction.
  - o Minimum column depth when different degrees of fire resistance and different load cases are considered.
  - o The amount of load resistance provided per used steel amount.
  - o The global warming potential and the energy use required for production of the constituent materials.
- The third part, chapter 5 is a case study, where a typical structure using steel columns is redesigned and optimized by using composite columns. The two designs will then be compared.
- The main part of the calculations and results are given as reference in Appendices, as well as the source codes written specifically for this thesis.

### 1.4 Limitations

- While an underlying intent of this thesis is to investigate whether composite structures can be utilized more in Norwegian building projects, the main part of the thesis will be limited to composite columns in order to reduce the scope. This exclusion also applies to the characteristics of the column joints such as column bases, column splices and beam-column connections. Other composite elements are briefly introduced in Chapter 2 in order to provide a general background/knowledge of composite structures.
- Composite structures are common in bridge engineering and the EC4, part 2 [5] details steel/concrete composite bridges. They are however not considered in this thesis.
- The dynamic behaviour of composite columns is only briefly discussed to limit the scope. Typical actions, when the dynamic behaviour of columns is considered, are seismic and blast/impact actions. Typically none of these type of actions are limiting design factors for columns in Norwegian buildings.
- The comparative and case study sections of the thesis will be limited mainly to structural considerations, i.e. the strengths and stiffnesses of the composite columns in ultimate and fire limit states when compared to ordinary steel columns. Due to the environmental footprint of building material production being relatively easy to determine by the available data from the

other studies, it has been done as an exception. Thus, multiple other topics which are relevant for construction are largely omitted, including:

- Economy
  - Construction time and schedule
  - Construction logistics
  - Maintainability
- This thesis compares composite and steel columns as they are calculated by the simple calculation rules provided in the relevant Eurocode standards. The real behaviour of such elements may differ from what is described in this thesis, due to simplifications, conservatism and/or possible errors in the standards.
  - Calculations with composite columns in sway buildings, requiring second order analysis have not been done. This would require not only studying the behaviour of the columns but also that of the horizontal members (e.g. beams) and the beam-column joints.

## 1.5 Abbreviations

ALS	Accidental Limit State
BMD	Bending Moment Diagram
CHS	Circular Hollow Section
CFD	Computational Fluid Dynamics
CFRT	Concrete Filled Rectangular Tubular
CFT	Concrete Filled Tubular
CTICM	Centre Technique Industriel de la Construction Métallique
EC	Eurocode
EHF	Equivalent Horizontal Force
EPD	Environmental Product Declaration
FEC	Fully Encased Composite
FEM	Finite Element Method
HE-A	European wide flange H beam, type A
HE-B	European wide flange H beam, type B
HE-M	European wide flange H beam, type M
ISRC	Isolated Steel Reinforced Composite
LTB	Lateral Torsional Buckling
MN	Moment-Neutral force
N/A	Not available/applicable
NOK	Norwegian Krone (unit of currency)
PEC	Partially Filled Composite

PNA	Plastic Neutral Axis
SFD	Shear Force Diagram
SRC	Steel Reinforced Concrete
ULS	Ultimate Limit State
VBA	(Microsoft) Visual Basic for Applications

## 1.6 Symbols

The symbols are chosen to match those used in the Eurocodes as far as possible.

### Roman letters, lower and upper case

$A$	Area of cross-section
$A_m/V$	Section factor, for steel sections in a fire scenario
$A_{eq}$	Equivalent steel area of cross-section
$b$	Width of steel cross-section
$b_c$	Width of composite cross-section
$c_p$	Specific heat
$E$	Modulus of elasticity
$E_{c,eff}$	Effective modulus of elasticity for concrete, including creep
$E_{cm}$	Secant modulus of elasticity, concrete
$E_{fi,d}$	Design effect of effects in a fire
$EHF_{imp}$	Equivalent horizontal force of member bow imperfection
$EHF_{sway}$	Equivalent horizontal force of sway action
$(EI)_{eff}$	Effective flexural rigidity, including creep
$(EI)_{eff,II}$	Effective flexural rigidity for 2 <sup>nd</sup> order member verification, including creep
$f_{cd}$	Design yield strength, concrete
$f_{ck}$	Characteristic yield strength, concrete
$f_s$	Characteristic yield strength, rebar
$f_{sd}$	Design yield strength, rebar
$f_y$	Characteristic yield strength, steel section
$f_{cd}$	Design yield strength, steel
$G_k$	Characteristic permanent load
$h$	Height of steel cross-section
$h_c$	Height of composite cross-section

$I$	Second moment of area
$I_{eq}$	Equivalent steel second moment of area
$k$	Moment amplification factor for 2 <sup>nd</sup> order member verification of composite column
$k_e$	Buckling correction factor
$L$	Column length
$L_{cr}$	Elastic buckling length
$L_{fi}$	Buckling length in a fire scenario
$M_{b,Rd}$	Moment resistance with combined axial load and 2 <sup>nd</sup> order effects
$M_{cr}$	Critical moment
$M_{Ed}$	Design moment
$M_{Ed,1}$	Design moment for first order member verification
$M_{Ed,2}$	Design moment for second order member verification
$M_{imp}$	Design moment from member bow imperfection
$M_{pl,Rd}$	Plastic moment resistance
$M_{max,Rd}$	Maximum plastic moment resistance in combination with axial load
$M_{N,Rd}$	Plastic moment resistance in combination with axial load
$n$	Design axial load resistance ratio
$N_{b,Rd}$	Buckling axial load resistance
$N_{Cr}$	Critical axial load / elastic buckling load
$N_{Cr,eff}$	Critical axial load for composite column and 2 <sup>nd</sup> order member verification
$N_{Ed}$	Design axial load
$N_{G,Ed}$	Permanent part of design axial load
$N_{pl,Rd}$	Design plastic axial load resistance
$N_{pm,Rd}$	Axial load resistance at point C on the simple polygonal MN interaction curve
$Q_k$	Characteristic imposed load
$r$	Radius
$R_d$	Design resistance in ambient temperature
$S$	Span length
$t$	Time

$t_f$	Thickness of steel flange
$t_w$	Thickness of steel web
$V_{Ed}$	Design shear load
$V_{pl,Rd}$	Design plastic shear resistance
$Z$	Plastic section modulus
$\emptyset_L$	Diameter, longitudinal rebars
$\emptyset_L$	Diameter, transverse rebars

Greek letters, upper case

$\alpha_{cr}$	Frame buckling factor
$\alpha_M$	Material reduction coefficient for combined axial load + bending of a composite column
$\beta$	Bending moment diagram factor for 2 <sup>nd</sup> order verification of composite column.
$\gamma_C$	Material property factor for concrete
$\gamma_G$	Safety factor for permanent actions
$\gamma_{M0}$	Material property partial factor for cross-sectional checks
$\gamma_{M1}$	Material property partial factor for instability
$\gamma_{M,fi}$	Material property factor for steel in a fire scenario
$\gamma_Q$	Safety factor for imposed actions
$\gamma_S$	Material property factor for reinforcement steel
$\delta_{H,Ed}$	Horizontal deflection of the top of the storey, relative the bottom of the storey
$\eta_{fi}$	Fire load reduction factor
$\eta_{fi,t}$	Fire design load level
$\theta_{a,cr}$	Critical steel temperature
$\theta_g$	Gas temperature from nominal fire curve
$\bar{\lambda}$	Relative slenderness
$\lambda_p$	Thermal conductivity
$\mu_D$	Moment resistance ratio for combined bending and compression
$\xi_M$	Ratio between major and minor axis design bending moment
$\tau_y$	Shear strength
$\phi$	Sway angle

$\phi_t$	Time dependent creep factor
$\chi$	Flexural buckling factor
$\chi_{comp}$	Steel efficiency, composite column
$\chi_{LT}$	Lateral-torsional buckling factor
$\chi_{steel}$	Steel efficiency, steel column
$\psi_0$	Partial factor for combined imposed action
$\psi_1$	Partial factor for frequent imposed action

### Subscripts

The following subscripts are exclusive and indicate the same thing, whenever they are used, unless listed specifically (such as for instance  $f_y$  being the characteristic yield strength of steel).

a	Steel section material
c	Concrete material
Ed	Design load, including load safety factors
Rd	Design resistance, including material partial factors
Rk	Characteristic resistance
s	Rebar steel material
y	About the y-axis (major axis)
z	About the z-axis (minor axis)

## 1.7 Definitions

**Composite member:** A structural member made of steel and concrete in accordance to the rules given by Eurocode 4, part 1-1 [3]

**Double curvature bending:** When the column is exerted to end moments of equal sign in both ends.

**Major axis:** The axis of a slender member in which a cross-section achieves the highest second moment of area about.

**Minor axis:** The axis of a slender member in which a cross-section achieves the smallest second moment of area about.

**Rebar:** Steel reinforcement bar

**Resistance:** The capacity for a structural member to withstand a specific type of load.

**Single curvature bending:** When the column is exerted to either only one end moment or to two opposite end moments.

**Steel efficiency:** A dimensionless ratio of how much structural resistance a column provides, per area unit of steel used.

**Utilization:** A ratio between the design load and the design resistance



## 2 Composite steel/concrete structures

### 2.1 Overview

Composite structures in the general definition consist of two or more different materials with significantly different properties in such manner that the materials are directly interacting with each other. A structure made of ordinary reinforced concrete is a good example of a composite structure, since the constituent materials steel and concrete have significantly different physical properties. Further the materials interact with each other, since forces are transferred between the materials due to mechanical and chemical bonding between the concrete and the ribbed steel reinforcement bars. The materials are located to maximize their strengths and minimize their weaknesses. The steel reinforcement remediate the concrete weaknesses due to being concentrated to regions of the structural element where either tensile or shear stresses dominate. It is furthermore located inside the concrete, which shields it from corrosion and heat (e.g. in a fire scenario).

Composite steel/concrete structural members as defined by the Eurocode 4, part 1-1 [3] differs from reinforced concrete by using a much larger fraction of steel, often in shapes conventional to steel constructions, e.g. I- and H-sections, hollow closed sections and corrugated plates. The increased amount of steel means that the steel material has a much larger contribution to the overall structural resistance, when compared to the contribution from reinforcement bars. Additionally, the increased ratio adds ductility to the structure.

The properties of a composite structure depends on the properties of the constituent materials as well as the how these materials are joined together. In section 2.3, the material properties will be discussed, while typical applications of composite structures are described in section 2.4.

### 2.2 A brief history of steel/concrete composite construction

The usage of steel/concrete composite structures dates back to the early 1900s. Eggemann [6] argues that an early composite construction was the Emperger column, in which a cast-iron member was encased in concrete with spiral reinforcement. The Austrian engineer Fritz von Emperger was granted a patent for the column in 1916 and it was employed in American building codes and multiple American high-rise buildings, for instance the McGraw-Hill building (demolished in 1988) and the Trustees System Service building, both in Chicago. In Europe, the column saw its use limited to Austria and Czechoslovakia due to not being approved in other building codes.

The steel-concrete bond between the concrete casing and the iron core in the Emperger column is adhesive and not sufficient to transfer the shear forces encountered in beams reliably. A breakthrough for composite beam construction was the introduction of shear connectors welded to the steel profile in order to provide a mechanical shear connection. Starting in the 1950s, composite beams using welded shear connectors were becoming commonly used. [1]

In the 1970s, a German research team led by Roik devised simplified calculations using perfect plastic theory, which was adapted into the German building codes at the time. These theories reduced the complexity of the earlier required elastic calculations (which had to account to a much larger degree for the creep and shrinkage behaviour of concrete). The simplicity of the plastic calculations increased the popularity of using composite constructions [1]. The theories also forms the basis of some of the simplified calculations in the current Eurocode 4, part 1-1 [7].

Work on developing the standards Eurocode (EC) 4 for steel-concrete composite structures was initiated in the early 1980s. In 1984 the first draft was finished and in 2004 the first revision was published. According to Stark, (a member of the EC4 drafting committee) the EC4 was developed in

parallel to the development of the Eurocodes for concrete (EC2) and steel (EC3) for cross-code consistency. [8]

## 2.3 Constituent materials

### 2.3.1 Structural steel

#### General

Structural steel is a collective name for a range of carbon steels, consisting of a mix of ductile ferrite and strong pearlite microstructures. In order to ensure good weldability, the carbon content of structural steel is usually kept at maximum 0,2% and other elements such as manganese, chromium or copper may be added to increase the material strength [9].

A common way to produce structural steel members is through hot rolling, where a steel billet heated above the recrystallization temperature is mechanically rolled to the desired shape. Thereafter, the member is cooled in a controlled manner in order to reduce the occurrence of thermally induced stresses. By shaping the member at a high temperature, the fabrication process is easier and cheaper due to the steel being more malleable. Hot rolling have practical consequences for the finished product, since in difference to cold-shaped steel which have oblong grains, the grains of hot rolled steel will regrow to a random alignment, resulting in an isotropic material. Strain-hardening is also avoided, which increases the ductility of the steel. Some negative consequences of hot rolling when compared to cold formed steel is reduced yield strength and larger dimensional variations of the end product [9].

#### Strength of material

Structural steels are ductile in ambient temperature and considered to show linear elastic behaviour for stresses up until the yield stress, where the steel will start to deform plastically. After the yield stress has been reached, the steel can yet resist higher stresses due to strain hardening in the plastic state. An idealized stress-strain curve for structural steel is shown in Figure 2-1.

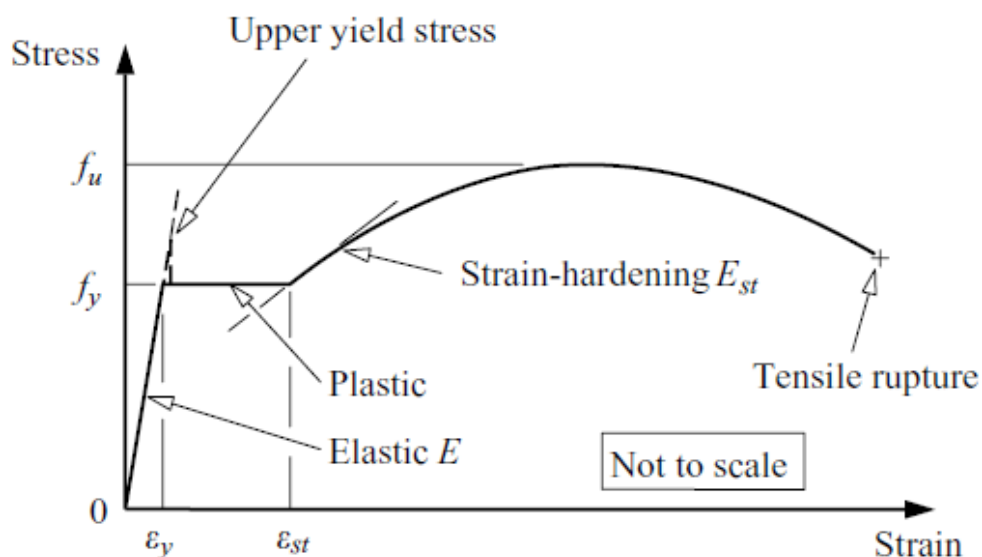


Figure 2-1: Typical stress-strain curve for structural steel [10].

Under some circumstances such as low temperatures or very rapid loading, even ductile structural steels can show brittle behaviour [9].

The European standard EN 10027-1 [11] classifies hot rolled structural steel against two criteria; characteristic yield strength and impact toughness. An example of a structural steel designation is S355J2, where “S” means structural steel, 355 indicates a yield strength of 355MPa and J2 indicates an impact toughness of class J2 (27 Joules at -20 degrees Celsius). In accordance with EC4 part 1-1 [3], the structural steel must have a characteristic yield strength between S235 and S460 for composite structures.

#### Thermal and fire behaviour:

Structural steel experiences thermal expansion at increased temperature and a linear expansion of  $11 \cdot 10^{-6} \text{ K}^{-1}$  can be assumed, with the exception of a thermal contraction that occurs between 700-800 degrees Celsius, when the ferritic steel transforms to its austenitic phase [12]. At about 350°C, the proportional limit strength (the upper value of linear elasticity) of structural steel is halved, when compared to its 20°C value. This is an issue for slender steel structures, which can buckle locally before plastic deformation occurs. According tables provided in EC3, part 1-2 [13] the effective yield strength (upper value of elasticity, including non-linear) of structural steel is halved at ~580°C, which is the relevant value for members that do not buckle locally until after yield.

Structural steel is not combustible but similar to other metals the heat conductivity is very high. The combination of a large strength loss at increased temperatures and a high heat conductivity means that steel members have a poor resistance towards fire loads. Due to this, load-bearing structural members are usually protected by thermally insulating materials if fire loads are relevant.

### 2.3.2 Concrete

#### General

*Note: The compendium by Jacobsen et al. [14] has been used as a comprehensive source of information for the general section.*

Norwegian concrete is usually made up from Portland cement (a mixture of inorganic oxides reactive to water), water and aggregate (sand and rocks). Other minerals commonly named pozzolans with reactive behaviour such as fly ash or silica are often added to enhance the properties of the concrete. Pozzolans may also provide environmental benefit as they are typically waste products from industry processes and may replace some of the required cement. Other specialized additives may also be added, to either enhance the casting properties or the final, mechanical properties.

The properties and composition of the aggregate, which makes up for ~70% of the final concrete volume are for economic/logistical reasons often depending on the sand and gravel qualities that is locally available to the building site/prefabrication factory for a normal weight concrete. Low-weight concretes use a low density aggregate, for example volcanic minerals or industrially made aggregate such as clay.

Concrete structural members may either be cast on site or prefabricated. The concrete ingredients are mixed together and poured into a formwork, in which reinforcement has been placed (see 2.3.3). Once the fresh concrete is set in place, the cement paste undergoes a physical phase shift as it changes from a liquid with solid aggregate particles to a solid, through a chemical process called hydration.

During hydration, significant amounts of heat is generated, which can cause permanent external cracks and/or internal stresses to the concrete material from thermal expansion effects. There is also a voluminous shrinkage associated with hydration, due to:

- Autogenous shrinkage due to the hydration reaction products occupying less volume than the reactants.
- Drying shrinkage from water lost due to drying to the external environment. If the concrete is exposed to high humidity, it may however absorb water and expand.

Pores of various sizes are always present in hardened concrete, due to water lost in the hydration process. Pores may also occur due to excessive water drying out to the atmosphere or intentionally for frost resistance. If the concrete was not sufficiently compacted during the casting, there may be unwanted pores or even larger voids.

### Mechanical properties

Since there are many uncertain factors related to the ingredients, mixing, casting and hardening of the concrete, the mechanical properties of the final, hardened concrete have a large range of possible values. This is manifested in the EC2, part 1-1 [15] by concrete having a high partial material factor of 1,5.

The compressive strength of concrete increases with time as more of the cement is hydrated and the characteristic yield strength values given in EC2 are taken at 28 days after casting. In a compressive stress-strain test, concrete shows elastic-plastic behaviour [16] and the measured strain varies non-linearly with the compressive stress. A reference value  $E_{cm}$  for the modulus of elasticity called the secant modulus is typically taken at 40% of the mean compressive strength [15]. Once the yield strength is reached, concrete shows strain-softening behaviour, meaning it will continue to deform even at lower stresses than the yield strength until fracture. See a typical concrete stress-strain curve in Figure 2-2.

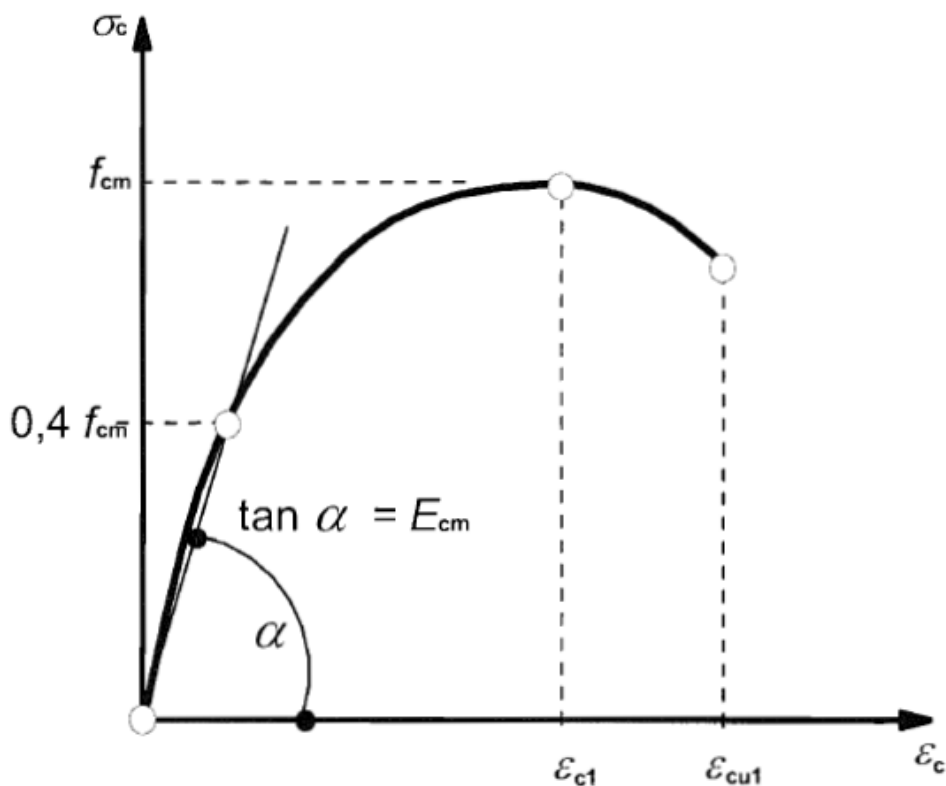


Figure 2-2: Typical stress-strain curve for reinforced concrete [15]

In order for concrete to be allowed for use in composite structures according to EC4, part 1-1 [3], the characteristic compressive yield stress must be between 20 and 60 MPa. Both light-weight and normal weight concrete may be used. The specific design rules for composite columns are slightly more restrictive, allowing normal-weight concrete only and a characteristic compressive yield stress between 20 and 50 MPa. The tensile strength of concrete is very low, owing to multiple pores, cracks, irregularities and other defects which causes stress concentrations. These stress concentrations are responsible for the brittle behaviour of concrete in tensile failure. The shear strength of concrete is also low, roughly 12% of the compressive strength [16]. The tensile strength of concrete is usually ignored in calculations, here it is assumed that the reinforcing steel provides the necessary tensile strength.

As response to loading over a long term duration, concrete experiences significant amounts of creep and will thus deform plastically over time for stresses which are smaller than the yield strength. The amount of creep is difficult to determine, since there are multiple factors affecting it, including load magnitude, load conditions, humidity and reinforcement. Annex B of EC2, part 1-1 [15] provides basic equations to quantify the creep.

#### Thermal and fire behaviour:

Hardened concrete experiences thermal expansion at increased temperatures. For normal concrete a linear expansion of  $12 \cdot 10^{-6} \text{ K}^{-1}$  can be assumed, but this may vary depending on which aggregate is used [16]. This is a similar rate to that of structural steel, which is one reason to why reinforced concrete can handle a relatively large range of temperature without loss of the concrete-steel bond. At roughly 700-800 degrees Celsius (depending on the aggregate composition), the compressive yield strength of concrete is halved when compared to the value in ambient temperature [12].

Concrete is not combustible and has a low heat conductivity; the latter property results in an insulating effect and a long duration for the outer temperature to reach the centre of the concrete in a fire scenario. Standards for the fire resistance of concrete constructions (including EC2, part 1-2 [17]) typically prescribe a minimum amount of concrete cover in order to provide fire insulation for the reinforcement steel. Fire may cause spalling and/or cracking of the concrete, due to tensile stresses from thermal expansion and/or increased pore pressure from heated retained or dehydrated water. Spalling and cracking may lead to loss of insulation of the steel reinforcement, subsequent loss of tensile strength due to heating of the rebars and this is the typical reason for a concrete structure to collapse in fire [12]. In total, when compared to other commonly used structural materials, concrete is viewed as a fire resistant material [18].

#### Durability

There are several effects that may cause direct deterioration of concrete or indirect weakening by harming the reinforcement steel, many of which have to be considered already during the member design and concrete proportioning [19], including:

- Carbonation. Calcium hydroxide within the hardened cement paste will react with atmospheric carbon dioxide, causing formation of calcium carbonate and a reduction of the concrete pH level. Carbonation starts at the surface and moves inwards over time but at a reduced rate. Once the carbonation front is in level with the reinforcement, the reduced pH results in de-passivation of the steel and subsequent loss of corrosion protection. The carbonation rate is the main factor for determining the required concrete cover of reinforcement steel in EC2, part 1-1 [15].
- Frost, by both voluminous expansions of retained pore water and from osmotic effects.

- Acidic conditions, for instance from bacterial activity.
- Internal pressure from the reaction products of sulphates or nitrates reacting with aluminates within the concrete.

### 2.3.3 Reinforcement steel

The requirements for reinforcement steel for composite structures are given by EC2, part 1-1 [15]. The yield strength of rebar is between 400-600 MPa, which is high when compared to that of typical structural steel.

In difference to structural steels, reinforcement steels are not standardized across Europe. The Norwegian standards for reinforcement steel bars are NS 3576-1 to 5 [20]. These standards defines four different grades, all with the characteristic yield strength of 500 MPa. The grades B500NA, B500NB and B500NC are made of carbon steel and differ by their ductility class, where B500NC is the most ductile. B500NCR is a stainless steel grade including at least 10,5 % of chromium. For further material behaviour of reinforcement steel, which similarly to structural steel is a carbon steel, refer to section 2.3.1.

## 2.4 Composite members

EC 4, part 1-1 [3] specifically mentions and describes beams, slabs and columns as different types of composite members. The seismic standard EC8, part 1 [21] also details composite shear walls. The typical approaches to design of such composite members as well as the means to join them are described in sections 2.4.1 to 2.4.6.

A major source of information regarding the different kinds of composite members is the Steel Designers' Manual, published by the UK Steel Construction Institute (SCI) [22,23,24].

### 2.4.1 Shear connection

In order to display composite behaviour, composite elements require means to transfer the forces between the materials. Without such a connection there will be a slip between the materials once the shear stresses at the steel/concrete interface is larger than the chemical steel-concrete bond formed during the casting of the concrete. As an illustration, consider a simply supported beam made up of two sections A and B of identical dimensions and material. It is uniformly loaded from the top by the line load  $q$ . In case a), the sections A and B are fully bonded to each other, while in case b), there is no bond between the sections and thus slip is allowed (the surface between A and B is here considered frictionless). The two cases are visualized in Figure 2-3.

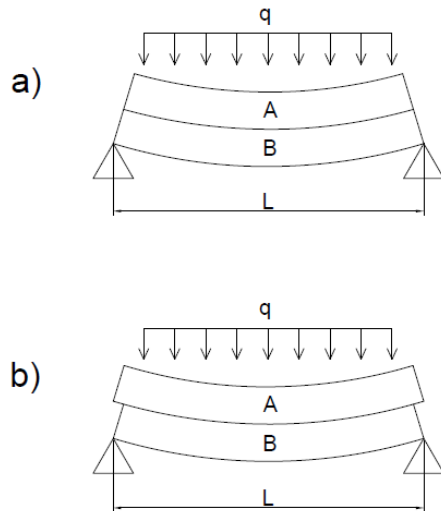


Figure 2-3: Simply supported composite beam with a) full shear connection; b) no shear connection.

Johnson [25] shows by using elementary beam theory that if the sections A and B are of the same material and have identical dimensions, the maximum bending stress in case a) is half that of b), while the mid span deflection in case a) is one fourth of that of b). He further shows that the total shear force at the intersection of A and B is significantly larger than the load  $qL$  carried by the beam. For the above example and with a beam length to height ratio of 20, this shear force is approximately equal to  $8qL$ .

EC 4, part 1-1 [3] defines shear connection as an interconnection between the steel and the concrete material so that they act as a composite member. The shear connection is said to be full, if having additional shear connectors would not increase the plastic cross-sectional bending resistance of the composite member. If this criteria is not met, the shear connection is said to be partial. A partial shear connection will result in a less than optimal shear connection and strength of the beam. Reasons to pursue a partial shear connection are given by Stark [26] as either due to the steel cross-section being oversized to handle an unpropped load during the concrete hardening, to limit deflections, or for economic reasons (if choosing an over-sized steel cross-section is cheaper than providing additional shear connectors).

As shear connectors are vital parts of a composite construction and since they have to transfer considerable forces to limited regions, they are associated with stress concentrations and their resistance to these forces has to be calculated. Both the shear resistance of the shear connectors and the crush resistance of the surrounding concrete is verified in the EC4 calculations. In addition to shear connection for longitudinal shear forces, a transverse tensile connection between the members may also be required [25]. If the distributed load  $q$  for instance would be applied upwards in Figure 2-3, the member B would not deflect together with the member A, unless there is a connection forcing it to do so. For this reason, shear connectors are also designed to handle such “uplift” forces.

The most common type of shear connector are headed studs, popularly named Nelson studs after the American inventor, which are welded onto the steel profile. Alternatively, steel claws nailed to the steel profile with a powder actuated gun, (commonly known as Hilti connectors) may be used. They are easier to install due to not requiring welding, but they have a lower resistance to shear force [23]. Kumar, Patnaik and Chaudhary [27] have studied usage of an adhesive bond by applying epoxy resin between the steel and the concrete. This type of connection is not covered by the EC4. Among the study conclusions, the adhesive bond shows promising results regarding the bond strength but there

are multiple factors which may affect the long-term durability negatively such as moisture and temperature. Additionally, the bond strength may be severely reduced in a fire scenario.

#### 2.4.2 Composite beam

EC4, part 1-1 [3] describes two different types of composite beams. The first type is a structural steel I or H-section which is connected through the flanges on the top side to either a concrete or composite slab (see chapter 2.4.4) by shear connectors; see Figure 2-4 for an illustration. The main advantage of this type of beam is the increased bending resistance of the slab/beam by allowing shear transfer between them. As shown by the simple example in section 2.4.1, shear transfer reduces the maximum bending stresses considerably which can allow for increased spans and/or reduced beam depths. As a result, a reduction of between 30-50% in steel material is stated for composite beams [23] when compared to a similar arrangement using ordinary steel beams without shear connectors. Another advantage is the lateral restraint provided by the slab to the compressive side of the steel beam (in regions of sagging moments), which prevents LTB of the beam and thus eliminates the need of additional lateral restraint.

The beam shown in Figure 2-4 can also be replaced by a steel truss, in which case it is called a composite truss. This type of member is not described in the EC4 codes for buildings but it is mentioned in the EC4, part 2 which is dedicated to composite bridge design [5].

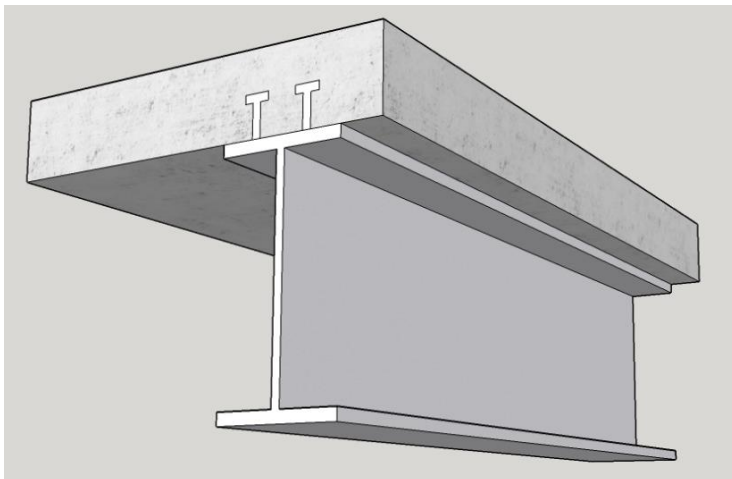


Figure 2-4: Steel I-beam connected to a concrete slab by shear connectors.

The second type of composite beam is the partially encased, which is a standard H- or I-section with the web encased in reinforced concrete. Shear connectors are provided between the web of the beam and the concrete in order to transfer shear forces. No literature has been found which clearly states the intended usage of this type of beam (given that the concrete clearly adds both self-weight and complexity). From structural theory it is evident that the stocky beam will not experience LTB, although this can also be achieved by the first type of composite beam. Fire and corrosion protection of the web is also an advantage. As argued by Kvočák and Drab [28] an advantage of a partially encased section when compared to the equivalent ordinary steel section is resistance towards local buckling, thus allowing an increased use of slender steel sections classified as class 4 in the EC3, part 1-1 [29].

See Figure 2-5 for an illustration of a partially encased composite beam.



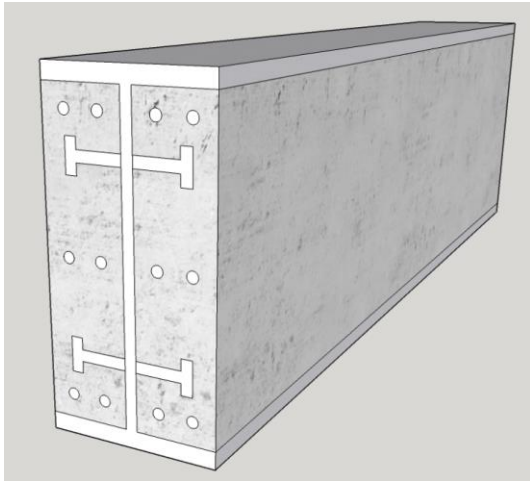


Figure 2-5: Partially encased composite beam.

The two types may also be combined, by using a partially encased composite beam connected to a slab through shear connectors, which will combine the advantages of both types of beams.

### 2.4.3 Composite slab

A composite slab as exemplified by EC4, part 1-1 [3] is constructed by laying profiled steel sheets onto supporting beams and thereafter cast a concrete slab on top of these sheets. Composite beams, see section 2.4.2 are typically utilized for supporting the slab, since the shear connectors on the beam will benefit both the slab and the beam [23].

There are lots of commercially available profiles for the steel sheets and manufacturers have their own specific designs. The two most commonly used profiles are the trapezoidal and dovetail. These corrugated shapes mainly gives the steel increased bending resistance (the dovetail also provides an interlock shear connection with the concrete) and are typically accompanied by smaller surface details such as indents, holes, embossments on the plates to provide a mechanical shear connection between the steel and concrete parts. The two types of steel profiles are principally shown in Figure 2-6. Transverse and longitudinal slab reinforcement is required by EC4. It is utilized for internal distribution of point loads, crack control and for fire scenarios [30]. If the slab is continuous, appropriate extra reinforcement must be provided in order to carry the tensile stresses due to the hogging moments occurring over the intermediate supports.

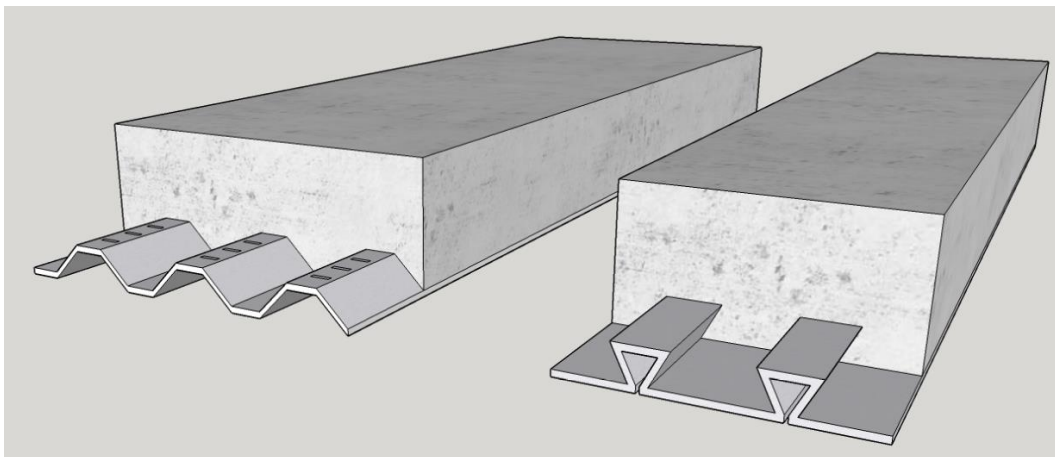


Figure 2-6: Composite slab steel profiles; trapezoidal (left) and dove-tail (right).

The preferred construction method with the above described composite slabs is to use an unpropred design. In this case, the profiled steel sheets are dimensioned strong enough to serve both as formwork for the hardening concrete and as a working platform. With no requirement of extra support during the concrete hardening, the building time may be reduced. The concrete used is typically in the lower scale of strength (cube strength C25-C32). Often lightweight concrete is utilized to reduce the self-weight, which is an important factor during unpropred design. [22]

Another type of composite structure which can be classified as a slab is the slim-floor, see Figure 2-7. In a slim-floor the supporting steel beams are encased in either a concrete or a composite slab such as described above, thus leading to a reduction of the total beam+slab height. Other benefits are also argued [31]:

- Increased fire resistance of the beam; up to R90 resistance without additional fire protection materials
- No underside interruption of the supporting beams. This can be practical for the planning and mounting of underlying utility installations.

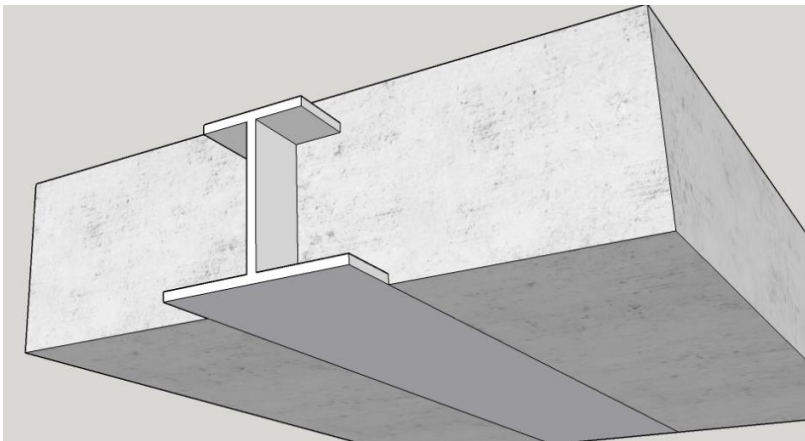


Figure 2-7: Slim-floor composite slab.

In difference to those solutions described above, the slim floor is not explicitly shown as a solution in EC4 and some simplified calculation methods in the standard e.g. fire resistance are not directly applicable. Various technical solutions for slim floors have been developed by different manufacturers. Typically the steel beams have larger lower flanges, increasing the tensile strength of the parts of the beam which are exerted to sagging moments. The beams may also have holes in the webs, to provide a steel-concrete shear connection by concrete dowels [31].

#### 2.4.4 Composite column

Arguably among the earliest incentives to utilize a composite column was the provision of increased fire resistance given by encasing steel profiles in concrete. Increased understanding of the composite column behaviour showed that in addition to the passive fire protection provided by the concrete, the composite member also showed a significant improvement in both strength and stiffness when compared to an ordinary steel member. [25]

EC4, part 1-1 [3] defines three principally different types of composite column cross-sections, which for the purpose of distinction are referenced as A, B and C according to Figure 2-8.

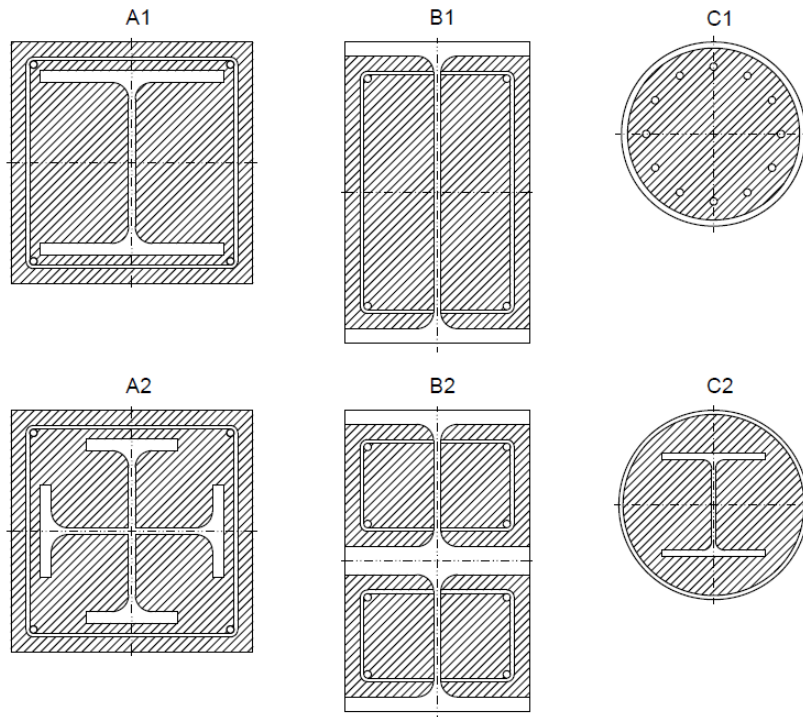


Figure 2-8: Examples of composite column cross-sections using standard steel sections, inspired by [3].

The different column cross-sections shown in Figure 2-8 are:

- Fully encased composite (FEC), (Type A1,A2)– in which the steel section is completely encased in reinforced concrete.
- Partially encased composite (PEC), (Type B1,B2)– in which the web of the steel section is encased in reinforced concrete. This cross-section is similar in appearance to the partially encased beam (see section 2.4.2) but unless shear forces are high, shear connectors may be omitted.
- Filled rectangular tubular (CFRT) or circular tubular (CFT) section (Type C1,C2) – in which a hollow steel section is filled with concrete.
- A cruciform of I-sections may be used, as shown in Type A2. This type is advantageous for beam-columns with significant bending moments about both the cross-sectional axes.
- Two or more steel sections may be welded together as shown by the double PEC section in type B2.
- Type A1 and C1 may be combined, as in type C2, in which an H/I section is enclosed within a hollow tubular member.

The different types of cross-sections offer different advantages. A concrete filled member does not require extra formwork, which is a great advantage during construction. The formwork required for a PEC column is relatively easy to erect, while construction of a FEC column requires more care with regards to the formwork and centralization of the steel member. FEC columns are expected to be resistant towards local buckling and therefore does not require any verification for this failure scenario, while the other two types of cross-sections require a class classification scheme similar to ordinary steel members.

In terms of fire resistance, the FEC column provides insulation to the whole steel member while the other types expose the steel member to some degree. In those cases, there is still benefit from the

concrete part, due to conductive heat loss into the concrete which results in a longer time needed to heat the steel to critical levels [24].

Notably, neither of the cross-sections are required to have shear connectors as described in 2.4.1 throughout the member when there are no fire resistance requirements. This is due to the relatively low shear forces encountered in columns. However in regions where shear forces are significant or in load introduction areas, shear connectors may still be required. PEC columns require shear connectors with a maximum interval of 0,5m if they are to be calculated for fire loads [4].

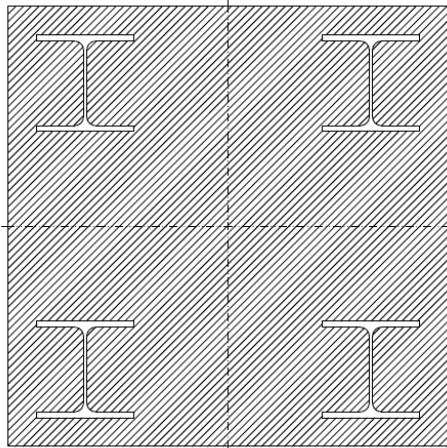


Figure 2-9: ISRC column, basic principle

Multiple, isolated steel sections may also be encased in a larger matrix of concrete, see Figure 2-9. This type of column is meant for very large building projects such as skyscrapers and their performance is described in a report by Fei [32], where they are named ISRC (Isolated Steel Reinforced Composite) columns. Due to utilizing multiple isolated steel sections, this type of column cannot be calculated according to the EC4 simplified rules (see Chapter 3), but it is still allowed in use, if specifically calculated according to guidelines given by the general rules section. The study concludes that the simplified rules for composite structures given by the Chinese building codes for ordinary composite columns such as shown in Figure 2-8 are applicable also for the ISRC column, but that the shear connections between steel and concrete are more important due to a larger relative load eccentricity.

#### 2.4.5 Beam to column joint

In a composite beam to column joint either the beam, the column or both may be a composite member. A sub-structure which consists of a composite beam, a composite column or both may be called a composite frame [3]. Traditional frame design often assumes either pinned or rigid joints. An ideally pinned joint does not transfer moments and has no rotational stiffness. An ideally rigid joint has unlimited rotational stiffness and the beam and column will always stay joined in the same angle. However, it has a limited moment resistance and will yield at a certain load. In reality both these cases are idealizations and the real behaviour is typically a joint with a moment resistance and rotational stiffness in between pinned and fixed.

Both EC3 and EC4 recognize this behaviour and a classification system is defined in EC3, part 1-8 [33] in which the beam-column joints either are defined as nominally pinned, semi-rigid or rigid depending on the rotational stiffness of the joint. Nominally pinned and rigid joints may be analysed by applying simple boundary conditions on the beams and columns, but for semi-rigid joints the stiffness of the joint has to be quantified and accounted for in the structural analysis.

Connecting either a steel or composite beam to a composite column introduces some specific issues. First, the steel section on the composite column is not very accessible for connection since either one or both sides are covered by concrete (making bolted connections more problematic). In the case of prefabricated composite columns, usually the connection details are welded in prefabrication. Secondly, the beam to column connection for continuous columns is often steel to steel and measures has to be taken to ensure transfer of the axial force from the column steel section to the concrete. Headed studs (see section 2.4.1) can be utilized for this purpose. Extra transverse reinforcement must also be applied in the load introduction area, to prevent failure of the concrete due to transverse shear.

In a joint where the beam is laid on top of the column with an endplate on the column, axial force transfer to the concrete can be accomplished without shear connectors if the end plate covers the concrete section [3]. This principle is also relevant for column bases and splices. Another method of load introduction which also directly transfer the load to the concrete section is a knife connection, where a vertical steel member is inserted through the centreline of the column.

Connecting a composite beam to either a steel or composite internal column will often mean that there is slab reinforcement in tension continuous above the joint and across the column. This steel reinforcement is contributing to the rigidity of the joint and have to be sized correctly to endure the bending stresses resulting from the desired moment capacity of the joint [25].

The typical solution for a composite beam to steel column joint is similar to steel joints. Trahair et al. [10] describes a number of joint solutions for connecting a beam onto the flanges of a column, including:

- rigid joints which are welded or bolted with large/stiff beam end plates
- nominally pinned joints in which the beam is seated on angle profiles fastened to the column and supplied with angle cleats to the top flange and web sides, or fastened with flexible beam end plates.
- semi-rigid joints, in which fin plates are welded onto the column and bolted to the web of the beam.

#### 2.4.6 Composite shear wall

Composite shear walls are not mentioned in the EC4. However the Eurocode for seismic actions EC8, part 1 [21] outlines different designs for this type of structural member. One design is to frame a reinforced concrete wall by steel or composite beams and columns. Shear connectors on the steel framework provide composite action between the concrete wall and the framing. Another design is a reinforced concrete wall with an internal or external steel plate. The steel plate is typically provided with shear connectors to the concrete section and fastened to the steel framework (e.g. welded).

The usage of composite shear walls in a construction typically allows for a higher ductility factor in seismic calculations than other types of walls offer. This in turn reduces the design response spectra essentially meaning that the structure will be exerted to less design shear force at its base and subsequently less design moments from seismically induced vibrations.

### 2.5 Usage of composite structural elements

It is difficult to find good references regarding the actual usage of composite structures for multiple reasons, including:

- It is not a primary target of structural research to describe what actually has been constructed (although there can arguably be many lessons learned from such an exercise).

- Composite construction methods are still developing and for instance a 15 year old report may not be indicative for the current situation.
- When experience from an existing building is documented, it usually regards large, unusual or prestigious projects. Experience from more modest projects (which arguably may be more relevant for the building industry at large) is harder to come by.

The following section briefly describes experiences from some composite constructions found in literature and where available, the given reasons why they were built with composite elements. Note that composite constructions outside of Europe typically are built in accordance to other building codes than the Eurocodes. The differences due to this are however not investigated.

### 2.5.1 Norway/Sweden

Claeson-Jonsson [34] provides experience from two Nordic buildings with composite elements, one in Norway and the other in Sweden:

#### Sørkedalsveien 6, Oslo

More commonly known as the KPMG building, this is an 18 storey high office building. CFT columns were chosen due to requiring no additional fire resistance measures other than reinforcement and for the speed of erection (here compared to concrete columns which require time for hardening before they can be loaded). The horizontal members were steel beams and pre-tensioned concrete slabs (i.e. not composite members).

#### Kista Science Tower, Stockholm

This is a 32 storey triangularly shaped building with office facilities. It has a bracing central core in concrete and a steel truss at the facade. Internal columns between the core and the facade have CFT cross-sections, with C65/80 grade concrete, which is a higher concrete strength than is allowed by the simple calculations rules of EC 4, part 1-1 [3]. The horizontal members were steel beams with filigree slabs, i.e. thin concrete slabs with truss-shaped reinforcement which similar to composite slabs allow for unpropped site casting. No specific reason as to why composite columns were used are described, although a discussion is provided regarding the different amounts of shrinkage between the steel facade and the concrete core. The shrinkage would naturally then have to be determined in the structural analysis and due to this, it is likely that an advanced calculation model including concrete shrinkage was used for the CFT columns.

### 2.5.2 Australia

Uy [35] describes a few Australian projects which utilize composite elements in ways that are not covered by the simple Eurocode calculation rules but exemplifies the versatility of composite construction methods.

#### Grosvenor Place, Sydney

At the ground level of this 44 storey building, composite multi-members each made of one vertical column and two diagonal struts in a trident shape are used to transfer vertical loads from three columns of the superstructure to one in the substructure. The columns and struts are all made up of FEC profiles. The purpose of this construction method is to reduce the column spacing in the underground parking facility.

### Star City complex, Sydney

In addition to using composite slabs in the casino areas for span length reasons, the 36m span roof construction in the theatres is made of a composite truss-slab, where the trusses are made of high strength steel and post-tensioned. Although not described in the report it is assumed the slab is made of light-weight concrete. All these strength-increasing measures was due to restrictions in crane access, which required light weight trusses. It is not stated how much lighter these trusses were, when compared to ordinary steel truss constructions.

### 2.5.3 Europe

#### Millenium Tower, Vienna

Huber [36] briefly describes the construction of the composite/concrete skyscraper Millenium Tower which is 202m high. It has a concrete core meant to brace the structure as well as carry vertical loads. The surrounding areas are shaped as twin circles in the shape of an “8” and made up of radially aligned composite frames with couples of composite columns supporting slim floor slabs. The main reason given for using composite elements was the fast erection time which was a project requirement. From the start of construction of the tower, it was finished within 8 months. Another reason which is given is lower facade costs due to the thin slim floor slabs.

In order to reduce the negative effects of the different shrinkage rates of the concrete core and the composite column pairs, the internal columns are circular FEC members with internal H-sections and the external columns have CFT cross-sections. This solution gives a gradient in concrete content from the core out to the external columns. Extra reinforcement in the concrete slab located above the slim floor beams ensure semi-rigid joints which increases the stiffness of the slab.

#### Netherlands

Stark and Schuurman [37] provides multiple examples of composite structures in the Netherlands of which two are given below. They argue that the reduced weight from composite slabs is beneficial for Dutch construction, since available construction sites are limited and existing buildings are often expanded. Here light-weight construction is important due to the limited strength of the existing structure and foundations.

#### Pathè Schouwburgplein cinema, Rotterdam

An existing underground parking facility with limited foundation strength was proposed as the base of a new large cinema building. By choosing a construction with composite slabs and beams, the overall weight was kept low and the subsequent foundation loads within the calculated limits.

#### Mammoet office, Schiedam

As a demonstration project for the heavy duty transport and lifting company Mammoet, a large office building of their own (now popularly named “the Bollard”) was constructed inside a workshop in Zwijndrecht and moved by barges to the already built foundations in Schiedam, where it was lifted in place onto a site-built steel foundation. Composite slabs were used to save weight, which was important due to barge tonnage limits. Multiple advantages for this type of “off-site construction” were listed, including in-door (weather independent) construction and simultaneous construction of foundation and building.

## 2.6 Previous research – composite columns

While the behaviour of composite columns is described in countless of reports, they are seldom explored in the sense of comparing their usefulness to that of other columns

Within a Norwegian context, no previous study on the topic has been found while a study was made 2008 in Sweden by Claeson-Jonsson [34] focusing on CFT columns only. That study described the general advantages and challenges of using composite columns, mainly from the construction method/time and economic aspects. A case study of a 9 storey building using either steel columns with intumescent paint or CFT columns was made and it was concluded that CFT columns potentially both were cheaper and can result in a reduced construction time. No research has been found (Norwegian or international) that does an extensive parametric comparison between steel and composite columns based on Eurocodes.



## 3 Column design according to Eurocodes

### 3.1 The column

Using a structural definition a column is a vertical, slender member which connects different horizontal levels and transfers predominantly compressive stresses. EC4, part 1-1 [3] defines a composite column as *“a composite member subjected mainly to compression or to compression and bending”*. Thus the definition provides no mention of the alignment or the shape of the column. A hypothetical composite load-bearing wall or a diagonal compressive composite strut may also fit the same definition. It is however assumed that EC4 refers to the general structural concept of a column, an assumption which is verified by the dimensional limitations to section shape given by further into the standard.

A column may in addition to axial compressive load be subjected to uniaxial or bi-axial bending moments due to end moments, loading eccentricities or transverse loads. Figure 3-1 shows an example column A-B, with an axial load  $N$ , end moment  $M$  due to a rigid beam-column joint; moment from loading eccentricity  $N \cdot e$  and a transverse distributed load  $q$ . When a member is subjected to moments in addition to axial force, it is often called a beam-column. For the purpose of this comparison, these members will still be referred to as columns in order to harmonize with the EC4 nomenclature.

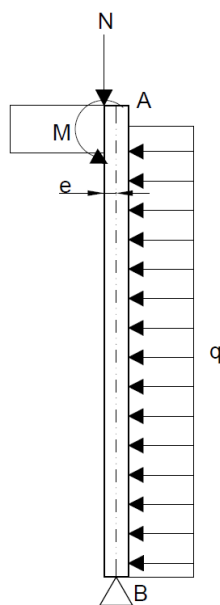


Figure 3-1: Illustration of load cases resulting in column moments

### 3.2 Worked examples - comparison of steel and composite column

This chapter will show by using simple worked examples, how steel and composite columns are calculated in accordance to the relevant Eurocodes and also highlight important structural theory. The relevant resistances of one structural steel column of a selected H-profile will be calculated for different ultimate limit state (ULS) criteria in accordance to EC3, part 1-1 [29] alongside the equivalent calculation of an FEC column in accordance to EC 4, part 1 [3], utilizing the same steel section but now fully encased in reinforced concrete. Thereafter the results will be compared as a ratio of the resistances. The same columns will be calculated for fire loads according to EC3, part 1-2 [13] (Steel) and EC4, part 1-2 [4] (Composite). Other accidental limit states (ALS) such as impact and blast loads are not calculated by using specific methods for composite members in the Eurocodes, however

composite columns may behave differently to such loads than those made of steel and a short literature survey regarding this has been made.

Note that some of the ULS criteria are two-dimensional, as for instance the case of combined uni-axial bending (M) and compressive force (N), section 3.3.2. A comparison of such criteria is better presented as a diagram instead of a ratio. In these cases, calculating sufficient values by hand to create good graphs require too many calculations to be practicable. Therefore the values are calculated by using spreadsheets in MS Excel.

The purpose of this chapter is not to explain in detail the justifications of the equations used in the Eurocodes, which would be a huge task and outside the scope of this thesis. The background for the EC3 rules for compression members can be found in literature from Trahair, Bradford, Nethercot and Gardner [10]. In a master's thesis, Basteskår, Birkeland and Knutsson describes the background for the EC4 composite column calculations [7], based largely on literature from Johnson [25].

The composite column is expected to out-perform the steel column for every ULS criteria. The reason is that it has a significantly higher squash load (yield resistance towards axial compressive force) due to having more material in the cross-section. The squash load design resistance  $N_{pl,Rd}$  does essentially contribute to every ULS criteria by increasing the associated design resistance. When reading this chapter, there are some important things to be aware of:

- There is a risk that mistakes were made during the creation of the earlier mentioned MS excel spreadsheets and such mistakes will not be visible to the reader of this report. As a safety measure, the results have been cross-checked against equivalent calculations made in the composite column verification software A3C (see section 4.1 for a software description).
- As there are only one of each type of column in the comparison, it is not possible to draw any well-founded conclusions on the differences between steel and composite columns in general based on this chapter only. In chapter 4, a larger selection of columns is calculated by software to determine the behavioural differences more accurately.

Table 3-1: Specifications of the worked example steel and FEC columns in chapter 3

<b>Specification, relevant for both columns</b>	
Column length	6000mm
Support	Nominally pinned at both ends
Steel section	HE-300B Hot-rolled [38], see Figure 3-2
Steel grade	S355
<b>Concrete specifications, only relevant for the composite column. Ref. EC2, part 1-1 [15]</b>	
Concrete strength	C30/37
Exposure class	XC1 (Low air humidity)
Structural class	S4
Relative humidity	50% (Indoors)
Design working life	50 year
Column loaded after	28 days
Reinforcement grade	B500NC
Composite section geometry	See Figure 3-3

The example columns are specified in Table 3-1. An additional description alongside cross-sectional illustrations are given below.

### Steel section:

The steel section is an HE-300B of S355 grade with measurements according Figure 3-2.

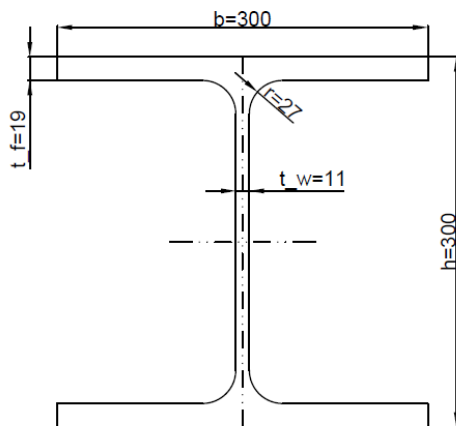


Figure 3-2: HE-300B profile with measurements in mm, according DIN 1025-5 [38].

### Composite section:

The steel profile (see Figure 3-2) is encased in the minimum required amount of normal-weight concrete of C30/37 grade to make a square section, with the minimum required B500NC grade reinforcement (See Table 3-1 for further details of the concrete used). This may not necessary be the most optimal way to design an FEC column cross-section, but it is a clear way of defining it, which is an advantage for a comparative study.

The minimum required amount of reinforcement is determined using a mix of rules originating from EC2, part 1-1 [15] and EC4, part 1-1 [3]. Notably, the total cross-sectional area of the reinforcement must at least be 0,3% of the concrete area and a maximum of 6%. The minimum required concrete is determined from the minimum required concrete cover of the steel section and the reinforcement bars. See Appendix B for detailed calculations of reinforcement and concrete cover, which concludes that the example composite cross-section should have dimensions according to Figure 3-3.

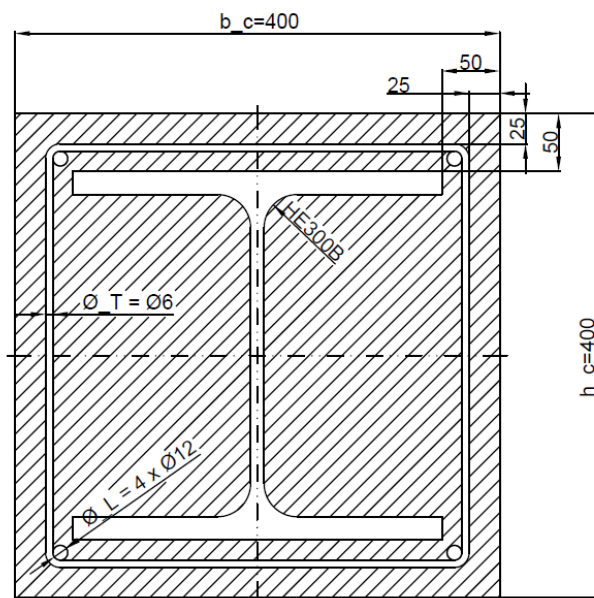


Figure 3-3: Fully encased composite HE-300B section. Measurements in mm.

### 3.3 Ultimate limit state (ULS)

#### General:

An ultimate limit states criteria for a column outlines the maximum amount of loads it can withstand before having a structural failure. It belong to one of these types of failure modes:

- Yielding of the cross-section due to axial compressive force, bending moments, shear force or combinations of these. See section 3.3.1 to 3.3.4.
- Instability of the member (i.e. buckling), considering member imperfections, load eccentricities and column deflections due to second order effects. See sections 3.3.5 & 3.3.6
- Failure at either the column base or at beam-column joints. This type of failure mode is not discussed or evaluated in detail in this thesis.

The criteria is typically expressed as  $R_d > E_d$ ; where  $R_d$  and  $E_d$  are the design resistance and design load respectively, which in turn are achieved by multiplying the listed/characteristic resistance and the structural loads from analysis with appropriate safety factors.

#### Steel:

The calculation methods given in EC3, part 1-1 [29] for ULS verification of compression members are either derived from elastic or plastic theory, pending on the predicted onset of local buckling. The material partial factors relevant to this thesis which account for deviations in the material strength are provided by the Norwegian national annex as:

- Yield of cross-section:  $\gamma_{M0} = 1,05$
- Instability:  $\gamma_{M1} = 1,05$

#### Composite:

EC4, part 1-1 [3] describes two different methods to calculate the ULS resistances for columns. The “general method” does not describe a specified calculation method but rather gives a guideline on how the structural analysis should be done, which assumptions are allowed and which considerations has to be taken. No restrictions for the shape of the composite cross-section are given.

The second method is the “simplified method”. When this method is used there are multiple restrictions regarding the shape of the column:

- a) The cross-section must be symmetrical about both axes.
- b) The cross-section must be uniform over the length of the column, except for shear connectors and transversal reinforcement where required.
- c) The cross-section can only have one steel section (for example ISRC columns such as shown in Figure 2-9 are not allowable).
- d) The maximum relative slenderness of  $\bar{\lambda}$  is 2,0.
- e) The steel contribution ratio  $\delta$  must be between 0,2 and 0,9
- f) The depth to width ratio of the total cross-section is within 0,2 and 5,0
- g) For FEC columns, the concrete cover is beneath 30% of the steel section height and 40% of the steel section width.

The criteria a), b), c), f) and g) of the example column are easily verifiable just by looking at the chosen cross-section. The steel contribution ratio e) will be verified in section 3.3.1 and the maximum relative slenderness d) in section 3.3.5. The material partial factors for the composite steel section are the

same as those given for pure steel sections. For the reinforced concrete, the partial material factors are provided by the EC2, part 1-1 [15] as:

- Concrete strength:  $\gamma_c = 1,5$
- Reinforcement strength:  $\gamma_s = 1,15$

### 3.3.1 Yield resistance of a cross-section towards compression (N)

#### General:

The plastic axial force resistance  $N_{pl}$  for a uniform member of a cross-sectional area  $A$  in pure compression can be derived directly from the elastic definition of stress. Equalling stress to the yield strength ( $f_y$ ) and rearranging, the maximum force before yield is found by:

$$N_{pl} = f_y/A \quad (3-1)$$

For thin sections, local instability effects due to the compressive force may occur before the compressive stresses in the member reach the yield strength. This results in so called local buckling which will reduce the yield resistance.

#### Steel:

For compression members such as columns, EC3, part 1-1 [29] classifies cross-sections according to the onset of local buckling. The web and flange sections of an H-profile are classified separately using dimensional ratios. Pending on the classification, the calculation rules for a certain resistance will be either be based upon plastic (class 1 and 2), elastic (class 3) or reduced elastic (class 4) theory. In pure compression, the plastic cross-sectional resistance is equal to the elastic resistance, since ideally all fibres yield and show plastic behaviour at the same time - at the yield strength. Therefore the same equation may be used for class 1 to 3 members. For class 4 members, the cross-sectional area  $A_A$  is reduced to compensate for local buckling.

The example HE300B column is classified to class 1 for both the web and the flange and the calculated yield resistance for a steel area  $A_a$  is directly based on equation (3-1), with the partial material factor  $\gamma_{M0}$  and equals:

$$N_{pl,a,Rd} = \frac{A_a f_y}{\gamma_{M0}} = 5040 \text{ kN (See Appendix A)} \quad (3-2)$$

#### Composite:

For an FEC cross-section, local buckling is not assumed to happen according to EC4, part 1-1 [3]. For CFT, CFRT or PEC sections the absence of local buckling must be verified through similar means as a pure steel section; by checking the steel section dimensions against defined limits. Unlike the calculation rules given by EC3, all rules given in the simplified method of EC4 are valid for perfectly plastic theory only and if the cross-section fails the defined limit, it cannot be calculated by the simplified method, due to the risk of local buckling before the cross-section reach the perfect plastic state.

The plastic cross-sectional resistance to compression is calculated by a simple addition rule and the contributions from the steel, concrete and longitudinal reinforcement cross-sectional areas  $A_a$ ,  $A_c$  and  $A_s$  are added as if they were calculated by EC3, part 1-1 [29] and EC2, part 1-1 [15] respectively:

$$N_{pl,Rd} = \frac{A_a f_y}{\gamma_{M0}} + \frac{0,85 A_c f_{ck}}{\gamma_c} + \frac{A_s f_s}{\gamma_s} = 7695 \text{ kN (see Appendix B)} \quad (3-3)$$

Notably, there is a factor of 0,85 for the concrete contribution. This is analogue to the long term strength factor  $\alpha_{cc}$  in EC2. For a CFRT or CFT cross-section, this factor can be taken as 1 due to confinement of the concrete [3,25]. EC4 provides additional calculation rules for confinement in CFT sections which increases the strength of the concrete and decreases that of the steel if certain criteria are met. A short explanation is that the Poisson's ratio for concrete is higher than that of steel at high compressive stress and when the concrete tries to expand in the radial direction it is confined by the steel tube. Thus counteractive stresses develop in the concrete, increasing the concrete strength. In addition, the friction bond between steel and concrete is strengthened [39]. The steel yield strength is however negatively affected due to the induced radial stresses from the concrete. The net result is an increase of plastic squash load resistance. The confinement effect and the limits for when it can be applied is further described by the Appendix J, in which a MATLAB model for CFT cross-sections is presented.

The steel contribution ratio describes to which degree the steel section contributes to carrying the squash load and it is calculated in Appendix B to be  $\delta = 0,655$  which is in between the allowed lower/upper limits of 0,2 and 0,9 respectively and therefore acceptable. If the steel contribution ratio is beneath 0,2 the member should be calculated by EC2, part 1-1 [15] rules as a reinforced concrete member and if it is above 0,9 the member should be calculated by EC3, part 1-1 [29] rules as a pure steel member [25].

#### Comparison of resistance:

The axial load cross-sectional resistances for the composite and steel sections can be compared directly by a ratio of equations (3-2) and (3-3):

$$\frac{N_{pl,Rd}}{N_{pl,a,Rd}} = \frac{7695}{5040} = 1,53 \quad (3-4)$$

### 3.3.2 Yield resistance of a cross-section towards compression (N) + uniaxial bending (M)

#### General:

It is reasonable to assume that a column always is exerted to axial loads, thus the plastic cross-sectional resistance towards bending only (when all fibres reach yield stress due to bending) is not a relevant case. However, bending moments in combination with axial loads are common (see Figure 3-1 for an illustration) and they must be accounted for.

In general, the plastic moment cross-sectional resistance  $M_{pl}$  is based on elementary beam theory. It can be determined accordingly for bending about major (y) and minor (z) axes of a section with the plastic section moduli  $Z_y$  and  $Z_z$  and the yield strength  $f_y$ :

$$\begin{cases} M_{pl,y} = Z_y * f_y \\ M_{pl,z} = Z_z * f_y \end{cases} \quad (3-5)$$

For a case of simultaneous axial force and uniaxial bending, the plastic cross-sectional moment resistance must be altered to account for the axial force. This may be visually represented by stress blocks of the perfectly plastic stress state, as shown in Figure 3-4.

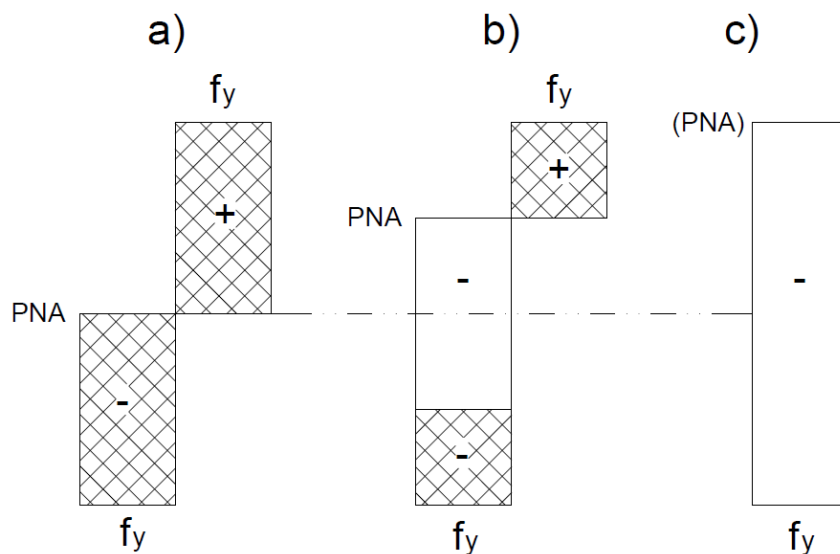


Figure 3-4: Stress blocks for plastic moment cross-sectional resistance in the presence of axial force

For a symmetrical member in pure bending (a), the areas in compression and tension will be of equal size, thus the plastic neutral axis (PNA) will coincide with the centroid of the member. Once a compressive axial force is present (b), this may be visually represented as dedicating the middle part of the cross-section to being in plastic stress due to pure compression. Meanwhile the top and bottom parts are in plastic stress due to pure bending. Notably both the plastic moment resistance (which relates to the size of the cross-hatched blocks) and the position of the PNA changes. If the compressive axial force is equal to the plastic axial force resistance of the member (c), the PNA can be said to be located at the very top of the member, meaning there is no moment resistance.

In order to determine the effect of the axial force for the moment resistance, interaction curves (also called M-N interaction diagrams) can be developed (as an example, see Figure 3-7). This method is also commonly used for reinforced concrete sections in EC2, part 1-1 [15]. By looking up the design axial force value  $N_{Ed}$  in the M-N interaction diagram it is possible to directly determine the altered moment resistance due to axial force  $M_{N,Rd}$ .

#### Steel:

Similar to the case of compression, see section (3.3.1); a class classification must be made in order to determine whether to analyse the member by plastic, elastic or reduced elastic theory. In major axis bending of an H/I section, one flange side will be in compression and must be classified as such. The web is likely in both compression and bending and can be classified according to rules for this. However, it is conservative to assume that it is in pure compression and since both the flange and web is determined as class 1 for pure compression in section 3.3.1, no further check is needed for this worked example.

Since structural steel have equal yield resistance towards compressive and tensile forces, the addition of a compressive force will always reduce the cross-sectional resistance against bending moment. For calculations of the M+N case EC3 do not require interaction curves, since the plastic cross-sectional moment resistances for the typical kinds of steel profiles are readily calculated with relative simple algebraic expressions, derived from plastic theory.

### Composite:

In difference to a steel section, but similar to a section in reinforced concrete - a composite section may show a higher moment resistance if a moderate compressive axial force is present. This is due to a reduction of the tensile forces on the outer fibres of the concrete [24].

To calculate the full MN interaction diagrams for a composite section is cumbersome and requires usage and addition of separate stress blocks for axial force and bending for the steel section, the reinforcement steel and the concrete. The main issue to calculate the maximum axial force at a specified bending moment is to find the location of the plastic neutral axis (PNA). By using the iterative possibilities of for instance a spreadsheet software, Johnson [25] suggests a method which first guesses the plastic neutral axis position, calculates the resultant axial force of the stress blocks at that position and the resultant bending moments about the section centroid. This can be repeated for other neutral axis positions up until pure compression, until there are enough points to draw a curve. A MATLAB code, which calculates the cross-sectional resistances for a reinforced CFT section was developed for the purpose of this thesis and it is further described in section 4.1.2.

EC4, part 1-1 [3] also allows using a simplified version of the MN interaction diagram, calculating a polygonal curve consisting of four points A to D at specific locations, see table Table 3-2. Johnson [25] argues to include an extra fifth point E between A and C for bending about the minor axis, since the diagram is too conservative otherwise.

Table 3-2: Point locations on the A to E polygonal curve suggested by EC4, part 1-1[3].

Point	Axial force (N)	Bending moment (M)
A	Plastic cross-sectional resistance to compressive force only, $N_{pl,Rd}$	0
B	0	Plastic cross-sectional resistance to moment only, $M_{pl,Rd}$
C	Upper value for axial force when the bending moment is at the $M_{pl,Rd}$ level, $N_{pm,Rd}$	Same moment as for point B, $M_{pl,Rd}$
D	Half value of point C $N_{pm,Rd}/2$	Maximum plastic cross-sectional resistance to bending moment, $M_{max,Rd}$
(E)	No guidance is given in EC4. For minor axis bending, the PNA for point E can for instance be set at half the width of the flanges on the tensile side. Thereafter axial force (N) and bending moment (M) are calculated from stress block equilibrium.	

The stress blocks of the perfectly plastic states for major axis bending of an FEC section, representative for the point A to D are shown in Figure 3-5. Compressive and tensile stresses are denoted by “-” and “+” respectively.

Note that the tensile strength of concrete is ignored, in accordance to the EC4 rules.



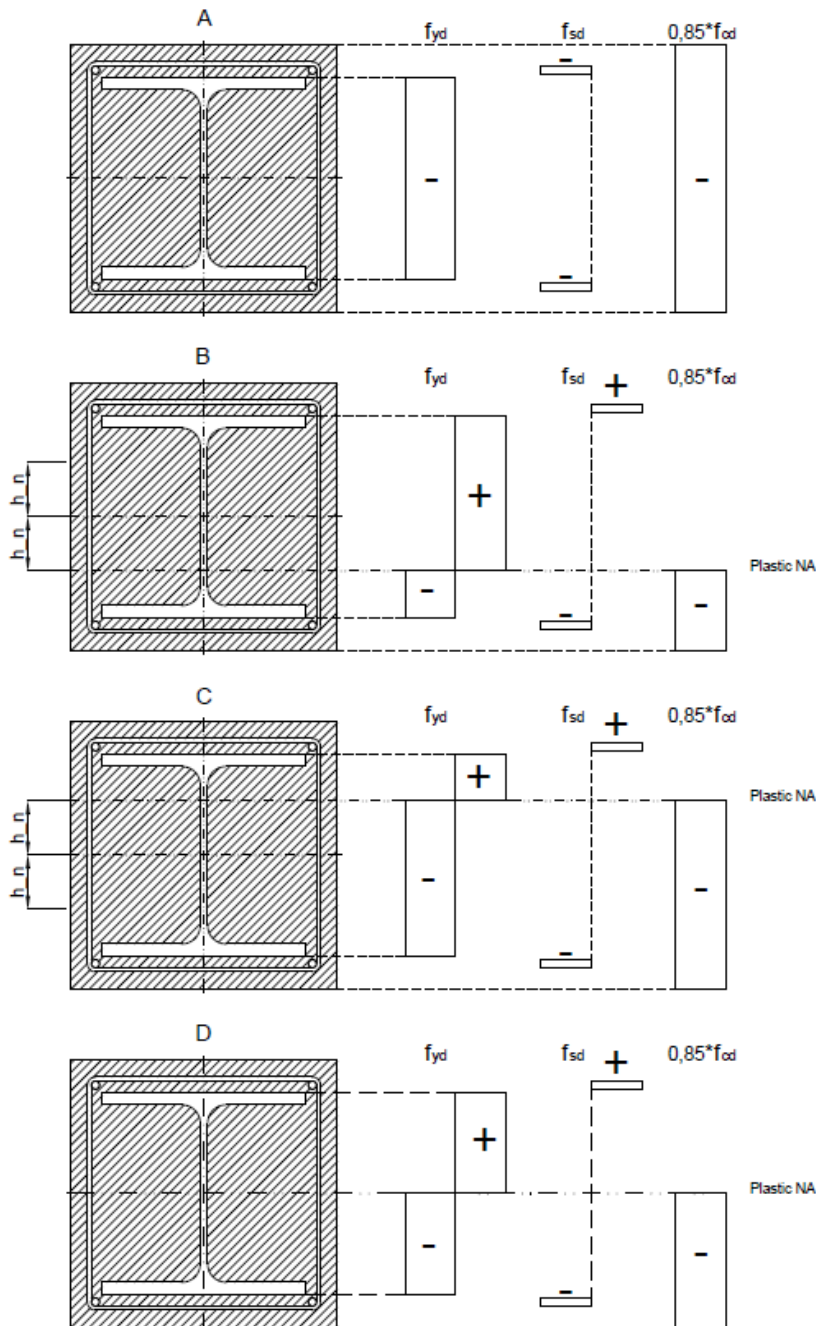


Figure 3-5: Stress blocks for polygonal curve points A to D for a fully encased composite section. Inspired by [24].

For our example composite column which is calculated in Appendix B, the corresponding A to D polygon version of the MN interaction diagram is developed. A step-wise procedure to calculate the  $\{M,N\}$  coordinates for an FEC H or I-section is established below, using [24] as guidance.

1. Point A is located at  $\{0, N_{Pl,Rd}\}$
2. Assume a position on the compressive side of the centreline for the position of the plastic neutral axis for pure bending (a sensible first guess is in between the fillets for bending about the major axis and through the flanges in compression for bending about the minor axis).
3. Calculate the position of the plastic neutral axis  $h_n$  at point B, using equilibrium of compressive and tensile forces given by the stress blocks.

4. Check whether the position of  $h_n$  is according to the assumption made in point 2, otherwise change the position and recalculate from step 2.
5. Calculate the plastic section moduli for the full section and for a section of  $\pm h_n$  distance from the section centreline for each of the constituent materials
6. Determine the plastic moment resistance for the composite cross-section  $M_{pl,Rd}$  by using the plastic section moduli from step 5, the position of the plastic neutral axis from point 2 and the design strengths of the constituent materials.  
Point B is located at  $\{M_{pl,Rd}, 0\}$
7. Assume the plastic neutral axis is now  $h_n$  away from the section centreline, now on the tensile side. Calculate the resistance to compressive force at this point,  $N_{pm,Rd}$  by the resultant of the stress blocks at this position.  
Point C is located at  $\{M_{pl,Rd}, N_{pm,Rd}\}$
8. Assume the plastic neutral axis is now coinciding with the centreline. Calculate the resistance to bending moment at this point,  $M_{max,Rd}$  by using the plastic section moduli for the full sections calculated in step 5.  
Point D is located at  $\{M_{max,Rd}, N_{pm,Rd}/2\}$

The resulting polygonal MN interaction diagrams for both axes of the example composite section are shown in Figure 3-6. Note that due to the PNA going through the fillet section for the calculation of the minor axis, the areas of the steel fillets are replaced by concrete in the calculations to simplify the algebraic expressions.

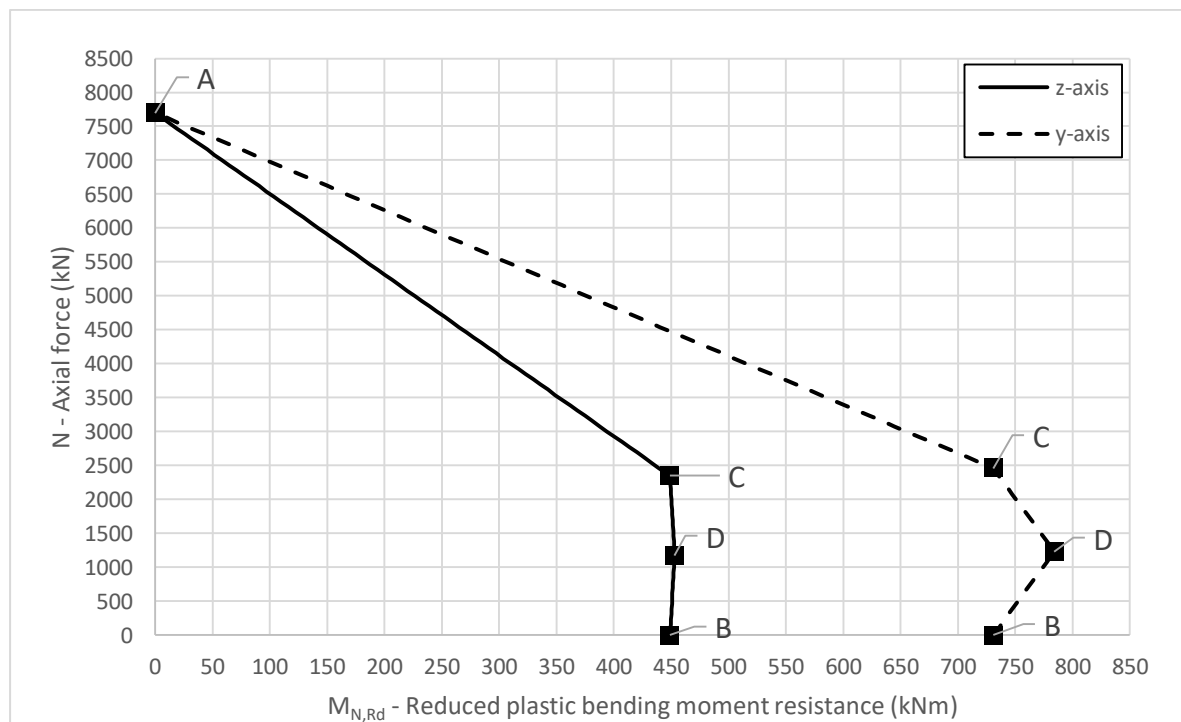


Figure 3-6: M-N polygonal interaction diagram for the fully encased HE300B section

The resistance found from the interaction diagram must be further reduced by multiplying it with a factor  $\alpha_M$  of 0,9 for steel section grades up to S355 and 0,8 to higher steel grades. This factor adjusts for inaccuracies regarding the plastic stress block assumption for the concrete section [25].

### Comparison of resistance:

In order to compare the design moment resistances for the steel and composite cross-sections, interaction curves for the steel section has to be developed. The EC3, part 1-1 [29] rules are applied and the maximum moments  $M_{N,Rd}$  the cross-section can carry for a certain design axial load  $N_{Ed}$ , are calculated and plotted on an M-N diagram for 100 evenly spaced axial force values of  $N_{Ed}$  between 0 and  $N_{pl,a,Rd}$  using an MS Excel spreadsheet. This is done for bending about both the major and minor axis.

Finding the reduced uniaxial moment resistances due to compression for the steel and composite columns can be done directly from the interaction diagrams, see Figure 3-7. Note that the composite section values are 10% lower than in Figure 3-6 due to application of the  $\alpha_M$  coefficient.

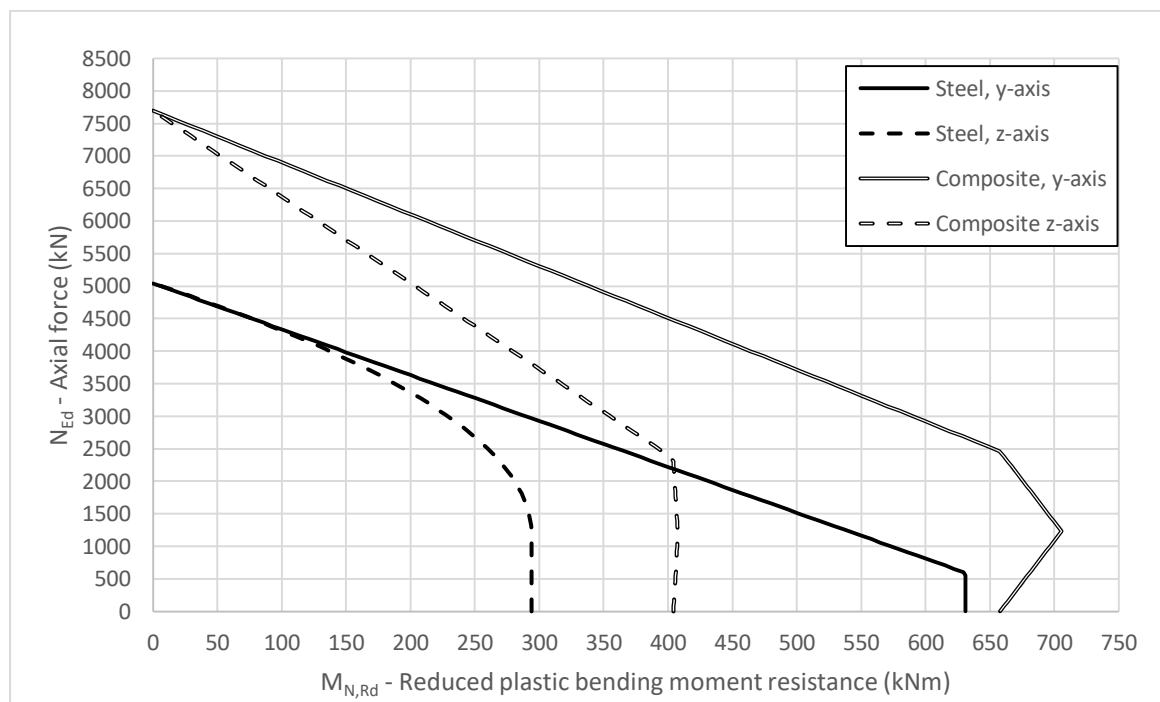


Figure 3-7: M-N interaction curves for HE300B. Comparison steel and FEC HE-300B cross-sections.

As can be seen, the steel and composite graphs for the major axis bending are close to parallel at lower values of  $M_{N,Rd}$ . For minor axis bending, the graph for the composite section has a higher slope. Arguably an extra point (E), according Table 3-2 would reduce the slope of the composite section for low  $M_{N,Rd}$  values, so that the minor axis graphs also would be close to parallel.

Since columns are primarily loaded axially, this linear section is usually the most interesting. The ratio between the composite and the steel section is determined by calculating the ratios of average design axial forces  $\bar{N}_{Ed}$  and  $\bar{N}_{a,Ed}$  respectively of the composite and steel cross-sections in the linear section of the graph, using MS Excel:

For bending about the major (y)-axis and  $M_{N,y,Rd}$  between 0-400 kNm:

$$\frac{\bar{N}_{Ed}}{\bar{N}_{a,Ed}} = \frac{6118}{3654} = 1,67 \quad (3-6)$$

For bending about the minor (z)-axis and  $M_{N,z,Rd}$  beneath 0-200 kNm;

$$\frac{\bar{N}_{Ed}}{\bar{N}_{a,Ed}} = \frac{6387}{4360} = 1,47 \quad (3-7)$$

### 3.3.3 Yield resistance of a cross-section towards compression (N)+ bi-axial bending ( $M_y$ & $M_z$ ) General

Bending moments may occur simultaneously about the major and minor axes. In such cases, bi-axial bending resistance must be checked, since the bending stresses will interact and cause two opposite corner areas with a higher compressive and tensile stress situation respectively, leading to a reduced overall plastic cross-sectional yield resistance.

#### Steel

The bi-axial moment + compression ULS verification for a steel H or I-section is determined in accordance to EC3, part 1-1 [29]; based on the design moments for the major and minor axes  $M_{i,Ed}$  as well as the reduced design moment resistances  $M_{N,i,Rd}$  found from the EC3 analytical expressions:

$$\left[ \frac{M_{y,Ed}}{M_{N,y,Rd}} \right]^2 + \left[ \frac{M_{z,Ed}}{M_{N,z,Rd}} \right]^{\max(5n; 1)} = 1 \quad (3-8)$$

Where  $n$  is the design axial resistance ratio of the design axial force  $N_{Ed}$  and the squash load resistance found from equation (3-2):

$$n = \frac{N_{Ed}}{N_{Pl,a,Rd}} \quad (3-9)$$

#### Composite

To determine the bi-axial moment + compression resistance for a composite section, first the M-N interaction diagrams for both the uniaxial bending + compression cases has to be developed and the uniaxial resistances verified (see section 3.3.2).

Thereafter the utilization factor  $\mu_d$  which describes the moment resistance ratios is calculated for both axes  $i = \{y, z\}$  as:

$$\mu_{di} = \frac{M_{N,i,Rd}}{M_{Pl,i,Rd}} \quad (3-10)$$

The criteria for the bi-axial moment + compression resistance is:

$$\frac{M_{y,Ed}}{\mu_{dy} M_{pl,y,Rd}} + \frac{M_{z,Ed}}{\mu_{dz} M_{pl,z,Rd}} \leq 1 \quad (3-11)$$

#### Comparison of resistance:

Similarly to the uniaxial bending case, the results for the steel and composite sections are compared by graphs rather than single value, since the allowable moments  $M_{y,Ed}$  and  $M_{z,Ed}$  varies according to how large the axial force  $N_{Ed}$  is.

As there are essentially three independent variables of the design loads ( $N_{Ed}$ ,  $M_{y,Ed}$  and  $M_{z,Ed}$ ) – a two dimensional graph is not sufficient to show a comparison between the bi-axial bending + compression plastic moment cross-sectional resistance for steel and composite. Therefore, a ratio  $\xi_M$  between the design moments about the major and minor axes is introduced. For this comparison, the following three sample ratios are used:

$$\xi_M = \frac{M_{y,Ed}}{M_{z,Ed}} = \begin{cases} 1/3 \\ 1 \\ 3 \end{cases} \quad (3-12)$$

The EC3, part 1-1 [29] and EC4, part 1-1 [3] rules for biaxial moment resistance for steel and composite sections respectively (including the uniaxial moment resistance verification for each axis as described in section 3.3.2) are applied and calculated for 100 evenly spaced values of  $N_{Ed}$  from 0 to  $N_{pl,Rd}$ . The target is to find the maximum allowable value of  $M_{y,Ed}$  when  $M_{z,Ed}$  equals  $\xi_M * M_{y,Ed}$ .

In the equation for the steel section (3-8) the  $M_{y,Ed}$  and  $M_{z,Ed}$  terms have different and varying exponents and it is therefore not easy to isolate  $M_{y,Ed}$  through algebraic means. Therefore the equation (3-12) is inserted into equation (3-8) and the equation is solved numerically. This is accomplished by using the goalseek function in MS Excel and a simple iterative loop written in VBA to solve the values of  $M_{y,Ed}$  for all 100 data points, which satisfies:

$$\left[ \frac{M_{y,Ed}}{M_{N,y,Rd}} \right]^2 + \left[ \frac{\xi_M M_{y,Ed}}{M_{N,z,Rd}} \right]^{\max\left(\frac{5 * N_{Ed}}{N_{pl,Rd}}, 1\right)} = 1 \quad (3-13)$$

Since it is known that the result of the equation equals 1, the errors which occurs during the numerical solving can be determined by comparing the achieved answers to 1. The errors calculated for the steel section values are in the magnitude of maximum 0,1% and therefore deemed insignificant.

The EC4 bi-axial equation (3-11) is easily rearranged through algebraic means accordingly:

$$M_{y,Ed} = \frac{1}{\frac{1}{\mu_{dy} M_{pl,y,Rd}} + \frac{\xi_M}{\mu_{dz} M_{pl,z,Rd}}} \quad (3-14)$$

The results for the biaxial moment design resistance comparison are shown in Figure 3-8. Notably, the moment design resistance for the steel section shows a strange inwards kink at low axial force and a  $\xi_M$  value of 1 and 3. This occurs at the location where the exponent for the  $M_{z,Ed}$  term shifts from 1 to  $5n$ , referring to equation (3-8).

Similarly to the results for combined uniaxial bending and compression, the steel and composite curves stay relatively parallel, but they would likely be even more parallel if more points are used for the composite MN interaction diagram.

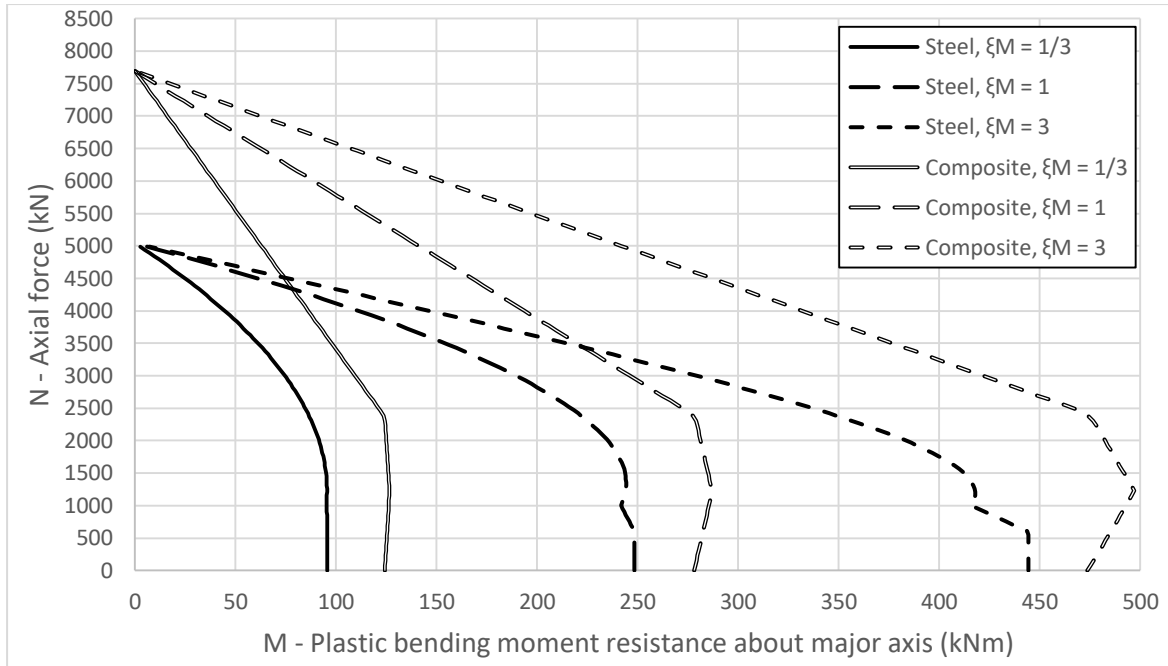


Figure 3-8: Reduced moment resistance about y-axis due to axial force, biaxial bending for three different ratios  $M_y/M_z$ . Comparison steel and FEC HE-300B cross-sections.

### 3.3.4 Yield resistance of a cross-section towards transverse shear force (V)

#### General:

Columns are usually not exposed to significant longitudinal shear stresses outside the near vicinity of the load introduction area and these kind of shear stresses are not treated in this section. If bending moments are introduced either from end moments or lateral loads, transverse shear stresses will occur unless the member is in pure bending. Yielding due to shear force is not the typical failure for a column and is mostly of consideration for accidental or seismic loads. For an elastic member in pure shear, the Von Mises yield criteria reduces to:

$$\tau_y = \frac{f_y}{\sqrt{3}} \quad (3-15)$$

Where  $\tau_y$  is the yield shear stress. Hereafter, the characteristic transverse shear resistance  $V_{pl,Rk}$  of an area A can be stated:

$$V_{pl,Rk} = \frac{\tau_y}{A} \quad (3-16)$$

In this section, the design resistance against pure shear force (V) is shown. A column is always subjected to axial loads and thus this is not a relevant verification. In a complete structural ULS verification, sufficient resistances towards shear + bending (M+V) and towards shear + bending + axial force (M+N+V) should be verified. This is done in the same principal way for both steel and composite column, where contribution from the shear force is ignored unless the design shear force equal more than 50% of the total shear resistance. After that, the yield strength of the shear area (essentially the area of the web for an I-section in major axis bending) is reduced by a factor, which affects the design plastic resistances to both bending and axial force. The resistances towards the M+V and M+N+V cases are not calculated in this chapter due to the complicity involved and since it rarely is relevant for a column.

### Steel:

As structural steel is assumed to behave perfectly elastic, the shear yield resistance  $V_{pl,a,Rd}$  of structural steel is assumed to be based on equation (3-15) and (3-16) i.e:

$$V_{pl,a,Rd} = \frac{f_y}{\sqrt{3}} A * \gamma_{M0} \quad (3-17)$$

### Composite:

An easy and conservative method to verify the horizontal shear resistance for a composite cross-section is to set it equal to that of the steel section and use the equation (3-17) [24]. Usually, the shear resistance of a composite column will not be dimensioning and shear stresses are only a local issue in load introduction areas. Calculation of these stresses is dependent on the joint solution and therefore not within the scope of this thesis. According EC4, part 1-1 [3] the design shear stress  $V_{Ed}$  may be divided onto the steel and the concrete section, where the ratio of the design steel shear force,  $V_{a,Ed}$  to the total design shear force is proportional to the ratio of the steel section plastic moment resistance against the total plastic moment resistances, which are calculated in section 3.3.2. Thus:

$$V_{a,Ed} = V_{Ed} * \frac{M_{pl,a,Rd}}{M_{pl,Rd}} \quad (3-18)$$

The design concrete shear force is equal to the remainder:

$$V_{c,Ed} = V_{Ed} - V_{a,Ed} \quad (3-19)$$

The rules to calculate the horizontal shear resistance of concrete is described in EC2, part 1-1 [15] and depends on whether the member requires shear reinforcement or not. For the composite section it is assumed that shear reinforcement is not required, since the transverse shear forces in a column are low and since the steel section already provides a large transverse shear resistance. The minimum required transverse shear reinforcement must however still be provided. For an FEC member the transverse reinforcement stirrups are typically laid in loops outside the longitudinal reinforcement bars (see Figure 2-8, case A1 for an example), while they would be welded to the web or drawn through drilled holes in the web for a PEC member.

How to calculate the additional shear resistance from the concrete is not clearly stated in EC4 or shown in the reference guidelines for EC4 calculations, since the typical approach seems to be to just verify that the steel section shear resistance is sufficient. The method chosen to include the concrete shear resistance is adopted from calculation examples by Bzdawka [40]. The shear resistance of concrete depends on the axial load. A compressive axial load increases the shear resistance of concrete up to a maximum level. For this example, a design axial load of  $N_{Ed} = 2000kN$  is chosen and distributed onto the concrete as  $N_{Ed,c}$  as per the ratio of the design squash load resistance of concrete to that of the full composite section:

$$N_{Ed,c} = N_{Ed} * \frac{N_{pl,c,Rd}}{N_{pl,Rd}} \quad (3-20)$$

Using the assumed axial design force of  $N_{Ed}$ , the positive effect from the compressive stress on the concrete shear resistance is above the upper limit given by EC2 and therefore further axial load would not improve the shear resistance.

Comparison of resistance:

The design cross-sectional resistances to shear for the steel and composite cross-sections are calculated in Appendix A and B respectively and can directly be stated by a ratio:

$$\frac{V_{pl,Rd}}{V_{pl,a,Rd}} = \frac{979}{925} = 1,06 \quad (3-21)$$

### 3.3.5 Buckling resistance of a column towards compression

General:

A straight member exerted to pure compression will become instable after the axial compression force reaches a critical value  $N_{cr}$ , derived by Leonhard Euler to equal:

$$N_{cr} = \frac{\pi^2 EI}{L_{cr}^2} \quad (3-22)$$

Once the axial load exceeds the critical axial force; even when exerted to very small moments the elastic restoring force is not sufficient to keep the member from continued bending, eventually leading to plastic collapse or a fracture of the member. This phenomena is named flexural buckling and it only occurs about the axis offering the least resistance towards bending. Here both the flexural rigidities  $EI$  and the buckling lengths  $L_{cr}$  of the axes must be considered. The buckling length depends on the end restraints and on intermediate lateral restraints (if available). For an H or I-section with no lateral restraint and similar support conditions for both axes, buckling always occurs about the minor (z) axis. For more complicated cases with uneven support conditions and lateral restraints for the major and minor axes, the safe approach is to calculate the critical force for both axes and select the lowest.

As a measure of the cross-sectional resistance to squash load relative the critical force, the relative slenderness concept is used, determined as:

$$\bar{\lambda} = \sqrt{\frac{Af_y}{N_{cr}}} \quad (3-23)$$

A low relative slenderness  $\bar{\lambda}$  indicates a stocky column which yields in compression before it buckles, while slender, unbraced columns typically always buckle before yielding. Real columns in pure compression will buckle before the critical load  $N_{cr}$  is reached due to for instance the load introduction not being perfectly applied to the member centroid, imperfections in the straightness of the column and/or material defects [41].

Steel:

The design resistance against flexural buckling due to pure compression is in EC3, part 1-1 [29] derived by a set of algebraic expressions, eventually finding a reduction factor  $\chi$  to account for the reduced axial resistance due to buckling. At the core of these expressions are empirically found member imperfection factors  $\alpha$  for different types of cross-sections and steel strengths.



The calculated buckling resistances to compressive force for the example column are (See Appendix A for the calculations):

For the major axis:  $N_{b,a,y,Rd} = 4198 \text{ kN}$

For the minor axis:  $N_{b,a,z,Rd} = 2605 \text{ kN}$

#### Composite:

The design flexural buckling resistance for composite sections in pure compression is treated by the same principle as that of steel sections, by being represented as a reduction factor  $\chi$  to the plastic axial cross-sectional resistance. The same intermediate factors and imperfection factors are used, and the buckling curves are selected pending section geometry and steel grade.

The relative slenderness in EC4, part 1-1 is calculated in the same manner as for EC3, using the ratio of the squash load characteristic resistance and the elastic buckling load:

$$\bar{\lambda} = \sqrt{N_{pl,Rk}/N_{cr}} \quad (3-24)$$

The characteristic plastic squash load resistance  $N_{pl,Rk}$  is here equivalent to the squash load resistance  $N_{pl,Rd}$  calculated in section 3.3.1 but without the partial factors. The long-term strength factor 0,85 is however still included for partially and fully encased cross-sections. An important notice in calculating the elastic buckling load  $N_{cr}$ , is to replace the flexural rigidity about the minor axis:  $E \cdot I_z$  from equation (3-22) with an effective flexural rigidity  $(EI)_{eff}$ :

$$N_{cr} = \frac{\pi^2 (EI)_{eff}}{L_{cr}^2} \quad (3-25)$$

The modified/effective expression for flexural rigidity  $(EI)_{eff}$ , is calculated to account for creep in the concrete, which over time reduces the modulus of elasticity, thus reducing the resistance towards buckling. To find the effective flexural rigidity of the cross-section, the moduli of elasticity and the second moments of area for bending about the minor axis for the constituent materials are calculated and added accordingly:

$$(EI)_{eff} = E_a I_{a,z} + E_s I_{s,z} + K_e E_{c,eff} I_{c,z} \quad (3-26)$$

Where  $K_e$  is a correction factor based on test results and recommended to be set at 0,6 [25]. The creep is calculated in accordance to EC2, part 1-1, Annex B [15] and expressed as a creep coefficient  $\phi_t$ , which for the example column is calculated to

$$\phi_t = 2,4 \text{ (See Appendix B for the calculations)}$$

For a concrete filled CFRT or CFT section a topic with no clear answer was found regarding determination of the creep coefficient. The EC2 rules require a value “u” which equals the concrete section perimeter exposed to air. Arguably, the steel section here shelters the concrete from drying to the air which should have an effect on the final creep value.

In the approach taken by the A3C software [42] for a CFT section with an internal H-steel profile, (see also section 4.1.1) the notional member size  $h_0$  is not calculated from the concrete perimeter, but rather set to the maximum available value in the figure 3.1 of EC2, part 1-1 [15] which is 1600mm. This is also the method which is used in the calculations for this thesis. Dujmović, Androić and Lukačević [39] uses the perimeter of the steel section for determination of the notional member size as if the whole section is made of concrete. This is on the conservative side, since it results in a larger creep coefficient. Hanswille [43] also uses the steel section perimeter to determine the creep

coefficient, but then argues that the final creep coefficient can be multiplied by a reduction factor 0,25 to account for the sheltering effect.

Using the creep coefficient, an effective modulus of elasticity of the concrete can be determined as a reduction of the elastic secant modulus value  $E_{cm}$ :

$$E_{c,eff} = E_{cm} \frac{1}{1 + \left(\frac{N_{G,Ed}}{N_{Ed}}\right)\phi_t} \quad (3-27)$$

The ratio of the permanent design axial force  $N_{G,Ed}$  to the total design axial force  $N_{Ed}$  compensates for the imposed loads not being applied permanently and therefore contributing less to the concrete creep. However, solving the problem with such a ratio can give counterintuitive results. As an example – consider a cross-section which is just above 2; the limit for relative slenderness according to equation (3-24). This cross-section is not allowed to be calculated according to the simplified EC4 rules. However, by increasing the size of the imposed design loads while keeping the permanent design load constant the ratio is reduced and the  $E_{c,eff}$  value is increased, thus giving a lower relative slenderness, possibly below 2. Another counterintuitive result is that the calculated effect of creep would be larger for a cross-section with only a small permanent design load than for a cross-section with 50/50% distribution of large permanent and imposed design loads. The ratio is set to 1 for the worked example in order to avoid a dependency of the magnitude of design loads for the creep evaluation. This is the ratio which gives the lowest elastic modulus  $E_{c,eff}$ .

The characteristic plastic resistance to compression and the elastic buckling load for the minor axis are calculated in Appendix B to equal:

$$N_{pl,Rk} = 9207 \text{ kN}$$

$$N_{cr} = 8836 \text{ kN}$$

Checking versus the EC4, part 1-1[3] criteria for maximum relative slenderness:

$$\bar{\lambda} = \sqrt{N_{pl,Rk}/N_{cr,z}} = \sqrt{9207/8836} = 1,021 < 2 \text{ (ok!)}$$

The calculated buckling resistances to compressive force are (See Appendix B for calculations):

$$\text{For the major axis: } N_{b,y,Rd} = 5971 \text{ kN}$$

$$\text{For the minor axis: } N_{b,z,Rd} = 4063 \text{ kN}$$

#### Comparison of resistance:

The design buckling resistance due to axial load only for the composite and steel columns can be compared directly by using a ratio:

For flexural buckling about the minor axis:

$$\frac{N_{b,z,Rd}}{N_{b,a,z,Rd}} = \frac{4063}{2605} = 1,56 \quad (3-28)$$

For buckling about the major axis (note that the minor axis would have to be laterally restrained and/or have different support conditions in order for the member to experience this buckling mode).

$$\frac{N_{b,y,Rd}}{N_{b,a,y,Rd}} = \frac{5971}{4198} = 1,42 \quad (3-29)$$

### 3.3.6 Buckling resistance of column towards compression + bending about major axis

#### General:

When there in addition to axial force is a bending moment about the minor axis, the member is still expected to buckle in flexural mode, but for a lower compressive force than when compared to the case of compression only due to the extra load eccentricity occurring from deflections of the bending moment.

With a bending moment about the major axis, one side of the column will experience compressive stress while the other will have at least some tensile stress. Thus instability will occur earlier on the pure compressive side than the other side. For an I or H steel member (open cross-section) the flanges on the more compressive side may start to twist due to instability, while the flanges on the less compressive side are still stable. This causes an unsymmetrical profile and the member may buckle in a combined flexural and torsional mode. This mode is usually called lateral torsional buckling (LTB) and occurs at lower levels of compressive load than flexural buckling.

For a closed steel cross-section such as a rectangular hollow section, the steel in the compressive side is supported at both ends and therefore has a much higher torsional stiffness, which counters the effect of LTB. Such members will usually buckle in flexural mode also for bending about the major axis. Similarly, in a composite FEC or PEC cross-section, the concrete will add torsional stiffness to the flanges and thus LTB is not relevant.

The effect of lateral torsional buckling depends on the shape of the bending moment diagram. A member which is in pure bending with a bending moment  $M_{Ed}$  throughout the whole member length is more prone to LTB than for instance a member subjected to a concentrated load in the middle. For the purpose of this comparison, these two different elementary loading scenarios are established. See also Figure 3-9.

{A}: Equal and opposite end moments  $M$  (pure bending) about the major axis:

{B}: Transverse point load  $P$  at the middle column length, applied in line with the web at the top of the flanges:

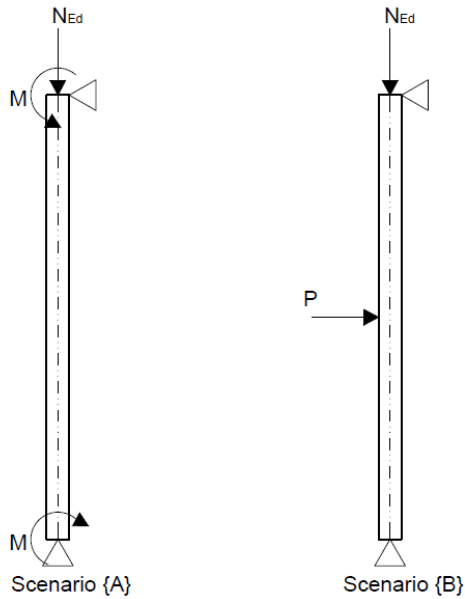


Figure 3-9: Load scenarios for buckling due to combined axial force and uniaxial bending.

### Steel:

Calculating the member resistance to buckling due to combined compression + bending about the major axis in accordance to EC3, part 1-1 [29] is relatively complicated and includes lengthy calculations of the critical moment and interaction factors to determine the potential influence of LTB. In order to determine whether LTB is a possible buckling mode for the member and to find the LTB reduction factor  $\chi_{LT}$  one first has to calculate the elastic critical moment  $M_{Cr}$ , which is the bending moment at which the cross-section of an ideal member would buckle (analogue to the critical load,  $N_{Cr}$ ). There are many available methods to calculate  $M_{Cr}$ , ranging from relatively simple analytical expressions to element methods that require computer software.

An analytical method which is published as a guideline on the official EC web page [44] is given below:

$$M_{cr} = C_1 \frac{\pi^2 EI_z}{(kL)^2} \sqrt{\left(\frac{k}{k_w}\right)^2 \frac{I_w}{I_z} + \frac{(kL)^2 GI_t}{\pi^2 EI_z} + (C_2 z_g)^2} - C_2 z_g \quad (3-30)$$

Where:

$C_1$  &  $C_2$  are BMD dependant coefficients

$k$  is the effective length factor of buckling length divided by actual length ( $L_{cr}/L$ )

$k_w$  is an effective length factor related to warping, set to 1 unless warping fixity is achieved

$I_z$  is the second moment of area for bending about the minor axis

$I_w$  is the warping constant

$I_t$  is the torsion constant

$E$  is the elastic modulus

$G$  is the shear modulus

$z_g$  is the distance between the load application and the shear centre

The factors  $C_1$  and  $C_2$  are given by the EC guideline [44] for the cases {A} and {B}.

$$\begin{cases} C_{1,\{A\}} = 1 \\ C_{2,\{A\}} = 0 \end{cases}$$

$$\begin{cases} C_{1,\{B\}} = 1,348 \\ C_{2,\{B\}} = 0,630 \end{cases}$$

The critical moments for case {A} and {B} are determined in Appendix A.

EC3, part 1-1 [29] have two criteria shown in equations (3-31) and (3-32) which both must be met for uniaxial bending + compression buckling resistance, here given in a reduced form due to lack of design bending moment about the minor axis. Hidden in the underlying equations are member imperfections (within  $\chi_y$ ,  $\chi_z$  and  $\chi_{LT}$ ) and moment amplification due to second order effects of the BMD (within  $k_{yy}$  and  $k_{zy}$ ):

$$\frac{N_{Ed}\gamma_{M1}}{\chi_y N_{Rk}} + \frac{k_{yy} M_{y,Ed}\gamma_{M1}}{\chi_{LT} M_{y,Rk}} \leq 1 \quad (3-31)$$

$$\frac{N_{Ed}\gamma_{M1}}{\chi_z N_{Rk}} + \frac{k_{zy} M_{y,Ed}\gamma_{M1}}{\chi_{LT} M_{y,Rk}} \leq 1 \quad (3-32)$$

For the determination of the interaction factors  $k_{yy}$  and  $k_{zy}$  required for uniaxial bending about the major axis, the Annex B of EC3, part 1-1 is used. For hand calculations, this is a simpler approach than following the rules given by the Annex A [10]. The relative slenderness of the member for LTB are above 0,4 for both load cases, thus LTB may occur in both of them, which is considered when calculating the interaction factors.

As can be seen, two design load input variables  $N_{Ed}$  and  $M_{y,Ed}$  are required. The calculation is therefore performed in an MS Excel spreadsheet and presented similarly to the MN interaction diagram in section 3.3.2, by showing the maximum allowable bending moment  $M_{N,b,a,y,Rd}$  for a certain force  $N_{Ed}$ . The resulting MN diagram for buckling of the steel member due to combined axial load and uniaxial bending is shown in Figure 3-11.

#### Composite:

The issue of buckling during uni- or bi-axial bending in the presence of axial force is treated in a similar way for a composite member as for a steel member. Shortly explained, in EC4, part 1-1 [3] the design moments from a first order analysis of the member are magnified by a factor  $k$  which is derived from the BMD and the buckling strength of the member. This factor correlates to the interaction factors  $k_{ij}$  used for the steel sections, but since lateral torsional buckling can be excluded, the calculation of  $k$  is much simpler.

A new, reduced effective flexural rigidity (here referring to the one calculated earlier in section 3.3.5), is calculated for the minor axis:

$$(EI)_{eff,II,z} = 0,9(E_a I_{a,z} + E_s I_{s,z} + 0,5E_{c,eff} I_{c,z}) \quad (3-33)$$

Using this value, a reduced critical buckling load  $N_{Cr,eff}$  may be determined:

$$N_{cr,eff} = \frac{\pi^2(EI)_{eff,II,z}}{L_{cr}^2} \quad (3-34)$$

The design moment found from the first order member analysis  $M_{Ed,1}$  is amplified by a modification factor  $k$ , which is calculated to consider the shape of the BMD by using a factor  $\beta$  given by the EC4:

$$k = \frac{\beta}{1 - \frac{N_{Ed}}{N_{cr,eff}}} \geq 1 \quad (3-35)$$

Here, Johnson [25] argues that having a minimum required value of  $k = 1$  is over-conservative if also the member imperfection is calculated for. In this worked example, it is not an issue. Since  $\beta$  is larger or equal to 1 for both the {A} and {B} cases,  $k$  will be larger or equal to 1 anyways.

An initial member imperfection should also be accounted for, which also is amplified by a  $k$ -value calculated from equation (3-35) using  $\beta = 1$ . Unless given otherwise, the member imperfection may be taken from EC4, part 1-1 [3]. For an FEC section, it is then equal to  $L/200$  for bending about the major axis and  $L/150$  for bending about the minor axis. For a nominally pinned column, this gives rise to a parabola-shaped BMD with the maximum design moment value  $M_{imp}$  in the middle of the member, equalling:

$$M_{imp} = N_{Ed} * \frac{L}{200} \text{ (major axis)} \quad (3-36)$$

$$M_{imp} = N_{Ed} * \frac{L}{150} \text{ (minor axis)} \quad (3-37)$$

The member imperfection is only applied onto the axis for which it is most critical (which is equivalent to the calculation of the steel section for which two verifications are made, one using the  $\chi_y$  and one with the  $\chi_z$  buckling reduction factor). If it is not obvious which axis is the most critical, a 2<sup>nd</sup> order member verification must be done for the two cases of either  $M_{Ed,imp}$  about the major or about the minor axis to determine the most adverse case. Since the design moment is largest in the middle for both the second order BMD and the BMD resulting from member imperfection; these moments can be added to find the 2<sup>nd</sup> order design moment value  $M_{Ed,2}$ :

$$M_{Ed,2} = M_{Ed,1} * k + M_{imp} * \frac{1}{1 - \frac{N_{Ed}}{N_{cr,eff}}} \quad (3-38)$$

Equation (3-38) can be rearranged, here for bending about the major axis:

$$M_{Ed,2} = \left( M_{Ed,1} * \beta + N_{Ed} * \frac{L}{200} \right) \left( \frac{1}{1 - \frac{N_{Ed}}{N_{cr,eff}}} \right) \quad (3-39)$$

Thereafter, the calculated  $M_{Ed,2}$  can be combined with  $N_{Ed}$  and verified by the same MN interaction diagrams similarly to section 3.3.2.

A typical representation of the first and second order bending moment diagrams for columns in double and single curvature bending is shown in Figure 3-10. The BMD for the second order member verification can regardless of the shape of the first order BMD be envisioned as a parabola, with the moment  $k * M_{Ed,1}$  in the middle and equal end moments of  $\beta * M_{Ed,1}$  [25]. Due to the higher  $k$ -factor, the column in single curvature bending gets a higher 2<sup>nd</sup> order design moment. This is correlating to the single curvature bending giving a larger column deflection.

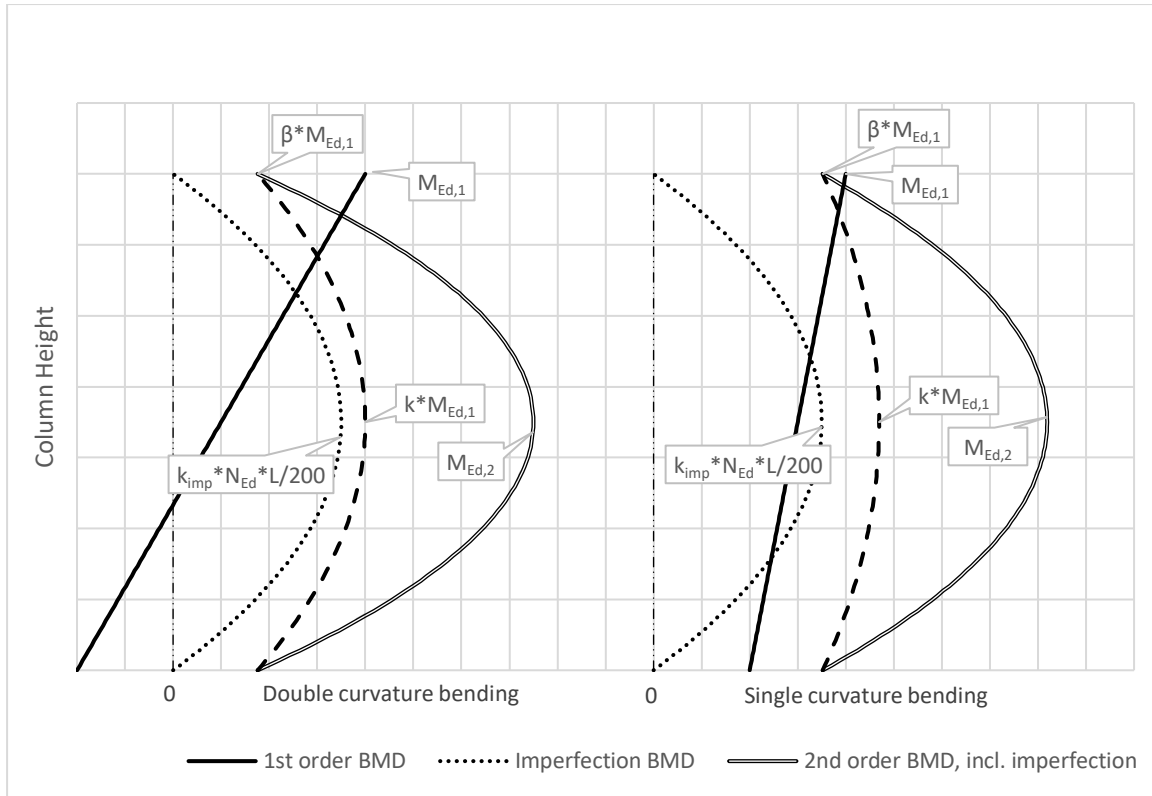


Figure 3-10: Typical 1st and 2nd order BMD for double/single curvature bending. Visually inspired by [25].

The method for calculation of members in compression + bending is evidently significantly different to that of members in pure compression as described in section 3.3.5. Perhaps most remarkable is the usage of the material dependent factor  $\alpha_M$  which is described in section 3.3.2 and now comes in play due to the bending moment. As a consequence, a S355 steel grade column in pure compression uses the same buckling curve as one of S420 steel. However, with even a minute design moment present, the calculations must consider that S355/S420 has an  $\alpha_M$  factor of 0,9 / 0,8 respectively.

#### Comparison of resistance:

The comparison may be presented as an MN interaction diagram, similar to what is used in section 3.3.2. For the steel column the two EC3 criteria, equations (3-31) and (3-32) are rewritten so that the maximum  $M_{y,Ed}$  allowed for a certain  $N_{Ed}$  is found. This design resistance, is here called  $M_{b,a,y,Rd}$ .

The rewritten function is:

$$M_{b,a,y,Rd} = \min \left[ \frac{\chi_{LT} M_{y,Rk}}{k_{yy}} \left( \frac{1}{\gamma_{M1}} - \frac{N_{Ed}}{\chi_y N_{Rk}} \right); \frac{\chi_{LT} M_{y,Rk}}{k_{zy}} \left( \frac{1}{\gamma_{M1}} - \frac{N_{Ed}}{\chi_z N_{Rk}} \right) \right] \quad (3-40)$$

For the composite column, the MN interaction diagram is plotted with the moment resistance values achieved from first order analysis ( $M_{Ed,1}$ ) since that is equivalent to the values used for the steel MN diagram.

This is done by equalling  $M_{Ed,2}$  to the reduced y-axis plastic moment resistances  $M_{N,y,Rd}$  in combined compression+bending shown in Figure 3-7.  $M_{Ed,1}$  is thereafter isolated from equation (3-39):

$$M_{b,y,Rd} = M_{Ed,1} = \frac{M_{N,y,Rd} \left( 1 - \frac{N_{Ed}}{N_{Cr,eff}} \right) - N_{Ed} * \frac{L}{200}}{\beta} \quad (3-41)$$

The design moment resistances for the steel and composite sections  $M_{N,b,a,Rd}$  and  $M_{N,b,Rd}$  are calculated and plotted on an M-N diagram for 100 evenly spaced axial force values of  $N$  between 0 and the flexural buckling resistances about the minor axis  $N_{b,z,a,Rd}$  and  $N_{b,z,Rd}$  using an MS Excel spreadsheet, see Figure 3-11.

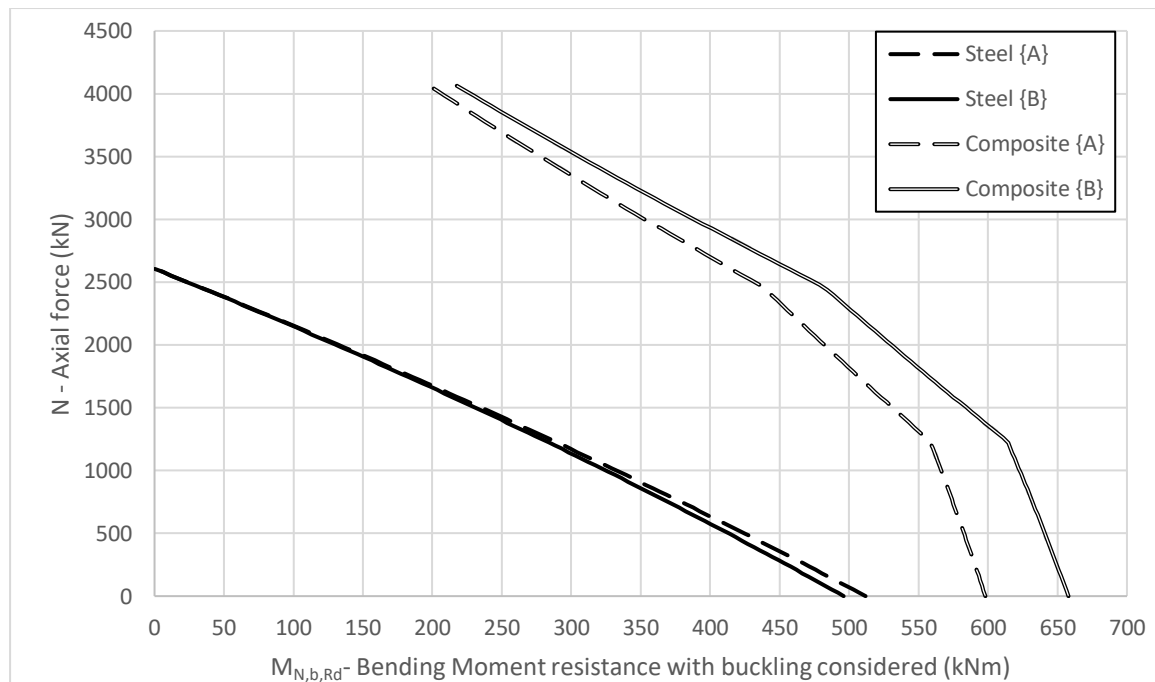


Figure 3-11: Reduced design moment resistance about the major axis due to buckling and axial force, comparison steel and FEC HE-300B columns.

#### Comments:

- The composite column axial force reach a maximum  $N_{Ed}$  of 4063kN, since the member will experience flexural buckling about the minor axis at that level, as shown in section 3.3.5.
- The maximum allowable bending moment for the composite column now occurs at zero axial force, in difference to the results when buckling is not considered (see Figure 3-7). This shows that the additional cross-sectional moment resistance gained between point B and D (refer Figure 3-6) is not necessarily representative for the column resistance when stability also is considered.
- It is noteworthy that the design moment resistance for case {A} is the clearly lowest for the composite column, while it is highest (slightly) for the steel column.

#### 3.3.7 Global structural behaviour

The sections 3.3.1 to 3.3.6 describe the resistances relevant to an isolated column. In order to arrive at the loads which are used for these member resistance checks, an analysis of the global structure must be made, where the relevant loads (e.g. structural, environmental, accidental) are applied onto the structure.

If the resulting member forces and moments from a structural analysis are taken as final results and the deformations of the structural members are ignored, the analysis is said to be linear or first order. For low levels of horizontal deformation a linear analysis is accepted by the Eurocodes. Large values of horizontal deformation will however result in significant extra moments onto the columns due to eccentric loading. In these cases the second order/non-linear effects must be taken into account. Second order analysis may be done iteratively by doing a first order analysis, retrieve the member



deformations, redo the analysis with these deformations as a starting condition and repeat until either the structure reaches an equilibrium position or collapses. Such analysis must typically be made by advanced computer software due to the amount of calculations involved. If such a method is used, there is no need for a further stability check of the column.

Alternatively, allowing for simpler calculations the methods described under section 3.3.6 can be utilized, where the member bending moments are amplified by a factor depending on the size and shape of the first order BMD. This is as demonstrated suitable for hand calculations or by simple computer spreadsheets. The amplified moment methods described in section 3.3.6 include a bow imperfection, in which imperfections to the column straightness, material quality and/or loading concentricity are accounted for (See Figure 3-10 for an example). In a global structure there may also be a sway imperfection where the whole building frame have a slight initial tilt. If the horizontal deflections in the building when lateral design loads such as for instance wind are applied are significant, a sway imperfection should also be included in the analysis.

Another way of classifying global structural analysis is whether it is elastic or plastic. An elastic analysis do not consider moment redistribution, so when a column reaches the ULS moment resistance it is a failure criteria. In a plastic analysis, if the ULS moment resistance is reached somewhere on a column it is assumed that a plastic hinge is formed at that point. If the structure or column is statically determinate, this will lead to a global or local structural collapse. If it however is statically indeterminate, it can potentially take more load until a sufficient amount of plastic hinges have formed to lead to local or global collapse. Thus a plastic analysis of a statically determinate building will lead to the same results as an elastic analysis, while it may provide higher structural resistance values for a statically indeterminate structure.

#### Steel:

Eurocode 3, part 1-1 [29] provides guidance on how to do a global structural analysis. A frame elastic critical factor  $\alpha_{cr}$  is determined either through plastic or elastic first order analysis. For plane rectangular frames where axial compression in the beams can be ignored,  $\alpha_{cr}$  can be determined through equation (3-42):

$$\alpha_{cr} = \frac{H_{Ed} * h}{V_{Ed} * \delta_{H,Ed}} \quad (3-42)$$

The value of  $\alpha_{cr}$  determines whether second order effects can be [10]:

- Ignored ( $\alpha_{cr} \geq 10$ )
- Dealt with by using the approximate amplified moments method given in section 3.3.6 ( $10 > \alpha_{cr} \geq 3$ )
- Or whether a more exact method/iterative approach must be taken, typically numerical analysis by computer software. Note that the above threshold values are only valid for elastic analysis.

In equation (3-42)  $H_{Ed}$  and  $V_{Ed}$  are the horizontal and vertical support reactions of the column,  $h$  is the height of the column and  $\delta_{H,Ed}$  is the calculated horizontal deflection at the top of the storey relative to the bottom. For this check, the equivalent horizontal force (EHF) of sway imperfection at the column base and top (in opposite directions) must be added in the analysis. This equals:

$$EHF_{sway} = N_{Ed} * \phi \quad (3-43)$$

Where  $N_{Ed}$  is the design axial load on the column and  $\phi$  is the sway imperfection angle which is calculated based on the height of the columns and the number of columns in a story.

The local member bow imperfections must be also included in the global analysis if second order analysis is required and if the following is true for the relative slenderness  $\bar{\lambda}$ :

$$\bar{\lambda} > 0,5 * \sqrt{\frac{N_{pl,Rk}}{N_{Ed}}} \quad (3-44)$$

Where  $N_{pl,Rk}$  is the characteristic plastic resistance equal to  $A * f_y$  for a steel section (refer to section 3.3.5) and  $N_{Ed}$  is the design force. For a bow imperfection of length  $e$ , this is done by defining an equivalent horizontal force  $EHF_{imp}$  as a transverse distributed load onto the column [10]:

$$EHF_{imp} = 8 \frac{N_{Ed} e}{L^2} \quad (3-45)$$

#### Composite:

The requirements for a global analysis of a composite structure according to EC4, part 1-1 [3] largely follows that of a steel structure, as long as the structure mostly contains composite or steel members. While a plastic global analysis is allowed it is not commonly utilized and elastic analysis is the most common method [25]. The frame elastic critical factor  $\alpha_{cr}$  cannot be calculated by simple means for complicated frame geometries or sway type frames. Based on searches for analysing tools on the internet, there are seemingly very few available tools for calculation of second order effects of frames with composite columns when compared to those with pure steel elements.

### 3.4 Fire loads

#### 3.4.1 Structural behaviour of a column subjected to fire

A fire may affect a single column and/or the global structure negatively in multiple ways. The specific material behaviour of steel and concrete in a fire is discussed in section 2.3. The following behaviour can be highlighted [12]:

- Reduced strength and stiffness:  
The material mechanical properties, including the strengths and modulus of elasticity are temperature dependant. Both the yield strength and the modulus of elasticity of a structural member in either steel or composite steel-concrete material are reduced when heated. Creep is also developing more rapidly in increased temperatures.
- Temperature induced strains/stresses:  
Steel and composite members which are heated will try to expand. If this is allowed, a beam may elongate and force the supporting columns to tilt outwards at the top, which results in eccentric loading, larger second order moments and possibly a buckling failure of a column. If this expansion is restricted, the beam will experience increased compressive stresses and may yield or buckle due to this.
- Heat conduction:  
Heat from a member directly exposed to fire may transfer to other members and/or finishes due to heat conduction. This can lead to temperature effects on adjoining members not exposed to the fire and it may also cause fire spread due to a heating of adjoining combustible materials
- Time-dependent degradation:

Structural members made of combustible material (e.g. timber) may have their cross-sectional area reduced by a material combustion. This will in addition add to the fire loads and promote fire spread.

Materials containing chemically bound water (e.g. concrete or gypsum) are fire resistant, but the water will gradually dehydrate and evaporate in a fire scenario. This can eventually cause spalling, loss of cross-sectional area and exposure of sheltered internal elements such as steel reinforcement.

Due to the reduction in both the material yield strength and stiffness, a fire exposed column will both yield and buckle for lower loads in the elevated temperature than it will in ambient temperature.

### 3.4.2 The Eurocode approach to fire design

#### General:

The purpose of a building during a fire scenario differs from that in a normal condition. Primarily, the structure must allow safe evacuation of people, allow safe entry and egress for rescue personnel and not put adjacent buildings in danger [45]. The requirements of a structure during a fire are given by EC1, part 1-2 [46]. In addition, criteria may be added as a result of fire risk assessment.

The fire resistance of a structure is detailed by giving the structural members functional ratings for fire loadbearing resistance (R), integrity against smoke and fire gasses (E) and/or thermal insulation (I). The loadbearing criteria is what will be discussed in this thesis. The functional rating is further given a minimum resistance duration in minutes. E.g. R120 means the member can provide loadbearing in the dimensioning fire scenario for at least 120 minutes. The Eurocodes do not detail which loadbearing resistance is required for a certain structural member, which is highly dependent on the consequences of a fire and stated at a national level [45]. In Norway, the requirements regarding load-bearing resistance are effectively given by the building regulations [47]. In short, the fire consequences of a building are categorized into a fire class between 1 and 4, where buildings in fire class 4 have the highest fire consequences. The fire class 1 and 2 requires structural loadbearing through a listed minimum fire duration, while fire class 3 and 4 are required to keep their loadbearing resistance for the full fire duration.

For buildings in fire class 1 to 3, there are pre-accepted values for loadbearing resistance. As an example, the main structural system of a fire class 1,2 and 3 building has to fulfil R30,R60 and R90 criteria respectively for loadbearing fire resistance in order to be pre-accepted (although there are exceptions to these requirements). Alternatively, the loadbearing fire resistance can be determined through fire analysis. The required loadbearing resistance for a fire class 4 building must always be determined through dedicated fire analysis.

The fire scenario may be modelled by different methods [48,49], including:

- Standardized time-temperature curves, directly given by the EC1, part 1-2 [46]
- Simple computer models such as the two-zone models, where an enclosure is divided into a hot layer and a cold layer and calculations are based on mass and energy conservation between these layers and the external environment.
- Advanced computer models using CFD simulations of the building volume. This type of analysis is common for complicated structural layouts [45].

## Steel:

The rules for fire design of structural steel columns are given in EC3, part 1-2 [13]. Three different methods are given to verify the fire resistance of a steel structural member.

- Simple calculations: Rules given directly by the EC3. The calculations can be in either load resistance, temperature or time domain [50].
  - o The load resistance calculations verifies that the member has sufficient load bearing resistance at the duration required for fire resistance (e.g. R30 = 30 minutes).
  - o The temperature calculations determine at which temperature the member will fail (critical temperature) and verifies that the member temperature is below that temperature at the required fire duration.
  - o The time calculations determines which time it takes for the steel cross-section to reach the critical temperature and verifies that the time is larger than the required duration.

Regardless of what calculation domain is chosen, the underlying equations are essentially the same. The member resistances are determined by using rules mimicking those for normal temperature ULS verification, section 3.3 but with additional parameters to account for the reduced strength and stiffness at elevated temperature. The steel temperature is determined through heat transfer equations based on the surrounding gas temperatures.

- Advanced: Only principal guidelines and requirements for advanced analysis are given by the EC3 standard. A structural analysis for fire scenarios using the advanced method is in practice using numerical calculations by computer software. It is important that the advanced model is validated with fire tests.
- Testing: Subjecting structural elements to a physical fire test according to approved methods.

## Composite:

The rules for fire design of composite columns are given in EC4, part 1-2 [4] and the same three principal types of methods as given by EC3 (see above) are allowed. The simplified calculation methods are however very different in detail than what is given by EC3. All types of composite column cross-sections which qualifies for the simplified calculation method in EC4, part 1-1 [3] (see section 3.3) are given tabulated values based on minimum cross-sectional dimensions, reinforcement details and for PEC, CFT and CFRT cross-sections the fire design load level.

For PEC, CFT and CFRT columns there are also simple calculation rules given by annexes G and H of EC4, part 1-2 [4]. In short, these calculation rules determine:

- the average temperatures in the steel section, the concrete and the reinforcement for a fire duration of 30,60,90 and 120 minutes.
- the reduced material properties (yield strength and flexural rigidity) in these temperatures
- the total squash load resistance and the axial load buckling resistance, from a summation of the resistances of the parts.

A worked example of Annex G calculations for a PEC column is made for the case study in this thesis and it is provided in Appendix K.

### 3.4.3 Global structural response in fire

A global structural response evaluation for a fire scenario, including for instance elongation of the members due to thermal expansion is not possible to do with the simplified rules provided by the EC.

Advanced structural calculation methods must therefore be employed if such effects are expected to govern the structural fire behaviour (this is not covered by this thesis).

A global structural topic which is mentioned in the simple fire calculations regards altered buckling lengths in a fire scenario. Larger buildings often include multiple fire partitions, which are meant to contain the fire for a certain amount of time, usually with requirements for both load-bearing (R), integrity (E) and thermal insulation (I). Thus, a fire acting on a column on the second story may not affect the same column on the first and third stories. This phenomena is captured by both EC3, part 1-2 [13] and EC4, part 1-2 [4] which includes rules for the buckling lengths in a fire situation, valid for braced rectangular frames with continuous columns, where fire partitions are included in the floors. A fire exposed intermediate continuous column of length L which normally also have a buckling length of L will lose so much stiffness in the middle section relative to the unaffected/cold column sections above and below so that it effectively will behave as fixed in the ends (buckling length = 0,5L). For a column in the top storey, there is not sufficient stiffness in the top joint for it to be considered fixed in a fire situation. Thus the top storey column buckling length equals a fixed-pinned column (buckling length = 0,7L).

No guidance for bottom storey columns are given in EC3, but arguably the above logic means that the top joint can be considered fixed in a fire situation, while the bottom joint depends on the rotational stiffness of the column base, meaning a buckling length between 0,5-0,7. In EC4, this is explicitly stated in the rules.

#### 3.4.4 Member fire resistance

##### General:

The fire load bearing resistances of the worked example steel and composite columns are calculated according EC3, part 1-2 [13] and EC4, part 1-2 [4]. The fire scenario is based on the standard ISO 834 fire curve which is visualized in Figure 3-12 where the gas temperature  $\theta_g$  in degrees Celsius at time t in minutes is given as:

$$\theta_g = 20 + 345 * \log(8t + 1) \quad (3-46)$$

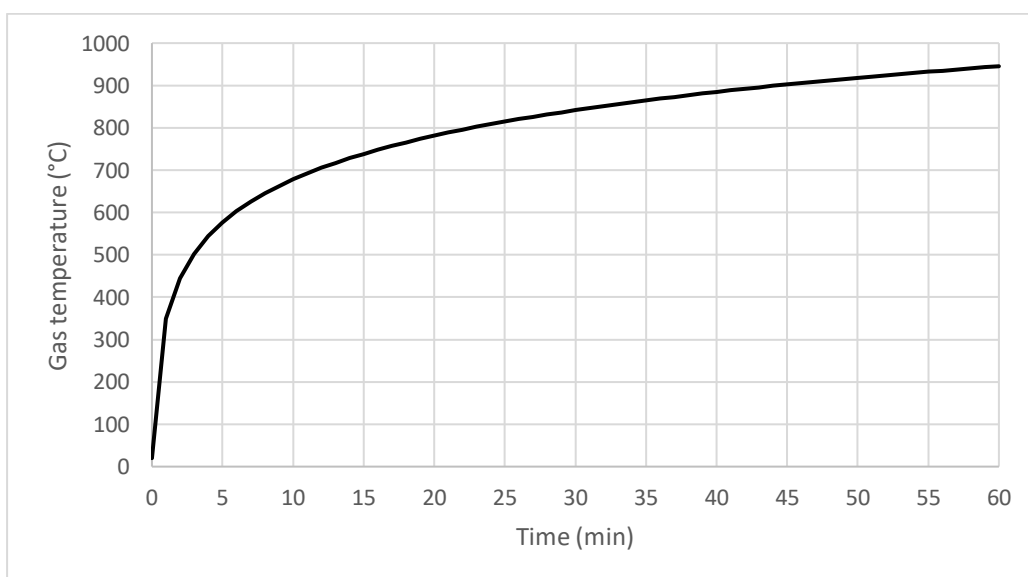


Figure 3-12: ISO 834 fire curve

### Steel:

The fire resistance of an unprotected steel column is calculated in accordance to a procedure shown by Vila Real [50]. For the sake of demonstration, it will be done for only one case, of a column in pure compression with a design load of  $N_{Ed} = 2000$  kN, which is reduced by a factor  $\eta_{fi}$  for the fire design load set to 0,65 as the simplified recommendation by EC3, part 1-2 [13].

The critical steel temperature  $\theta_{a,cr}$  is the temperature at which the column is no longer able to provide the required load bearing resistance due to the associated reduction in steel yield strength. For a column in axial compression, it is calculated by first determining temperature dependent material and buckling parameters at ambient temperature and arrive at a fire utilization degree  $\mu_0$  which through a logarithmic relation can provide a value for  $\theta_{a,cr}$ . The calculation is iterated, with the previously calculated  $\theta_{a,cr}$  as the temperature input for the calculations until the resulting  $\theta_{a,cr}$  no longer changes. For the worked example, the critical steel temperature is calculated to 547°C. The time for the steel column to reach this temperature is calculated using radiative and convective heat transfer equations using the gas temperature from the ISO 834 curve to determine the heat transfer into the member. The calculated fire resistance duration is 17 minutes. Note that the above description does not describe all aspects of calculating the steel fire resistance duration since steel columns is not the main focus of this thesis. A full calculation of the unprotected fire resistance duration of the worked example, with limited explanations is given in Appendix C.

In order to utilize structural steel columns in a fire scenario in practice, insulating passive fire protection is typically required. Therefore the thickness and efficiency of the added passive fire protection is more relevant for fire design than a re-sizing of the steel member. Passive fire protection for steel members may come in the shape of:

- Insulating boards
- Intumescent paint
- Spray on fire resistant material (e.g. fibre reinforced cement)

For the insulating boards and the spray-on material, the thickness may be calculated according EC3, part 1-2 [4] if the specific heat,  $C_p$  and thermal conductivity  $\lambda_p$  of the fire protection material are known. Alternatively, they may be directly provided by the manufacturer of these products.

The intumescent paint expands and chars when exposed to heat, causing an insulating layer. The expanding function means the thickness of the passive fire protection in a normal state can be significantly reduced. However, care must be taken to ensure that sufficient space is required for expansion of the paint in a fire scenario (for instance when placing the column within a wall). The dimensioning thickness calculations of intumescent paints are developed by the paint manufacturers.

### Composite:

The EC4, part 1-2 [4] tabulated values for FEC columns are based only on the concrete cover and longitudinal reinforcement positions. For PEC and CFRT/CFT cross-sections the tabulated values additionally depends on the fire design load level  $\eta_{fi,t}$ , which is the maximum ratio of the design fire action  $E_{fi,d}$ , to the normal temperature resistance  $R_d$ . If the actions vary over time (for instance when thermal elongation of building elements is considered) the time-dependent value  $E_{fi,d,t}$  should be used instead.

$$\eta_{fi,t} = \frac{E_{fi,d}}{R_d} \quad (3-47)$$

Even though specific partial material factors are provided in EC4 for steel, concrete and reinforcement for a fire situation,  $R_d$  is stated as the “normal temperature resistance”. Thus the normal temperature partial factors should be used for calculating the fire design load level. The fire material partial factors are still relevant if other methods than the tabulated values are employed.

The  $R_d$  value needs to be calculated using a buckling length which is double the buckling length assumed in a fire scenario. Nominally pinned columns in a fire may therefore result in a large increase of required resistance, since the buckling length for calculation of the  $R_d$  value then must equal 2 times the column height. There are some restrictions for the tabulated values, namely:

- The columns must be located within a braced frame
- The length of the columns cannot exceed the smallest side length of the column cross-section (or diameter for CFT members) multiplied by 30.
- Minimum requirements for the reinforcement ratio and cover.

As an alternative to the tabulated values, annexes with calculation rules are provided for the determination of the fire resistance of PEC, CFT and CFRT cross-sections. These calculation rules have additional limitations, including maximum buckling length, concrete grade and in the case of PEC cross-sections they are valid for bending about the minor axis only, although worked examples by Vassart et al. [45] shows how the method can be used for bending about the major axis. These annexes have however been rejected by multiple nationalities and are likely subject for revision in the next EC4, part 1-2 revision according to Dujmović [39]. In Norway, the status of these calculation rules is “informative” meaning that they may be used.

Due to the multiple limitations of the simple calculation rules (both tabulated and annex values), composite columns may in practical applications often have to be calculated by advanced calculation models. This is far more complex, involving 2 dimensional heat transfer and preferably also simulating the spalling of concrete. Thus the advanced calculations requires the use of dedicated or general purpose thermal and structural FEM software.

Rodrigues, Correria and Pires [51] tested different FEC cross-sections with HE-A profiles, using different degrees of end restraint and load levels for their behaviour in a fire scenario. The critical times (the time until one or more design actions exceeds their resistance) were determined and compared to the fire resistance values given by EC4. The fire tests showed an 83% to 230% improvement in duration when compared to the tabulated values. They concluded that the EC4 tabulated values underestimates the fire resistance of fully encased composite columns and that they should be reviewed. Furthermore they suggest that the load level and support conditions have a significant effect on the resulting fire resistance.

Another fire test study by Mao and Kodur [52] also indicates that the EC4 tabulated values for FEC columns are conservative. During the tests, concrete spalling occurred for some specimen and this had a significant negative effect on the fire resistance due to heat exposure of the internal steel section.

The accuracy of the EC4, part 1-2 [4] for PEC columns were investigated by Fellouh et al. [53] who studied the columns for R30 to R120 fire resistance by using a general purpose FEM software. They concluded that the tabulated values are conservative, while there are situations in which the Annex G calculations are unsafe.

## Comparison of fire resistance

Due to the poor performance of unprotected steel in a fire scenario and due to the tabulated EC4 values which for an FEC cross-section does not consider the load scenario or support conditions, a criteria-by-criteria comparison for fire resistance similar to what is done for ULS verification in section 3.3 is not meaningful. A study of the required cross-sectional area to provide a certain load-bearing fire resistance is given in section 0, where the steel column is assumed to be covered in insulating fire protection boards.

## 3.5 Impact loads

### Impact loads:

Impacts loads are described in EC1, part 1-7 [54]. In its initial part, a risk management approach to impact design is suggested, both considering the consequence and the likelihood, which can be exemplified accordingly:

- A column which collapses from impact of a forklift, but with no resulting global structural collapse may be allowed due to the low consequence.
- An internal column in a supermarket does usually not have to be designed to handle a car collision due to low likelihood.

A vehicular impact load is a dynamic event in which the kinetic energy of a moving vehicle transfers to transient elastic and/or permanent plastic deformation of both the structure and the vehicle. For simplicity, EC1 provides static EHF for different collision scenarios. As an example, a car collision in a substructure parking garage has a static EHF of 50 kN.

Alternatively, a dynamic analysis may be done. The kinetic energy  $W_K$  of the vehicle equals:

$$W_K = 0,5mv^2 \quad (3-48)$$

Where  $m$  and  $v$  are the mass and velocity of the vehicle respectively.

The vehicle may be considered an elastic spring during impact, with a spring constant of  $k$ , a displacement of  $x$  and a potential energy  $W_p$  ultimately reaching:

$$W_p = 0,5kx^2 \quad (3-49)$$

Hooke's law describes the linear force-displacement relation for a spring, where  $F$  equals the force.

$$F = kx \rightarrow k = F/x \quad (3-50)$$

By conservation of energy, the following can be derived from equations (3-48) to (3-50) which is equivalent to the equation given by EC1:

$$W_K = W_p \rightarrow 0,5mv^2 = 0,5F^2/k \rightarrow F = v\sqrt{km} \quad (3-51)$$

EC1 provides the following statistical data for the involved parameters, (car collision in a parking garage):  $v = 10 \text{ km/h}$ ;  $k = 300 \text{ kN/m}$ ;  $m = 1500 \text{ kg}$ .

Thus, the maximum dynamic impact force  $F_{max}$  of a car collision in a parking garage, based on the EC1 statistical values equals:

$$F_{max} = \frac{10}{3,6} \sqrt{1500 * 300000} \text{ kN} = 58,9 \text{ kN} \quad (3-52)$$

This force is applied at  $h=0,5\text{m}$  above the road level and for an  $L=3\text{m}$  high nominally pinned column, this gives rise to a design moment (using no partial factor as this is an accidental load) equalling:



$$M_{Ed, coll} = \frac{F_{max} * h * (L - h)}{h} = \frac{58,9 * 0,5 * (3 - 0,5)}{3} kNm = 24,5 kNm \quad (3-53)$$

Neither the design impact moment  $M_{Ed, coll}$  or shear force ( $V_{Ed, coll}$  which equals  $F_{max}$ ) are comparatively large compared to typical structural loads and it is therefore not likely that a composite cross-section would be chosen over a steel cross-section to withstand them.

Steel profiles used for columns are typically made of relatively thin steel and can experience local plastic deformation in an impact, leading to an asymmetrical cross-section/loading and a reduced load bearing ability. No calculation method for this type of scenario is given in the Eurocodes, but it is fair to assume that such local damage can be significantly decreased with any composite cross-section, since the concrete part either shelters the steel section or restricts local deformation of the steel. Impact tests with a drop hammer applied transversely onto hollow and concrete filled tubular steel sections were made by Han, Hou, Zhao and Rasmussen[55]. While the hollow steel sections showed severe denting, the CFT specimen had nearly intact cross-sections, although they were permanently bent. The tests also showed that the CFT members had increased flexural resistance for a dynamic load than what they had under static loading. Furthermore, it was shown that the concrete strength did not have a large influence on the flexural resistance in an impact. As a remark, the tested members were not axially loaded during the test, so it is not possible to directly conclude the impact behaviour for a real column. The article concludes that CFT members have a good impact resistance.

A research project called COSIMB initiated by the European Commission research fund for coal and steel studied the impact and blast resistances (including post-impact fire loads) of composite columns and composite column-wall systems. The study was performed mainly in the context of resistance of buildings against terrorist attacks and the results are presented in a report by Hauke et al. [56]. A moving carriage of approximately 1450 kg (representing a car) was impacted transversely onto PEC sections and CFRT sections with internal H-sections at different speeds and thereafter the elastic and plastic deflections were measured. This study did not load the test specimen axially, primarily to not cause deflections from second order effects/buckling which would obscure the results.

Thereafter, transient element models were developed to describe the dynamic behaviour by using a two degree of freedom spring model with viscous damping, where the impacting carriage and the column were the two moving bodies. Axial loads were implemented in the model by using results from a static test on the columns. The model was used on a full scale building case study, where a composite wall-column system was used. The results showed that the building was well suited to withstand impact loads. No benchmark test on a building constructed by other means than composite elements was done, thus it is difficult to determine from the report whether the composite structure was significantly more effective in resisting the impact than a steel structure would have been.

### 3.6 Blast loads

Blast loads can come from many different sources and their impact on structures is different depending mainly on whether the blast pressure wave is sub-sonic (deflagration) or super-sonic (detonation). Most blasts resulting from ignited gas clouds are deflagrations, while blasts initiated by explosives typically are detonations [57].

Blasts may damage structural members in its sightline due to:

- Direct overpressure from the pressure wave. When the wave has passed, there will also be a period of under-pressure and a secondary pressure wave from air rushing back to fill voids.
- Drag forces from the pressure wave

- Flying debris

Structural members may also be affected due to transfer of stresses and deformations of adjoining members. An additional issue is that an explosion may damage the passive fire protection and subsequent fires may thereafter collapse the building.

Blast or explosion loads due to dust or gas explosions are described by EC1, part 1-7 [54], providing simple guidance for sizing ventilation panels and the equivalent static pressures on the structure resulting from gas explosions (given that adequate explosion venting is installed). Such venting areas are either directly open to the outside atmosphere or through specifically designed weak panels venting to the outside atmosphere. The largest static pressure to be applied on the structure for such a scenario is stated as  $p_{D,max} = 50 \text{ kPa}$ , which can be reduced by appropriate design of the explosion vent area. It should be noted that designing a structure to withstand this maximum pressure value is not common. At 7-15 kPa ordinary building panels will yield or blow out, while ordinary steel framed buildings may collapse starting at 20 kPa blast pressure [57]. Thus, for a room with a defined blast accidental load, it is very likely that the blast venting is designed to release at quite low pressures in order to avoid dimensioning the structure to withstand a 50kPa blast load. No guidance in the EC1, part 1-7 [54] is given for drag forces, which owing to the slender shape of columns may be more relevant for them than loads from the pressure wave.

No guidance regarding blast loads from explosives is given by the EC1 1-7. Traditionally, this has mostly been a topic for military structures but in recent history it has become a topic discussed also for ordinary buildings due to the risk of terrorist attacks. The COSIMB project [56] studied the resistance of composite structures against explosive loads, concluding that composite structures were efficient in resisting blast loads from explosives. An important remark was that columns as singular members may experience a temporary change of sign for the axial stress during a blast; from compressive to tensile (presumably due to displacement of the floor and ceiling). While steel columns as isolated members are stronger in tensile stress than in compressive due to the absence of instability effects, the same is not necessarily true for composite columns which have a reduced resistance to tensile stresses due to the concrete part. However, by connecting composite columns to composite shear walls they become restrained in the axial direction and therefore the tensile stress scenario can be ignored.

### 3.7 Seismic loads

The determination of seismic loads and calculations of structural resistance to seismic loads are described in EC8, part 1 [21] where one chapter is dedicated to design rules for steel/concrete composite members. For dissipative composite structures (where the structure dampens seismic action by dissipating seismic energy by plastic deformation) there are multiple design limitations in addition to those given by EC4 regarding for instance slenderness and longitudinal/transverse reinforcement placement, mostly for FEC and PEC columns.

A structure with composite columns together with reinforced concrete walls is able to dissipate a lot of seismically induced kinetic energy. This is quantified by such structures being able to reach high behaviour factors,  $q$ . The design seismic shear forces acting at the base of the building and subsequently the design actions experienced at higher levels are essentially linearly inversely proportional to  $q$ , meaning composite columns can provide a high resistance towards seismic loads.

That being said, seismic activity in Norway is low when compared to many other countries. According Rønnquist, Remseth and Lindholm [58], the typical Norwegian approach to seismic design is to assume a low ductility class, setting  $q$  to 1,5 (far beneath what is achievable by both steel and composite

structures). The national Norwegian annex to EC8 restricts the ductility class to being medium at most, meaning  $q$  is limited to 4. This behaviour factor is also achievable by steel structures and therefore there is seemingly little merit in using composite columns in Norway in order to withstand seismic loads.

## 4 Parametric studies of composite and steel columns.

In order to better understand the different behaviours of composite and steel columns, software-assisted parametric studies have been made. As the main purpose of this thesis is to evaluate whether composite structures may be utilized to a larger degree in Norwegian building projects, the selected cases have been developed together with Rambøll using relevant factors for the Norwegian construction industry.

The following topics are selected as study targets:

- Span maximizing, section 4.2:  
The maximum achievable span between two bottom columns located within a 4 storey rectangular plane frame is determined.
- Column depth reduction for a normal temperature and fire protected column, section 0.  
The minimum achievable column depth/cross-sectional side lengths for different fire load bearing resistances are determined based on a single column.
- Steel efficiency, section 4.4  
The achieved column resistance towards axial load and bending, per unit cross-sectional steel area is determined.
- Environmental foot-print, section 4.5  
The amount of CO<sub>2</sub> mass equivalents as well as the energy use involved in producing the required building materials for one meter of column length, when the columns are dimensioned as per the normal temperature case of section 0.

Within these comparisons, two different principal approaches have been taken and both have weaknesses which should be highlighted.

The first approach is to select a number of load cases and determine the minimum required cross-section to withstand the loads. This approach is taken for the column depth reduction and the environmental foot-print studies. An issue is that this approach may require many load scenarios in order to ensure statistical fairness. In this thesis, 15 load cases are considered. Since member sizes are available with 20mm steps for standard H-profiles up to HE-360 and with multiple configurations of diameter and thickness for CHS profiles, the statistical error is deemed small.

The second approach is to determine the maximum resistance of a certain cross-section, which is the approach taken for the two other studies. An issue of this approach is that it is not realistic in real construction to be able to “design the load”. Rather, a cross-section has to be selected to match a certain load (similar to the first approach) which usually leads to over-capacity of the cross-section. An effect that cannot be adequately showcased by using this approach is for example the increased possibilities to adjust the composite cross-sectional parameters and fine-tune the cross-section with dimensioning of rebar amount and concrete amount/strength to reduce the over-capacity.

## 4.1 Software

### 4.1.1 A3C

The software primarily used in this chapter is named A3C (“Verification of members in bending and axial compression”). It is developed by the French technology centre CTICM for the steel manufacturing company ArcelorMittal and it is freely available on that company’s website [42]. The software is dedicated to ULS and fire verification of steel and composite columns and beam-columns in accordance to EC3, part 1-1 and 1-2 [29,13] and EC4, part 1-1 and 1-2 [3,4]. Two revisions of the software were used for this thesis:

2.89: This revision was used for the span study in section 4.2 and verification of the hand-calculations in chapter 3.

2.93: During the thesis work, this revision came out and it was used for all other studies. In order to use the steel yield strength vs. thickness relations of table 3.1 in EC3, part 1-1 [29]; the steel profile data base of A3C rev. 2.89 still had to be used since it for some reason was not included in rev. 2.93 where only the EN-10025 yield strength vs. thickness relations are available.

The range of composite columns that may be verified in A3C are:

- FEC with steel H/I - profile and reinforced concrete in a square/rectangular shape.
- FEC with steel H/I - profile and reinforced concrete in a circular shape.
- PEC with steel H/I - profile and reinforced concrete.
- CFT section with internal steel H/I -profile and no additional reinforcement.

The software can also verify structural steel H/I -profile columns to EC3. Here, the commonly used element method for calculation of critical moments for LTB which is called LTBeam (also developed by CTICM) is implemented.

The reason for why this software was selected is due to being free of charge, quick to set up the calculations in and deemed trustworthy due to being developed by the well-known steel institute CTICM. Documentation of most of the program features is included within the software help section. There are some draw-backs by using the software:

- It is a verification tool and it does not contain any features for design optimization.
- It is configurable to the general EC rules or French national annexes only. Thus verification is required to ensure that the calculation rules according Norwegian national annexes are followed.
- The range of available composite profiles are limited. CFRT and CFT sections with non-reinforced or reinforced concrete (but without internal I-beam) are common types of composite columns which are not possible to select.

There are two potential flaws with the software related to the handling of member verification of 2<sup>nd</sup> order effects (see 3.3.6 for the relevant theory).

- If there is a design moment about both the y and z axes, the effect of 2<sup>nd</sup> order effects due to member imperfection is accounted for about both the axes, while EC4, part 1-1 [3] states that it only needs to be added for the most adverse axis. The issue can easily be exemplified through an example:

A pin supported 3,5m high, FEC S355 HE-200A section with C25/30 concrete and 4xØ12mm longitudinal reinforcement with the minimum required concrete cover is exerted to:

- 1800 kN design axial load + 0,001 kNm design moment about the y-axis.  
Result: A3C verifies the member as ok, with the most critical ULS criteria being buckling about the z axis (90,5% utilization)
- 1800 kN design axial load + 0,001 kNm design moment about both the y-axis and z-axis.  
Result: The member is by combined compression + design bi-axial moment (primarily from double member imperfections) verified as not ok in A3C (105,6% utilization).

Due to this, none of the studied examples use bi-axial design moments.

- The interaction factor  $k$  which determines the effect of the BMD when calculating 2<sup>nd</sup> order effects should according Johnson be calculated using a  $\beta$  value of 1,0 for the member imperfection, regardless of the end moments [25]. However when the A3C software is set to calculate to the setting: “Approached method (EN 1994-1-1 §6.7.3.4)”, the member imperfection is calculated with the same  $k$ -factor as found from the end moments. When the first order analysis yields a double curvature BMD, the beta factor can reach as low as 0,44. (This is the case for many of the columns in the rigid frame span study). Assuming a beta factor equal to 0,44 for the member imperfection typically gives a lower  $k$  factor and it is therefore non-conservative. The consequences can be exemplified:

A pin supported 3,5m high, FEC S355 HE-200A column with C25/30 concrete and 4xØ12mm longitudinal reinforcement with the minimum required concrete cover is exerted to:

- 1800 kN design axial load + 0,001 kNm single curvature design moment about the z-axis.  
Result: The 2<sup>nd</sup> order effect of combined axial force + moment action about the z axis is 78,4% of the resistance.
- 1800 kN design axial load + 0,001 kNm double curvature design moment about the z-axis.  
Result: The 2<sup>nd</sup> order effect of combined axial force + moment action about the z axis is 41,6% of the resistance.

Since end moments resulting in double curvature BMD are required for the rigid frame span study, A3C is set to calculate the local imperfection according to “Exact calculation”. In difference to the erroneous “Approached method” which is documented by the software help section, the rules governing the “exact calculation” are unknown. However, by trial calculation they seem to yield the desired results.

#### 4.1.2 MATLAB model – ULS and fire verification of CFT column

The largest short-coming of the A3C software with regards to this thesis is the lack of available cross-sections. Particularly the CFRT and CFT sections are missed, since they are commonly used for composite columns in Norway. A3C includes a CFT section with an internal steel H-section (see type C2 in Figure 2-8), but obviously this type of cross-section differs largely in terms of strength and stiffness to a tubular filled with only pure or reinforced concrete.

Since no calculation tools for concrete filled composite members are easily available, a verification tool has been developed for this thesis, using the multipurpose calculation software MATLAB R2018a and taking inspiration from the available functions in A3C. This includes the exact calculation of the MN interaction diagram which is relatively complicated for the selected cross-section (CFT). A similar

endeavour, but with a simplified polygonal MN-diagram was made by Bzdawka [40]. Only a small part of the source code is provided in his report and it has not been used for this thesis.

For transparency and for possible further usage and/or modification, the source code developed for this thesis along with a few development comments is provided in Appendix J. The MATLAB model mostly follows the same calculation methods as presented in chapter 3.3. Some key notes for the model, including its limitations and a verification towards a worked example by Dujmović, Androić and Lukačević [39] are included in Appendix J.

#### 4.1.3 CALFEM

In order to analyse the pinned and rigid frames in section 4.2, CALFEM version 3.4 has been used. CALFEM is an add-on set of finite element method (FEM) functions to MATLAB and it is aimed towards learning structural analysis by the element method. It is developed by the faculty of engineering at Lund University in Sweden and is free to download/use. A huge advantage of using this tool for a comparative study is that it is integrated in MATLAB. This makes it easy to write code to allow for parametric studies. For instance, the rigid frame case is written so that the user is free to design the size of the rectangular frame by inserting values for the number of columns, number of stories and beam to beam span. A manual for CALFEM, including element descriptions is accessible on the internet [59].

All beams and columns in this study are modelled using 2-dimensional Euler-Bernoulli beam elements with 3 degrees of freedom per node; see Figure 4-1 for a visualization.

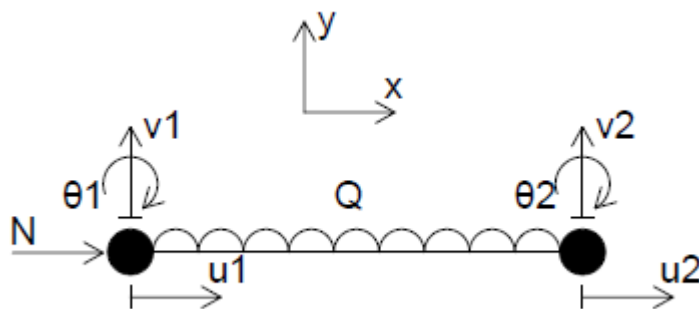


Figure 4-1: 2-dimensional Euler beam element with axial and distributed loads

The beam element uses a stiffness matrix  $\mathbb{k}$  equal to:

$$\mathbb{k} = \frac{EI}{L^3} \begin{bmatrix} AL^2/I & 0 & 0 & -AL^2/I & 0 & 0 \\ 0 & 12 & 6L & 0 & -12 & 6L \\ 0 & 6L & 4L^2 & 0 & -6L & 2L^2 \\ -AL^2/I & 0 & 0 & AL^2/I & 0 & 0 \\ 0 & -12 & -6L & 0 & 12 & -6L \\ 0 & 6L & 2L^2 & 0 & -6L & 4L^2 \end{bmatrix} \quad (4-1)$$

Where E, A and I are the modulus of elasticity, cross-sectional area and second moment of area for the axis of bending respectively. L is the length of the beam element.

The element displacement vector  $\mathbb{d}$  uses displacements illustrated by Figure 4-1 and equals (here shown in transpose):

$$\mathbb{d}^T = [u_1 \quad v_1 \quad \theta_1 \quad u_2 \quad v_2 \quad \theta_2] \quad (4-2)$$

The consistent vector of external loads for the element  $r_e$  equals (here shown in transpose):

$$r_e^T = \left[ \frac{NL}{2} \quad \frac{QL}{2} \quad \frac{QL^2}{2} \quad \frac{NL}{2} \quad \frac{QL}{2} \quad -\frac{QL^2}{2} \right] \quad (4-3)$$

Where N and Q are the applied axial and uniformly distributed loads on the element as illustrated by Figure 4-1.

The correlation between the stiffness matrix and the displacement/load vectors in equations (4-4) to (4-3) is Hooke's law expressed in matrix form:

$$r_e = k d \quad (4-4)$$

Using the Euler-Bernoulli beam element implies some assumptions [60]:

- Shear deformation is not accounted for. This may give errors of significant magnitude at beam length to height ratios of below 10.
- The cross-section remains uniformly aligned in the plane (i.e. no twisting occurs, which would result in a varying value of the second moment of area along the element length).
- Plane cross-sections remain plane under bending.

The beam element is described by only one modulus of elasticity, which is selected as that of structural steel (210GPa). For a composite section, the cross-sectional area A used for the element formulation must be re-calculated to that of an equivalent steel area  $A_{eq}$ . When accounting for long term creep, this is done accordingly (using the creep adjusted concrete modulus of elasticity  $E_{c,eff}$ ):

$$A_{eq} = A_a + A_c * \frac{E_{c,eff}}{E_a} + A_s \quad (4-5)$$

An issue with equation (4-5) is that  $E_{c,eff}$  depends on the ratio of permanent to total design axial load ( $N_{G,Ed}/N_{Ed}$ ) (see section 3.3.5). This can be determined for each beam/column individually, but a simpler, conservative approach is to assume that the permanent load is as high as possible, i.e. use the equation 6.10a in EC0 [61]:

$$\frac{N_{G,Ed}}{N_{Ed}} = \frac{1,35G_k}{1,35G_k + \psi_0 * 1,5 * Q_k} \quad (4-6)$$

The second moment of area is calculated similarly as a steel equivalent  $I_{eq}$ , by taking the effective flexural rigidity calculated by A3C and dividing it by the modulus of elasticity of structural steel, here shown for bending about the major axis:

$$I_{eq,y} = \frac{(EI_y)_{eff}}{E_a} \quad (4-7)$$

A more exact composite beam element formulation than described above is proposed by Gonçalves and Carvalho [62] in which the stress-strain behaviour of concrete is argued to be more accurately modelled than in the EC4 simplified approach (refer section 3.3.6). The authors note that the EC4 approach leads to large conservatism due to an exaggerated effect of member imperfections but do not recommend using their own approach until more studies are conducted. No attempt to use their beam element formulation has been made for this thesis.

## 4.2 Maximum span

The maximum achievable span between two columns is an important factor in construction, since it limits the utilizable free volume in buildings. In addition, having fewer columns can reduce the building time and possibly the material costs. How large the span can be for a given load scenario does not only depend on the design of the columns, but also on the horizontal members that connect them (e.g. beams) and the rigidities of the column bases and beam to column joints. Another important factor is the magnitude of bracing against sway mode.

In this study, the maximum spans of various steel and composite cross-sections are determined separately for a pinned and a rigid rectangular braced frame with equal number of columns and stories.

### 4.2.1 Study set-up

#### Pinned frame

A pinned structure with typical loads is given by Rambøll as a reference case. It is an idealized rectangular frame with pinned end single-story columns and continuous beams, braced against sway mode. In this idealization, there are no resulting moments on the columns – only axial loads equal to the reaction forces of the continuous beams. Having pinned columns and continuous beams instead of the opposite gives lower mid-beam moments and typically increases the beam spans.

It is assumed that the wind bracing is sufficient to neglect sway effects. The reason for omitting sway imperfections is that it would complicate the calculation model considerably. Furthermore, the magnitude of effects due to sway imperfections are largely affected by the specifics of the frame (total building height and number of in-plane columns) and variations of these parameters are not investigated in this study.

The relevant geometry and load data of the structure are given in Table 4-1. The permanent and imposed characteristic area loads  $\dot{G}_k$  and  $\dot{Q}_k$  on the top deck/roof are for simplicity assumed equal to those of the intermediate floor decks.

Table 4-1: Maximum span frame input data

Geometrical data		Value	Unit
Column length (m)	L	3,5	m
Distance between beams	C	7,2	m
Number of stories	$n_{tot}$	4	
Number of beam spans	$n_{span}$	5	
<b>Load data</b>			
Permanent load per area	$\dot{G}_k$	5	kN/m <sup>2</sup>
Imposed load per area	$\dot{Q}_k$	3	kN/m <sup>2</sup>

The structure is reduced from a 3d frame to a plane frame with line loads acting on the beams and further transferred to the columns through nominally pinned joints. No continuity of the slab in transverse direction is considered and the characteristic line loads  $G_k$  and  $Q_k$  are thus described accordingly on a beam which is not at the building edge.

$$G_k = \dot{G}_k * C = 5 * 7,2 \text{ kN/m} = 36 \text{ kN/m} \quad (4-8)$$

$$Q_k = \dot{Q}_k * C = 3 * 7,2 \text{ kN/m} = 21,6 \text{ kN/m} \quad (4-9)$$



The columns are referenced as A1 to F4 in accordance to Figure 4-2. The imposed load distribution which results in the highest axial load on a column is to disregard the imposed loads on the mid spans and the most loaded columns are then B1 and E1.

The design permanent line load G and imposed line load Q are calculated for each story according to EC0 rules [61], see Appendix E. For the composite sections, the permanent to total axial design load ratio  $N_{G,Ed}/N_{Ed}$  which is required to determine the creep-adjusted concrete modulus of elasticity  $E_{c,eff}$  (see also section 4.1.3) is assumed constant for all columns, equal to equation (4-10) which is based on the equation 6.10a in EC0 [61]. This approach is conservative, since equation 6.10b would result in smaller permanent loads and a lower permanent load ratio.

$$\frac{N_{G,Ed}}{N_{Ed}} = \frac{1,35G_k}{1,35G_k + \psi_0 * 1,5 * Q_k} = \frac{1,35 * 36}{1,35 * 36 + 0,7 * 1,5 * 21,6} \approx 0,68 \quad (4-10)$$

For each story, the beams may be treated as 5-span continuous beams and the distributed line loads acting on the beams are transferred to the supporting columns equal to that of the reaction forces for the beam. These reaction forces are constant ratios of  $G*S$  (for the permanent load G) and  $Q*S$  (for the imposed load Q) and these ratios are calculated in CALFEM, with the results given in Figure 4-2. The CALFEM source code for these calculations is provided in Appendix I.

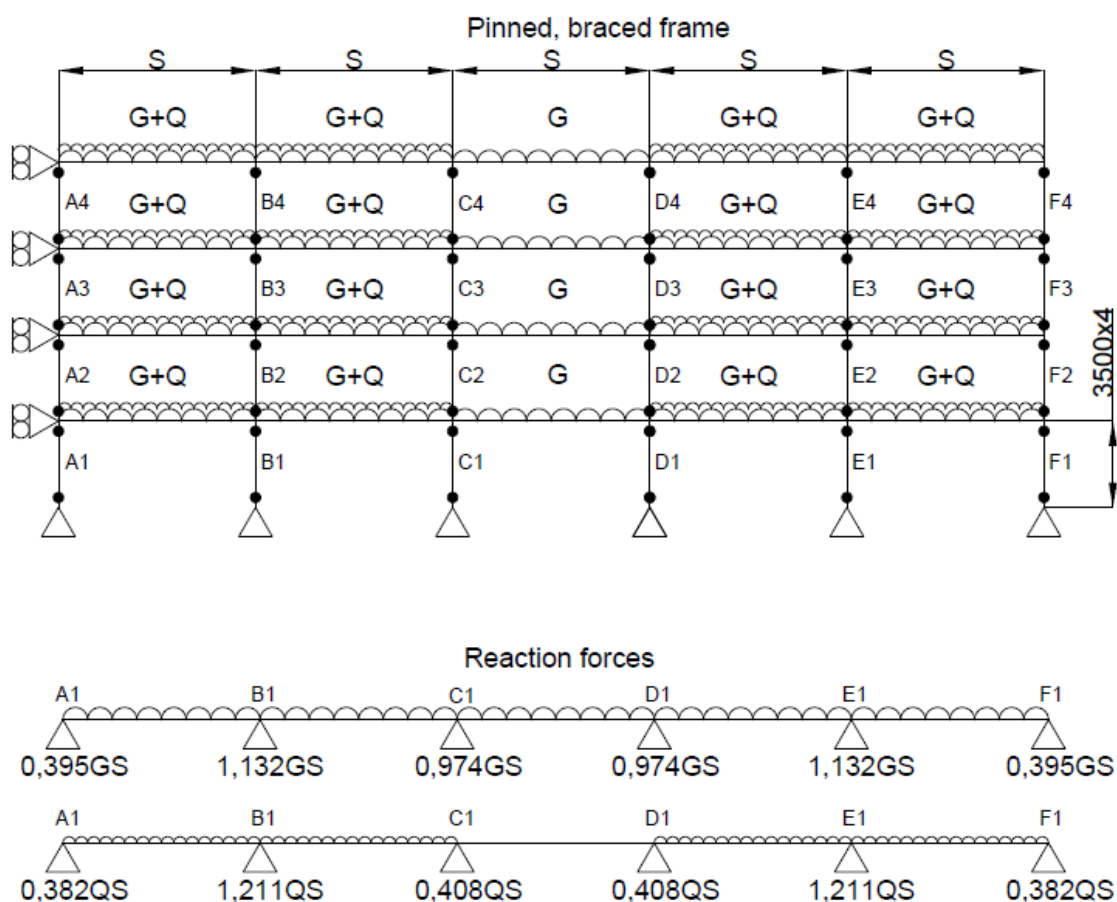


Figure 4-2: Idealized pinned plane frame for span study, with design load distribution and the calculated reaction forces of the beams

The steel cross-sections of the columns are chosen from three nominal sizes (200,300 and 400mm) and the studied cross-sections are listed in Appendix D. The outer diameter of the CFT sections are set to the closest available to the nominal sizes, i.e. 193,7mm, 323,9mm and 406,4mm. The reinforced concrete is described for a base case and for two variations where either the concrete strength or the reinforcement amount is changed. See Table 4-2.

Table 4-2: Concrete and reinforcement specification for maximum span study

	Base Case	Variation 1 (Concrete strength)	Variation 2 (Reinforcement amount)
Concrete Strength	C50/60	C25/30	C50/60
Longitudinal reinforcement	4xØ12mm	4xØ12mm	4xØ25mm
Transverse reinforcement	Ø6mm	Ø6mm	Ø8mm
Reinforcement grade	B500NC		
Age at loading	28 days		
Structural class	S4		
Relative humidity	50%		
Exposure class	XC1		
Reinforcement cover	According to Table D-2 in Appendix D. 20mm between the flanges and rebars for the PEC cross-section.		

The only influence of the cross-sectional size of the beams on the calculations is the self-weight. Longer spans typically require larger beam steel sections with a higher self-weight per length unit. For simplification, the sum of the self-weight of the construction and other permanent loads are assumed to have a constant characteristic value of  $\dot{G}_k$ , regardless of the beam span length and column cross-section.

For the given load scenario, the largest column sections in the study allow for spans up to  $S=40m$  which are not realistic to handle with standard steel profile beams (for such spans, the horizontal supporting members would likely be trusses). However, the purpose of this study is to investigate whether significant changes to column spacing can be achieved by using composite instead of steel cross-sections and the maximum span is used as an effective way to visualize the difference. Even with unrealistic span lengths, the results are still relevant. Instead of for example a 4 storey building with 40m beam spans, the building could have been 16 stories high with 10m beam spans, putting similar axial loads onto the bottom columns.

The resulting axial loads on column B1 are calculated in MATLAB for 1000 span lengths between 5m and 20m and a linear regression (see Figure E-1 in Appendix E) of the resulting data yields a very close match to the equation (4-11) for the design axial load:

$$N_{Ed} = 329,253 * S + 10,146 \text{ kN (with } S \text{ in meter)} \quad (4-11)$$

Since there are no moments applied to the columns, the design axial force  $N_{Ed}$  at the maximum achievable span before the column fails is equal to the minor axis flexural buckling resistance  $N_{b,z,Rd}$  and the maximum span length for the scenario can thus directly be determined by a reformulation of equation (4-11) as:

$$S = \frac{N_{b,z,Rd} - 10,146}{329,253} \quad (4-12)$$

Values of  $N_{b,z,Rd}$  are calculated in A3C for the steel, FEC and PEC columns and in the developed MATLAB model for the CFT columns. This then directly gives the maximum span lengths of the example frame by using equation (4-12).

### Rigid frame span comparison

Calculations are also made for a rigid moment frame, which is kept equal to the pinned frame in the geometrical and load aspects, i.e. Table 4-1 is still valid. The difference is that it has rigid joints and rigid bases. A 2d-idealization of the rigid frame, with a span length of 12500mm is shown in Figure 4-3. Similarly to the pinned structure, the frame is considered to be braced against sway and no sway imperfection is considered for this idealization, due to the same reasons as for the pinned case.

This type of frame is not commonly employed in construction due to the complexity and costs related to ensuring rigid joints. In constructions with for instance continuous composite columns and composite slabs, a semi-rigid behaviour of the joints is likely the best description due to the added rotational stiffness from the slab reinforcement [25] and therefore such a model is of interest. Modelling a frame with semi-rigid joints, using the available software and within the scope of the thesis was not deemed viable, thus a rigid frame was modelled. The semi-rigid behaviour is assumed to be in between the pinned and the rigid so therefore an idea of semi-rigid frame behaviour may be derived by noticing the differences between a pinned and a rigid frame. This assumption is supported by the research of Vellasco et al. [63] who used element methods to analyze steel and composite portal frames according to the Eurocodes. For all investigated beams in their study, the beam hogging and sagging moments where semi-rigid joints were used were in between those encountered in frames with pinned and rigid joints, typically closer to those of the rigid joints.

The rigid frame is statically indeterminate and the resulting column forces and moments depend on the chosen cross-sections of both the beams and columns. In a real design, the columns would likely have been sized differently for the different stories since the upper columns have much lower axial loads than the lower. For this comparison it is however assumed that all the columns are of equal cross-sectional size for simplicity.

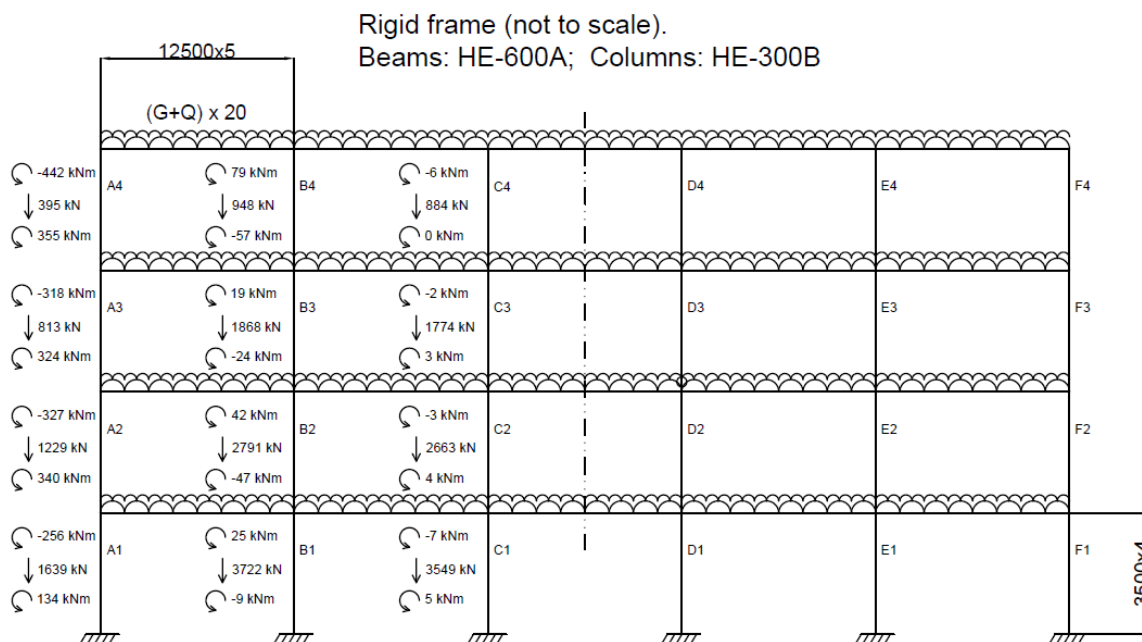


Figure 4-3: Idealization of rigid frame, plus example of the first order elastic rigid steel frame analysis results.

Unlike the pinned frame, this rigid structure cannot be analysed by simply calculating the reaction forces of the beams. There exist multiple software which can analyse a rigid frame, but few or possibly none are able to also verify a structural member to the EC4 rules and easily determine the maximum span length. Therefore an FEM model has been developed in CALFEM (see section 4.1.3) which does a first order analysis of the frame and finds the axial forces and end moments on the beams and columns for a set number of span lengths. The source code of this frame analysis is given in Appendix I.

With an assumption of a non-sway frame, no additional second order analysis is required, since second order effects of end moments and member imperfections are taken care of by the methods described in section 3.3.6. The columns can directly be verified as single members in A3C for the PEC/FEC sections and the MATLAB model for the CFT section by using the first order analysis end moments and axial forces.

It is not easy to determine which column will fail first, as the span length is increased. To save time and to reduce the complicity of the calculations, only the maximum spans based on the resistances of two specific columns are considered. The location of these columns are selected based on a trial calculation of an example steel frame, using steel HE-600A beams and HE-300B columns (Figure 4-3) and they are:

- B1 (the equivalent column as in the pinned case). This has the highest axial load and is also the dimensioning column for the trial frame. However, the end moments are relatively small, thus the comparison results are expected to be similar to those of the pinned case.
- A2, which have large end moments, while still the axial force is considerable.

The worst case distribution of the imposed loads (considering the combined effect of axial force and end moments) is also hard to determine and it may possibly also change, pending on the span length. The chosen approach is to regardless of the span length follow the thumb rule suggested by Johnson [25]. For an internal column, removing one of the imposed loads on the beams connected to the top end of the column and the imposed load on the beam on the other side in the bottom end, usually gives the most critical combination of axial force and moment. Since B1 is a bottom column, only top end imposed loads are present. Thus, the imposed load on the first story beam between B1 and C1 is removed. For an external column, the line load at the bottom of the column is removed. Thus for the A2 column, the imposed load on the first story beam between A1 and B1 is removed.

No special consideration when it regards the  $N_{G,Ed}/N_{Ed}$  ratio is taken for the imposed load that is removed in order to get the most adverse end moments. On column B2 it approximately means that 1/8 of the imposed axial load is removed. By modifying the calculations, the  $N_{G,Ed}/N_{Ed}$  ratio would go from 0,68 to 0,71 which is non-conservative. However, this only have a minor effect on  $E_{c,eff}$  and even less so on the calculated equivalent steel area used in the FEM analysis, since the concrete contribution is only a part of it. Therefore this error is ignored.

In difference to the pinned case (where increased self-weight is the only issue related to the beam cross-sectional dimensions), the size of the beams here also influence the moment transfer to the columns. Using an unrealistically stiff beam gives unrealistically low bending moments on the columns. The beams are therefore sized to handle the maximum spans achieved by using FEC columns, meaning they are likely oversized for the spans achievable by the steel columns. However, using different beam sizes for cross-sections of the same nominal size would make a direct comparison between steel and composite sections difficult to interpret, which is the reason why it is not done. It is assumed that the

beams are sufficiently restrained against LTB and thus are dimensioned for cross-sectional yield in bending.

No standard HE-A or HE-B beam can handle the maximum spans achieved by using the fully encased composite columns with the nominal steel cross-sectional size 400mm. Therefore (and to reduce the number of calculations), the only nominal section sizes which are calculated are 200 and 300mm, see Table 4-3. For similar reasons, no HE-M column cross-section is included in the study.

Table 4-3: Selected beam sections for the rigid span study

Column section (FEC section, C50/60 concrete with 4x12Ø longitudinal reinforcement)	Maximum span (taken from pinned case calculations) mm	Beam section Calculated as the minimum steel section required to support a uniformly distributed line load on the maximum span; 1,2G + 1,5Q (here assuming the beam is simply supported).
HE-200B	9771	HE 400A
HE-300B	22146	HE 1000B

The maximum beam moments (occurring anywhere in the frame) are calculated for both the pinned and the rigid frame, using the respective load cases for the B1 column for simplicity. For these calculations, the span length is set to the maximum span length calculated for the pinned frame.

#### 4.2.2 Study results

The maximum span lengths of composite columns using a certain steel section and concrete specifications of the base case (see Table 4-2) are compared to those achieved by using the steel section only. The results are presented in Figure 4-4, where the percentage numbers above the composite section indicates the improvement in maximum span, when compared to the steel section.

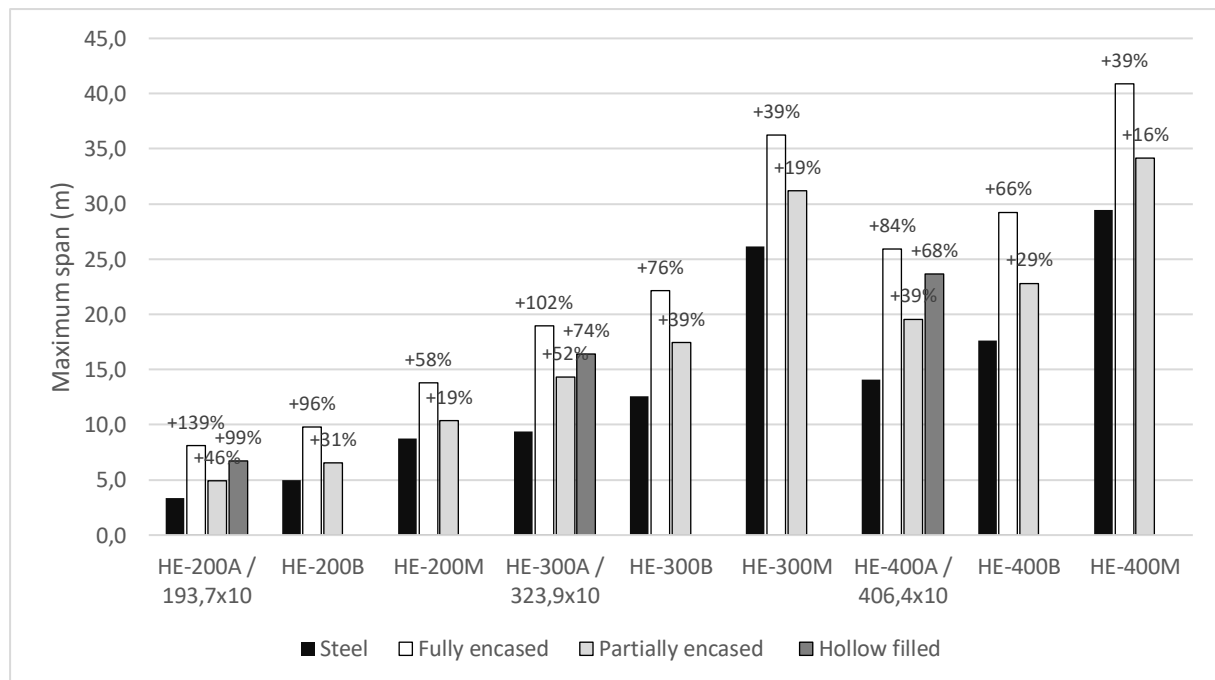


Figure 4-4: Pinned frame maximum span study results.

The CFT composite steel sections use a steel circular hollow section (CHS) which is neither comparable in steel area or column depth to an H-profile. Therefore only the sections with the most similar steel section areas are compared, which are 10mm thick CHS profiles vs. HE-A profiles. The differences in steel section areas for a 10mm thick CHS versus an HE-A profile are 7% and 5% larger for the sizes 200 and 300mm respectively and 22% smaller for the 400mm size.

The effect of changing the concrete strength is studied, by comparing the maximum span length achieved by a composite column with C25/30 strength concrete towards one with C50/60 grade; the highest concrete strength allowed by the simple calculation rules in EC4, part 1-1 [3]. All cross-sections are reinforced by 4xØ12mm longitudinal rebars. On average, the FEC and CFT profiles increase their span length by 22% and 24% respectively by using the stronger concrete. The PEC cross-section experiences a notably smaller increase; on average 11%. The full set of data are given in Appendix E by Table E-2.

In addition, the effect of changing the column longitudinal reinforcement cross-sectional area has also been studied, by comparing the maximum span length of cross-sections of C50/60 grade concrete with either 4xØ12mm or 4xØ25mm longitudinal reinforcement bars of B500NC grade. The FEC cross-section had a span length increase of 27% in average for the larger reinforcement diameter, while the PEC and CFT sections showed notably smaller differences, with 8% and 7% respectively. The full set of data are given in Appendix E by Table E-3.

The average differences in the maximum achievable span length by using a rigid frame instead of a pinned frame is shown in Table 4-4 as  $\Delta_1$ . These results are based on a verification of column B1 only and a 12% increase in span length is noted for the rigid frame for all H-profile based cross-sections. The CFT sections have a much lower increase in average maximum span length by only 4-5 %. The full set of data are given in Appendix E by Table E-4.

The average differences in maximum span length for a rigid frame when column A2 instead of B1 is selected as the dimensioning column is shown in Table 4-4 as  $\Delta_2$ . Notably, the steel profile shows the largest increase, followed by the PEC and the CFT profiles. The FEC section have a remarkably lower increase in span length; in the case of the stiffest member (HE-300B encased in C50/60 concrete), the span length is actually decreased by 5%; meaning that for that case the A2 column is more critical than the B1 column in the rigid frame. The full set of data are given in Appendix E by Table E-4.

Finally, the maximum beam bending moments of all beams in the frame is calculated and compared between the pinned and rigid frames as  $\Delta_3$  in Table 4-4. As expected, the maximum moments in the beams are decreasing when a rigid frame is used. The different cross-sections show relatively similar differences in maximum beam bending moments at about 10% decrease for the rigid frame. The full set of data are given in Appendix E by Table E-5.

Table 4-4: Average differences between pinned and rigid frames.

Profile (All composite sections use 4xØ12mm longitudinal rebar)	$\Delta_1$ Average increase: Span length in rigid instead of pinned frame, based on column B1	$\Delta_2$ Average increase: Span length by dimensioning to column A2 instead of B1 in the rigid frame.	$\Delta_3$ Average increase: Maximum beam bending moment in rigid instead of pinned frame.
Steel	12%	79%	-16%
FEC, C25/30 concrete	12%	28%	-11%
FEC, C50/60 concrete	12%	6%	-10%

<b>Profile</b> (All composite sections use 4xØ12mm longitudinal rebar)	<b>Δ<sub>1</sub></b> Average increase: Span length in rigid instead of pinned frame, based on column B1	<b>Δ<sub>2</sub></b> Average increase: Span length by dimensioning to column A2 instead of B1 in the rigid frame.	<b>Δ<sub>3</sub></b> Average increase: Maximum beam bending moment in rigid instead of pinned frame.
PEC, C25/30 concrete	12%	57%	-14%
PEC, C50/60 concrete	12%	46%	-12%
CFT, C25/30 concrete	5%	62%	-13%
CFT, C50/60 concrete	4%	45%	-10%

### 4.3 Column depth reduction

PEC and CFT columns do not increase in depth when concrete is added to the steel section. However they increase in strength and stiffness and therefore the column depth might be possible to reduce for a given load, when compared to pure steel columns. The concrete in an FEC section will however add on significantly to the depth and therefore it will not necessarily be thinner than the equivalent steel section if only ULS verification is considered.

Composite columns have an inherent fire protection of the steel due to the concrete part, which in the case of encased steel sections acts as insulation and in the case of filled steel sections acts as a heat sink [24]. In contrast, steel columns typically requires added insulation to achieve the desired fire resistance. It is therefore reasonable to assume that the cross-sectional area of a column can be reduced if a steel section is replaced by a composite, since the insulation material in the latter case also contributes to the column strength and stiffness. Another smaller factor is the increased possibility to fine-tune the dimensions of the composite section by changing both the dimensions of the concrete section and the reinforcement, thus reducing the overcapacity and size of the section.

Reducing the cross-sectional area of a column may lead to more utilizable volume in a building, since columns often are located within the open floor spaces. More slender columns also means a larger flexibility for usage when the space allocated to structural members is tight. Therefore, it may be of interest to better understand whether/when composite members offer a distinct reduction of column size.

#### 4.3.1 Study set-up

The minimum required column depths of steel HE-B members with the necessary amount of fire protective boards are compared to those of FEC and PEC cross-sections using HE-B steel members and CFT members for a number of different structural load cases with no required loadbearing fire resistance and for the classes R30, R60, R90, R120 and R180.

Most of the variables and software settings are held constant in order to reduce the number of total calculations, see Table 4-5. This causes room for errors in the comparison. It can be argued that there for instance may be other types of fire protection boards which require less thickness for certain combinations of structural and fire loads. On the other hand, some of the composite cross-sections could be reduced in area by using a stronger concrete and/or more longitudinal reinforcement bars. The steel grade for all steel sections is set to S355 since that is the largest allowable steel grade in order to use the EC4, part 1-2 [4] tabulated fire resistance rules for PEC sections.

Table 4-5: Cross-sectional area due to fire protection study - constant parameters

<b>Steel material properties:</b>	
Steel section	HE-B, standard sizes up to HE-500B For CFT columns - CHS, standard sizes up to CHS 508x12,5 See Appendix D for a list of all section sizes considered.
Steel grade	S355
<b>Fire protection board material properties:</b>	
Type	Rockwool CONLIT 150 [64]
<b>Concrete material properties:</b>	
Concrete strength	C40/50
Age at loading	28 days
Relative humidity	50% (in-doors)
Structural class	S4
Exposure class	XC1
<b>Reinforcement properties</b>	
Reinforcement grade	B500NC
Longitudinal bars	4 rebars, one in each corner; using the minimum distance to the cross-sectional edge as required by EC4, part 1-1 or part 1-2 [3,4]. <i>In some cases 6 rebars are required for the PEC section, (three on each side of the web) in order to meet the minimum reinforcement criteria.</i> See Appendix D for a list of the reinforcement diameters considered.
Transverse bars/stirrups	$\varnothing = \min(6\text{mm} ; 0,25 * \varnothing_l)$
<b>Steel column calculation settings in A3C:</b>	
Plastic design to M-N and M-N-V	Exact calculation
Buckling resistance of members in bending	Clause 6.3.2.2 (EN 1993-1-1)
Interaction factors $k_{ij}$	Annex A (EN 1993-1-1)
Evaluation of the critical moment	Modal buckling analysis (LTBeamN)
Factor for shear resistance	$\eta=1.20$
Partial factor for fire calculation	$\gamma_{M,fi,a} = 1.00$
Fire exposure	4 sides
Buckling length in a fire situation	$L_{fi} = 0,5L$ (intermediate storey)
<b>Composite column calculation settings in A3C:</b>	
Local imperfection and second order effects	Exact calculation
<b>Fire resistance calculation settings in A3C:</b>	
Fire exposure	4 sides
Buckling length in a fire situation, $L_{fi}$	$0,5 * L$ (Intermediate storey)

Using a larger number of reinforcement bars than 4 (one in each corner) may possibly reduce the size of the FEC cross-section somewhat further, but it would add a lot of complexity in optimizing the cross-sections for this study and has therefore not been done. For the PEC cross-section, 4 reinforcement



bars are used normally, but sometimes 6 reinforcement bars are needed to achieve the minimum required reinforcement area.

The study is primarily meant to investigate the column depth differences between steel and composite columns for different load bearing resistances and how variations in loading parameters affect the column depths. Finding the required cross-sectional areas includes a lot of trials for section optimization in the A3C software and thereafter (for the steel section) consulting tables to adjust the fire protection thickness. To limit the work scope, the amount of load cases is limited to 15. The reference case is a 3m long column, pinned in both ends with 2500kN axial load and no end moment. The axial load, column length and bending moment parameters are then each varied in turn to see the changes in minimum column depth for R30 to R180 fire resistance. In the cases where an end moment is applied, it is a point moment at the top end of the column. See Table 4-6 for the established structural load cases.

Table 4-6: Column depth reduction – structural load cases.

Axial load (N)		Column length (L)		Major axis bending moment (M)	
Case	Load (kN)	Case	Length (m)	Case	Bending moment (kNm)
N1	1500	L1	1,5	M1	0
N2	2000	L2	2,25	M2	50
N3	2500	L3	3	M3	100
N4	3000	L4	3,75	M4	150
N5	3500	L5	4,5	M5	200
N6	4000			M6	250

Notes:

1. For a given group of load cases (Nx,Lx,Mx) the values of the other two parameters are set to that which is indicated in a gray shaded background. As an example, all load cases Lx uses 2500 kN axial load and no major axis bending moment.
2. The loads are given as the ambient temperature design loads.

For a steel section, first the required cross-section for a load case in normal temperature is determined in A3C. Thereafter the critical temperature is calculated in A3C for the given load case, but with loads reduced to 65% of the normal temperature design loads. This reduction is chosen as per the general recommendation given in EC3, part 1-2 [13]. Finally product data tables for fire protection boards [64] are consulted to find the required thickness of the fire protection board.

For the composite sections, the columns are optimized for the load cases in normal temperature and the minimum required section size determined in A3C. The permanent to total axial design load ratio  $N_{G,Ed}/N_{Ed}$  can be visually determined based on the figure 2.1 in EC4, part 1-2 [4]. The frequent variable action factor  $\psi_1$  is assumed to be 0,5 (typical for residential buildings or office areas) according EC0 [61]. With a fire load reduction factor  $\eta_{fi}$  equal to 0,65 as assumed earlier for the steel section; the ratio of characteristic imposed to permanent load  $Q_{k,1}/G_k$  then equals  $\sim 0,25$ . This ratio is used in equations (4-13) and (4-14) which are a comparison of the results of equations 6.10a and 6.10b of EC0 [61], expressed as a multiple of  $G_k$ :

$$N_{Ed,6.10a} = \gamma_G G_k + \gamma_Q \psi_0 Q_k = 1,35G_k + 1,5 * 0,7 * 0,25G_k = 1,61G_k \quad (4-13)$$

$$N_{Ed,6.10b} = \gamma_G \xi G_k + \gamma_Q Q_k = 1,2G_k + 1,5 * 0,25G_k = 1,58G_k \quad (4-14)$$

The largest result and the dimensioning equation is equation (4-13) and the design permanent to total axial design load ratio used when defining design loads in A3C and the MATLAK model is found by using equation (4-6) and (4-13):

$$\frac{N_{G,Ed}}{N_{Ed}} = \frac{1,35G_k}{1,61G_k} = 0,84 \quad (4-15)$$

Different calculation procedures are then applied for the different types of composite sections:

- For an FEC column the section size and/or reinforcement amount is increased if required according EC4, part 1-2 table 4.4 [4] for each fire load bearing resistance. For this cross-section, the magnitude of the structural loads does not affect the values given by the EC4 table.
- For a PEC or a CRT column the fire design loads are reduced to 65% of the normal temperature design loads, equal to the reduction for the steel column. Thereafter, the required cross-sections is determined by EC4, part 1-2 table 4.6 or 4.7 [4] respectively for each fire load bearing resistance.

A more detailed description of the calculation procedures is given in Appendix F.

#### 4.3.2 Study results

For free-standing columns, the FEC and CFT and possibly also the PEC columns could be used directly with a concrete or painted steel finish. The steel column would however for aesthetical and durability reasons likely be using gypsum boards or similar on top of the fire protection board. The added depth from such extra finishes have not been included in the results. The results are presented in a condensed form in Table 4-7. Graphs showing the depth reduction of composite columns when compared to steel columns are given in Appendix F, by Figure F-2 to Figure F-7. The calculated cross-sections are given in Appendix F, by Table F-1 to Table F-4.

Table 4-7: Results, column depth reduction study. Average and minimum reductions.

Fire load bearing resistance	Load case group, ref. Table 4-6.	Fully Encased (mm)		Partially encased (mm)		Filled Tubular (mm)	
		Average	Min	Average	Min	Average	Min
R0	N	-13	-26	47	20	<b>54</b>	32
	L	-25	-30	36	20	<b>45</b>	26
	M	-19	-26	<b>50</b>	40	9	-24
	Total Average:	-19		<b>44</b>		36	
R30	N	27	14	<b>87</b>	60	19	-33
	L	15	10	<b>76</b>	60	11	-13
	M	21	14	<b>90</b>	80	13	-4
	Total Average:	21		<b>84</b>		14	
R60	N	<b>27</b>	14	20	0	-4	-33
	L	<b>15</b>	10	0	-20	11	-13
	M	21	14	<b>23</b>	0	0	-24
	Total Average:	<b>21</b>		14		2	
R90	N	<b>47</b>	20	23	-40	-39	-66
	L	<b>40</b>	24	6	-10	-56	-76
	M	<b>69</b>	44	52	10	-21	-46
	Total Average:	<b>52</b>		27		-38	

Fire load bearing resistance	Load case group, ref. Table 4-6.	Fully Encased		Partially encased		Filled Tubular	
		(mm)		(mm)		(mm)	
		Average	Min	Average	Min	Average	Min
R120	N	47	10			0	-47
	L	40	30			2	-26
	M	70	30			37	4
	Total Average:	52				13	
R180	N	147	90			77	34
	L	130	130			74	74
	M	173	130			120	74
	Total Average:	150				90	

#### 4.4 Steel efficiency

The cost related to the steel material is a substantial part of the total economic cost of a steel or composite column. According price guidance dated January 2019 from a large Norwegian steel distributor [65], the prices for rebar of grade B500NC and HE-A/HE-B/CHS profiles of grade S355J2 up to nominal size 400mm were as indicated by Table 4-8. As a comment, there is not a very large difference in material cost between the different steel application and when labour costs also are included as well, the rebar is likely not the cheapest steel section.

Table 4-8: Price comparison of steel profiles

Steel Profile	Size 1	Size 2	Size 3	Average
Rebar, grade B500NC	(8mm) 22,84 NOK/kg	(16mm) 21,40 NOK/kg	(25mm) 21,40 NOK/kg	21,88 NOK/kg
HE-A (hot rolled), grade S355J2	(HE-A 200) 24,55 NOK/kg	(HE-A 300) 25,09 NOK/kg	(HE-A 400) 25,45 NOK/kg	25,03 NOK/kg
HE-B (hot rolled), grade S355J2	(HE-B 200) 24,37 NOK/kg	(HE-B 300) 24,37 NOK/kg	(HE-B 400) 25,09 NOK/kg	24,61 NOK/kg
CHS (cold formed), grade S355J2	(193,7x6mm) 27,61 NOK/kg	(323,9x8mm)* 27,61 NOK/kg	(508,0x8mm)* 27,25 NOK/kg	27,49 NOK/kg
Notes: * The CHS dimensions used in the study are not available in the price guide and therefore the price of the closest larger profile is used.				

In the following comparison, it is investigated how much load resistance per steel cross-sectional area that steel and composite columns can provide. In addition to the area of the steel profile, the areas of longitudinal and transverse steel reinforcement are also included in the calculations. Since the steel cross-sectional area is uniform across the length of the column, the mass and subsequently the cost of the constituent steel is considered to be directly proportional to the steel area.

These calculations can provide some insight into which type of steel cross-section and what amount of reinforcement is economical within a certain category of column. However it is not accurate from an economic perspective to compare the results for steel columns towards e.g. PEC columns since there will be large costs attributed to for instance concrete material and reinforcement and casting labour. For instance the construction method and the construction time also plays a role, as well as the pricing of the particular steel profile. For composite columns, the amount and type of concrete and reinforcement material naturally also plays a role in the total costs.

#### 4.4.1 Study set-up

While a PEC or a CFT column is directly restricted in its size to the dimensions of the steel member, there is no such limit for an FEC column. The cross-section which will provide the most load resistance per steel area for an FEC column is clearly the one that maximizes the concrete amount. In practice this will be limited by the maximum concrete cover of the cross-section, see restriction g) in section 3.3. Only with very thin steel sections of low steel grade and with very high amounts of longitudinal reinforcement the minimum steel contribution ratio becomes limiting. FEC columns are excluded from this comparison, since they would be more relevant to compare to reinforced concrete columns.

PEC and CFT cross-sections are studied, using the highest strength concrete allowed by the simple calculation rules (C50/60). The PEC cross-sections have the minimum amount of B500NC grade reinforcement required to reach a 0,3% reinforcement ratio, which is 8 mm diameter for the HE-200 A/B and 10 mm diameter for the HE-300 A/B and 400 A/B section. In addition, 6mm diameter transverse reinforcement is included. The CFT cross-sections are not reinforced. A few composite columns are tried with higher amounts of reinforcement to see whether that increases the steel efficiency. No consideration is given to the amount of steel used for joints or for steel-concrete shear connection close to the load introduction area.

Two primary types of load cases are evaluated; a column in pure compression and in combined compression and bending. For a steel column, the maximum axial force resistance (considering both cross-sectional yield and buckling) is called  $N_{Rd,steel}$ . By dividing this value by the steel cross-sectional area  $A_a$  a measure of the average axial stress in the column at its maximum axial force resistance is achieved. That value can then be divided by the design steel yield strength for buckling mode in order to get a dimensionless ratio of how the steel section compares towards one which is in cross-sectional yield.  $\chi_{steel}$  actually measures the reduction effect of buckling for a steel section and in pure compression it will be equal to the  $\chi$  factor calculated in section 3.3.5:

$$\chi_{steel} = \frac{N_{Rd,steel} / A_a}{f_y / \gamma_{M1}} \quad (4-16)$$

A similar value can be derived for the composite column but here the steel area is considered to also include the longitudinal ( $A_s$ ) and transverse ( $A_t$ ) reinforcement areas. The permanent design load ratio  $N_{G,Ed} / N_{Ed}$  is set equal to that in the maximum span study from equation (4-10) = 0,68. The transverse reinforcement cross-sectional area is not taken directly but rather converted into an equivalent longitudinal cross-sectional area (see Appendix G for a description of these calculations). Similarly to the expression for  $\chi_{steel}$ , equation (4-17) provides a value for how much axial load the column can take per steel unit area. While the yield strength of rebar is higher than that of the steel section, the same divisor  $f_y / \gamma_{M1}$  is still used, in order to be able to compare the steel and composite results.

$$\chi_{comp} = \frac{N_{Rd,comp} / (A_a + A_s + A_t)}{f_y / \gamma_{M1}} \quad (4-17)$$

Within this thesis, the ratios  $\chi_{steel}$  in equation (4-16) and  $\chi_{comp}$  in equation (4-17) will be referred to as “steel efficiencies”, which is however not common nomenclature.

For a pin-ended column in pure compression, the dimensioning ULS criteria is always equal to the buckling resistance about the minor axis  $N_{b,z,Rd}$  (see section 3.3.5), since that resistance tends towards the squash load resistance for stocky columns. For a given steel/composite column buckling length and cross-section, this value can be directly determined in A3C.

For the beam-column, a design bending moment  $M_{Ed}$  is applied about the major axis at the top of the column. Since the dimensioning ULS criteria of this type of column is not given (it may buckle either about the minor or the major axis), the value  $N_{Rd}$  is determined iteratively in A3C, where axial loads divisible by 10 are applied until the highest acceptable is found. Three design bending moment ratios are studied, equal to 15%, 30% and 45% of the pure bending moment resistance of the steel section. These moments are calculated and presented in Appendix G.

#### 4.4.2 Study results

The steel efficiencies of steel and PEC columns as described in equations (4-16) and (4-17) are determined and compared using yet another ratio  $r_\chi$  accordingly:

$$r_\chi = \chi_{comp} / \chi_{steel}. \quad (4-18)$$

The results are given in Figure 4-5 and Figure 4-6. They indicate as expected that the PEC columns have a larger steel efficiency than the steel columns. Additionally the results show that an increased column/buckling length leads to a less difference in steel efficiency, while increased bending moments leads to a larger difference in steel efficiency. For both the column and the beam-column, it seems that the difference is larger for a nominal section size of 300mm than for 200mm or 400mm.

Results for the CFT column cannot be directly compared to the H-profile steel sections with a ratio. Results of the individual steel efficiencies  $\chi_{comp}$  and  $\chi_{steel}$  are given for the steel and PEC/CFT cross-sections in Table G-2 of Appendix G. For axially loaded columns, it is shown that the CFT columns (without reinforcement) on average have approximately twice the steel efficiency of the steel columns, while PET columns have 20-30% increased steel efficiency.

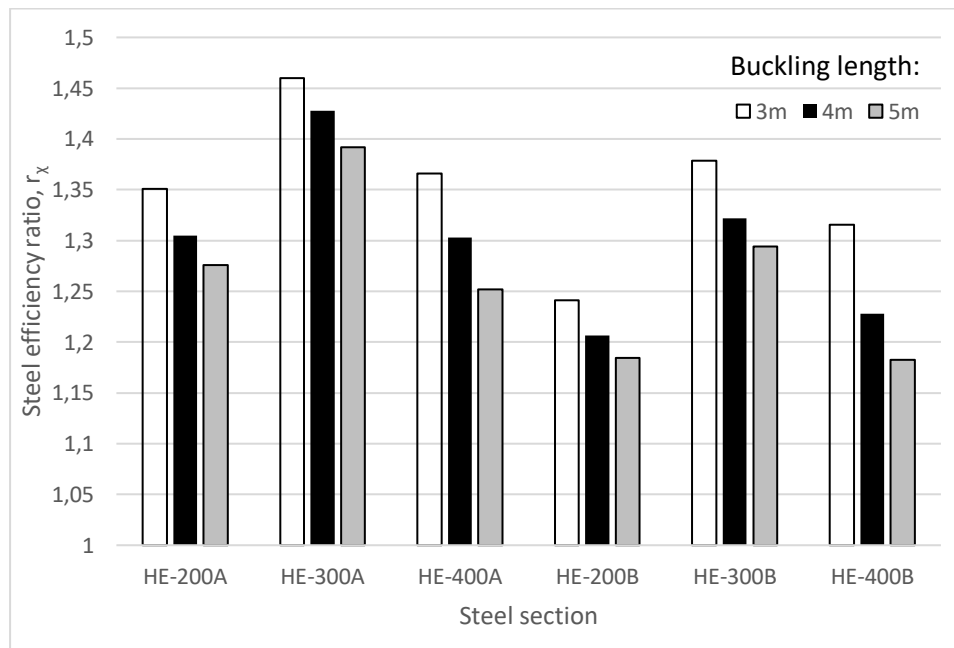


Figure 4-5: Composite to steel ratio of steel efficiency for a column in compression

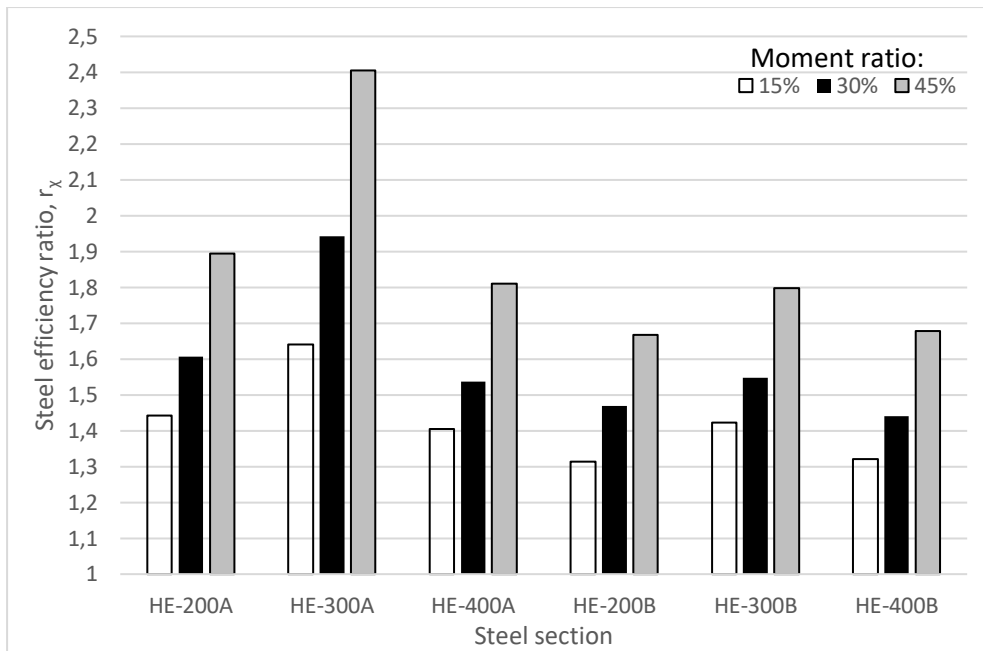


Figure 4-6 Composite to steel ratio of steel efficiency for a column in combined compression+ bending

The optimum amount of reinforcement was investigated. It was first studied for the most slender cross-sections, which are the PEC HE-200A and 193,7x6mm CFT sections. They were exerted to the largest buckling length in the study and for the PEC section also for the largest moment used in the study. The steel efficiency was not increased significantly by adding reinforcement for either of the sections. It was actually notably reduced for a CFT when a large amount of reinforcement was used, due to the less favourable buckling curve required for reinforcement ratios above 3%.

#### 4.5 Environmental foot-print

A basic study has been made to investigate the differences in environmental footprint between a steel and a composite column. This study is not comprehensive and only considers the production of the included building materials. A 2006 note from Bernhard and Jørgensen [66] states that the production of building materials was responsible for 7% of the total greenhouse gas emissions in Norway (measured as CO<sub>2</sub> mass equivalents) while construction activity was responsible for 1,2%. While the accuracy of these numbers can be questioned since this is a single, dated note and since the topic is complex, it is still reasonable to assume that the greenhouse gas emissions from the production of building materials used is a relevant indicator for the environmental footprint of a building element.

Building elements which are documented under the voluntary environmental product declaration (EPD) scheme shall be listed with various environmentally relevant factors as described by ISO 14025 [67]. The EPD is owned and developed by the building material manufacturing company, but it must be verified by a third party and reviewed periodically. It contains multiple values related to the environmental footprint, including the global warming potential expressed in CO<sub>2</sub> mass equivalents and the required energy use. These two values are often stated on the first page of the EPD and they are the key factors compared in this study. The values are specified for a selected, suitable unit (this can be by mass, by volume or by one building element unit).

Even for the same type of building material (e.g. structural steel) and the same manufacturer; different types of profiles may have substantially different values, mainly due to the differences in production method and the amount of recycled material used in the process:

The key factor values are limited to the production of the building materials, or in detail:

### Steel/Rebar

- Raw materials (e.g. mining, melting, recycling)
- Producing finished steel products (e.g. H, CHS profiles and rebars)
- Handling/transport between the above production phases.

### Fresh concrete

- Raw materials (e.g. production of cement, aggregate and additives)
- Mixing the raw materials including water to a fresh concrete mix
- Handling/transport between the above production phases.

Not included in this comparison are the EPD key factors that depends on the location of the specific building site, the construction method employed and the intended purpose of the building. These are for instance:

- Transportation of the building materials to the construction site.
- Construction/installation, including casting of the concrete.
- Building usage/maintenance
- Uptake of CO<sub>2</sub> through carbonation during the building life-time (For concrete).
- End-of-life considerations (e.g. decommissioning, disposal and potential for further recycling).

The EPD factors for the constituent materials are shown in Table 4-9. They are taken from typical Norwegian suppliers of Steel/Concrete respectively. No EPD has been found for Norwegian composite columns as they typically are site-constructed CFT sections, where steel is delivered from one supplier and concrete from another. Thus one EPD is provided from the steel manufacturer and another from the concrete manufacturer. If FEC or PEC columns became more common in Norway, they would likely be pre-fabricated and possibly the EPD values would be given for the column as an element.

Table 4-9: Key EPD factors for 1 kg of building material

	Fraction of recycled steel	CO <sub>2</sub> equivalents (kg) ***	Energy use (MJ) ***	Reference
Hot rolled I or H section	85%	1,16 (3,4 g/MPa)	14,8 (43,8 kJ/MPa)	[68]
Hot formed CHS section	13%	2,1 (6,2 g/MPa)	21,6 (63,9 kJ/MPa)	[69]
Cold formed CHS section	13%	2,29 (6,8 g/MPa)	24,0 (71,0 kJ/MPa)	[70]
Rebar, B500NC	100%	0,33 (0,8 g/MPa)	8,1 (18,6 kJ/MPa)	[71]
C45/55 concrete, slump <200mm*	N/A	0,1 (3,9 g/MPa)	0,87 (34,1 kJ/MPa)	[72]**

#### Notes:

\* No reference EPD for the studied concrete strength C40/50 has been found. C45/55 is selected as the closest available concrete strength.

\*\* The reference EPD uses values per m<sup>3</sup> of fresh concrete. These are converted to kg by dividing them by a density of 2450 kg/m<sup>3</sup>, which is the mean concrete density of the span 2300-2600 kg/m<sup>3</sup> given by the EPD.

\*\*\* The value within parenthesis is the EPD value divided by the compression yield strength  $f_{yd}$  with Eurocode material partial factors applied as follows;

Steel sections:  $f_{yd} = 355/\gamma_{M0} = 338$  MPa

Rebar:  $f_{sd} = 500/\gamma_s$  MPa = 435 MPa

Concrete:  $f_{cd} = 0,85 \cdot 45/\gamma_c$  MPa = 25,5 MPa

As can be seen, there is a very large difference between steel and concrete in EPD values per unit mass. By dividing the values by the Eurocode design compression yield strength (the values within parenthesis in Table 4-9), a more fair comparison is arguably achieved and now the concrete and steel H-profile show EPD values of similar magnitude. Differences are large between different types of steel sections, where CHS sections have much higher values than H-profiles, likely due to the much lower fraction of recycled steel.

#### 4.5.1 Study set-up

To reduce the scope; the optimized steel, FEC and PEC cross-sections already found for the 15 load cases (see Table F-1 to Table F-3 , Appendix F) of the normal temperature case in the column depth study (section 0) are used as input.

The CFT cross-sections in the column depth study are however typically selected with steel CHS cross-sections of 10mm or 12,5mm thickness. Unless reducing column depth is a very important target, it is reasonable that thinner steel sections and somewhat stockier columns would be used since that saves steel material. Thus the CFT cross-sections are recalculated for this study, with a maximum allowed thickness of 8mm and a minimum rebar diameter of 12mm, but without changing the concrete specification (Table 4-5). The resulting cross-sections are shown in Table H-1 of Appendix H.

The cross-sectional areas of the steel section, the reinforcement and the concrete sections for the cross-sections are determined. By multiplying these areas with the relevant material density and the EPD value per mass unit from Table 4-9 and adding it together, the EPD values per column unit length are achieved.

#### 4.5.2 Study results

The average results of the study are presented in Table 4-10, while more detailed values for each load case are presented in Figure H-1 and Figure H-2 in Appendix H. The building materials required for producing FEC and PEC columns emits less greenhouse gases and are more energy efficient than steel columns, while CFT columns emits more greenhouse gases while still being more energy efficient.

*Table 4-10: EPD values for production of building materials for one meter of column, average values for all load cases*

	CO <sub>2</sub> mass equivalents		Energy use	
	Average (kg)	Vs. Steel	Average (MJ)	Vs. Steel
<b>Steel</b>	106,3		1355,9	
<b>PEC</b>	81,4	-23%	989,7	-27%
<b>FEC</b>	91,5	-14%	1142,5	-16%
<b>CFT</b>	112,2	6%	1194,0	-12%



## 5 Case study

### 5.1 Case selection

In a session together with Rambøll, a case study was selected where steel columns are replaced with composite columns to investigate whether benefits are gained. The main focus is to reduce the column depth. The original idea was to choose an earlier building project from Rambøll which utilize steel columns and see whether the building would have been optimized by using composite columns instead. However, no suitable candidate was found (the criteria was a relatively simple construction with steel columns where either the axial or fire loads were high).

Thus a fictive building proposed by Rambøll was selected, representative of a relatively common building type in Norway. This is a hall for indoor sports activities with a single-storey steel frame, using lattice girders as horizontal members to allow for a large roof span. To provide safety for the users of the facility, the columns are hid inside the exterior walls to avoid protrusions into the playing field. An illustration of the building, with two exterior walls and the roof construction removed for main structure visibility is shown in Figure 5-1. The size of the columns effectively decides the building footprint and thus there may be significant savings in building material by using slimmer columns.

A similar type of steel frame is used in industrial buildings. In such a case there is usually no requirement for the columns to be hidden inside the walls. However, having slimmer columns provides more available area and increased flexibility of building utilization (e.g. forklift corridors).

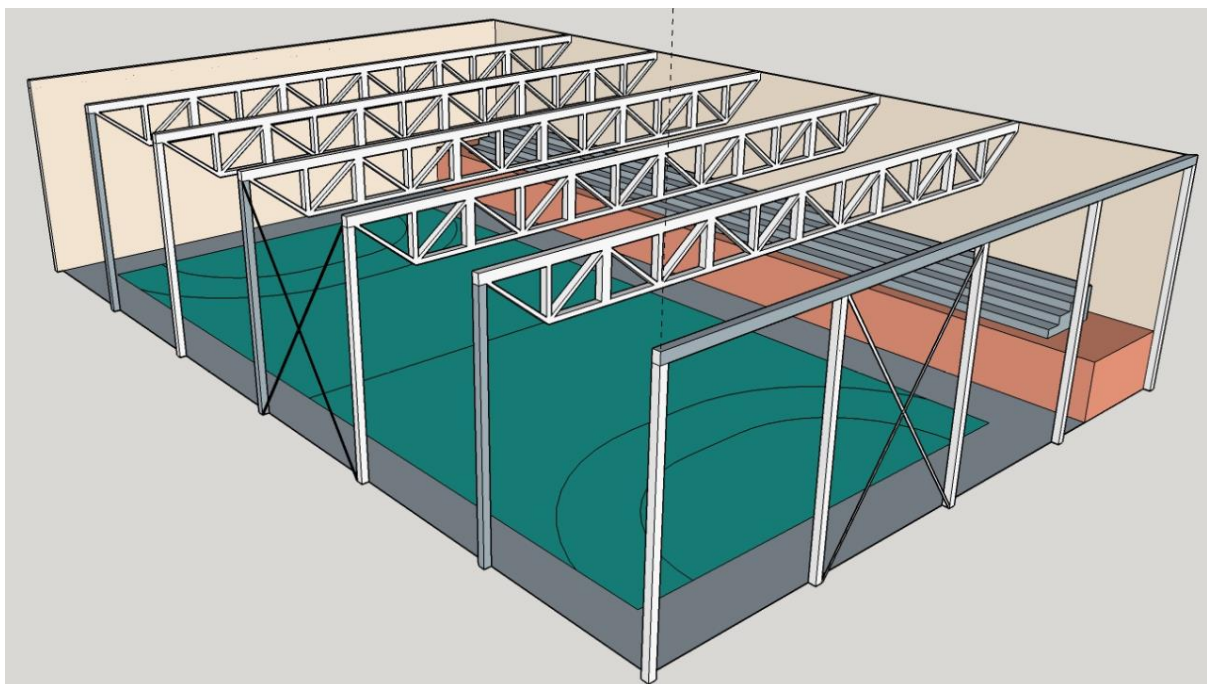


Figure 5-1: Case study - In-door sports hall

### 5.2 Case description

#### Design and dimensions:

The selected case is a typical hall for indoor sports activities, measuring  $45 \times 30 \text{ m}^2$  internally (length x width). Guidance on how to size and design such a building is given by the cultural department of Norway [73]. The height of the building is 10 m in total, which gives roughly 7,5 m free height under the lattice girders. The minimum free height for this type of building is 7m, thus there is space available for technical installations such as lighting. The field for sports activities measures  $45 \times 25 \text{ m}^2$ , which is

the normal size for a handball field with safety perimeter. In addition, 5m width on one long end is dedicated to storage, wardrobes and mezzanine seating.

The flat roof construction is considered sufficiently stiff to prevent individual lattice girders from side movement. The roof is supported by 5 trusses of 2,0 m height and 2 end wall beams running across the width of the building. The girders are each supported by two 9 m high columns at the ends of their top rafters and they transfer axial loads onto the columns concentrically using nominally pinned joints. The columns are not given lateral restraint and their bases are also nominally pinned.

The end wall rafters are supported by 5 columns which are not considered in this study since they carry much less axial load than the long wall columns. Lateral and torsional stability of the building is accomplished by a cross bracing on all exterior walls. The column spacing is shown in Figure 5-2.

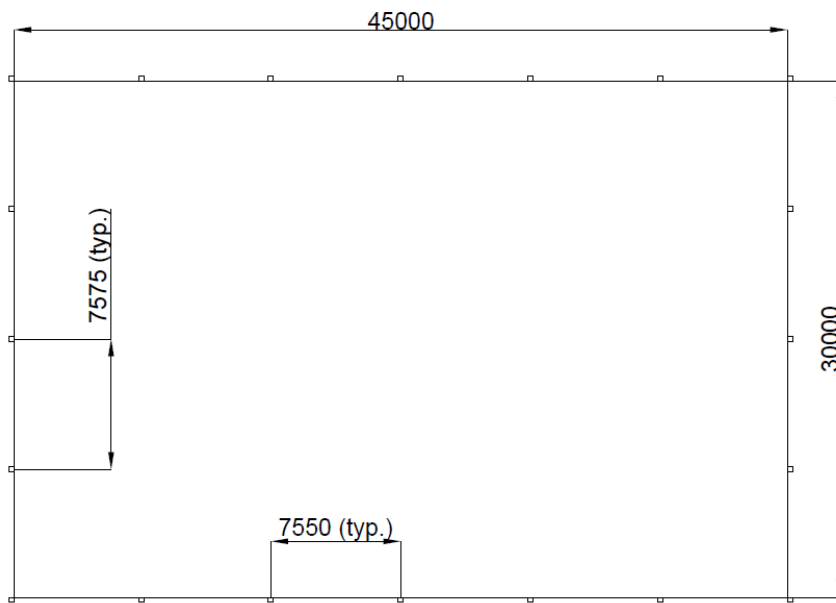


Figure 5-2: Column spacing, case study (measurements in mm)

#### Loads:

The building is envisioned to be located in the Kristiansand County in Norway directly adjacent to the sea. The snow and wind loads were calculated and provided by Rambøll with the following results:

- The snow load  $q_{\text{snow}}$  is 3,2 kN/m<sup>2</sup> for the whole roof area.
- The wind load onto the windward side wall is  $q_{\text{wind}}$  1,34 kN/m<sup>2</sup>, which is the sum of the external and internal wind pressures 0,94 kN/m<sup>2</sup> and 0,4 kN/m<sup>2</sup> respectively.

The snow and wind load calculations are attached in Appendix K. Seismic loads were ignored as it is located in an area of low seismic activity and it is assumed that the wind load will be dimensioning.

The self-weight of the roof construction (excluding the lattice girders) is assumed as  $g_{\text{roof}} = 1,0$  kN/m<sup>2</sup>. The self-weight of the girders and technical installations mounted on them is assumed as  $g_{\text{truss}} = 100$  kN per truss, see Figure K-1 in Appendix K. The self-weight of one column plus the supported wall plates and secondary wall structure is assumed to be  $g_{\text{wall}} = 30$  kN (regardless of the column size). The load eccentricity of the self-weight of the wall structure is assumed to be neglectible.

Three different fire resistances are considered: R15, R30 and R60. The first two are typical required resistances for this type of building. Sports halls are categorized as risk class 5 and for a one storey

building R15 is a pre-accepted fire resistance value for the main load bearing structure [47]. However, risk considerations, taking into account for instance the mezzanine seating and utilization of the building by handicapped persons, may increase the requirement to R30.

R60 load-bearing resistance is not typically required, but it may be required for a single wall if it is adjacent to another building.

#### Assumptions on loads:

- The wall and roof constructions are not provided in detail. Both are assumed to have some continuity over the columns and trusses with a continuity factor for the reaction forces assumed to be equal to  $k_c = 1,1$ .
- Regardless of the column size, the total width of the roof construction is considered to be equal to  $w_{\text{roof}} = 30,6$  m.
- The wind loads on the roof are not considered, since they give suction pressure on the windward side and only a low down pressure on the leeward side.

### 5.3 Case calculations

Two load combinations are calculated according to equation 6.10b in EC0 [61], with snow and wind as the leading imposed loads respectively. Due to the low self-weight in comparison to the snow load, the load cases using equation 6.10a will not be dimensioning. The load combination which will give the highest design loads in a fire scenario is using snow as the leading imposed load with factor  $\psi_1 = 0,5$  since the Norwegian Annex to EC0 states that wind then also should be considered with a factor  $\psi_1 = 0,2$ .

#### Calculation assumptions:

- It is assumed that regardless of column size, there is available space for thermal insulation and technical installations inside the wall.
- The wall cladding on the inner side of the exterior walls is not expected to provide any fire protection to the columns.
- Column bases and beam-to-column joints are adequately sized to provide the required structural and fire resistances.
- No design or verification of lattice girders, roof and wall constructions or wind bracing is done.
- The frame is non-sway due to wind bracing (a limited justification of this is given in Appendix K).
- The buckling length in a fire situation is set to  $L_{\text{et}} = 0,7h$  which is a conservative approach assuming that the rotational stiffness of the column base is limited. See also section 3.4.2.

The design actions are calculated in Appendix K and summarized in Table 5-1.

Table 5-1: Design actions, case study

$g=\text{permanent}$ $s=\text{snow}; w=\text{wind}$		<b>Snow (S)</b> $1,2g + 1,5s + 0,6*1,5w.$	<b>Wind (W)</b> $1,2g + 1,5w + 0,7*1,5s.$	<b>Fire (Fi)</b> $1g + 0,5s + 0,2s.$
<b>Axial force, due to permanent actions (kN)</b>	$N_{Ed,G}$	254,5	254,5	254,5
<b>Axial force, total (kN)</b>	$N_{Ed}$	864,4	681,4	415,4
<b>Distributed transverse load (kN/m)</b>	$Q_{Ed}$	10,0	16,7	2,2

### Steel section:

The required minimum steel column size (only HE-B sections are considered) to resist the design actions for the snow and wind load combinations is determined by a member verification in A3C:

- Snow load combination: HE-300B -> utilized capacity of 0,759.
- Wind load combination: HE-300B -> utilized capacity of 0,791.

Thus the selected steel reference member is HE-300B. A fire resistance verification for the fire loads in A3C yields that the maximum fire resistance duration is 22 minutes and the critical temperature  $\theta_{a,cr}$  is 648 °C. With a section factor  $A_m/V = 116 \text{ m}^{-1}$  the required thickness of fire protection board is taken from the product documentation [64] as 20 mm for both R30 and R60 sections (R15 resistance is ok without additional fire protection).

### Composite section:

Based on the results from chapter 0 the PEC cross-section clearly offers the best column depth reduction over steel for the fire load bearing resistances of R30 and R60 and therefore it is seemingly the preferred choice for all fire resistance levels in the case study. However as described under section 3.4.2 the minimum side must at least equal the column height divided by 30 (regardless of which type of composite cross-section is used). This means the cross-section must have sides of at least  $9000/30 \text{ mm} = 300 \text{ mm}$  to use the tabulated values. Furthermore, the cross-section must be calculated with twice the buckling length  $L_{fi}$  assumed in a fire situation:

$$L_{fi} = 2 * 0,7h = 2 * 0,7 * 9 = 12,6m$$

In order to achieve the minimum relative slenderness beneath 2 for a PEC profile with a steel H section and a buckling length of 12,6m; lateral restraint valid in a fire scenario for the minor axis must be provided. This can be difficult to provide for a PEC profile in practice since the web is encased. By instead following the simplified rules for PEC cross-sections in EC4, part 1-2 Annex G [4] it is stated that the buckling length in a fire situation can assume a maximum value of  $13,5b$ ; where  $b$  is the width of the cross-section. For the selected case, this gives a minimum cross-sectional side value of  $9000*0,7/13,5 = 467\text{mm}$ .

## 5.4 Case results

The column is calculated in A3C for the snow and wind load scenarios to find the minimum cross-sectional dimensions. The results are shown in Table 5-2. Note that the required steel sections in a fire scenario are taken as the minimum required for the snow and wind loads.

Table 5-2: Case study results

	Snow (S)	Wind (S)	Fire (Fi) – R15	Fire (Fi) – R30	Fire (Fi) – R60
<b>Steel column</b>					
Steel section	HE-300B	HE-300B	HE-300B	HE-300B	HE-300B
Fire protection board thickness	0mm	0mm	0mm	20mm	20mm
Total steel area	14908 mm <sup>2</sup>	14908 mm <sup>2</sup>	14908 mm <sup>2</sup>	14908 mm <sup>2</sup>	14908 mm <sup>2</sup>
Minimum depth of column	300mm	300mm	300mm	340mm	340mm
<b>Partially encased composite (PEC) column</b>					
Steel section	HE-240A	HE-240A	HE-240B*	N/A**	N/A**
Concrete	C40/50	C40/50	C40/50	N/A	N/A
Reinforcement	4 x Ø14mm	4 x Ø20mm	4xØ25mm	N/A	N/A
Minimum depth of column	230mm	230mm	N/A	N/A	N/A
<b>Comparison</b>					
Difference, depth of column (Steel – PEC)	70mm	70mm	60mm		
Comments: * The PEC cross-section is calculated as the constituent unprotected steel section for the R15 fire resistance, using EC3, part 1-2 [13]. ** Cannot be calculated by the EC4, part 1-2 [4]					

Due to time restraint within the thesis, the PEC column have not been calculated using advanced calculation rules, which would be necessary to confirm the load-bearing fire resistances for R30 and R60. In order to get an indication on how the PEC column would behave in R30 and R60 fire scenarios, a column is calculated in accordance to the rules of Annex G of EC4, part 1-2 [4]. The results are only indicative since the buckling length in a fire scenario exceeds the given limitations. The calculations require determination of the buckling resistance of a composite member with an eccentric axial load. The moment from the wind loads is therefore converted into an eccentricity. There is limited guidance on how to determine the buckling resistance for eccentric loads; thus a method recommended by Arezki et al. is used. This is the Campus-Massonet criteria, originally developed for buckling of an eccentrically loaded steel columns [74].

The cross-section which is chosen is an HE-240B profile of S355 grade, with C40/50 grade concrete and 4xØ25 mm longitudinal rebars of B500NC grade. This dimension is chosen since it has been calculated in A3C to provide 16 min fire load bearing resistance as a bare steel column against the dimensioning fire loads and therefore assumed to provide R15 load bearing resistance also for the PEC column. This is a justifiable assumption, since the concrete provides thermal insulation of the steel web and flange backsides. In addition, the concrete and reinforcement provides additional strength and stiffness.

The indicative Annex G calculations are provided in Appendix K and the resulting utilization grades (design loads divided by design load resistances) are given by Table 5-3.

Table 5-3: Indicative calculation of the utilization of the case study column in a fire scenario, using EC4 part 1-2 Annex G [4]

<b>ULS criteria</b>	<b>R30 - utilization</b>	<b>R60 -utilization</b>
Yield due to axial force:	0,13	0,2
Axial force buckling resistance about the minor axis:	0,59	1,0 (slightly above)
Axial force buckling resistance about the major axis (including a load eccentricity):	0,58	1,0 (slightly above)

As can be seen by the results, the buckling resistances are essentially equal for buckling about the major/minor axes. However, the major axis buckling resistance is calculated with a conservative consideration that the maximum moment from the wind load (parabolic BMD) is directly used as a load eccentricity (constant BMD). Therefore, likely the minor axis buckling resistance is dimensioning if a more exact approach is taken.

## 6 Discussion/Conclusions

### 6.1 Discussion

Already by the worked example in chapter 3, it is shown that an a large improvement in all ULS member resistances can be achieved by encasing a steel HE-300B profile in concrete, with the exception of shear resistance which rarely is an issue for a column. However, the chapter is only meant to display the Eurocode calculation methods and the results given are not necessarily indicative for other cases. Below are discussions for the results from each of the parametric studies as well as the case study.

#### Span length, ref section 4.2

The span length in an ideally pinned frame structure is significantly increased by using an FEC or PEC column instead of a steel column. The effect is larger for thin steel profiles; using a column with a FEC HE-A section with C50/60 concrete and 4xØ12mm rebar could more than double the span achieved by the steel section alone, while the span is increased by roughly 50% by using a PEC HE-A member. For a HE-B section the gains in span length are smaller, but they still reach 70% and above for the FEC and 30% for the PEC column. Even for the thick flanged HE-M members, there is a notable increase in span length by using a composite member. Since CFT profiles uses CHS steel sections it is difficult to compare them directly to H-profiles. However the cross-sectional area of a CHS steel section of 10mm thickness compares reasonable to HE-A members of similar depth. By using these cross-sections; CFT sections show an improvement in span length of between 70% and 100% compared to steel HE-A members.

Increasing the concrete strength in order to gain increased column strength and stiffness is likely economical. Much of the extra costs attributed to the concrete is due to formwork, reinforcement work/material and transporting logistics, all which are not related to the strength of the concrete. Thus; unless there are good reasons (such as availability) it is reasonable to use the strongest concrete allowed (C50/60). This approach is also good in fire scenarios, since concrete is less adversely affected in temperature than steel. Calculations on the pinned frame show that frames with FEC and CFT columns in average gain 20-25% in span length with C50/60 when compared to concrete of half the strength. Frames with PEC columns gain on average 11% span length.

Changing the diameter of the rebars have the largest effect on the FEC member, since the rebar is located furthest away from the neutral axis and thus have the largest effect on bending or buckling resistance. An increase in span length of 27% on average (and above 40% for some cases) is noted by using 4xØ25mm instead of 4xØ12mm longitudinal reinforcement. Rebar also have a larger yield strength than structural steel members and the material cost is cheaper, as shown in section 4.4. Thus for an FEC member it is wise to dimension the rebar as large as allowed (maximum 6% reinforcement ratio).

The diameter of the rebars in the PEC section has a relatively low effect on the maximum span length which also can be seen by the calculations in section 4.4. The calculated example showed an increase in span length of 8% by using Ø25 instead of Ø12 rebar. Longitudinal reinforcement is required for the PEC member, but unless extra is required for fire protection purpose, it may be economical to keep the reinforcement area at the minimum required size (0,03% reinforcement ratio or 12mm if fire protection is required) and instead increase the steel section dimensions if more strength is required.

CFT members also have a relatively low gain in span length from using the larger sized reinforcement bars (10% increase in average). Reinforcement is not required unless for fire protection purpose. Thus

for a column without fire protection requirements it may be beneficial to avoid reinforcement altogether in order to simplify the casting work and to reduce the cost and construction time.

By having a rigid instead of a pinned frame, the column span lengths are increased by an average of 12% for both FEC and PEC columns and 4% for the CFT columns. This effect is due to a more even distribution of the beam reaction forces onto the columns. If the columns are continuous instead of the beams for the pinned frame (this was not tested in the study) it is possible that the span lengths of the pinned frame would exceed those of the rigid frame, due to a lower end moments in the columns. However, an increased span length for the rigid frame may still be possible if the dimensioning members are the beams, since the sagging moments in them are reduced. The reasoning for the rigid frame is assumed to be valid also for a semi-rigid frame, although with a less difference to the pinned frame.

#### Column depth reduction, ref section 0

Based on the results using the tabulated EC4 values, it is not possible to describe the difference in the required column depth between steel columns and any of the composite columns in a consistent matter. For instance, the CFT cross-section is thicker than the steel section for R90 protection, while it is more slender both for R30 and R180. This general behaviour is expected, due to the way the EC4-1-2 tables 4.4 to 4.7 are formulated, where the cross-section either is calculated from the design loads or set to a constant (whichever is the smallest).

The results are too wide-spread to allow for a definitive answer on how much the column depth be reduced. However, it is possible to see which type of composite column provides the largest depth reduction when compared to a steel column:

- R0: PEC, or CFT if the moments are low
- R30: PEC to a large degree
- R60: None, unless the loads are high; in that case PEC.
- R90: FEC, or PEC if the loads are high.
- R120: FEC.
- R180: FEC

The R0 graph (see Figure F-2 in Appendix F) provides some indicative results on how the different cross-sections compare towards steel for a certain type of loading. The most striking observation is that the CFT section has a decrease in depth reduction for increasing end moments. This is likely due to the comparatively lower plastic section modulus of a circular hollow steel section to that of an H-profile of the same depth, making it less resistant to bending.

#### Steel efficiency, ref section 4.4

The steel efficiency (a term developed in this thesis to compare the column resistance vs. the amount of steel used) is compared between steel, PEC and to a limited degree CFT columns. The CFT columns have a very high steel efficiency in axial compression; on average double that of steel H profiles for columns with a depth of approximately 200 to 400mm. This is largely due to being able to increase the long-term concrete strength factor from 0,85 to 1 and due to the more favourable buckling curve for this type of cross-section. The PEC column which requires a less favourable buckling curve showed more moderate improvements in steel efficiency, on average 20% to 30%.

A more extensive comparison between the steel and PEC cross-section shows that the type of cross-section matters largely. The largest difference for H-profiles of nominal sizes 200,300 and 400mm is



interestingly shown for the HE-300 cross-section, since the steel section has an unfavourable buckling curve when the height to depth ratio is beneath 1,2.

In general, the buckling curve is less favourable for the PEC cross-section and therefore the steel efficiency difference is less at larger buckling lengths. The opposite behaviour is noted for increasing bending moments, which should be a result of a lesser slope in the MN interaction diagram for the PEC column.

#### Environmental footprint, ref section 4.5

Both the production of FEC and PEC columns shows potential to have a lower total global warming potential and lower energy use than that of producing the steel columns required for equivalent structural loads. These composite columns are likely to be pre-fabricated due to the complexity involved with formwork and reinforcement. What type of effect this has on the environmental calculations is not estimated; but assumedly it is beneficial since it requires less energy on the construction site but more in the factory where it should be easier to provide green energy. The production process can be more optimized and the amount of material waste can likely be reduced. The production of a CFT column, (which by far is the most commonly employed type of composite column in Norway) has a larger global warming potential than a steel H-section.

While not studied, the transport and construction work for composite columns will reasonably require more energy and emit more CO<sub>2</sub> mass equivalents than that of steel columns. This is due to the double transport (both from the steel and the concrete manufacturer) and the extra labour involved with formwork, reinforcing and casting of the concrete. On the other hand, the composite column may possibly provide other advantages, such as no need for fire protection material and CO<sub>2</sub> uptake through carbonation. The potentially beneficial effects from recycling the building materials at the end of the column life span (here assumed as 50 year) is a topic which is very hard to predict, but the composite columns are reasonably more difficult to recycle since the concrete have to be separated from the steel.

The EPD for the H-profile and CHS steel sections [68,69,70] used as basis in this study all have a validity to June 2019 and they will assumedly be revised afterwards. If significantly new values are given, it would be interesting to see the effect on this study.

#### Case study, ref chapter 5

In the selected case, the column depth has a direct impact in the exterior foot-print of the building. If the column depth can be reduced, savings in building material can be made both in steel amount in the columns but also for the wall, roof and foundation constructions. Similar results should be expected for all cases when the columns are hid inside walls. In many other applications such as industrial, the columns can be visible and therefore a building footprint reduction is not necessarily accomplished by using a composite cross-section. However, thinner columns may increase the flexibility in usage of the building when for instance available paths for fork lifts or bridge cranes are considered. If the composite columns are pre-fabricated, there is likely also a saving in construction time when compared to a fire protected steel column since fire protection boards typically have to be mounted on-site.

The case study showed that the cross-sectional size of the columns can be reduced significantly for the normal temperature scenarios, when using a PEC cross-section (HE-240A) instead of a steel section (HE-300B). However, due to the height restrictions in EC4 part 1-2 [4], the fire resistance of the composite columns cannot be determined through simple means unless the smallest side of the

column is at least  $1/30^{\text{th}}$  of the height. For the 9 m high columns in the case study, this means the PEC columns require at least 300 mm side lengths, which is a profile which equals that of the unprotected steel section (HE-300B). For R15 fire resistance, the steel section of the PEC column should be possible to calculate as an unprotected steel column in accordance to EC3, part 1-2 [13] and then pass the design fire loads with a partially encased steel section of HE-240B.

Advanced fire calculations may also show that the PEC cross-section also is sufficient for R30 resistance, since an indicative calculation using the Annex G of EC 4, part 1-2 [4] showed that the utilization is only  $\sim 60\%$  in the R30 fire scenario. It is not likely that the cross-section will be sufficient for R60 fire resistance since the utilization is slightly above 100% for that scenario. Still, the typical fire resistance requirements in single-storey halls such as the one used for the case study is R15 or R30 and the PEC column may thus be possible to use with a HE-240B profile which is a significant decrease in depth compared to the steel HE-300B section required.

## 6.2 Conclusions

These conclusions regards the behaviour of composite columns compared to structural steel columns when calculated according to the simplified Eurocode rules.

- Composite columns increases the maximum possible span between columns in a braced rectangular frame considerable. The increase is similar for a pinned frame with continuous beams and for a rigid frame. For many frames with composite columns, the horizontal members will be dimensioning for the span. Composite columns are therefore mostly useful when the axial loads are high (for instance bottom columns in a high-rise building) or when the horizontal members have a high moment resistance (e.g. trusses).
- The column cross-sectional depth can usually be decreased for any design fire resistance when using the proper type of composite column. This reduction is most consistent and significant for the PEC cross-section at R30 and the FEC cross-section at R90 to R180. The depth reduction for a free-standing composite column will be higher if additional boards (e.g. gypsum) are provided on top of the fire protection boards for the steel column. On the other hand, it will be less if the steel column is protected by intumescent paint.
- CFT columns have above double the structural resistance to that of a steel column per steel amount used when exerted to axial loads only. CFT columns can be made without reinforcement (when fire loads are not relevant). Doing so is economic with regards to the steel amount used, for not requiring reinforcement work and likely for making the concrete compacting easier.

Using PEC columns instead of CFT on saves considerably less on steel material on average, although for high bending moments and short buckling lengths they can also reach up to and above double the structural resistance when compared to a steel column.

- Considering only the production of the constituent materials and using available data, PEC and FEC have a smaller environmental footprint, both when considering the generation of greenhouse gasses and the energy use. The CFT columns are seemingly environmentally worse than steel H-profiles when the generation of greenhouse gases is concerned.
- Both the tabulated values and the simple calculation rules in the fire design section of Eurocode 4, part 1-2 [4] include multiple restrictions and requirements to the dimensions and reinforcement of composite columns. In ambient temperatures long composite columns with low axial loads are limited by their relative slenderness, but they are restricted to 30 times their smallest side length in a fire scenario. This limits the benefits of using composite columns in a high ceiling, hall type of building. Based on an investigative study it seems likely that

advanced fire calculations can show that a PEC column can endure up to R30 fire loads with a significantly smaller depth than a steel column.

All in all, there are multiple benefits of using composite instead of steel columns and each of the parametric studies showed significant improvements for the studied criterion. For uncomplicated geometries, where members can be verified as single members or for simple, braced frame geometries, the composite columns are not significantly more difficult to calculate than steel columns. With a design perspective, they are easier to optimize due to having more configurable parameters. However, for geometries where second order effects must be analysed by advanced methods (such as sway frames or complicated geometries) there is little clear guidance on how to calculate composite columns and few available tools to do so.

### 6.3 Further work

The following further work in the fields of composite columns is proposed to get an even better insight into whether they could be utilized more in Norway:

- This thesis focuses on finding whether there are situations where composite columns would be preferred instead of steel columns. For a more complete picture, they should also be compared to ordinary reinforced concrete columns.
- Two important but uncovered topics which are relevant for choosing the best type of column for a building project are the advantages/disadvantages for the construction method/time and economic differences, which could be studied (in Norwegian perspective).
- In difference to CFT columns; FEC or PEC columns show potential to be an environmentally preferred option when slender columns are required. More comprehensive studies including factors related to transport, construction and long life considerations may show whether this is correct.
- The case study shows that there is a potential to get a decrease in the column cross-section for long columns with a low axial load by using a PEC instead of a steel section. Typical uses of such columns are single-storey hall structures. However, if the columns are meant to resist fire they cannot be calculated according to the simple calculation rules given by EC4 due to dimensional limitations. It may be possible to use advanced FEM calculations or fire tests to determine the behaviour of such columns and possibly show that they are ok for low fire loads (up to R30).

## 7 References

- [1] Kurrer KE. The History of the Theory of Structures (English translation). Berlin: Ernst & Sohn Verlag für Architektur und technische Wissenschaften; 2008
- [2] Company information on Rambøll webpage [Internet]. [cited 2019 Apr 14]. Available from: <https://no.ramboll.com/about-us>.
- [3] Standard Norge. NS-EN 1994-1-1:2004+NA:2009. Eurocode 4: Design of composite steel and concrete structures, Part 1-1: General rules and rules for buildings. Oslo: SN; 2009.
- [4] Standard Norge. NS-EN 1994-1-2:2005+A1:2014+NA:2018. Eurocode 4: Design of composite steel and concrete structures, Part 1-2: General rules – Structural fire design. Oslo: SN; 2005.
- [5] Standard Norge. NS-EN 1994-2:2005+NA:2009. Eurocode 4: Design of composite steel and concrete structures – Part 2: General rules and rules for bridges. Oslo: SN; 2002.
- [6] Eggemann H. Development of composite columns: Emperger's effort. In: Huerta S, Juan de Herrera I, Benvenuto AE, Dragados F, editors. Proceedings of the First International Congress of Construction History, 20th-24th January 2003. Madrid; 2003.
- [7] Basteskår M, Birkeland M, Knutsson Koren A. Bakgrunn for beregningsregler etter Eurokode for slanke betongsøyler, samvirkesøyler og forankring av lengdearmering. [Unpublished master's thesis]. Trondheim: NTNU; 2014.
- [8] Stark JWB. New developments in Eurocode 4. In: Easterling WS, Roddis KWM editors. Proceedings of An Engineering Foundation Conference, 14th-19th June. Trout Lodge Potosi Missouri; 1992.
- [9] Thackery R, Burdekin M. Applied metallurgy of steel. In: Davison B, Owens GW, editors. Steel designers' manual. 7th ed. Chichester: Wiley-Blackwell; 2012. p. 305-330.
- [10] Trahair NS, Bradford MA, Nethercot DA, Gardner L, The behaviour and design of steel structures to EC3. 4th ed. Abingdon: Taylor & Francis; 2008.
- [11] Comité Européen de Normalisation. EN10027-1, Designation systems for steels – Part 1: Steel names. Brussels: CEN; 2005.
- [12] Kodur VKR, Harmathy TZ. Properties of Building Materials. In: Hurley MJ, Gottuk D, Hall JR, Harada K, et al. editors. SFPE Handbook of Fire Protection Engineering. 5th ed. New York:Springer; 2016. p. 277-324.
- [13] Standard Norge. NS-EN 1993-1-2:2005+NA:2009. Eurocode 3: Design of steel structures, Part 1-2: General rules – Structural fire design. Oslo: SN; 2005.
- [14] S. Jacobsen, editor. Concrete Technology. Trondheim: NTNU; 2016.
- [15] Standard Norge. NS-EN 1992-1-1:2004+A1:2014+NA:2018. Eurocode 2: Design of concrete structures, Part 1-1: General rules and rules for buildings. Oslo: SN; 2004.
- [16] Hassoun MN, Al-Manaseer A. Structural concrete theory and design, 6th ed. Hoboken: Wiley; 2015.
- [17] Standard Norge. NS-EN 1992-1-2:2004+NA:2010. Eurocode 2: Design of concrete structures– Part 1-2: General rules - Structural fire design. Oslo: SN; 2004.

- [18] Fletcher IA, Welch S, Torero JL, Carvel RO, Usmani A. The behaviour of concrete structures in fire. Edinburgh: BRE Centre for Fire Safety Engineering, The University of Edinburgh; 2007
- [19] Sandvik M, Fjell B, Betongteknologi 2, Hefte 3. Herdet Betong. Ullandhaug: Høgskolesenteret i Rogaland; 1992.
- [20] Standard Norge. NS 3576-3:2012. Armeringsstål – Mål og egenskaper – Del 1-5. Oslo: SN; 2012.
- [21] Standard Norge. NS-EN 1998-1:2004+A1:2013+NA:2014. Eurocode 8: Design of structures for earthquake resistance – Part 1: General rules, seismic actions and rules for buildings. Oslo: SN; 2002.
- [22] Lawson M. Composite slabs. In: Davison B, Owens GW, editors. Steel designers' manual. 7th ed. Chichester: Wiley-Blackwell; 2012. p. 623-646.
- [23] Lawson M, Chung KF. Composite beams. In: Davison B, Owens GW, editors. Steel designers' manual. 7th ed. Chichester: Wiley-Blackwell; 2012. p. 647-700.
- [24] Chung KF, Lawson M. Composite columns. In: Davison B, Owens GW, editors. Steel designers' manual. 7th ed. Chichester: Wiley-Blackwell; 2012. p. 701-732.
- [25] Johnson RP. Composite structures of steel and concrete. 3rd ed. Oxford: Blackwell Publishing; 2004.
- [26] Stark JWB. Composite steel and concrete beams with partial shear connection. Delft: HERON vol.34 no.4;1989.
- [27] Kumar P, Patnaik A, Chaudhary S. A review on application of structural adhesives in concrete and steel–concrete composite and factors influencing the performance of composite connections. Int J Adhes Adhes. 2017; 77: 1-14.
- [28] Kvočák V, Drab L. Partially-encased composite thin-walled steel beams. Procedia Engineer. 2012; 40:91-95.
- [29] Standard Norge. NS-EN 1993-1-1:2005+A1:2014+NA:2015. Eurocode 3: Design of steel structures, Part 1-1: General rules and rules for buildings. Oslo: SN; 2005.
- [30] Rackham JW, Couchman GH, Hicks SJ. Composite Slabs and Beams using Steel Decking: Best Practice for Design and Construction. London: MCRMA; 2009. MCRMA Technical Paper No.13 (Revised edition).
- [31] Bemessungshilfe Integrierte Deckenträger in Verbundbauweise CoSFB [Internet]. Düsseldorf: Bauforumstahl; 2016 [cited 2019 Mar 11]. Available from: [https://bauforumstahl.de/upload/documents/publikationen/Bemessungshilfe\\_Deckentrager\\_neu.pdf](https://bauforumstahl.de/upload/documents/publikationen/Bemessungshilfe_Deckentrager_neu.pdf)
- [32] Fei D, Tao C. Performance and capacity of isolated steel reinforced concrete columns and design approaches [Internet]. Beijing: CABR. Available from: [http://sections.arcelormittal.com/uploads/tx\\_abdownloads/files/CompositeMegaColumns\\_Full\\_Report.pdf](http://sections.arcelormittal.com/uploads/tx_abdownloads/files/CompositeMegaColumns_Full_Report.pdf)
- [33] Standard Norge. NS-EN 1993-1-8:2005+NA:2009. Eurocode 3: Design of steel structures, Part 1-8: Design of joints. Oslo: SN; 2005.

- [34] Claeson-Jonsson C. Användning av samverkanspelare. Göteborg: FOU-Väst; 2003. Report 0301.
- [35] Uy, B. Modern design, construction and maintenance of composite steel-concrete structures: Australian experiences. Selected Key Note papers from MPDCMS 1 1st International Conference on Modern Design, Construction and Maintenance of Structures – Hanoi, Vietnam; 2007
- [36] Huber, G. Semi-Continuous Beam-to-column joints at the Millennium tower in Vienna, Austria. Fourth International Workshop on Connections in Steel Structures Oct 22-25, Roanoke, USA; 2000
- [37] Stark R, Schuurman R. Practical experience with composite structures in the Netherlands. In: Leon RT, Lange J editors. Proceedings of Composite Construction in Steel and Concrete V, 18th-23th July. Kruger National Park, South Africa; 2004.
- [38] Deutsches Institut für Normung. DIN 1025-5. Hot rolled I and H sections (IPB series) – Dimensions, mass and static parameters. Berlin: DIN; 1995
- [39] Dujmović D, Androić B, Lukačević I. Composite structures according to Eurocode 4 – Worked examples. Berlin: Wiley/Ernst & Sohn; 2015.
- [40] Bzdawka K. Composite Column – Calculation Examples. Tampere: Tampere University of Technology; 2010. Research Report 147
- [41] Boresi AP, Schmidt RJ. Advanced mechanics of materials. 6th ed. Hoboken: Wiley; 2003
- [42] A3C. v 2.89 [Internet]. Luxembourg: ArcelorMittal and CTICM; 2018. [cited 2018 Dec 16]. Available from: <http://sections.arcelormittal.com/download-center/design-software/composite-solutions.html>
- [43] Hanswille G. Eurocode 4 Composite Columns [Internet]. Wuppertal: University of Wuppertal; 2008 [cited 2019 Mar 11]. Available from: [https://eurocodes.jrc.ec.europa.eu/doc/WS2008/EN1994\\_4\\_Hanswille.pdf](https://eurocodes.jrc.ec.europa.eu/doc/WS2008/EN1994_4_Hanswille.pdf)
- [44] Bureau A, Galéa. Elastic critical moment for lateral torsional buckling [Internet]. Access steel; 2008 [cited 2019 Mar 03]. Available from: <https://eurocodes.jrc.ec.europa.eu/doc/WS2008/SN003a-EN-EU.pdf>
- [45] Vassart O, Zhao B, Cajot LG, Robert F, Meyer U, Frangi A. Eurocodes: Background & Applications Structural Fire Design, Worked examples. In: Poljanšek M, Nikolova B, Sousa L, Dimova S, Pinto A editors. Luxemburg: Joint Research Centre; 2014. Report EUR 26698 EN.
- [46] Standard Norge. NS-EN 1991-1-2:2002+NA:2008. Eurocode 1: Actions on structures, Part 1-2: General actions – Actions on structures exposed to fire. Oslo: SN; 2002.
- [47] Direktoratet for byggkvalitet. Veiledning om tekniske krav til byggverk, Byggteknisk forskrift (TEK17) med veiledning. Oslo: DiBK; 2017.
- [48] Walton WD, Carpenter DJ, Wood CB. Zone Computer Fire Models for Enclosures. In: Hurley MJ, Gottuk D, Hall JR, Harada K, et al. editors. SFPE Handbook of Fire Protection Engineering. 5th ed. New York:Springer; 2016. p. 1024-1033.

- [49] McGrattan K, Miles S. Modeling Fires Using Computational Fluid Dynamics (CFD). In: Hurley MJ, Gottuk D, Hall JR, Harada K, et al. editors. SFPE Handbook of Fire Protection Engineering. 5th ed. New York:Springer; 2016. p. 1025-1065
- [50] Real PV, EN 1993-1-2 Resistance of members and connections to fire [Internet]. Brussels: European commission; 2014 [cited 2019 Mar 11]. Available from: [https://eurocodes.jrc.ec.europa.eu/doc/2014\\_07\\_WS\\_Steel/presentations/10\\_Eurocodes\\_Steel\\_Workshop\\_VILA\\_REAL.pdf](https://eurocodes.jrc.ec.europa.eu/doc/2014_07_WS_Steel/presentations/10_Eurocodes_Steel_Workshop_VILA_REAL.pdf)
- [51] Rodrigues JPC, Correia AJM, Pires TAC. Behaviour of composite columns made of totally encased steel sections in fire. J Constr Steel Res. 2015;105:97-106.
- [52] Mao X, Kodur VKR. Fire resistance of concrete encased steel columns under 3- and 4-side standard heating. J Constr Steel Res. 2011;67:270-280.
- [53] Fellouh A, Benlakehal N, Piloto P, Ramos A, Mesquita L. Load carrying capacity of partially encased columns for different fire ratings. Fire res. 2017; 1:23:13-19.
- [54] Standard Norge. NS-EN 1991-1-7:2006+NA:2008. Eurocode 1: Actions on structures, Part 1-7: General actions – Accidental actions. Oslo: SN; 2006.
- [55] Han LH, Hou CC, Zhao, XL, Rasmussen, KJR. Behaviour of high-strength concrete filled steel tubes under transverse impact loading. J Constr Steel Res. 2014;92:25-39.
- [56] Hauke B, et al. COSIMB Composite column and wall systems for impact and blast resistance [Internet]. Brussels: EC Research Fund for Coal and Steel; 2007 [cited 2019 Apr 2]. Available from: <https://publications.europa.eu/en/publication-detail/-/publication/283ca9a3-42c3-4825-a46a-ff11c3611ace>
- [57] Zalosh R. Flammable Gas and Vapor Explosions. In: Hurley MJ, Gottuk D, Hall JR, Harada K, et al. editors. SFPE Handbook of Fire Protection Engineering. 5th ed. New York:Springer; 2016. p. 2738-2765.
- [58] Rønnquist A, Remseth S, Lindholm C. Earthquake engineering design practice in Norway: Implementation of Eurocode 8. 15th World Conference on Earthquake engineering 15WCEE, Lisbon, 2012.
- [59] Austrell PA, Dahlblom O, Lindeman J, Olsson A, et al. CALFEM A Finite element toolbox version 3.4 [Internet]. Lund: Lund University; 2004 [cited 2019 11 Mar 03]. Available from: [http://www.solid.lth.se/fileadmin/hallfasthetslara/utbildning/kurser/FHL064\\_FEM/calfem34.pdf](http://www.solid.lth.se/fileadmin/hallfasthetslara/utbildning/kurser/FHL064_FEM/calfem34.pdf)
- [60] Mathisen KM. Finite element modelling of structural mechanics problems [Internet] [cited 2019 Apr 27]; 2012. Available from <https://www.sintef.no/globalassets/project/evitameeting/2012/kmm-geilo-2012-lecture-10.pdf>.
- [61] Standard Norge. NS-EN 1990:2002+A1:2005+NA:2016. Eurocode: Basis of structural design. Oslo: SN; 2002.
- [62] Gonçalves R, Carvalho J. An efficient geometrically exact beam element for composite columns and its application to concrete encased steel I-sections. Eng Struct. 2014; 75:213-224.
- [63] da S Vellasco PCGdS, de Andrade SAL, da Silva JGS, de Lima LRO, Brito Jr O. A parametric analysis of steel and composite portal frames with semi-rigid connections. Eng Struct. 2006. 28:543-556

- [64] Produktdokumentasjon SINTEF 010-0253 (Rockwool Conlit 150/150P). Trondheim: SINTEF; 2013.
- [65] Norsk Stål. Prislister Januar 2019 [Internet]. [Cited 2019 Jan 19]. Available from <https://produktkatalog.norskstaal.no/>
- [66] Bernhard P, Jørgensen PF. Byggsektorens CO<sub>2</sub>-utslipp. KanEnergi. Oslo; 2006.
- [67] Standard Norge. NS-EN ISO 14025:2010. Environmental labels and declarations – Type III environmental declarations – Principles and procedures. Oslo: SN; 2010.
- [68] Norwegian Steel Association. Environmental product declaration, Generic EPD I,H,U,L,T and wide flats hot-rolled sections (Type 2.1) [Internet] [Cited 2019 May 23]. Oslo; 2014. Declaration number NEPD 00252E. Available from <https://norskstaal.no/produkter/epd-environmental-product-declaration/>.
- [69] Norwegian Steel Association. Environmental product declaration, Generic EPD Hot finished structural hollow sections (Type 4.1) [Internet] [Cited 2019 May 23]. Oslo; 2014. Declaration number NEPD 00254E. Available from <https://norskstaal.no/produkter/epd-environmental-product-declaration/>.
- [70] Norwegian Steel Association. Environmental product declaration, Generic EPD Cold formed welded structural hollow sections (Type 3.1) [Internet] [Cited 2019 May 23]. Oslo; 2014. Declaration number NEPD 00253E. Available from <https://norskstaal.no/produkter/epd-environmental-product-declaration/>.
- [71] Norsk Stål AS. Environmental product declaration, Ribbed reinforcement bars [Internet] [Cited 2019 May 23]. Søgne; 2015. Declaration number NEPD-347-238-EN. Available from <https://norskstaal.no/produkter/epd-environmental-product-declaration/>.
- [72] Velde Betong AS. 1M3.B45 M40 <200mm [Internet] [Cited 2019 May 23]. Sandnes; 2015. Declaration number NEPD-33-217-NO. Available from <https://www.epd-norge.no/ferdig-betong/category317.html>
- [73] Kulturdepartementet. Idrettshaller, Planlegging og Bygging. Oslo; 2016. Report V-0989 B.
- [74] Arezki S, Illouli S. In: Diouri A, Khachan N, Talbi MA editors. Practical fire design of partially encased composite steel-concrete columns according to Eurocode 4. MATEC Web of Conferences vol.11, 26th-30th November 2013. Rabat; 2014.
- [75] Standard Norge. NS-EN 1991-1-1:2002+NA:2008. Eurocode 1: Actions on structures, Part 1-2: General actions – Densities, self-weight, imposed loads for buildings. Oslo: SN; 2002.
- [76] Calculation tool for lattice girders, Maku webpage [Internet]. [cited 2019 Jun 06]. Available from: <http://maku.se/default.asp?ID=OFFERT&sLang=sv-se>.



## Appendix A. Worked example – ULS verification of HE-300B steel column

This appendix displays the ULS verification calculations for a HE-300B steel cross-section, which are done according to EC3, part 1-1 [29].

Where the resistance is dependent on the magnitude of the loads and multiple values are calculated (e.g. moment resistance dependency of design axial force); only the formulae are given. The calculations themselves are done in an MS Excel spreadsheet.

The relevant section geometry and material properties are given in Table A-1.

Table A-1: HEB-300 steel section geometrical and material properties:

<b>Geometrical properties – HE300B cross-section, from [42]</b>		
	Section dimensions	See Figure 3-2
$A_a$	Cross-section area	14908mm <sup>2</sup>
$I_{a,y}$	Second moment of area, Major axis	251,66*10 <sup>6</sup> mm <sup>4</sup>
$I_{a,z}$	Second moment of area, Minor axis	85,63*10 <sup>6</sup> mm <sup>4</sup>
$I_{a,t}$	Torsional constant	1858*10 <sup>3</sup> mm <sup>4</sup>
$I_{a,w}$	Warping constant	1688*10 <sup>9</sup> mm <sup>6</sup>
$W_{a,z}$	Elastic section modulus, minor axis	1680*10 <sup>3</sup> mm <sup>3</sup>
$Z_{a,y}$	Plastic section modulus, major axis	1869*10 <sup>3</sup> mm <sup>3</sup>
$Z_{a,z}$	Plastic section modulus, minor axis	870*10 <sup>3</sup> mm <sup>3</sup>
<b>Material properties (S355, t&lt;40mm) – EC3, part 1-1 [29]</b>		
$f_y$	Yield strength	355 MPa
$E_a$	Elastic Modulus	210 GPa
$G_a$	Shear Modulus	81 GPa
$\nu_a$	Poisson's ratio	0,3
$\epsilon$	Coefficient for class classification	0,81

### Cross-sectional compression resistance:

Class classification to compression:

Web:

$$\frac{c}{t\epsilon} = \frac{h - 2(r + t_f)}{t_w\epsilon} = \frac{300 - 2(27 + 19)}{11 * 0,81} = 23,3 < 33 \text{ (Class 1!)}$$

Flanges:

$$\frac{c}{t\epsilon} = \frac{b - t_w - 2r}{2t_f\epsilon} = \frac{300 - 11 - 2 * 27}{2 * 19 * 0,81} = 7,6 < 9 \text{ (Class 1!)}$$

Conclusion: HEB-300 cross-section classified to class 1.

Resistance towards squash load:

$$N_{pl,a,Rd} = \frac{A_a f_y}{\gamma_{M0}} = \frac{14908 * 355}{1,05} N = 5040 \text{ kN}$$

### Cross-sectional compression + uniaxial bending resistance:

Class 1: Calculating the plastic moment resistance for uni-axial bending, one for each axis:

For bending about the major axis:

$$M_{pl,a,y,Rd} = \frac{Z_{a,y} * f_y}{\gamma_{M0}} = \frac{1869 * 10^3 * 355}{1,05} Nmm = 631kNm$$

For bending about the minor axis:

$$M_{pl,a,z,Rd} = \frac{Z_{a,z} * f_y}{\gamma_{M0}} = \frac{870 * 10^3 * 355}{1,05} Nmm = 294kNm$$

Thresholds when axial force should not be considered:

For bending about the major axis:

$$\begin{aligned} N_{Ed} &\leq \min\left(0,25N_{pl,Rd}; \frac{0,5h_w t_w f_y}{\gamma_{M0}}\right) \\ &= \min\left(0,25 * 5040000; \frac{0,5 * (300 - 2 * (19 + 27)) * 11 * 355}{1,05}\right) \text{ kN} \\ &= 387 \text{ kN} \end{aligned}$$

For bending about the minor axis:

$$N_{Ed} \leq \frac{h_w t_w f_y}{\gamma_{M0}} = \frac{(300 - 2 * (19 + 27)) * 11 * 355}{1,05} \text{ kN} = 774 \text{ kN}$$

Factors for moment resistance:

$$a = \min\left(\frac{A - 2bt_f}{A}; 0,5\right) = \min\left(\frac{14908 - 2 * 300 * 11}{14908}; 0,5\right) = 0,235$$

$$n = \frac{N_{Ed}}{N_{pl,Rd}}$$

Calculated by an MS Excel spreadsheet due to dependency of  $N_{Ed}$ .

Moment resistance for bending about the major axis:

$$M_{N,a,y,Rd} = M_{pl,a,y,Rd}(1 - n)/(1 - 0,5a)$$

(Calculated by an MS Excel spreadsheet due to dependency of  $N_{Ed}$ )

Moment resistance for bending about the minor axis:

$$\begin{cases} M_{N,a,z,Rd} = M_{pl,a,z,Rd} \left[1 - \left(\frac{n - a}{1 - a}\right)^2\right] & (n > a) \\ M_{N,a,z,Rd} = M_{pl,a,z,Rd} & (n \leq a) \end{cases}$$

(Calculated by an MS Excel spreadsheet due to dependency of  $N_{Ed}$ )

### Cross-sectional compression + bi-axial bending resistance:

Bi-axial moment resistance criteria of class 1 H-profile:

$$\left[ \frac{M_{y,Ed}}{M_{N,a,y,Rd}} \right]^2 + \left[ \frac{M_{z,Ed}}{M_{N,a,z,Rd}} \right]^{5n} \leq 1$$

This equation is solved numerically by the goal seek algorithm in MS Excel.

### Cross-sectional shear resistance:

Shear resistance factor:

$$\eta = 1,2$$

The shear area is calculated (I-profile, load parallel to web):

$$\begin{aligned} A_{av} &= \max(A - 2bt_f + (t_w + 2r)t_f; \eta h_w t_w) \\ &= \max\left( \begin{array}{l} 14908 - 2 * 300 * 19 + 19(11 + 2 * 27) \\ 1,2 * (300 - 2(19 + 27)) * 11 \end{array} \right) mm^2 = 4743 mm^2 \end{aligned}$$

The plastic cross-sectional shear resistance is calculated:

$$V_{pl,a,Rd} = \frac{A_v * \left(\frac{f_y}{\sqrt{3}}\right)}{\gamma_{M0}} = \frac{4743 * 355 / \sqrt{3}}{1,05} kN = 925 kN$$

### Resistance towards flexural buckling in compression:

Buckling lengths (pin-ended):

$$L_{cr,y} = L_{cr,z} = L = 6000 mm$$

Radii of gyration:

$$i_{ay} = \sqrt{\frac{I_{ay}}{A_a}} = \sqrt{\frac{251,66 * 10^6}{14908}} mm = 129,9 mm$$

$$i_{az} = \sqrt{\frac{I_{az}}{A_a}} = \sqrt{\frac{85,63 * 10^6}{14908}} mm = 75,8 mm$$

Non-dimensional slenderness (Class 1)

$$\bar{\lambda}_{ay} = \frac{L_{cr,y}}{i_{ay} * 93,9\varepsilon} = \frac{6000}{129,9 * 93,9 * 0,81} = 0,607$$

$$\bar{\lambda}_{az} = \frac{L_{cr,z}}{i_{az} * 93,9\varepsilon} = \frac{6000}{75,8 * 93,9 * 0,81} = 1,041$$

Member imperfection factors:

y-axis: Buckling curve b selected ( $h/b < 1,2$ ;  $t_f < 100\text{mm}$ ; S355)  $\rightarrow \alpha_{ay}=0,34$

z-axis: Buckling curve c selected ( $h/b < 1,2$ ;  $t_f < 100\text{mm}$ ; S355)  $\rightarrow \alpha_{az}=0,49$

$\phi$ -factors:

$$\phi_{ay} = 0,5 \left[ 1 + \alpha_{ay}(\bar{\lambda}_{ay} - 0,2) + \bar{\lambda}_{ay}^2 \right] = 0,5[1 + 0,34(0,607 - 0,2) + 0,607^2] = 0,754$$

$$\phi_{az} = 0,5 \left[ 1 + \alpha_{az}(\bar{\lambda}_{az} - 0,2) + \bar{\lambda}_{az}^2 \right] = 0,5[1 + 0,49(1,041 - 0,2) + 1,041^2] = 1,248$$

$\chi$ -factors:

$$\chi_{ay} = \frac{1}{\phi_{ay} + \sqrt{\phi_{ay}^2 - \bar{\lambda}_{ay}^2}} = \frac{1}{0,754 + \sqrt{0,754^2 - 0,607^2}} = 0,833$$

$$\chi_{az} = \frac{1}{\phi_{az} + \sqrt{\phi_{az}^2 - \bar{\lambda}_{az}^2}} = \frac{1}{1,248 + \sqrt{1,248^2 - 1,041^2}} = 0,517$$

Flexural buckling resistances:

$$N_{b,a,y,Rd} = \frac{\chi_{ay} A_a f_y}{\gamma_{M1}} = \frac{0,833 * 14908 * 355}{1,05} \text{ kN} = 4198 \text{ kN}$$

$$N_{b,a,z,Rd} = \frac{\chi_{zy} A_a f_y}{\gamma_{M1}} = \frac{0,517 * 14908 * 355}{1,05} \text{ kN} = 2605 \text{ kN}$$

With no lateral restraints to any of the axes, the design buckling resistance is about the minor axis:

$$N_{b,a,Rd} = 2605 \text{ kN}$$

### Resistance towards buckling in combined compression+ major axis bending:

Calculating for scenarios {A} and {B}, as described in section 3.3.6. The subscript shows which scenario is calculated.

Bending moment diagram factors:

$$\begin{cases} C_{1,\{A\}} = 1 \\ C_{2,\{A\}} = 0 \end{cases}$$

$$\begin{cases} C_{1,\{B\}} = 1,348 \\ C_{2,\{B\}} = 0,630 \end{cases}$$

Effective length factors:

$$k = \frac{L_{cr,z}}{L} = 1 \text{ (pin - pin connection)}$$

$$k_w = 1 \text{ (No special provision for warping fixity)}$$

Distance between point of load application and shear centre:

$$z_g = \frac{h}{2} = 150\text{mm} \text{ (doubly symmetrical member, shear centre is in the centroid)}$$

Critical moments, calculated according to [44]:

$$N_{cr,a,z} = \frac{\pi^2 E_a I_{a,z}}{(kL)^2} = \frac{\pi^2 * 210000 * 85,63 * 10^6}{6000^2} N = 4930 kN$$

$$M_{cr,\{A\}} = C_{1,\{A\}} * N_{cr,a,z} \left[ \sqrt{\left(\frac{k}{k_w}\right)^2 \frac{I_{a,w}}{I_{a,z}} + \frac{GI_{a,t}}{N_{cr,a,z}} + (C_{2,\{A\}} Z_g)^2} - C_{2,\{A\}} Z_g \right]$$

$$= 4930 \left[ \sqrt{\frac{1688 * 10^9}{85,63 * 10^6} + \frac{81 * 1858 * 10^3}{4930}} \right] kNm = 1105 kNm$$

$$M_{cr,\{B\}} = C_{1,\{B\}} * N_{cr,a,z} \left[ \sqrt{\left(\frac{k}{k_w}\right)^2 \frac{I_{a,w}}{I_{a,z}} + \frac{GI_{a,t}}{N_{cr,a,z}} + (C_{2,\{B\}} Z_g)^2} - C_{2,\{B\}} Z_g \right]$$

$$= 1,348 * 4930 \left[ \sqrt{\frac{1688 * 10^9}{85,63 * 10^6} + \frac{81 * 1858 * 10^3}{4930} + (0,63 * 150)^2} - 0,63 * 150 \right]$$

$$= 989 kNm$$

Relative lateral torsional slenderness:

$$\bar{\lambda}_{LT,0} = 0,4 \text{ (Lower boundary when LTB may occur)}$$

$$\bar{\lambda}_{aLT\{A\}} = \sqrt{\frac{Z_{ay} f_y}{M_{cr,\{A\}}}} = \sqrt{\frac{1869 * 10^3 * 355}{1105 * 10^6}} = 0,775 > \bar{\lambda}_{LT,0} \text{ (LTB may occur)}$$

$$\bar{\lambda}_{aLT\{B\}} = \sqrt{\frac{Z_{ay} f_y}{M_{cr,\{B\}}}} = \sqrt{\frac{1869 * 10^3 * 355}{989 * 10^6}} = 0,819 > \bar{\lambda}_{LT,0} \text{ (LTB may occur)}$$

Imperfection factor for LTB:

Buckling curve "a" selected (rolled I-section  $h/b < 2$ )  $\rightarrow \alpha_{aLT}=0,21$

$\phi$ -factors:

$$\phi_{aLT\{A\}} = 0,5 \left[ 1 + \alpha_{aLT} (\bar{\lambda}_{aLT\{A\}} - 0,2) + \bar{\lambda}_{aLT\{A\}}^2 \right]$$

$$= 0,5 [1 + 0,21(0,775 - 0,2) + 0,775^2] = 0,861$$

$$\phi_{aLT\{B\}} = 0,5 \left[ 1 + \alpha_{aLT} (\bar{\lambda}_{aLT\{B\}} - 0,2) + \bar{\lambda}_{aLT\{B\}}^2 \right]$$

$$= 0,5 [1 + 0,21(0,819 - 0,2) + 0,819^2] = 0,900$$

$\chi$ -factors:

$$\chi_{aLT\{A\}} = \frac{1}{\phi_{aLT\{A\}} + \sqrt{\phi_{aLT\{A\}}^2 - \bar{\lambda}_{aLT\{A\}}^2}} = \frac{1}{0,861 + \sqrt{0,861^2 - 0,775^2}} = 0,810$$

$$\chi_{aLT\{B\}} = \frac{1}{\phi_{aLT\{B\}} + \sqrt{\phi_{aLT\{B\}}^2 - \bar{\lambda}_{aLT\{B\}}^2}} = \frac{1}{0,900 + \sqrt{0,900^2 - 0,819^2}} = 0,785$$

Calculating the equivalent uniform moment factors, required for interaction factors.

Case {A}, pure bending

$$\psi = 1$$

$$C_{m_y,\{A\}} = C_{m_{LT},\{A\}} = 0,6 + 0,4\psi = 1$$

Case {B}, concentrated load:

$$\alpha_h = \frac{M_h}{M_s} = 0 \quad (M_h = 0)$$

$$C_{m_y,\{B\}} = C_{m_{LT},\{B\}} = 0,90 + 0,10\alpha_h = 0,9$$

The HE300B cross-section is open without torsional restraint, both  $\chi$  factors are smaller than 1 -> thus torsional deformations may occur.

Calculating the interaction factors  $k_{yy}$  &  $k_{zy}$  according to Annex B:

$$k_{yy} = C_{m_y,\{i\}} * \min \left[ \left( 1 + (\bar{\lambda}_y - 0,2) \frac{N_{Ed}}{\chi_y N_{Rk}} \right); \left( 1 + 0,8 \frac{N_{Ed}}{\chi_y N_{Rk}} \right) \right]$$

$$k_{zy} = \max \left[ \left( 1 - \frac{0,1\bar{\lambda}_z}{(C_{m_{LT},\{i\}} - 0,25)} \frac{N_{Ed}}{\chi_z N_{Rk}} \right); \left( 1 - \frac{0,1}{(C_{m_{LT},\{i\}} - 0,25)} \frac{N_{Ed}}{\chi_z N_{Rk}} \right) \right]$$

The interaction factors are calculated by an MS Excel spreadsheet due to dependency of  $N_{Ed}$ .

Calculating stability of column, according formulae for the 2<sup>nd</sup> order effects of applied bending, axial force and member imperfection:

$$\frac{N_{Ed}}{\chi_y N_{Rk}} + \frac{k_{yy} M_{y,Ed} + \Delta M_{y,Ed}}{\chi_{LT} \frac{M_{y,Rk}}{\gamma_{M1}}} + \frac{k_{yz} M_{z,Ed} + \Delta M_{z,Ed}}{\frac{M_{z,Rk}}{\gamma_{M1}}} \leq 1 \quad (A1)$$

$$\frac{N_{Ed}}{\chi_z N_{Rk}} + \frac{k_{zy} M_{y,Ed} + \Delta M_{y,Ed}}{\chi_{LT} \frac{M_{y,Rk}}{\gamma_{M1}}} + \frac{k_{zz} M_{z,Ed} + \Delta M_{z,Ed}}{\frac{M_{z,Rk}}{\gamma_{M1}}} \leq 1 \quad (A2)$$

The criteria A1 and A2 are rewritten to find the maximum  $M_{y,Ed}$  at a given  $N_{Ed}$ .  $M_z$  terms are omitted since there is no minor axis bending moment:

$$M_{b,a,y,Rd} = \min \left[ \frac{\chi_{LT} M_{y,Rk}}{k_{yy}} \left( \frac{1}{\gamma_{M1}} - \frac{N_{Ed}}{\chi_y N_{Rk}} \right); \frac{\chi_{LT} M_{y,Rk}}{k_{zy}} \left( \frac{1}{\gamma_{M1}} - \frac{N_{Ed}}{\chi_z N_{Rk}} \right) \right]$$

(Calculated by an MS Excel spreadsheet due to dependency of  $M_{y,Ed}$  and  $N_{Ed}$ .)

## Appendix B. Worked example – ULS verification of FEC, HE300B column

This appendix displays the ULS verification calculations for a fully encased composite HE-300B cross-section, which are done according to EC4, part 1-1 [3].

Where the resistance is dependent on the magnitude of the loads and multiple values are calculated (e.g. moment resistance dependency of design axial force); only the formulae are given. The calculations themselves are done in an MS Excel spreadsheet.

Relevant section geometry and material properties of the steel section is given in Table 3-1 and Table A-1.

### Determination of minimum required reinforcement and cover:

Minimum required cover of flange:

$$c_{fl,min} = \max(40; b/6) = \max(40; 300/6) \text{ mm} = 50 \text{ mm}$$

Assume a concrete envelope with sides  $b_{c,trial} = h_{c,trial} = b + 2 * c_{fl,min} = 400 \text{ mm}$ . This gives the area:

$$A_{c,trial} = b_{c,trial} * h_{c,trial} - A_a = 400 * 400 - 14908 \text{ mm}^2 = 145092 \text{ mm}^2$$

Minimum area per longitudinal rebar (4 bars) to have 0,3% reinforcement ratio:

$$A_{s,bar,min} = \frac{A_{c,trial} * 0,003}{4} = \frac{145092 * 0,003}{4} \text{ mm}^2 = 109 \text{ mm}^2$$

Selected longitudinal rebar diameter:

$$\varnothing_L = 12 \text{ mm} > \text{Longitudinal rebar area } A_{s,bar} = 113 \text{ mm}^2$$

Minimum cover of reinforcement (assume  $c_{min,b} < c_{min,dur}$ ).

$$c_{min,dur} = 15 \text{ mm (XC1)}$$

Accepted deviation of cover:

$$\Delta c_{dev} = 10 \text{ mm}$$

Nominal concrete cover:

$$c_{nom} = c_{min,dur} + \Delta c_{dev} = 15 + 10 \text{ mm} = 25 \text{ mm}$$

Minimum transverse rebar diameter:

$$\varnothing_T = 6 \text{ mm}$$

Sum of minimum reinforcement cover and the diameters of rebars:

$$c_{nom} + \varnothing_T + \varnothing_L = 43 \text{ mm} < c_{fl,min} \text{ (} c_{fl,min} \text{ is dimensioning for concrete envelope)}$$

Concrete envelope height/width:

$$h_c = h + 2 * (c_{fl,min}) = 300 + 2 * 50 \text{ mm} = 400 \text{ mm}$$

$$b_c = b + 2 * (c_{fl,min}) = 300 + 2 * 50 \text{ mm} = 400 \text{ mm}$$

Area of concrete:

$$A_c = b_c * h_c - A_a - 4 * A_{s,bar} \text{ mm}^2 = 300^2 - 14908 - 4 * 113 = 144640 \text{ mm}^2$$

Check vs. maximum cover of flange for y and z axes:

$$c_y = \frac{b_c - b}{2} = \frac{400 - 300}{2} \text{ mm} = 50 \text{ mm} < 0,4 * b \text{ (ok!)}$$

$$c_z = \frac{h_c - h}{2} = \frac{400 - 300}{2} \text{ mm} = 50 \text{ mm} < 0,3 * h \text{ (ok!)}$$

Check vs. minimum required (0,003) and maximum recommended (0,06) reinforcement ratio:

$$\frac{A_s}{A_c} = \frac{4 * A_{s,bar}}{A_c} = \frac{4 * 113}{144640} = 0,0031 \text{ (Ok!)}$$

### Compressive cross-sectional resistance and steel contribution:

Resistance towards squash load:

$$N_{pl,Rd} = \frac{A_A f_y}{\gamma_{M0}} + \frac{0,85 A_c f_{ck}}{\gamma_c} + \frac{A_s f_s}{\gamma_s} = \frac{14908 * 355}{1,05} + \frac{0,85 * 144640 * 30}{1,5} + \frac{452 * 500}{1,15} \text{ N}$$

$$= 7695 \text{ kN}$$

Check whether the steel contribution ratio  $\delta$  is between 0,2 and 0,9:

$$\delta = \frac{A_a f_{yd}}{N_{pl,Rd,c}} = \frac{14908 * 355}{7695 * 1000 * 1,05} = 0,655 \text{ (Ok!)}$$

### Determination of points A to D on a polygonal MN interaction curve, y axis bending:

**Point A:**

$$N_{A,y} = N_{pl,Rd} = 7695 \text{ kN}$$

$$M_{A,y} = 0 \text{ kNm}$$

**Point B:**

$$N_{B,y} = 0 \text{ kN}$$

The distance between the PNA and the centreline ( $h_{n,y}$ ) is found by force equilibrium of stress blocks (Assuming the PNA lies on the web, between the fillets of the steel section):

Area of steel in compression & tension: (Flanges and section with fillets cancel each other out and are omitted)

$$A_{a,y,com} = t_w \left[ \frac{h - 2(t_f + r)}{2} - h_{n,y} \right] = 11 \left[ \frac{300 - 2(19 + 27)}{2} - h_{n,y} \right] = 1144 - 11h_{n,y}$$

$$A_{a,y,ten} = t_w \left[ \frac{h - 2(t_f + r)}{2} + h_{n,y} \right] = 11 \left[ \frac{300 - 2(19 + 27)}{2} + h_{n,y} \right] = 1144 + 11h_{n,y}$$



Areas of rebars in compression & tension cancel each other out and are omitted.

Area of concrete in compression, deducting areas of the steel section and rebars in compression:

$$A_{c,y,com} = b_c \left( \frac{h_c}{2} - h_{n,y} \right) - t_f b - t_w \left( \frac{h}{2} - h_{n,y} - t_f \right) - 2r^2 \left( 1 - \frac{\pi}{4} \right) - 2A_{s,bar}$$

$$A_{c,y,com} = 400 \left( \frac{400}{2} - h_{n,y} \right) - 19 * 300 - 11 \left( \frac{300}{2} - h_{n,y} - 19 \right) - 2 * 27^2 \left( 1 - \frac{\pi}{4} \right) - 2 * 113 = 72320 - 389h_{n,y}$$

The PNA to centreline distance  $h_{n,y}$  is determined from equilibrium of stress blocks:

$$\frac{f_y}{\gamma_{M0}} (A_{a,y,com} - A_{a,y,ten}) + 0,85 \frac{f_{ck}}{\gamma_c} * A_{c,c} = 0$$

$$\frac{f_y}{\gamma_{M0}} (-22h_{n,y}) + 0,85 \frac{f_{ck}}{\gamma_c} (72320 - 389h_{n,y}) = 0$$

$$h_{n,y} = \frac{72320 * 0,85 * \frac{30}{1,5}}{22 * \frac{355}{1,05} + 389 * 0,85 * \frac{30}{1,5}} mm = 87,5 mm$$

Check that the assumption regarding the position of the PNA is correct:

$$h_{n,y} = 87,5 mm \leq \frac{h}{2} - r - t_f = 104 mm (ok!)$$

Calculation of plastic resistance towards major axis bending is done by moment equilibrium about the PNA:

Plastic section modulus of the whole steel section about the centreline:

$$Z_{a,y} = 1869 * 10^3 mm^3$$

Plastic section modulus of steel section within region +/-  $h_n$  from the centreline

$$Z_{an,y} = t_w * \frac{(2h_{n,y})^2}{4} = 11 * 87,5^2 mm^3 = 84 * 10^3 mm^3$$

Plastic section modulus of the longitudinal rebars about the centreline:

$$Z_{s,y} = 4 * A_{s,bar} * \left( \frac{h_c}{2} - c_{nom} - \frac{\emptyset_L}{2} \right) = 4 * 113 * \left( \frac{400}{2} - 25 - \frac{12}{2} \right) mm^3 = 76 * 10^3 mm^3$$

No rebar inside the region +/-  $h_n$  from centreline:

$$Z_{sn,y} = 0$$

Plastic section modulus of the whole concrete section about the centreline:

$$Z_{c,y} = \frac{b_c h_c^2}{4} - Z_{a,y} - Z_{s,y} = \frac{400^3}{4} - (1869 + 76) * 10^3 mm^3 = 14055 * 10^3 mm^3$$

Plastic section modulus of concrete section within region +/-  $h_n$  from centreline:

$$Z_{cn,y} = \frac{(b_c - t_w) * (2h_{n,y})^2}{4} = (400 - 11) * 87,5^2 mm^3 = 2978 * 10^3 mm^3$$

Plastic moment resistance for bending about major axis. Equation according to [10]:

$$M_{B,y} = M_{pl,y,Rd} = \frac{f_y}{\gamma_{M0}} (Z_{a,y} - Z_{an,y}) + 0,5\alpha_c \frac{f_{ck}}{\gamma_c} (Z_{c,y} - Z_{cn,y}) + \frac{f_s}{\gamma_s} (Z_{s,y} - Z_{sn,y}) =$$

$$\left[ \frac{355}{1,05} (1869 - 84) + \frac{0,5 * 0,85 * 30}{1,5} (14055 - 2978) + \frac{500}{1,15} (76) \right] * 10^3 Nmm$$

$$= 731 kNm$$

**Point C:**

To find the axial force at point C, the PNA is set at  $h_{n,y}$  (calculated for point B) in the opposite side of the centreline, if compared to the PNA location for point B. The axial force is the sum of the forces from the stress blocks, refer Figure 3-5.

Steel section: (Sections outside  $2h_{n,y}$  cancel each other out).

$$N_{C,a,y} = \frac{f_y}{\gamma_{M0}} * t_w * 2h_{n,y} = \frac{355}{1,05} * 11 * 2 * 87,5 N = 651 kN$$

Reinforcement section – rebars in tension/compression cancel each other out

Concrete section

$$N_{C,c,y} = \frac{f_{ck}}{\gamma_c} * 0,85 * \left[ \frac{A_c}{2} + (b_c - t_w) * h_n \right] = \frac{30}{1,5} * 0,85 * \left[ \frac{144640}{2} + (400 - 11) * 87,5 \right] N$$

$$= 1808 kN$$

$$N_{C,y} = N_{C,a,y} + N_{C,c,y} = 651 + 1808 = 2459 kN$$

$$M_{C,y} = M_{pl,y,Rd} = 731 kNm \text{ (see calculation for point B)}$$

**Point D:**

$$N_{D,y} = \frac{N_{C,y}}{2} = \frac{2459}{2} = 1229 N$$

The maximum moment resistance is achieved when the PNA coincides with the centreline. It can be calculated by using the plastic section moduli of the constituent materials for the whole section, which are already calculated for point B:

$$M_{D,y} = M_{max,y,Rd} = \frac{f_y}{\gamma_{M0}} * Z_{a,y} + \frac{f_s}{\gamma_s} * Z_{s,y} + 0,5 * 0,85 * \frac{f_{ck}}{\gamma_c} * Z_{c,y}$$

$$= \left[ \frac{355}{1,05} * 1869 + \frac{500}{1,15} * 76 + 0,5 * 0,85 * \frac{30}{1,5} * 14055 \right] * 10^3 Nmm$$

$$= 784 kNm$$

Determination of points A to D on polygonal MN interaction curve, minor axis bending:

**Point A:**

$$N_{A,z} = N_{Pl,Rd} = 7695 kN \text{ (From section 3.3.1)}$$

$$M_{A,z} = 0 kNm$$

**Point B:**

$$N_{B,z} = 0 \text{ kN}$$

We find the distance between the PNA and the centreline ( $h_{n,z}$ ) by force equilibrium of stress blocks :

By assuming the PNA run through the flanges,  $h_{n,z}$  calculates to 2,5mm, which is not correct (that position is in the web). By assuming the PNA runs through the web,  $h_{n,z}$  calculates to 6mm which is not correct either (that position is in the fillet section). Thus it is clear that the PNA runs through the fillet section.

In order to simplify the algebraic expressions, the fillets are omitted and the areas of the four fillets are considered to be in concrete instead of steel.

Area of steel in compression & tension:

$$A_{a,z,com} = 2 * t_f * \left(\frac{b}{2} - h_{n,z}\right) = 38 * \left(\frac{300}{2} - h_{n,z}\right) = 5700 - 38h_{n,z}$$

$$\begin{aligned} A_{a,z,ten} &= A_a - A_{a,z,com} - 4r^2 \left(1 - \frac{\pi}{4}\right) = 14908 - 5700 + 38h_{n,z} - 4 * 27^2 \left(1 - \frac{\pi}{4}\right) \\ &= 8582 + 38h_{n,z} \end{aligned}$$

Areas of rebars in compression & tension cancel each other out:

Area of concrete in compression, deducting area for steel section and rebars in compression:

$$\begin{aligned} A_{c,z,com} &= h_c \left(\frac{b_c}{2} - h_{n,z}\right) - A_{a,z,com} - 2A_{s,bar} \\ &= 400 \left(\frac{400}{2} - h_{n,z}\right) - 5700 + 38h_{n,z} - 2 * 113 = 74074 - 362h_{n,z} \end{aligned}$$

The PNA to centreline distance  $h_{n,z}$  is determined from equilibrium of stress blocks:

$$\frac{f_y}{\gamma_{M0}} (A_{a,z,com} - A_{a,z,ten}) + 0,85 \frac{f_{ck}}{\gamma_c} * A_{c,z,com} = 0$$

$$\frac{f_y}{\gamma_{M0}} (-2882 - 76h_{n,z}) + 0,85 \frac{f_{ck}}{\gamma_c} * (74074 - 362h_{n,z}) = 0$$

$$h_{n,z} = \frac{74074 * 0,85 * \frac{30}{1,5} - 2882 * \frac{355}{1,05}}{362 * 0,85 * \frac{30}{1,5} + 76 * \frac{355}{1,05}} \text{ mm} = 8,9 \text{ mm}$$

Check that the assumption regarding position of the neutral axis is correct:

$$h_{n,z} = \frac{t_w}{2} \leq 8,9 \leq \frac{t_w}{2} + r \text{ (ok!)}$$

Calculation of plastic resistance towards minor axis bending is done by moment equilibrium about the PNA.

Plastic section modulus of the whole steel section about the centreline:

$$Z_{a,z} = \frac{2t_f * b^2}{4} + \frac{(h - 2t_f) * t_w^2}{4} = \frac{19 * 300^2}{2} + \frac{(300 - 2 * 19) * 11^2}{4} = 863 * 10^3 \text{ mm}^3$$

Plastic section modulus of steel section within region +/-  $h_n$  from the centreline

$$Z_{an,z} = \frac{2t_f * (2h_{n,z})^2}{4} + \frac{(h - 2t_f) * t_w^2}{4} = 2 * 19 * 8,9^2 + \frac{(300 - 2 * 19) * 11^2}{4} = 11 * 10^3 mm^3$$

Plastic section modulus of the whole reinforcement about the centreline:

$$Z_{s,z} = 4 * \pi * \left(\frac{\emptyset_L}{2}\right)^2 * \left(\frac{h_c}{2} - c_{nom} - \frac{\emptyset_L}{2}\right) = 4 * \pi * \left(\frac{12}{2}\right)^2 * \left(\frac{400}{2} - 25 - \frac{12}{2}\right) mm^3 = 76 * 10^3 mm^3$$

The reinforcement section is outside region +/-  $h_n$  from centreline:

$$Z_{sn,z} = 0$$

Plastic section modulus of the whole concrete section about the centreline:

$$Z_{c,z} = \frac{b_c h_c^2}{4} - Z_{a,z} - Z_{s,z} = \frac{400^3}{4} - (863 + 76) * 10^3 mm^3 = 15061 * 10^3 mm^3$$

Plastic section modulus of concrete section within region +/-  $h_n$  from centreline:

$$Z_{cn,z} = \frac{b_c (2h_{n,z})^2}{4} - Z_{an,z} = \frac{400 * (2 * 8,9)^2}{4} - 11 * 10^3 = 21 * 10^3 mm^3$$

Plastic moment resistance for bending about major axis. Equation according to [10]:

$$M_{B,z} = M_{pl,z,Rd} = \frac{f_y}{\gamma_{M0}} (Z_{a,z} - Z_{an,z}) + 0,5\alpha_c \frac{f_{ck}}{\gamma_c} (Z_{c,z} - Z_{cn,z}) + \frac{f_s}{\gamma_s} (Z_{s,z} - Z_{sn,z}) = \left[ \frac{355}{1,05} (863 - 11) + \frac{0,5 * 0,85 * 30}{1,5} (15061 - 21) + \frac{500}{1,15} (76) \right] * 10^3 Nmm = 449 kNm$$

### Point C:

To find the axial force at point C, the PNA is set at  $h_{n,z}$  (calculated for point B) in the opposite side of the centreline, when compared to calculations for point B. The axial force is the sum of the forces from the stress blocks, refer Figure 3-5.

Axial force for steel section (Sections outside  $2h_{n,z}$  cancel each other out):

$$N_{C,a,z} = \frac{f_y}{\gamma_{M0}} * [2h_{n,z}t_f + t_w(h - 2t_f)] = \frac{355}{1,05} * [2 * 8,9 * 19 + 11(300 - 38)] = 1089 kN$$

Axial force for reinforcement section – rebars in tension/compression cancel each other out

$$N_{C,s,z} = 0$$

Axial force for concrete section:

$$N_{C,c,z} = \frac{f_{ck}}{\gamma_c} * 0,85 * \left[ \frac{A_c}{2} + 4r^2 \left(1 - \frac{\pi}{4}\right) + \frac{t_w}{2} (h_c - h) + \left(h_{n,z} - \frac{t_w}{2}\right) (h_c - 2t_f) \right] =$$

$$= \frac{30}{1,5} * 0,85 * \left[ \frac{144640}{2} + 2 * 27^2 \left( 1 - \frac{\pi}{4} \right) + \frac{11}{2} (400 - 300) + \left( 8,9 - \frac{11}{2} \right) (300 - 2 * 19) \right] N = 1259 \text{ kN}$$

$$N_{C,z} = N_{C,a,z} + N_{C,s,z} + N_{C,c,z} = 1089 + 0 + 1259 = 2348 \text{ kN}$$

$$M_{C,z} = M_{pl,z,Rd} = 449 \text{ kNm (see calculation for point B)}$$

**Point D:**

$$N_{D,z} = \frac{N_{C,z}}{2} = \frac{2348}{2} = 1174 \text{ N}$$

The maximum moment resistance is achieved when the PNA coincides with the centreline. It can be calculated by using the plastic section moduli of the constituent materials for the whole section, which are already calculated for point B:

$$\begin{aligned} M_{D,z} = M_{max,z,Rd} &= \frac{f_y}{\gamma_{M0}} * Z_a + \frac{f_s}{\gamma_s} * Z_s + 0,5 * 0,85 * \frac{f_{ck}}{\gamma_c} * Z_c \\ &= \left[ \frac{355}{1,05} * 863 + \frac{500}{1,15} * 76 + 0,5 * 0,85 * \frac{30}{1,5} * 15061 \right] * 10^3 \text{ Nmm} \\ &= 453 \text{ kNm} \end{aligned}$$

### Cross-sectional shear resistance:

The plastic shear resistance for the steel section is calculated in Appendix A:

$$V_{pl,a,Rd} = 925 \text{ kN}$$

Calculating the shear resistance of the concrete section (assuming no extra shear reinforcement is needed) according EC2, part 1-1 [15]:

Distance from the compressive edge to the centre of the tensile reinforcement:

$$d = h_c - c_{nom} - \emptyset_T - \frac{\emptyset_L}{2} = 400 - 25 - 6 - \frac{12}{2} \text{ mm} = 363 \text{ mm}$$

Minimum width of the cross-section in tensile area:

$$b_w = b_c - t_w = 400 - 11 \text{ mm} = 389 \text{ mm}$$

Plastic resistance towards compression for the concrete section:

$$N_{pl,c,Rd} = A_c * 0,85 * \frac{f_{ck}}{\gamma_c} = 144640 * 0,85 * \frac{30}{1,5} \text{ N} = 2458 \text{ kN}$$

Compressive stress due to axial load: (Assuming design axial force:  $N_{Ed} = 2000 \text{ kN}$ ). Also, assuming the concrete section takes a fraction of the design load equal to the ratio of concrete plastic compressive resistance to total plastic compressive resistance:

$$\begin{aligned} \sigma_{cp} &= \min \left( \frac{N_{pl,c,Rd} * N_{Ed}}{N_{pl,Rd} * A_c}; 0,2 * 0,85 * \frac{f_{ck}}{\gamma_c} \right) \\ &= \min \left( \frac{2458 * 2000 * 10^3}{7695 * 144640}; 0,2 * 0,85 * \frac{30}{1,5} \right) \text{ MPa} = 3,4 \text{ MPa} \end{aligned}$$

Factors to determine the shear resistance of concrete:

$$C_{Rd,c} = \frac{0,18}{\gamma_c} = \frac{0,18}{1,5} = 0,12$$

$$k = \min\left(1 + \sqrt{\frac{200}{d}}; 2\right) = \min\left(1 + \sqrt{\frac{200}{363}}; 2\right) = 1,74$$

$$k_1 = 0,15$$

$$\rho_l = \min\left(\frac{A_s}{b_w d}; 0,02\right) = \min\left(\frac{4 * 113}{389 * 363}; 0,02\right) = 0,0032$$

$$v_{min} = 0,035 k^{\frac{3}{2}} * f_{ck}^{\frac{1}{2}} = 0,035 * 1,74^{\frac{3}{2}} * 30^{\frac{1}{2}} = 0,44$$

$$\begin{aligned} V_{c,Rd,1} &= \left[ C_{Rd,c} * k * (100 * \rho_l * f_{ck})^{\frac{1}{3}} + k_1 * \sigma_{cp} \right] * b_w * d \\ &= \left[ 0,12 * 1,74 * (100 * 0,0032 * 30)^{\frac{1}{3}} + 0,15 * 3,4 \right] * 389 * 363 \text{ N} \\ &= 134 \text{ kN} \end{aligned}$$

$$V_{c,Rd,2} = (v_{min} + k_1 * \sigma_{cp}) * b_w * d = (0,44 + 0,15 * 3,4) * 389 * 363 = 134 \text{ kN}$$

Shear resistance of concrete

$$V_{c,Rd} = \max(V_{c,Rd,1}; V_{c,Rd,2}) = 134 \text{ kN}$$

Assuming shear forces are working in the z-axis.

Distribution ratio of shear force into steel section,  $\xi_V$ :

$$\xi_V = \frac{M_{pl,a,y,Rd}}{M_{pl,y,Rd}} = \frac{631}{731} = 0,863$$

Effective cross-sectional shear resistance of the steel section, assuming it takes a  $\xi_V$  ratio of the total shear resistance:

$$V_{pl,a,eff,Rd} = \frac{V_{pl,a,Rd}}{\xi_V} = \frac{925}{0,863} \text{ kN} = 1071 \text{ kN}$$

Effective cross-sectional shear resistance of the concrete, assuming it takes a  $(1 - \xi_V)$  ratio of the total shear resistance:

$$V_{pl,c,eff,Rd} = \frac{V_{c,Rd}}{1 - \xi_V} = \frac{134}{1 - 0,863} \text{ kN} = 979 \text{ kN}$$

Cross-sectional shear resistance of composite section selected as the smallest of the above results:

$$V_{pl,Rd} = \min(V_{pl,a,eff,Rd}; V_{pl,c,eff,Rd}) = 979 \text{ kN}$$

### Determination of the creep coefficient:

The creep coefficient is calculated according to EC2, part 1-1 Annex B [15]:

Perimeter exposed to air:

$$u = 2 * (h_c + b_c) = 2 * (400 + 400)mm = 1600mm$$

Notional member size:

$$h_0 = \frac{2A_c}{u} = 2 * \frac{144640}{1600}mm = 180,8mm$$

Mean value of the compressive strength for C30/37 grade concrete is tabulated in EC2 [Table 3.1]:

$$f_{cm} = 38 \text{ MPa}$$

Coefficients for having a  $f_{cm}$  larger than 35 MPa:

$$\alpha_1 = (35/f_{cm})^{0,7} = (35/38)^{0,7} = 0,944$$

$$\alpha_2 = (35/f_{cm})^{0,2} = (35/38)^{0,2} = 0,984$$

$$\alpha_3 = (35/f_{cm})^{0,5} = (35/38)^{0,5} = 0,960$$

Factor for relative humidity ( $f_{cm} > 35$  MPa):

$$\phi_{RH} = \alpha_2 \left[ 1 + \frac{1 - \frac{RH}{100}}{0,1 * \sqrt[3]{h_0}} * \alpha_1 \right] = 0,984 * \left[ 1 + \frac{1 - \frac{50}{100}}{0,1 * \sqrt[3]{180,8}} * 0,944 \right] = 1,805$$

Factor for effect of concrete strength:

$$\beta(f_{cm}) = \frac{16,8}{\sqrt{f_{cm}}} = \frac{16,8}{\sqrt{38}} = 2,725$$

Factor for effect of concrete age at loading

$$\beta(t_0) = \frac{1}{0,1 + t_0^{0,2}} = \frac{1}{0,1 + 28^{0,2}} = 0,488$$

Notional creep coefficient:

$$\phi_0 = \phi_{RH} * \beta(f_{cm}) * \beta(t_0) = 1,805 * 2,725 * 0,488 = 2,400$$

Factor for development of creep with time after loading; assumed to be 1,0 to conservatively estimate for the full life-time of (50 years).

$$\beta_c(t, t_0) = 1,0$$

Creep coefficient:

$$\phi(t, t_0) = \phi_0 * \beta_c(t, t_0) = 2,4 * 1 = 2,4$$

### Determination of elastic buckling loads:

Characteristic resistance to axial (squash) load:

$$N_{pl,Rk} = A_A f_y + 0,85 A_c f_{ck} + A_s f_s \\ = 14908 * 355 + 0,85 * 144640 * 30 + 4 * 113 * 500 \text{ N} = 9207 \text{ kN}$$

Secant modulus of elasticity for C30/37 grade concrete, according EC2, part 1-1 [15]:

$$E_{cm} = 33 \text{ GPa}$$

Effective concrete modulus of elasticity:

$$E_{c,eff} = E_{cm} \frac{1}{1 + \left( \frac{N_{G,Ed}}{N_{Ed}} \right) \phi_t} = 33 * \frac{1}{1 + 1 * 2,4} \text{ GPa} = 9,7 \text{ GPa}$$

Second moments of area for the steel section (major & minor axes):

$$I_{ay} = 251,6 * 10^6 mm^4$$

$$I_{az} = 85,6 * 10^6 mm^4$$

Second moments of area for rebars: (both axes) with radius  $r_L = \phi_L/2 = 6mm$

$$I_{sy} = I_{sz} = 4 * \left[ \frac{\pi}{4} r_L^4 + \pi r^2 * \left( \frac{h_c}{2} - c_{nom} - \phi_T - r_L \right)^2 \right] = 12,0 * 10^6 mm^4$$

Second moments of area for concrete section:

$$I_{cy} = \frac{h_c b_c^3}{12} - I_{ay} - I_{sy} = 1869,7 * 10^6 mm^4$$

$$I_{cz} = \frac{h_c b_c^3}{12} - I_{az} - I_{sz} = 2036,7 * 10^6 mm^4$$

The total effective flexural rigidities for both axes, using recommended  $K_e$  factor of 0,6 for the concrete:

$$\begin{aligned} (EI)_{eff,y} &= E_a I_{ay} + E_s I_{sy} + K_e E_{c,eff} I_{cy} \\ &= 10^9 * (210 * 251,6 + 200 * 12 + 0,6 * 9,7 * 1869,7) Nmm^2 \\ &= 6612 * 10^{10} Nmm^2 \end{aligned}$$

$$\begin{aligned} (EI)_{eff,z} &= E_a I_{az} + E_s I_{sz} + K_e E_{c,eff} I_{cz} \\ &= 10^9 * (210 * 85,6 + 200 * 12 + 0,6 * 9,7 * 2036,7) Nmm^2 \\ &= 3223 * 10^{10} Nmm^2 \end{aligned}$$

Buckling lengths (pin-pin connection):

$$L_{cr,y} = L_{cr,z} = 6000mm$$

Calculating the elastic buckling loads.

$$N_{cr,y} = \frac{\pi^2 (EI)_{eff,y}}{L_{cr}^2} = \frac{\pi^2 * 6612 * 10^{10}}{6000^2} N = 18127 kN$$

$$N_{cr,z} = \frac{\pi^2 (EI)_{eff,z}}{L_{cr}^2} = \frac{\pi^2 * 3223 * 10^{10}}{6000^2} N = 8836 kN$$

### Resistance towards flexural buckling in compression:

Relative slendernesses using earlier derived elastic buckling loads:

$$\bar{\lambda}_y = \sqrt{N_{pl,Rk} / N_{cr,y}} = \sqrt{9207 / 18127} = 0,713$$

$$\bar{\lambda}_z = \sqrt{N_{pl,Rk} / N_{cr,z}} = \sqrt{9207 / 8836} = 1,021$$

Member imperfection factors:

For y-axis - buckling curve b selected  $\rightarrow \alpha_y = 0,34$

For z-axis - buckling curve c selected  $\rightarrow \alpha_z = 0,49$



$\phi$ -factors:

$$\phi_y = 0,5 \left[ 1 + \alpha_z (\bar{\lambda}_z - 0,2) + \bar{\lambda}_z^2 \right] = 0,5 [1 + 0,34(0,713 - 0,2) + 0,713^2] = 0,841$$

$$\phi_z = 0,5 \left[ 1 + \alpha_z (\bar{\lambda}_z - 0,2) + \bar{\lambda}_z^2 \right] = 0,5 [1 + 0,49(1,021 - 0,2) + 1,021^2] = 1,222$$

$\chi$ -factors:

$$\chi_y = \frac{1}{\phi_z + \sqrt{\phi_z^2 - \bar{\lambda}_z^2}} = \frac{1}{0,841 + \sqrt{0,841^2 - 0,713^2}} = 0,776$$

$$\chi_z = \frac{1}{\phi_z + \sqrt{\phi_z^2 - \bar{\lambda}_z^2}} = \frac{1}{1,222 + \sqrt{1,222^2 - 1,021^2}} = 0,528$$

Flexural buckling resistances:

$$N_{b,y,Rd} = \chi_y N_{pl,Rd} = 0,776 * 7695 \text{ kN} = 5973 \text{ kN}$$

$$N_{b,z,Rd} = \chi_z N_{pl,Rd} = 0,528 * 7695 \text{ kN} = 4063 \text{ kN}$$

With no lateral restraints to any of the axes, the design buckling resistance is about the minor axis:

$$N_{b,Rd} = 4063 \text{ kN}$$

### Resistance to flexural buckling in compression+ major axis bending:

Determination of reduced, effective flexural rigidity about major axis:

$$\begin{aligned} (EI)_{eff,II,y} &= 0,9(E_a I_{a,y} + E_s I_{s,y} + 0,5 E_{c,eff} I_{c,y}) \\ &= 0,9 * 10^9 (210 * 251,6 + 200 * 12 + 0,5 * 9,7 * 1869,7) \text{ Nmm}^2 \\ &= 5787 * 10^{10} \text{ Nmm}^2 \end{aligned}$$

Critical effective elastic buckling load:

$$N_{cr,eff,y} = \frac{\pi^2 (EI)_{eff,II,y}}{L_{cr}^2} = \frac{\pi^2 * 5787 * 10^{10}}{6000^2} \text{ N} = 15866 \text{ kN}$$

Determination of  $\beta$ -factors for case {A} and {B}:

$$\beta_{\{A\}} = 0,66 + (0,44 * 1) = 1,1$$

$$\beta_{\{B\}} = 1$$

Member imperfection for major axis equals  $L/200$

2nd order design moment:

$$M_{Ed,2} = \left( M_{Ed,1} * \beta_{\{i\}} + N_{Ed} * \frac{L}{200} \right) \left( \frac{1}{1 - \frac{N_{Ed}}{N_{cr,eff}}} \right) \quad (B1)$$

The maximum allowable 2<sup>nd</sup> order moment is equal to the max allowable moment (reduced for axial force) for the cross-section as provided by the MN diagram:

$$M_{Ed,2} = M_{N,y,Rd} \quad (B2)$$

Using equation B1 and B2 and solving for the maximum allowable 1<sup>st</sup> order moment, here called  $M_{b,y,Rd}$ . The expression is calculated in an MS Excel spreadsheet, due to dependence on  $N_{Ed}$ .

$$M_{b,y,Rd} = M_{Ed,1} = \frac{M_{N,y,Rd} \left(1 - \frac{N_{Ed}}{N_{Cr,eff}}\right) - N_{Ed} * \frac{L}{200}}{\beta}$$

## Appendix C. Worked example – fire resistance verification of HE-300B steel column

The fire resistance of a steel HE-300B column is verified in this appendix, in accordance to EC3, part 1-2 [13].

The relevant section geometry and material properties of the steel section are given in Table A-1.

### Critical temperature for pure compression

Calculation of the reduced local buckling factor  $\varepsilon_{fi}$  for fire:

$$\varepsilon_{fi} = 0,85 \sqrt{\frac{235}{f_y}} = 0,85 \sqrt{\frac{235}{355}} = 0,69$$

Class classification to compression in fire scenario:

Web:

$$\frac{c}{t\varepsilon} = \frac{h - 2(r + t_f)}{t_w \varepsilon_{fi}} = \frac{300 - 2(27 + 19)}{11 * 0,69} = 27,4 < 33 \text{ (Class 1!)}$$

Flanges:

$$\frac{c}{t\varepsilon} = \frac{b - t_w - 2r}{2t_f \varepsilon_{fi}} = \frac{300 - 11 - 2 * 27}{2 * 19 * 0,69} = 9,0 = 9 \text{ (Class 1!)}$$

The cross-section is thus class 1 in a fire scenario.

Fire buckling length (here assumed as pin-pin connection):

$$L_{fi} = L = 6000mm$$

Fire reduction factor for load level, simplification as recommended by EC3.

$$\eta_{fi} = 0,65$$

Design axial load during fire:

$$N_{fi,Ed} = \eta_{fi} * N_{Ed} = 0,65 * 2000 \text{ kN} = 1300kN$$

Normal temperature relative slenderness for the minor axis (from Appendix A):

$$\bar{\lambda}_{az} = 1,041$$

Imperfection factor during fire:

$$\alpha_{fi} = 0,65 * \sqrt{\frac{235}{f_y}} = 0,65 * \sqrt{\frac{235}{355}} = 0,529$$

The critical temperature for the design load is found by an iterative process adopted from [50], where:

- The temperature dependent reduction factors for yield strength and elastic modulus ( $k_{y,\theta}$  and  $k_{y,\theta}$  respectively) are interpolated from EC3, part 1-2 Table 3.1. For the first iteration the average steel temperature  $\theta$  is assumed to be 20 °C.

- The reduced slenderness due to temperature is calculated as:

$$\bar{\lambda}_{\theta} = \bar{\lambda}_{az} \sqrt{\frac{k_{y,\theta}}{k_{E,\theta}}}$$

- The  $\phi_{fi}$  and  $\chi_{fi}$  buckling curve factors for fire are calculated similarly for a normal temperature (see Appendix A), now using the  $\bar{\lambda}_{\phi}$  and  $\alpha_{fi}$  values
- The reduced axial load resistance due to buckling in fire is calculated as:

$$N_{fi,\theta,Rd} = \frac{\chi_{fi} * A_a * f_y}{\gamma_{M,fi}}$$

- The utilization factor is calculated:

$$\mu_0 = \frac{N_{fi,Ed}}{N_{fi,\theta,Rd}}$$

- The critical temperature in °C is calculated:

$$\theta_{a,cr} = 39,19 * \ln\left(\frac{1}{0,9674 * \mu_0^{3,833}} - 1\right) + 482$$

- If  $\theta_{a,cr} = \theta$  then the calculations are finished, else the steel temperature  $\theta$  is set to  $\theta_{a,cr}$  and a new iteration is made.

A numerical analysis using the method above of the critical steel temperature for the example column is shown in Table C-1, which concludes that the critical steel temperature  $\theta_{a,cr}$  equals 547 °C.

Table C-1: Example calculation of the critical steel temperature

$\theta$	$k_{y,\theta}$	$k_{E,\theta}$	$\lambda_{\theta}$	$\phi_{fi}$	$\chi_{fi}$	$N_{fi,\theta,Rd}$	$\mu_0$	$\theta_{a,cr}$
°C						kN		°C
20	1	1	1,041	1,317	0,471	2492	0,522	578
578	0,538	0,374	1,249	1,610	0,381	2016	0,645	541
541	0,653	0,481	1,213	1,556	0,395	2091	0,622	548
548	0,631	0,461	1,218	1,564	0,393	2080	0,625	547
547	0,634	0,464	1,217	1,562	0,393	2082	0,624	547

## Duration for an unprotected member to reach the critical temperature

Calculation of the section factor (unprotected HE-300B), exposure at 4 sides, approximating the fillets as square angles, equalling the perimeter of the cross-section divided by the area.

$$\frac{A_m}{V} \approx \frac{2(b+h) + 2(b-t_w)}{A_a} = \frac{2(300+300) + 2(300-11)}{14908} mm^{-1} = 119m^{-1}$$

Box value section factor (HE-300B):

$$\frac{A_m}{V_b} \approx \frac{2(b+h)}{A_a} = \frac{2(300+300)}{14908} mm^{-1} = 80m^{-1}$$

Shadow effect:

$$k_{sh} = 0,9 * \frac{\frac{A_m}{V} b}{\frac{A_m}{V}} = 0,9 * \frac{80}{119} = 0,605$$

Density of steel:  $\rho_a = 7850 \text{ kg/m}^3$

Convective heat transfer coefficient:  $\rho_a = 25 \text{ W/m}^2\text{K}$

Configuration factor:  $\Phi = 1$

Emissivity, steel:  $\varepsilon_m = 0,7$

Emissivity, fire:  $\varepsilon_f = 1$

Stefan-Boltzmann constant:  $\sigma = 5,67 * 10^{-8} \text{ W/m}^2\text{K}^4$

Time step:  $\Delta t = 60\text{s}$

The result of the following equations are determined by a time-step MS Excel spreadsheet, using standard thermodynamical formulations for radiative and convective heat, given by [50]:

Fire gas temperature (from ISO 834 curve):

$$\theta_g = 20 + 345 * \log(8t + 1); t = \text{fire duration in minutes}$$

Heat capacity of steel, valid up to a steel temperature of 600 °C (which is above the critical temperature):

$$c_a = 425 + 0,773\theta_a - 1,69 * 10^{-3}\theta_a^2 + 2,22 * 10^{-6} * \theta_a^3$$

Net convective heat flux to the steel member:

$$\dot{h}_{net,c} = \alpha_c(\theta_g - \theta_a)$$

Net radiative heat flux to the steel member:

$$\dot{h}_{net,r} = \phi * \varepsilon_m * \varepsilon_f * \sigma * [(\theta_g + 273)^4 - (\theta_m + 273)^4]$$

Total net heat flux to the steel member:

$$\dot{h}_{net,d} = \dot{h}_{net,c} + \dot{h}_{net,r}$$

Increase in steel temperature per minute:

$$\Delta\theta_{a,t} = k_{sh} * \frac{\frac{A_m}{V}}{c_a\rho_a} * \dot{h}_{net,d} * 60$$

Table C-2 shows the steel member temperature at a given time. After a duration of 17 minutes and before 18 minutes, the steel temperature  $\theta_a$  reaches above the critical temperature  $\theta_{a,cr}$ . Therefore, the fire resistance is assumed to be 17 minutes.

Table C-2: Temperature development in steel member exerted to ISO 834 fire curve

<b>t</b>	<b><math>\theta_g</math></b>	<b><math>\theta_a</math></b>	<b><math>c_a</math></b>	<b><math>\dot{h}_{net,c}</math></b>	<b><math>\dot{h}_{net,r}</math></b>	<b><math>\dot{h}_{net,d}</math></b>	<b><math>\Delta\theta_{a,t}</math></b>
(min)	(°C)	(°C)	(J/kgK)	(W/m <sup>2</sup> )	(W/m <sup>2</sup> )	(W/m <sup>2</sup> )	(°C)
0	20,0	20,0	440	0	0	0	0,0
1	349,2	20,0	440	8230	5656	13887	17,4
2	444,5	37,4	452	10178	10151	20329	24,8
3	502,3	62,1	467	11004	13839	24842	29,3
4	543,9	91,4	483	11312	16974	28286	32,2
5	576,4	123,6	499	11320	19679	30998	34,2
6	603,1	157,8	514	11133	22017	33150	35,5
7	625,8	193,3	527	10811	24022	34834	36,4
8	645,5	229,7	540	10394	25709	36103	36,8
9	662,8	266,5	553	9910	27083	36993	36,8
10	678,4	303,3	566	9379	28146	37525	36,5
11	692,5	339,8	580	8820	28900	37720	35,8
12	705,4	375,6	595	8247	29353	37600	34,8
13	717,3	410,4	611	7674	29519	37192	33,5
14	728,3	443,9	629	7111	29418	36529	31,9
15	738,6	475,8	649	6569	29080	35649	30,2
16	748,2	506,0	671	6054	28539	34593	28,4
17	757,2	534,4	694	5570	27836	33405	26,5
18	765,7	560,9	719	5120	27006	32127	24,6

## Appendix D. Cross-sections and reinforcement sizes used in parametric studies

The steel cross-sections which were considered in the parametric studies chapter (ref chapter 4) are given in Table D-1. All cross-sections used in the studies are of S355 steel.

Table D-1: Cross-section sizes used in studies

<b>HE-A, HE-B, HE-M</b> (Wide flange H-beams)		<b>CHS</b> (Circular hollow section) <i>Note:</i> Sections which doesn't meet the dimensional criteria $\frac{t}{D} \leq \frac{1}{25}$ are shown in gray background and they are not considered for fire resistance calculations.				
Nominal size, mm	Study	Outer diameter (D), mm	Thickness (t) 6mm	Thickness (t) 8mm	Thickness (t) 10mm	Thickness (t) 12.5mm
160	F,E	168.3	F,E			
180	F,E	193.7	S,F,A,E	S,A	S	
200	S,F,A,E	219.1	F,E	F,E		
220	F,E	244.5	F,E	F,E		
240	F,E	273.0	F,E	F,E	F	
260	F,E	323.9	S,F,A,E	S,F,A,E	S,F	F
280	F,E	355.6	F,E	F,E	F	F
300	S,F,A,E	406.4	*	S,F,A,E	S,F	F
320	F,E	457.0	*	F,E	F	F
360	F,E	508.0	*	*	F	F
400	S,F,A,E					
450	F,E					
500	F,E					

*Legend:*  
*S = Span length study; F = Fire protection study; A = Steel amount study;*  
*E = Environmental foot-print study; \* = Not included, does not fulfil local buckling criteria.*

The longitudinal rebar diameters used in the parametric studies are those which are available in A3C. These are shown in Table D-2. All rebar used in the studies are of B500NC grade.

Table D-2: Reinforcement bar sizes used in studies

$\phi_L$ Longitudinal rebar diameter (mm)*	$\phi_L$ Minimum transverse rebar diameter (mm)	$c_{nom,XC1}$ Minimum concrete cover (mm) Exposure XC1
8	6	25
10	6	25
12	6	25
14	6	25
16	6	26
20	6	30
25	8	35
28	8	38
32	8	42
40	10	50
Note: * For the column depth study, the minimum required longitudinal diameter is $\phi 12$ mm.		



## Appendix E. Maximum span study supporting calculations

This appendix is connected to the maximum span study in section 4.2.

- The maximum span length is determined as a function of the minor axis buckling resistance of the columns, for the pinned frame.
- Steel equivalent areas and second moment of areas for the composite cross-sections used for FEM calculation of the rigid frame are determined.
- Detailed results of the maximum span study are provided.

### Structural analysis, pinned frame

The structural loads are determined in accordance to EC0 [61] and EC1, part 1-1 [75].

Column center-center span:  $S = \text{unknown}$

Column width:  $b = \text{selected to } 0,3\text{m (assumed average)}$ .

Permanent surface load, including self-weight:  $\dot{G}_k = 5\text{kN/m}^2$

Imposed surface load:  $\dot{Q}_k = 3\text{kN/m}^2$

Beam to beam center-center distance:  $C = 7,2\text{m}$

Number of stories:  $n_{\text{tot}} = 4$

Number of beam spans:  $n_{\text{span}} = 5$

Characteristic permanent line load:

$$G_k = \dot{G}_k * C = 5 * 7,2 \text{ kN/m} = 36\text{kN/m}$$

Characteristic imposed line load:

$$Q_k = \dot{Q}_k * C = 3 * 7,2 \text{ kN/m} = 21,6\text{kN/m}$$

Reduction combination factor:  $\psi_0 = 0,7$

Reduction factor  $\alpha_A$  for beams:

$$\alpha_{A,1} = \min\left(\frac{5}{7}\psi_0 + \frac{A_0}{C(S-b)}; 1\right) = \min\left(0,5 + \frac{15}{7,2(S-0,3)}; 1\right)$$

$$\alpha_A = \max(\alpha_{A,1}; \psi_0; 0,6) = \max\left(\min\left(0,5 + \frac{15}{7,2(L-0,3)}; 1\right); 0,7\right)$$

Reduction factor for columns on storey 1 ( $\alpha_{n,1}$ ) and 2 ( $\alpha_{n,2}$ ):

$n_s = \text{stories above column (n>2)}$ :

$$\alpha_{n,1} = \frac{2 + (n_s - 2)\psi_0}{n_s} = \frac{2 + (4 - 2) * 0,7}{4} = 0,85$$

$$\alpha_{n,2} = \frac{2 + (n_s - 2)\psi_0}{n_s} = \frac{2 + (3 - 2) * 0,7}{3} = 0,9$$

Smallest reduction factor for multiple stories, level 1 to 4:

$$\alpha_{\text{min},1} = \min(\alpha_{n,1}; \alpha_A)$$

$$\alpha_{min,2} = \min(\alpha_{n,2}; \alpha_A)$$

$$\alpha_{min,3} = \alpha_A$$

$$\alpha_{min,4} = \alpha_A$$

G and Q are the design permanent and imposed loads for floor level i. These are determined by taking the relevant factor from the lowest total of:

$$(1,35 * G_k) + (1,5 * \psi_0 * Q_k) \quad [\text{EC0; Equation 6.10a}]$$

$$(1,2 * G_k) + (1,5 * \alpha_{min,i} * Q_k) [\text{EC0; Equation 6.10b}]$$

The worst case distribution of imposed loads is determined in CALFEM and it is shown in Figure 4-2. For this load case, the dimensioning columns are found to be B1 and E1 and the axial design load on these columns is:

$$N_{Ed} = \sum_{i=1}^{n_{tot}} S * ((1,132 * G) + (1,211 * Q))$$

The design imposed load Q may include the reduction factor  $\alpha_A$ , which depends on the span length S and therefore it may be non-linear.  $N_{Ed}$  is therefore calculated for 1000 different span lengths between S = 5m and S = 20m using a CALFEM model of a continuous beam with 5 spans made from 5 beam elements. The source code of this model is given in Appendix I. The results are exported into MS Excel and are shown in Figure E-1, including a linear regression of the results.

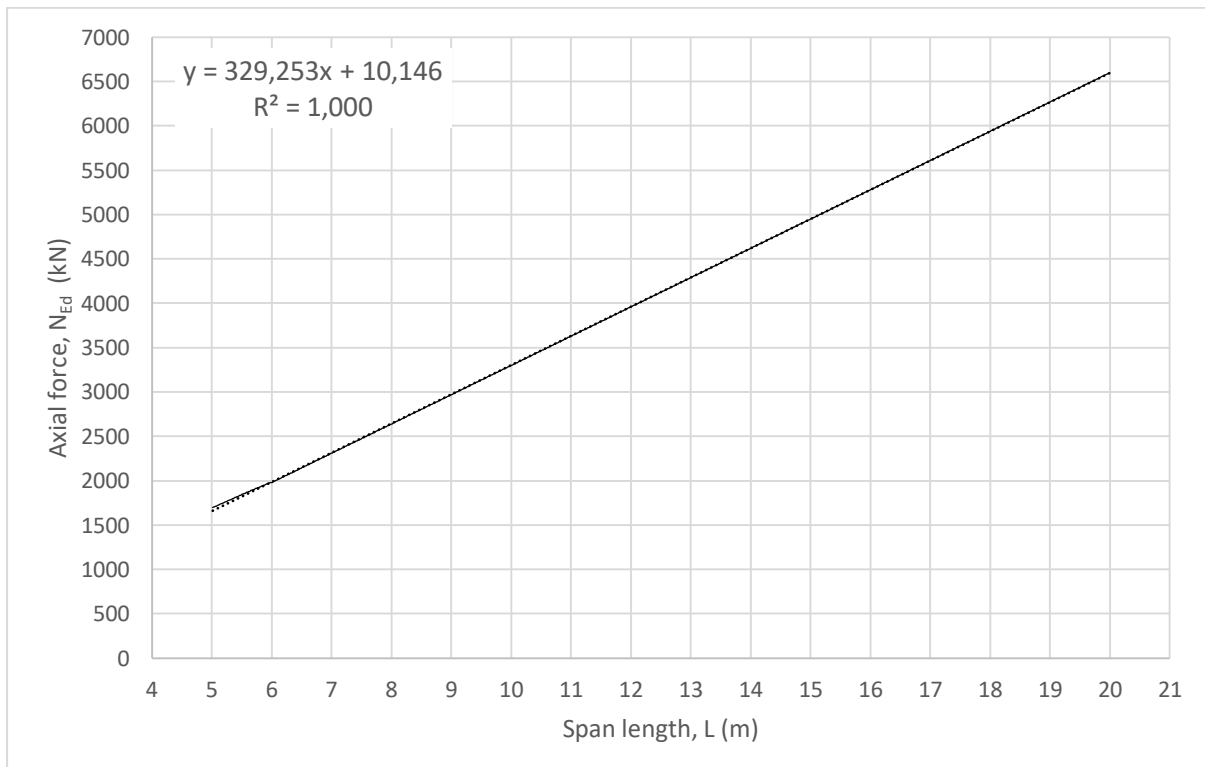


Figure E-1: Relation between span length and axial force on column B1/E1.

It can visually be determined that the graph has a linear fit and from the linear regression, the following relationship between the span length S and the column B1 design axial force  $N_{Ed}$  is derived:

$$N_{Ed} = 329,3S + 10,146 \text{ kN (with } S \text{ in meter)}$$

Without applied moments, the dimensioning resistance of the column is buckling about minor axis,  $N_{b,z,Rd}$ . Thus:

$$S = \frac{N_{b,z,Rd} - 10,146}{329,253}$$

The full results of the pinned frame study comparison are given by Table E-2 and Table E-3.

### Structural analysis, rigid frame

A global first order elastic analysis is done for the rigid frame, using FEM. This is done in CALFEM using the direct stiffness method and Euler-Bernoulli beam elements. The beam element definition requires singular values for the cross-sectional area “A” and the second moment of area about the bending axis “I”. For the composite column, the A and I values are converted to steel equivalents, using the methods described in section 4.1.2. The results of these conversions are presented in Table E-1.

Table E-1: Steel equivalent area and second moment of area for the maximum span study cross-sections

Section/ Concrete strength	HE-200A		HE-200B		HE-300A		HE-300B	
	A cm <sup>2</sup>	I cm <sup>4</sup>	A cm <sup>2</sup>	I cm <sup>4</sup>	A cm <sup>2</sup>	I cm <sup>4</sup>	A cm <sup>2</sup>	I cm <sup>4</sup>
<b>Steel</b>	53,83	3692	78,08	5696	112,53	18263	149,08	25166
<b>FEC C25/30</b>	95	5543	119,6	7700	186,46	24027	223	31212
<b>FEC C50/60</b>	119	6444	144	8672	230,19	27012	266,83	34336
<b>PEC C25/30</b>	75,21	4063	99,21	6069	158,62	20116	194,27	26994
<b>PEC C50/360</b>	85,77	4213	109,63	6217	182,9	20933	218,85	27821
	<b>6mm thickness</b>		<b>8mm thickness</b>		<b>10mm thickness</b>			
	A cm <sup>2</sup>	I cm <sup>4</sup>	A cm <sup>2</sup>	I cm <sup>4</sup>	A cm <sup>2</sup>	I cm <sup>4</sup>		
<b>CFT 193,7mm C25/30</b>	54,43	1933	65,08	2362	75,49	2762		
<b>CFT 323,9mm C25/30</b>	107,75	9911	126,12	12146	144,24	14295		
<b>CFT 193,7mm C50/60</b>	64,35	2053	74,56	2472	84,54	2862		
<b>CFT 323,9mm C50/60</b>	137,32	10978	154,92	13159	172,3	15256		

The source code of the CALFEM rigid frame structural analysis is given in Appendix I.

## Maximum span study results - detailed

The differences in the maximum column span for a composite column in the pinned frame study by using either C25/30 concrete grade or the double strength grade C50/60 is shown in Table E-2 while the difference in using  $\varnothing 12$  or  $\varnothing 25$  rebar is shown in Table E-3. The relative differences between span lengths for a pinned and a rigid frame are shown in Table E-4 along with the relative differences in span length of the rigid frame by basing the resistance on either column B1 or A2. The maximum beam moments in the pinned and rigid frames are shown in Table E-5.

Table E-2: Pinned frame study, effect of using C25/30 or C50/60 concrete strength

Profile	Fully encased H-profile, 4x $\varnothing 12$ mm rebar			Partially encased H-profile, 4x $\varnothing 12$ mm rebar			Concrete filled CHS profile, 4x $\varnothing 12$ mm rebar			
	Span (mm)			Span (mm)			Span (mm)			
	C25/30	C50/C60	$\Delta$	C25/30	C50/C60	$\Delta$	Profile	C25/30	C50/C60	$\Delta$
200A	6295	8086	28%	4425	4938	12%	193,7x6	4273	4883	14%
300A	14793	18975	28%	12270	14316	17%	193,7x8	5213	5826	12%
400A	20404	25920	27%	16830	19550	16%	193,7x10	6116	6718	10%
200B	7966	9771	23%	6033	6546	8%	323,9x6	9729	12891	32%
300B	17955	22146	23%	15389	17430	13%	323,9x8	11546	14665	27%
400B	23723	29245	23%	20094	22801	13%	323,9x10	13332	16391	23%
200M	11878	13797	16%	9822	10371	6%	406,4x8	16057	21409	33%
300M	31816	36238	14%	29069	31198	7%	406,4x10	18374	23643	29%
400M	35142	40858	16%	31349	34136	9%				
	Average $\Delta$ : 22%			Average $\Delta$ : 11%			Average $\Delta$ : 24%			

Table E-3: Pinned frame study, effect of using 4x $\varnothing 12$ mm or 4x $\varnothing 25$ mm longitudinal reinforcement

Profile	Fully encased H-profile, C50/60 concrete			Partially encased H-profile, C50/60 concrete			Concrete filled CHS profile, C50/60 concrete			
	Span (mm)			Span (mm)			Span (mm)			
	4x $\varnothing 12$	4x $\varnothing 25$	$\Delta$	4x $\varnothing 12$	4x $\varnothing 25$	$\Delta$	Profile	4x $\varnothing 12$	4x $\varnothing 25$	$\Delta$
200A	8086	12014	49%	4938	5594	13%	193,7x6	4883	5098	4%
300A	18975	24416	29%	14316	15781	10%	193,7x8	5826	6001	3%
400A	25920	31115	20%	19550	21017	8%	193,7x10	6718	6845	2%
200B	9771	13962	43%	6546	7201	10%	323,9x6	12891	14397	12%
300B	22146	27655	25%	17430	18892	8%	323,9x8	14665	16178	10%
400B	29245	34515	18%	22801	24266	6%	323,9x10	16391	17908	9%
200M	13797	18514	34%	10371	11097	7%	406,4x8	21409	23100	8%
300M	36238	42062	16%	31198	32694	5%	406,4x10	23643	25337	7%
400M	40858	46345	13%	34136	35626	4%				
	Average $\Delta$ : 27%			Average $\Delta$ : 8%			Average $\Delta$ : 7%			

Table E-4: Pinned and rigid frame span length comparison

Profile		Pinned B1 Span (mm)	Rigid B1 Span (mm)	$\Delta_1$	Rigid A2 Span (mm)	$\Delta_2$
Steel	200A	3381	4000	18%	8600	115%
	300A	9414	10200	8%	17400	71%
	200B	4997	5600	12%	10000	79%
	300B	12551	13600	8%	20400	50%
			<b>Average <math>\Delta</math>:</b>	12%		79%
<b>C25/30</b>						
Profile		Pinned B1 Span (mm)	Rigid B1 Span (mm)	$\Delta_1$	Rigid A2 Span (mm)	$\Delta_2$
Fully Encased	200A	6295	7100	13%	10500	48%
	300A	14793	16400	11%	20900	27%
	200B	7966	9100	14%	11400	25%
	300B	17955	20000	11%	21900	10%
			<b>Average <math>\Delta</math>:</b>	12%		28%
Partially Encased	200A	4425	5000	13%	9900	98%
	300A	12270	13600	11%	20200	49%
	200B	6033	6800	13%	10800	59%
	300B	15389	17200	12%	21300	24%
			<b>Average <math>\Delta</math>:</b>	12%		57%
Filled tubular	193,7x6	4273	4700	10%	8600	83%
	193,7x8	5213	5500	6%	9100	65%
	193,7x10	6116	6300	3%	9500	51%
	323,9x6	9729	10400	7%	18000	73%
	323,9x8	11546	12000	4%	18700	56%
	323,9x10	13332	13600	2%	19300	42%
			<b>Average <math>\Delta</math>:</b>	5%		62%
<b>C50/60</b>						
Profile		Pinned B1 Span (mm)	Rigid B1 Span (mm)	$\Delta_1$	Rigid A2 Span (mm)	$\Delta_2$
Fully Encased	200A	8086	9200	14%	11100	21%
	300A	18975	21200	12%	21800	3%
	200B	9771	11200	15%	12000	7%
	300B	22146	24000	8%	22800	-5%
			<b>Average <math>\Delta</math>:</b>	12%		6%
Partially Encased	200A	4938	5600	13%	10500	88%
	300A	14316	15900	11%	20900	31%
	200B	6546	7400	13%	11300	53%
	300B	17430	19500	12%	22200	14%
			<b>Average <math>\Delta</math>:</b>	12%		46%
Filled tubular	193,7x6	4883	5400	11%	9200	70%
	193,7x8	5826	6200	6%	9600	55%
	193,7x10	6718	6900	3%	9900	43%
	323,9x6	12891	13500	5%	19300	43%
	323,9x8	14665	15000	2%	19800	32%
	323,9x10	16391	16300	0%	20200	24%
			<b>Average <math>\Delta</math>:</b>	4%		45%

Table E-5: Pinned and rigid frame beam maximum moment comparison

Profile		Span (mm)	Pinned $M_{max}$ (kNm)	Rigid $M_{max}$ (kNm)	$\Delta_3$
Steel	200A	3300	85	70	-18%
	300A	9400	689	565	-18%
	200B	4900	187	154	-18%
	300B	12500	1219	1066	-13%
				<b>Average <math>\Delta</math>:</b>	-16%
<b>C25/30</b>					
Profile		Span (mm)	Pinned $M_{max}$ (kNm)	Rigid $M_{max}$ (kNm)	$\Delta_3$
Fully Encased	200A	6200	300	260	-13%
	300A	14700	1686	1511	-10%
	200B	7900	487	429	-12%
	300B	17900	2500	2280	-9%
				<b>Average <math>\Delta</math>:</b>	-11%
Partially Encased	200A	4400	151	122	-19%
	300A	12200	1161	1027	-12%
	200B	6000	281	242	-14%
	300B	15300	1826	1640	-10%
				<b>Average <math>\Delta</math>:</b>	-14%
Filled tubular	193,7x6	4300	144	117	-19%
	193,7x8	5200	211	179	-15%
	193,7x10	6100	290	255	-12%
	323,9x6	9700	734	614	-16%
	323,9x8	11500	1032	905	-12%
	323,9x10	13300	1380	1237	-10%
				<b>Average <math>\Delta</math>:</b>	-13%
<b>C50/60</b>					
Profile		Span (mm)	Pinned $M_{max}$ (kNm)	Rigid $M_{max}$ (kNm)	$\Delta_3$
Fully Encased	200A	8000	499	443	-11%
	300A	18900	2787	2558	-8%
	200B	9700	734	654	-11%
	300B	22100	3810	3505	-8%
				<b>Average <math>\Delta</math>:</b>	-10%
Partially Encased	200A	4900	187	157	-16%
	300A	14300	1595	1434	-10%
	200B	6500	330	287	-13%
	300B	17400	2362	2154	-9%
				<b>Average <math>\Delta</math>:</b>	-12%
Filled tubular	193,7x6	4900	187	157	-16%
	193,7x8	5800	262	229	-13%
	193,7x10	6700	350	312	-11%
	323,9x6	12800	1278	1145	-10%
	323,9x8	14500	1640	1486	-9%
	323,9x10	16300	2073	1887	-9%
				<b>Average <math>\Delta</math>:</b>	-10%

## Appendix F. Minimum depth of fire protected column supporting calculations

This appendix relates to the study of the minimum column depth, with reference to section 0. It describes:

- The fire resistance calculation procedures, which differ pending on which type of steel or composite cross-section is calculated. Steel sections are calculated according to EC3, part 1-1 [29] and 1-2 [13]. Composite sections are calculated according to EC4, part 1-1 [3] and 1-2 [4].
- Detailed results of the column depth study are provided, both as the resulting cross-sections in tabulated form and as graphs of the depth differences between composite and steel columns.

### Calculation procedure, steel column:

#### Step 0 (R0)

- Set up the design load scenario in A3C and determine the minimum required steel section for normal temperature by standard ULS verification of a steel member.

#### Step 1 (R30 to R120)

- Reduce the design loads/moments by multiplying them with the fire load reduction factor  $\eta_{fi} = 0,65$  and calculate the critical temperature  $\theta_{cr}$  of the steel in A3C.
- Use the CONLIT 150/150P data tables [64], with glued end joints to find the minimum required fire protection board thickness for R30 to R120, using the value for the equal or closest higher shape factor ( $A_m/V$ ) and the equal or closest smaller critical temperature ( $\theta_{cr}$ ).
- The total cross-sectional area is taken as that of the box surrounding the H-profile, with fire protection boards added on all four sides. See Figure F-1 for an example.
- For R120, the steel section was tried for one size larger to see whether the combination of the increased steel size and potentially lower fire protection board thickness gave a smaller total size.

#### Step 2 (R180)

- By using CONLIT 150, it was discovered that the steel section calculated in step 0 never have a sufficiently low shape factor to allow for R180 protection. Therefore, the steel section must be increased and the critical temperature  $\theta_{cr}$  re-calculated until the CONLIT 150 tables [64] provides a minimum fire protection thickness.
- The area is taken as that of the box surrounding the H-profile, with fire protection boards added on all four sides. See Figure F-1 for an example.

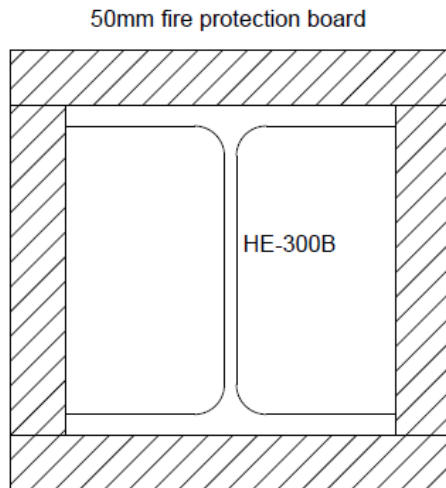


Figure F-1: Example of H-profile boxed in by 50mm of fire protection board.

### Calculation procedure, fully encased composite column, acc. EC4, part 1-2 [4] table 4.4:

#### Step 0 (R0)

- Set up the scenario loading in A3C and calculate the minimum required steel sections for normal temperature by standard ULS verification. The cross-section is provided with the minimum required amount of concrete cover and  $4 \times \varnothing 12\text{mm}$  longitudinal rebars.
- Check if the closest smaller steel section, with an increased reinforcement diameter and the required minimum concrete cover can fulfil ULS criteria. If it is a near-miss, then also increase the concrete dimensions slightly.  
If a smaller total cross-sectional area is found, this is used as the result.

#### Step 1 (R30 to R180)

- Check the cross-section found in step 0 in A3C for R30 to R180 fire resistance according the EC4 table and increase the concrete encasement and the reinforcement cover if required by the tables.
- If the cover exceeds 30% of the total column depth, a larger steel section must be selected and step 1 recalculated.

### Calculation procedure, partially encased composite column, acc. EC4, part 1-2 [4] table 4.6:

The web to flange thickness of the steel member must minimum be 0,5 in order to use the simplified rules for PEC columns given by table 4.6. This requirement is fulfilled for all the HE-B members which are considered. Since HE-B members are only 300mm wide, the tabulated criteria which requires a minimum width of 400mm are impossible to fulfil. This means that a fire rating higher than R90 is not possible to achieve with a partially encased HE-B member and the tabulated values.

#### Step 0 (R0)

- Set up the scenario loading in A3C and calculate the minimum required section by standard ULS verification.



Step 1 (for R30 to R90)

- The required cross-section can be iteratively determined in A3C for each load-bearing fire resistance & load case by selecting the same steel section size as found in step 0, with the maximum allowed amount (as close to 6% reinforcement ratio as possible) of reinforcement and check whether that is sufficient, else increase the steel section. Once the steel section size has been found, the reinforcement is reduced as much as allowable.

#### Calculation procedure, concrete filled tubular section, acc. EC4, part 1-2 [4] table 4.7:

To determine the fire resistance of a CFT section according to the tabulated approach in EC4 includes several limitations:

- The yield strength of the steel  $f_y$  is assumed to be 235 MPa, regardless of what it is in normal temperature.
- Unlike the partially and fully encased cross-sections which allow to account for the reinforcement contribution for reinforcement ratios up to 6%, the concrete filled hollow section only allow to account for the reinforcement contribution for reinforcement ratios up to 3%. Simultaneously, the minimum required reinforcement ratio is 6% for many cases, meaning at least half of the reinforcement steel cannot be included in these calculations.
- Where applicable, the minimum required reinforcement ratio of 6% causes ambiguity between EC4, part 1-1 [3] and EC4, part 1-2 [4] since the buckling curves are only valid for up to a maximum 6% reinforcement ratio.

No guidance on this issue has been found and it is therefore assumed that regardless of the actual reinforcement ratio, the buckling curves for 3% reinforcement can be used since this ratio is that which can be accounted for.

- The wall thickness of the steel section can maximum be 1/25 of the outer diameter in order to account for the full wall thickness. This is controlled by only allowing steel sections with sufficiently thin walls. These sections are given by Table D-1 in Appendix D.

The developed MATLAB model for the CFT section does not include these limitations, so therefore they are enforced by the calculation procedures as shown below. This sometimes causes a small error on the unsafe side, in which the concrete area is taken as that for a reinforcement ratio of 3% even if it the true concrete area is lower due to a higher reinforcement ratio. It is however assumed that the difference in concrete area (which in reality is a steel rebar instead of concrete) at least can match the yield strength of concrete and therefore this error is ignored.

Note that EC4, part 1-2 [4] uses a slightly different definition of the reinforcement ratio  $\rho_s$  than EC4, 1-1 [3].

$$\rho_s = A_s/A_c \text{ (EC4-1-1)}$$

$$\rho_s = A_s/(A_c + A_s) \text{ (EC4-1-2)}$$

The required reinforcement diameter to achieve a 3% reinforcement ratio with 4 rebars as per EC4-1-2 rules can be stated:

$$\emptyset_{L,3\%} = 2 \sqrt{\frac{0,03 * \pi * (\frac{D}{2} - t)^2}{4 * \pi}} \approx 0,17 * (\frac{D}{2} - t)$$

Where D and t are the outer diameter and thickness of the steel section respectively.

### Step 0 (R0)

- Set up the scenario loading in the MATLAB model and calculate the minimum required section by standard ULS verification.

### Step 1 (for R30 to R180)

- The required cross-section can be iteratively determined in the fire mode of the MATLAB model for each load-bearing fire resistance & load case by selecting the same steel section size as found in step 0, with 3% amount of reinforcement and the largest steel section thickness. Once the steel section diameter has been found, the steel section thickness is reduced as much as allowable.

## Detailed results of minimum column depth study

The load cases used in the study are as per Table 4-6.

The required cross-sections and the thickness of fire protection board for the different load cases are given by Table F-1 to Table F-4.

The depth reduction results are presented as column graphs in Figure F-2 to Figure F-7, where the depth reductions achieved by using a composite section instead of a steel HE-B member with fire protection boards are presented.

*Table F-1: Steel cross-sections and passive fire protection thickness, column depth study.*

	R0		R30		R60		R90		R120		R180	
Load case	HE-B:	PFP th. (mm)	HE-B:	PFP th. (mm)	HE-B:	PFP th. (mm)	HE-B:	PFP th. (mm)	HE-B:	PFP th. (mm)	HE-B:	PFP th. (mm)
N1	200	0	200	20	200	20	200	30	200	55	240	100
N2	220	0	220	20	220	20	220	35	220	70	280	100
N3	240	0	240	20	240	20	240	35	240	60	280	100
N4	280	0	280	20	280	20	280	30	280	60	300	100
N5	300	0	300	20	300	20	300	30	300	55	340	100
N6	320	0	320	20	320	20	320	30	320	55	360	100
L1	220	0	220	20	220	20	220	35	220	70	280	100
L2	220	0	220	20	220	20	220	35	220	70	280	100
L3	240	0	240	20	240	20	240	35	240	60	280	100
L4	260	0	260	20	260	20	260	35	260	60	280	100
L5	280	0	280	20	280	20	280	25	280	50	280	100
M1	240	0	240	20	240	20	240	35	240	60	280	100
M2	240	0	240	20	240	20	240	40	240	70	300	100
M3	260	0	260	20	260	20	260	50	260	80	320	100
M4	260	0	260	20	260	20	260	50	260	80	340	100
M5	280	0	280	20	280	20	280	50	280	80	360	100
M6	300	0	300	20	300	20	300	40	300	70	360	100

Steel grade: S355

Table F-2: FEC steel sections and concrete cover thickness, column depth study

	R0		R30		R60		R90		R120		R180	
Load case	HE-B:	Cover (mm)	HE-B:	Cover (mm)	HE-B:	Cover (mm)	HE-B:	Cover (mm)	HE-B:	Cover (mm)	HE-B:	Cover (mm)
N1	140	43	140	43	140	43	140	50	140	80	140	105
N2	160	43	160	43	160	43	160	45	160	75	160	95
N3	180	43	180	43	180	43	180	43	180	75	180	85
N4	200	43	200	43	200	43	200	43	200	75	200	75
N5	200	49	200	49	200	49	200	51	200	75	200	75
N6	220	47	220	47	220	47	220	48	220	65	220	75
										0		
L1	140	48	140	48	140	48	140	50	140	80	140	105
L2	160	45	160	45	160	45	160	45	160	75	160	95
L3	180	43	180	43	180	43	180	43	180	75	180	85
L4	200	43	200	43	200	43	200	43	200	75	200	75
L5	200	53	200	53	200	53	200	53	200	75	200	75
										0		
M1	180	43	180	43	180	43	180	43	180	75	180	85
M2	180	43	180	43	180	43	180	43	180	75	180	85
M3	180	46	180	46	180	46	180	47	180	75	180	85
M4	200	43	200	43	200	43	200	43	200	75	200	75
M5	200	48	200	48	200	48	200	48	200	75	200	75
M6	220	43	220	43	220	43	220	43	220	65	220	75
Steel grade: S355 Concrete: C40/50, XC1, 28 days hardening before load, 50% RH Rebar: B500NC grade												

Table F-3: Partially encased steel sections, column depth study

	R0	R30	R60	R90
Load case	HE-B:	HE-B:	HE-B:	HE-B:
N1	180	180	240	300
N2	200	200	260	300
N3	200	200	280	300
N4	220	220	300	300
N5	240	240	300	300
N6	240	240	300	300
L1	180	180	260	300
L2	200	200	280	300
L3	200	200	280	300
L4	220	220	300	300
L5	240	240	300	320
M1	200	200	280	300
M2	200	200	280	300
M3	200	200	280	300
M4	220	220	280	300
M5	220	220	280	300
M6	240	240	280	300
Steel grade: S355 Concrete: C40/50, XC1, 28 days hardening before load, 50% RH Rebar: B500NC grade				

Table F-4: CFT steel CHS cross-section diameter (D) and thickness (t), column depth study

Load case	R0		R30		R60		R90		R120		R180	
	CHS $\phi$ (mm)	CHS t (mm)	CHS $\phi$ (mm)	CHS t (mm)	CHS $\phi$ (mm)	CHS t (mm)	CHS $\phi$ (mm)	CHS t (mm)	CHS $\phi$ (mm)	CHS t (mm)	CHS $\phi$ (mm)	CHS t (mm)
N1	168,3	8	273	6	273	6	273	10	273	10	406,4	6
N2	168,3	12,5	273	6	273	6	323,9	10	323,9	10	406,4	6
N3	193,7	12,5	273	6	273	6	355,6	12,5	355,6	12,5	406,4	6
N4	219,1	12,5	273	6	323,9	6	406,4	6	406,4	10	406,4	10
N5	244,5	10	273	6	323,9	8	406,4	6	457	6	457	8
N6	244,5	12,5	323,9	6	355,6	6	406,4	6	457	6	457	12,5
L1	168,3	12,5	273	6	273	6	355,6	10	355,6	10	406,4	6
L2	193,7	10	273	6	273	6	355,6	12,5	355,6	12,5	406,4	6
L3	193,7	12,5	273	6	273	6	355,6	12,5	355,6	12,5	406,4	6
L4	219,1	10	273	6	273	6	355,6	12,5	355,6	12,5	406,4	6
L5	219,1	12,5	273	6	273	6	406,4	6	406,4	8	406,4	8
M1	193,7	12,5	273	6	273	6	355,6	12,5	355,6	12,5	406,4	6
M2	219,1	12,5	273	6	273	6	355,6	12,5	355,6	12,5	406,4	6
M3	244,5	12,5	273	6	273	8	355,6	12,5	355,6	12,5	406,4	6
M4	273	10	273	6	323,9	10	355,6	12,5	355,6	12,5	406,4	6
M5	273	12,5	323,9	6	323,9	6	406,4	6	406,4	8	406,4	8
M6	323,9	8	323,9	6	355,6	6	406,4	6	406,4	12,5	406,4	12,5

Steel grade: S355  
 Concrete: C40/50, XC1, 28 days hardening before load, 50% RH  
 Rebar: B500NC grade

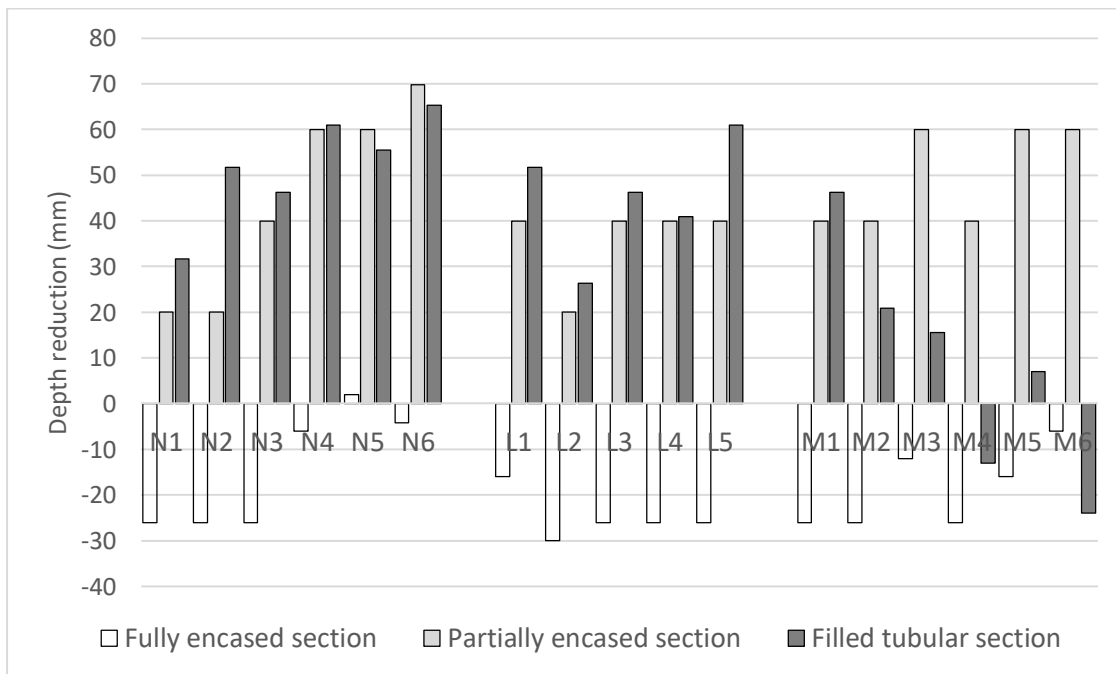


Figure F-2: Depth reduction for columns with no loadbearing fire criteria (R0)

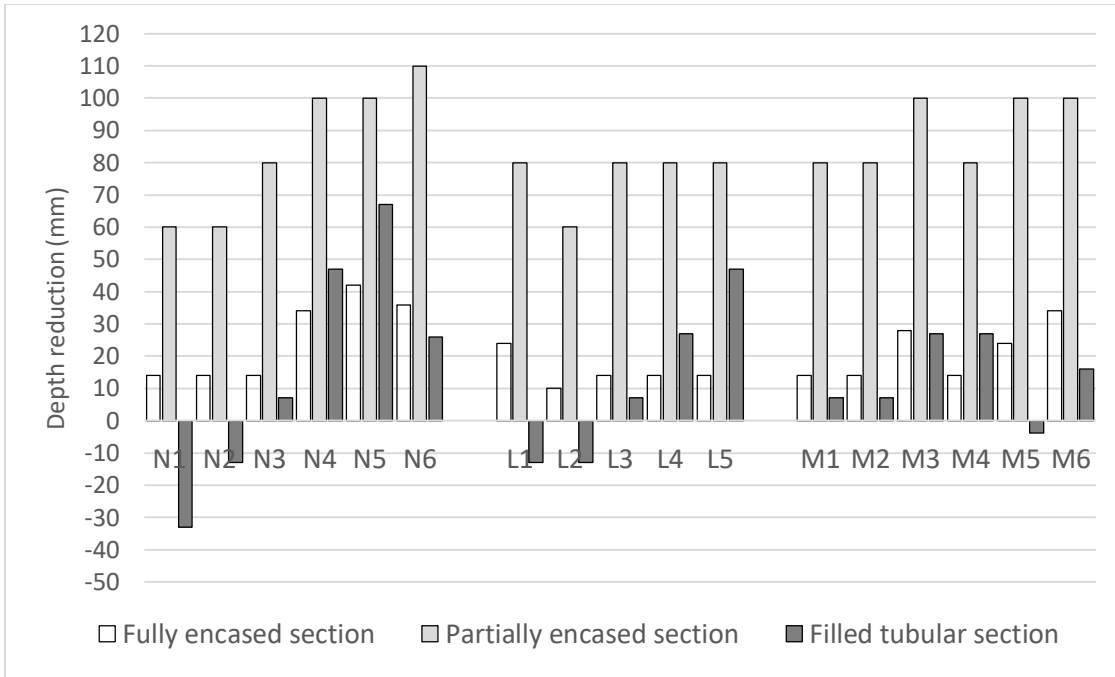


Figure F-3: Depth reduction for columns with 30 min. loadbearing fire criteria (R30)

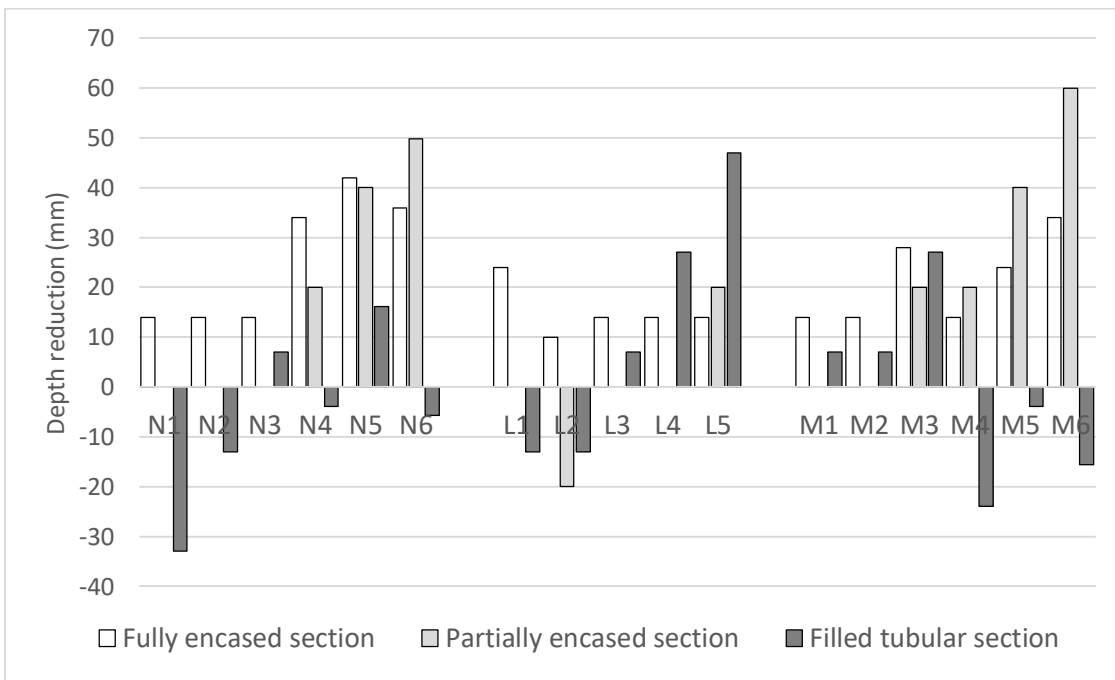


Figure F-4: Depth reduction for columns with 60 min. loadbearing fire criteria (R60)

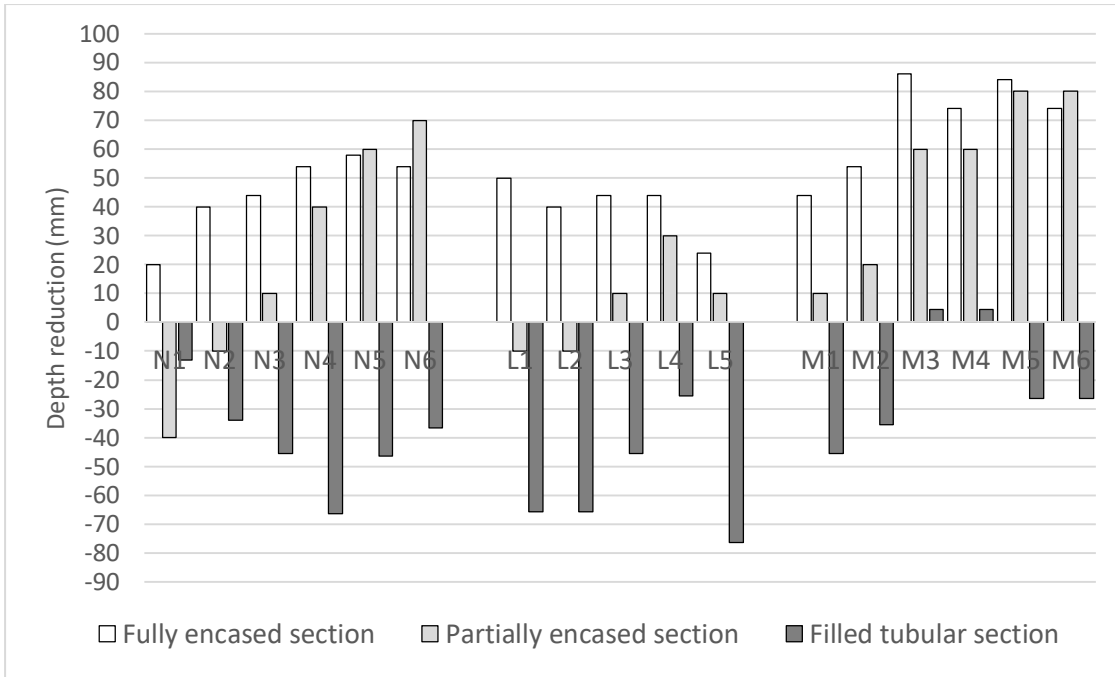


Figure F-5: Depth reduction for columns with 90 min. loadbearing fire criteria (R90)

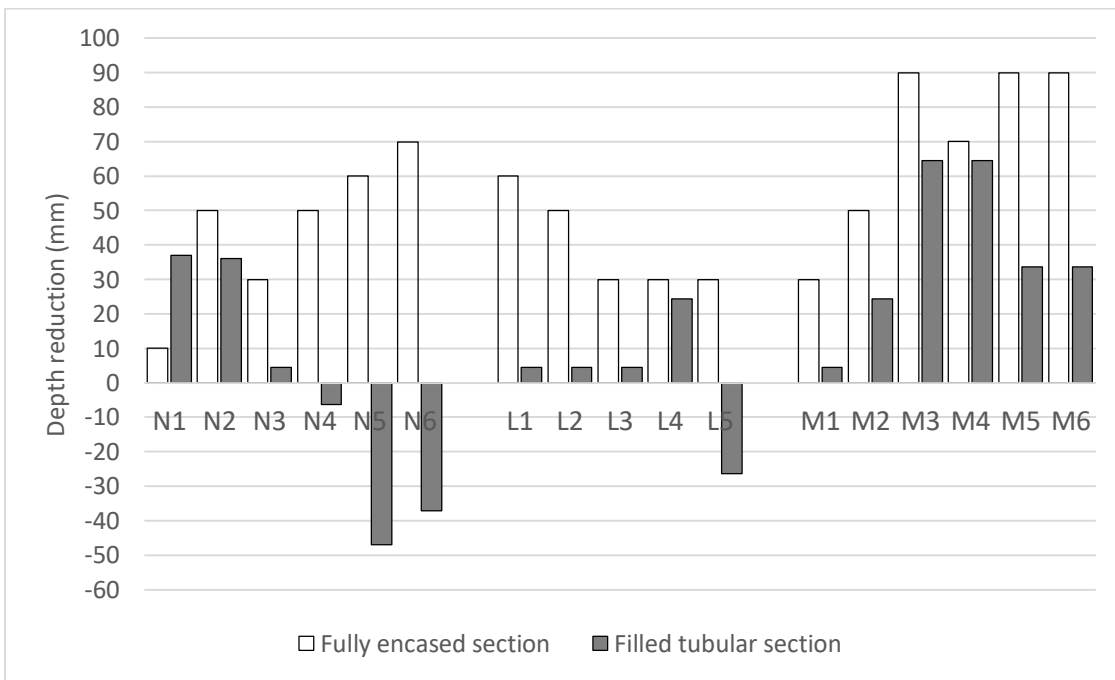


Figure F-6: Depth reduction for columns with 120 min. loadbearing fire criteria (R120)

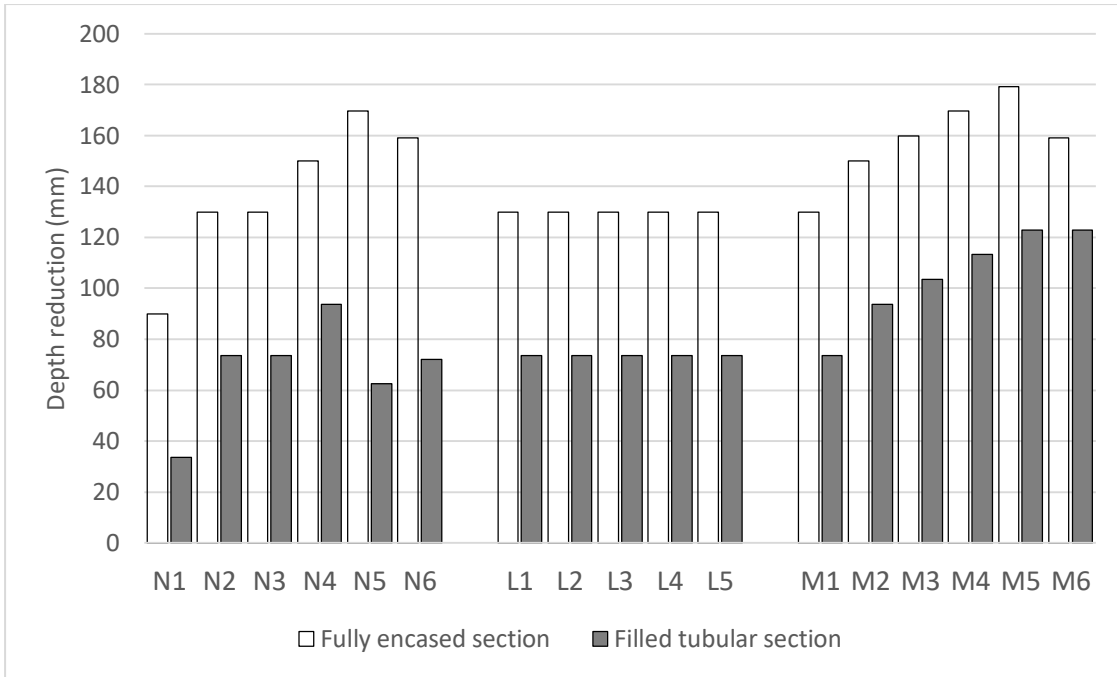


Figure F-7: Depth reduction for columns with 180 min. loadbearing fire criteria (R180)

## Appendix G. Steel efficiency study

This appendix relates to the steel efficiency study in section 4.4 and provides the following information:

- Description on how the cross-sectional area of the transverse reinforcement is converted to an equivalent longitudinal steel area.
- Determination of the bending moments applied on beam-columns.
- Detailed results of the study

### Determination of the minimum required transverse reinforcement cross-sectional area per unit length of PEC column

The transverse reinforcement will add up to the total amount reinforcement of a column and for the steel amount study, this is accounted for. It is assumed that the transverse rebars are evenly distributed along the column length. Note that the extra required transverse reinforcement in the load introduction region is not considered as it has a marginal effect on the total amount used.

The minimum amount of steel used for transverse reinforcement of a PEC column is determined and converted to an equivalent longitudinal cross-sectional steel area. Dimensional variable names are visualized in Figure G-1.

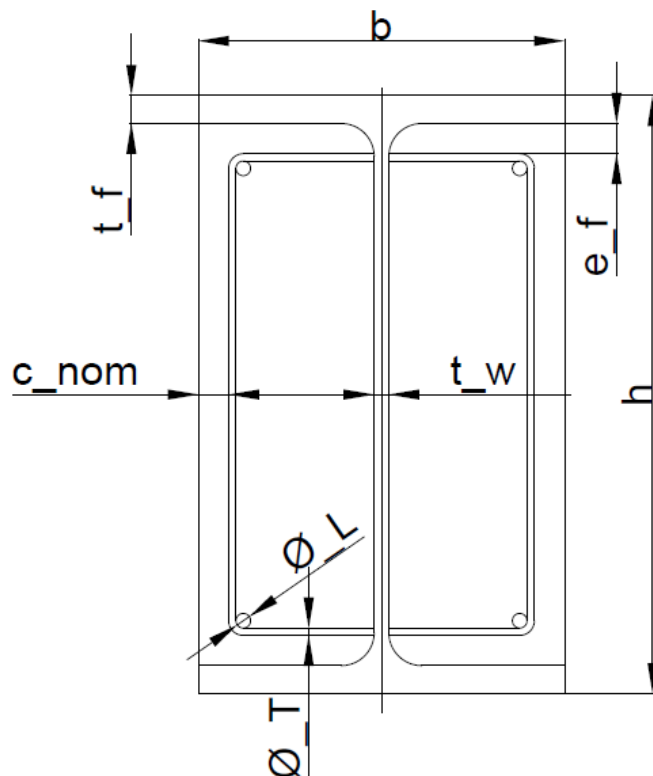


Figure G-1: PEC section dimensions (typical)

The amount of transverse reinforcement is assumed as the minimum required by EC2, part 1-2 [15], which is having a spacing  $s_{cl,max}$  equalling:

$$s_{cl,max} = \min(20 * \varnothing_L; h; 400) \text{ mm}$$



The diameter of the transverse reinforcement  $\varnothing_T$  is selected as the closest available profile which satisfies:

$$\varnothing_T = \max\left(6; \frac{\varnothing_L}{4}\right) mm$$

The reinforcement is laid as stirrups on the outside of the longitudinal reinforcement, with a cover  $c_{nom}$  and a distance to steel flange of  $e_f$ . The length of one stirrup  $L_{st}$ , assuming the radius is a straight corner thus equals:

$$L_{st} = h - 2(t_f + e_f) + b - t_w - 2c_{nom}$$

The total transverse reinforcement length (in mm) per meter of column length, using one stirrup on each side of the web:

$$L_T = \frac{1000}{s_{cl,max}} * 2L_{st}$$

Assuming the transverse reinforcement is laid out similarly as the longitudinal reinforcement, the cross-sectional area would equal:

$$A_T = \pi \left(\frac{\varnothing_T}{2}\right)^2 * \frac{L_T}{1000}$$

This area  $A_T$  is included in the MS Excel sheet which determines the required steel amount for a certain cross-section.

### Determination of design moments for beam-column

The design moments are set as 15%,30% and 45% of the uniaxial pure bending moment resistance about the major axis  $M_{y,Rd}$  of the steel section, equalling:

$$M_{y,Rd} = \frac{W_{y,Pl} * f_y}{\gamma_{M0}} \text{ (class 1,2)}$$

$$M_{y,Rd} = \frac{W_{y,El} * f_y}{\gamma_{M0}} \text{ (class 3)}$$

The calculated values are given in Table G-1.

Table G-1: Design moments for steel amount study

Member	Class	Section modulus	15% $M_{y,Rd}$	30% $M_{y,Rd}$	45% $M_{y,Rd}$
Grade S355 ( $f_y=355MPa$ )	Ref. EC3, part 1-1 [29]	$W_{y,Pl}$ (class 1,2) $W_{y,El}$ (class 3) $mm^3$	kNm	kNm	kNm
HE-A 200	2	429500	21,8	43,6	65,3
HE-A 300	3	1259600	63,9	127,8	191,6
HE-A 400	1	2561800	129,9	259,8	389,8
HE-B 200	1	642500	32,6	65,2	97,8
HE-B 300	1	1868700	94,8	189,5	284,3
HE-B 400	1	3231700	163,9	327,8	491,7

## Detailed results of steel efficiency

The main results of the steel efficiency study are given in Table G-2 and

Table G-3. The effect of changing reinforcement dimensions is given in Table G-4.

Table G-2: Steel efficiency for steel, PEC and CFT columns with axial load

Buckling length	Steel, $\chi_{steel}$			PEC, $\chi_{comp}$		
	3m	4m	5m	3m	4m	5m
HE-200A	0,70	0,54	0,40	0,95	0,70	0,51
HE-300A	0,87	0,76	0,65	1,27	1,09	0,90
HE-400A	0,91	0,81	0,70	1,25	1,06	0,88
HE-200B	0,71	0,55	0,41	0,88	0,66	0,49
HE-300B	0,85	0,77	0,65	1,18	1,01	0,85
HE-400B	0,89	0,82	0,70	1,17	1,00	0,83
<b>Average</b>	<b>0,82</b>	<b>0,71</b>	<b>0,59</b>	<b>1,12</b>	<b>0,92</b>	<b>0,74</b>
	CFT, $\chi_{comp}$					
	3m	4m	5m			
193,7x6	1,40	1,11	0,82			
193,7x8	1,26	1,03	0,78			
323,9x6	2,08	1,94	1,75			
323,9x8	1,79	1,68	1,53			
406,4x8	2,08	1,99	1,89			
<b>Average</b>	<b>1,72</b>	<b>1,55</b>	<b>1,35</b>			

Table G-3: Steel efficiency for steel and PEC columns with axially load + bending moment

Moment ratio, ref. Table G-1	Steel, $\chi_{steel}$			PEC, $\chi_{comp}$		
	15%	30%	45%	15%	30%	45%
HE-200A	0,48	0,43	0,37	0,70	0,70	0,70
HE-300A	0,66	0,56	0,45	1,09	1,09	1,09
HE-400A	0,76	0,69	0,59	1,06	1,06	1,06
HE-200B	0,50	0,45	0,39	0,66	0,66	0,66
HE-300B	0,71	0,65	0,56	1,01	1,01	1,01
HE-400B	0,76	0,70	0,60	1,00	1,00	1,00
<b>Average</b>	<b>0,65</b>	<b>0,58</b>	<b>0,49</b>	<b>0,92</b>	<b>0,92</b>	<b>0,92</b>

Table G-4: Steel efficiency for PEC and CFT columns with varying degrees of reinforcement

Longitudinal reinforcement	PEC HE-200A, $\chi_{comp}$		CFT 193,7x6mm, $\chi_{comp}$
	5m length No end moment	4m length 45% end moment	5m length No end moment
None	N/A	N/A	0,824
4x $\varnothing$ 8mm	0,513	0,698	0,772
8x $\varnothing$ 8mm	0,514	0,699	N/A
4x $\varnothing$ 16mm	0,509	0,693	0,655

6xØ20mm	0,485	0,66	N/A
---------	-------	------	-----

## Appendix H. Environmental foot-print study

This appendix shows the detailed results of the environmental footprint study in section 4.5.

- The calculated CFT cross-sections used in the environmental foot-print study are given in Table H-1.
- The detailed results of the environmental foot-print study are given by Figure H-1 and Figure H-2.

Table H-1: CFT cross-sections for the environmental foot-print study

Load case	CHS section diameter (mm)	CHS section thickness (mm)	Longitudinal reinforcement diameter (mm) (4 off)
<b>N1</b>	168,3	8	12
<b>N2</b>	168,3	12,5	14
<b>N3</b>	193,7	12,5	16
<b>N4</b>	219,1	12,5	16
<b>N5</b>	244,5	10	16
<b>N6</b>	244,5	12,5	16
<b>L1</b>	168,3	12,5	20
<b>L2</b>	193,7	10	25
<b>L3</b>	193,7	12,5	16
<b>L4</b>	219,1	10	28
<b>L5</b>	219,1	12,5	28
<b>M1</b>	193,7	12,5	16
<b>M2</b>	219,1	12,5	14
<b>M3</b>	244,5	12,5	16
<b>M4</b>	273	10	12
<b>M5</b>	273	12,5	32
<b>M6</b>	323,9	8	25
Steel grade: S355 Concrete: C40/50, XC1, 28 days hardening before load, 50% RH Rebar: B500NC grade			

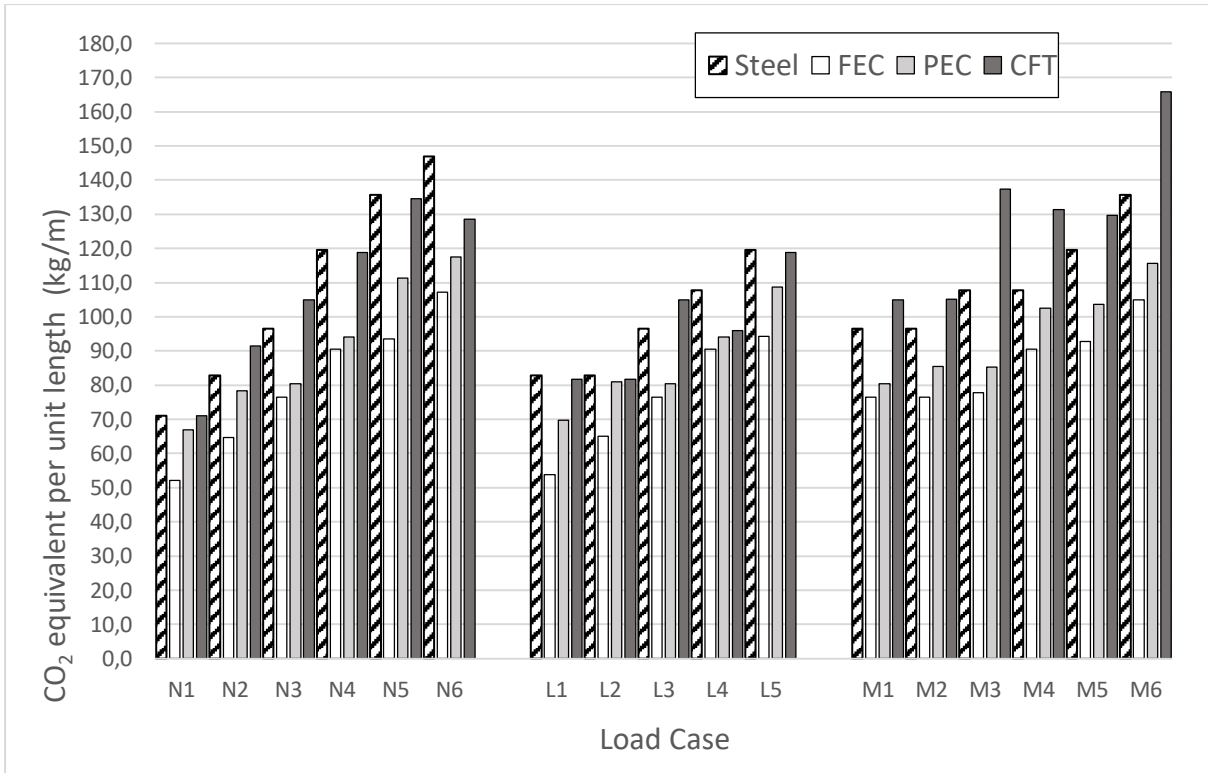


Figure H-1: CO2 mass equivalents per m of column length for each load case

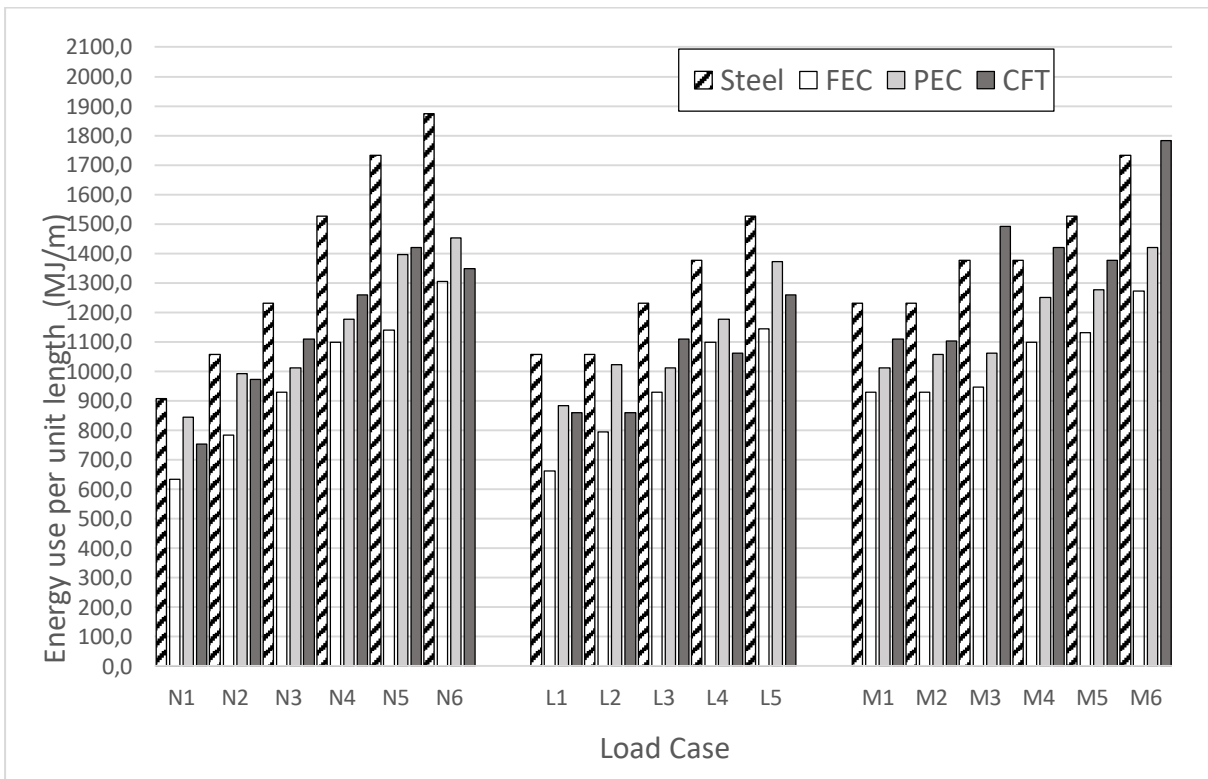


Figure H-2: Energy use per m of column length for each load case

## Appendix I. MATLAB/CALFEM Codes for span study

In this appendix, the MATLAB+CALFEM source codes used in the span study in section 4.2 are given for:

- Calculation of the reaction forces of a uniformly loaded and spanned continuous beam as a variable of the uniformly distributed load, times the span length.
- Calculation of the relationship between the span and axial load of a pinned rectangular frame, when loaded in accordance to Eurocode rules; for spans between 5-25m.
- Calculation of the axial loads and end moments for a given column in a rectangular, rigid frame as well as the hogging beam moments at the beam-column joints and the sagging mid-beam moments.

### Reaction forces , continuous beam

```
%This program calculates the ratios of continuous beam reaction forces  
%to the force Q*L for a chosen number of spans. It further presents the  
%maximum (absolute) moment encountered.
```

```
clear all  
close all  
clc  
%Variables by user (Span in mm, Q in N/mm, Number of spans)  
L=16300;  
Q=75.6;  
Spans=5;  
  
% El.Modulus, Crossection area, 2nd area moment - beam (HE-1000A)  
% (MPa, mm^2, mm^4)  
E=210000;  
A=346.85*100;  
I=553846*10000;  
  
% CALCULATIONS  
%Establish the beam elements, with node numbers and coordinates  
%BC is boundary conditions (pinned supports)  
Edof=[1 1 2 3 4 5 6];  
Ex=[0 L];  
Ey=[0 0];  
BC=[1 0;2 0];  
for i=2:Spans+1  
    Edof=[Edof;i i*3-2 i*3-1 i*3 i*3+1 i*3+2 i*3+3];  
    Ex=[Ex;L*(i-1) L*i];  
    Ey=[Ey;0 0];  
    BC=[BC;i*3-2 0;i*3-1 0];  
  
end  
for i=1:Spans  
    Eq(i,1)=0;  
    Eq(i,2)=-Q;  
end  
%Edit load/loads  
Eq(3,2)=0; %Imposed load in the middle is removed  
  
%Material data and distributed load vector  
Ep=[E A I];  
  
%Establish load vector and assemble stiffness matrix  
f=zeros(3*(Spans+1),1);  
K=zeros(3*(Spans+1),3*(Spans+1));
```

```

for i=1:Spans
    [Ke,fe]=beam2e (Ex (i, :),Ey (i, :),Ep,Eq (i, :));
    [K,f]=assem (Edof (i, :),K,Ke,f,fe);
end

% Solve unknown displacements(a) and support reactions (r)
[a,r]=solveq(K,f,BC);
% Store support reactions as a ratio of Q*Span in N
N=zeros (Spans+1,2);
for i=1:Spans+1
    N(i,1)=i;
    N(i,2)=round(r(i*3-1,:)/(Q*L),3);
end
N
%get element displacements in global coordinates
for i=1:Spans
    Ed(i,:)=extract (Edof (i, :),a);
end
%* Find max moment and deflection, beam
MaxM=0; MaxMx=0;
MaxD=0; MaxDx=0;

for i=1:Spans
    [Es,Edi,Eci]=beam2s (Ex (i, :),Ey (i, :),Ep,Ed (i, :),Eq (i, :),100);           %Check
    moments and deflections for 100 positions
    for j=1:100
        %if max moment, then update value
        if (abs (MaxM)<abs (Es (j,3)))
            MaxM=Es (j,3);
        end
    end
end
end
%Present max moment in kNm,
abs (MaxM/1e6)

```

The calculated reaction force WS-factors for a continuous beam with uniformly distributed load W and 5 equally long spans S:

(Column number    Reaction force WL factor)

1.0000    0.3950

**2.0000    1.1320 (Used as Gfac in pinned frame analysis)**

3.0000    0.9740

4.0000    0.9740

5.0000    1.1320

6.0000    0.3950

Output of reaction force WL-factor, 5 span beam with middle span removed.

1.0000    0.3820

**2.0000    1.2110 (Used as Qfac in pinned frame analysis)**

3.0000    0.4080

4.0000 0.4080

5.0000 1.2110

6.0000 0.3820

## Pinned frame analysis

```
%This program calculates the reaction force NEd for 1000 different span
lengths,
%for a 4 story building with Eurocode reduction factors implemented
GGk = 5; %Characteristic surface permanent load (kN/m2)
QQk = 3; %Characteristic surface imposed load (kN/m2)
D = 7.2; % Beam to beam distance (m)
Lmin=5; %Min span(m)
Lmax=20; %Max span (m)
b=0.3; %Column depth, must be recalculated by trial (m)
ntot=4; %Number of stories, should be at least 2
Gfac=1.132; %WL-Factor for permanent load 5 spans, calculated seperately
Qfac=1.211; %WL-Factor for imposed load 5 spans, calculated seperately
psi0=0.7; %EC0 reduction factor on imposed load
%CALCULATIONS
NEd = zeros(1000,2); %Init NEd
for i = 1:1000

    L=Lmin+(Lmax-Lmin)*(i/1000); %Span length (m)
    Gk=GGk*D; %Characteristic permanent line load on beam (kN/m)
    Qk=QQk*D; %Characteristic imposed line load on beam (kN/m)
    alphaA=max(0.7,min(0.5+15/(7.2*(L-b)),1)); %Reduction factor for beam
    alphaN(ntot)=1; %Column reduction factor, top story
    alphaN(ntot-1)=1; %Column reduction factor, top-1 story
    %Determination of the rest of column reduction factors, for bottom
stories:
    if ntot > 2
        for j=1:(ntot-2)
            n=ntot-j+1;
            alphaN(j)=(2+(n-2)*psi0)/n;
        end
    end
    %Determination of dimensioning axial load, (kN):

    NEd(i,1)=L; %Insert span length in first column of NED matrix
    for j=1:ntot
        alphamin=min(alphaA,alphaN(j));
        E610a=1.35*Gk+1.5*psi0*Qk %Equation 6.10a
        E610b=1.2*Gk+1.5*alphamin*Qk %Equation 6.10b
        if E610a>=E610b
            Gi=1.35*Gk;
            Qi=1.5*psi0*Qk;
        else
            Gi=1.2*Gk;
            Qi=1.5*alphamin*Qk;
        end
        NEd(i,2) = NEd(i,2) + L*(Gfac*Gi + Qfac*Qi); %Add load contribution
    from story
    end
end
```

## Rigid frame analysis

```
% This program establishes and analyses a rigid frame with user set number
of columns
% and stories, with user set span and column height.
clear all;
close all;
clc;
disp("Please wait...")
% ----- SETTINGS BY USER
% Column height (mm)
H=3500;
% Column-Column distance (mm)
D=7200;
%Min, max- span lengths (mm)
SpanMin=0;
SpanMax=25000;
%Data points
Spanpoints=250;
% Characteristic Loads (kN/m)
Gk=5;
Qk=3;
%EC0 factor
psi0=0.7;
%Beams without imposed load (Beams are numbered from bottom to top, then
%left to right)
%A2 column = 2; B1 column = 5
NoneImp=[25];
%Number of columns and stories
Columns=6;
Stories=4;
%Bases rigid (true) or pinned (false)?
Rigidbases=true;
%Braced left columns (vertical rollers)?
Bracedleft=false;
%Span length to find maximum moment (mm)
CheckMSpan=12500;
%Calculate all columns (takes more time)?
AllResults=true;
% El.Modulus, Crossection area & 2nd area moment - column (HE200A)
% (MPa, mm^2, mm^4)
EC=210000;
% Section area and 2nd moment of area properties calculated in A3C and
converted to steel equivalent for composite members.
%Uncomment the section which is to be calculated

% Steel sections
%AC=53.83*100; %HE200A
%IC=3692*10000; %HE200A
%AC=78.081*100; %HE200B
%IC=5696*10000; %HE200B
%AC=112.53*100; %HE300A
%IC=18263*10000; %HE300A
AC=149.08*100; %HE300B
IC=25166*10000; %HE300B
%Fully encased, C25 sections
%AC=95*100; %Full C25Ø12 HE200A
%IC=5543*10000; %Full C25Ø12 HE200A
%AC=119.6*100; %Full C25Ø12 HE200B
%IC=7700*10000; %Full C25Ø12 HE200B
%AC=186.46*100; %Full C25Ø12 HE300A
```



```

%IC=24027*10000; %Full C25Ø12 HE300A
%AC=223*100; %Full C25Ø12 HE300B
%IC=31212*10000; %Full C25Ø12 HE300B
%Fully encased, C50 sections
%AC=119*100; %Full C50Ø12 HE200A
%IC=6444*10000; %Full C50Ø12 HE200A
%AC=144*100; %Full C50Ø12 HE200B
%IC=8672*10000; %Full C50Ø12 HE200B
%AC=230.19*100; %Full C50Ø12 HE300A
%IC=27012*10000; %Full C50Ø12 HE300A
%AC=266.83*100; %Full C50Ø12 HE300B
%IC=34336*10000; %Full C50Ø12 HE300B
%Partially encased, C25 sections
%AC=75.21*100; %Part C25Ø12 HE200A
%IC=4063*10000; %Part C25Ø12 HE200A
%AC=99.21*100; %Part C25Ø12 HE200B
%IC=6069*10000; %Part C25Ø12 HE200B
%AC=158.62*100; %Part C25Ø12 HE300A
%IC=20116*10000; %Part C25Ø12 HE300A
%AC=194.27*100; %Part C25Ø12 HE300B
%IC=26994*10000; %Part C25Ø12 HE300B
%Partially encased, C50 sections
%AC=85.77*100; %Part C50Ø12 HE200A
%IC=4213*10000; %Part C50Ø12 HE200A
%AC=109.63*100; %Part C50Ø12 HE200B
%IC=6217*10000; %Part C50Ø12 HE200B
%AC=182.9*100; %Part C50Ø12 HE300A
%IC=20933*10000; %Part C50Ø12 HE300A
%AC=218.85*100; %Part C50Ø12 HE300B
%IC=27821*10000; %Part C50Ø12 HE300B
%Hollow filled, C25 sections
%AC=54.43*100; %Filled C25Ø12 193,7x6
%IC=1933*10000; %Filled C25Ø12 193,7x6
%AC=65.08*100; %Filled C25Ø12 193,7x8
%IC=2362*10000; %Filled C25Ø12 193,7x8
%AC=75.49*100; %Filled C25Ø12 193,7x10
%IC=2762*10000; %Filled C25Ø12 193,7x10
%AC=107.75*100; %Filled C25Ø12 323,9x6
%IC=9911*10000; %Filled C25Ø12 323,9x6
%AC=126.12*100; %Filled C25Ø12 323,9x8
%IC=12146*10000; %Filled C25Ø12 323,9x8
%AC=144.24*100; %Filled C25Ø12 323,9x10
%IC=14295*10000; %Filled C25Ø12 323,9x10
%Hollow filled, C50 sections
%AC=64.35*100; %Filled C50Ø12 193,7x6
%IC=2053*10000; %Filled C50Ø12 193,7x6
%AC=74.56*100; %Filled C50Ø12 193,7x8
%IC=2472*10000; %Filled C50Ø12 193,7x8
%AC=84.54*100; %Filled C50Ø12 193,7x10
%IC=2862*10000; %Filled C50Ø12 193,7x10
%AC=137.32*100; %Filled C50Ø12 323,9x6
%IC=10978*10000; %Filled C50Ø12 323,9x6
%AC=154.92*100; %Filled C50Ø12 323,9x8
%IC=13159*10000; %Filled C50Ø12 323,9x8
%AC=172.3*100; %Filled C50Ø12 323,9x10
%IC=15256*10000; %Filled C50Ø12 323,9x10
BCol=300; %Column Depth
% El.Modulus, Crossection area & 2nd area moment - beam
% (MPa, mm^2, mm^4)
EB=210000;
%AB=158.98*100; %HE400A for nom size 200

```

```

%IB=45069*10000;    %HE400A for nom size 200
AB=400.05*100;     %HE1000B for nom size 300
IB=644748*10000;  %HE1000B for nom size 300
% ----- CALCULATIONS
NoCol=Columns*Stories;
NoBeam=(Columns-1)*Stories;
%Setup result matrices.
%Axial force (kN), lower and upper end moments (kNm) for columns
ResultNC=zeros(NoCol+1,Spanpoints+1);
ResultMCs=zeros(NoCol+1,Spanpoints+1);
ResultMCE=zeros(NoCol+1,Spanpoints+1);
%Provide column number in results
for i = 1:NoCol
    ResultNC(i+1,1)=i;
    ResultMCs(i+1,1)=i;
    ResultMCE(i+1,1)=i;
end
%Axial force (kN), left, mid and right end moments (kNm) for beams
ResultNB=zeros(NoBeam+1,201);
ResultMBS=zeros(NoBeam+1,201);
ResultMBm=zeros(NoBeam+1,201);
ResultMBe=zeros(NoBeam+1,201);
%Provide beam number in results
for i = 1:NoBeam
    ResultNB(i+1,1)=i;
    ResultMBS(i+1,1)=i;
    ResultMBm(i+1,1)=i;
    ResultMBe(i+1,1)=i;
end
MaxM=0;    %Init maxmoment check
%Loop to get readings for lots of spans,from Spanmin to Spanmax
%distance
for ii=1:Spanpoints
    Span=round(SpanMin+(SpanMax-SpanMin)*(ii/Spanpoints));
    %Establish column elements, from bottom to top, then left to right
    for i = 1:Columns
        for j = 1:Stories
            if (i==1)&&(j==1)
                %Create array EdofC
                k = 1;
                EdofC = [k 1 2 3 4 5 6];
                ExC=[0 0];
                EyC=[0 H];
            else
                k = k + 1;
                l = j*3+(i-1)*(Stories*3+3);
                % [Column Element no, 1x 1y 1theta 2x 2y 2theta]
                EdofC = [EdofC;[k l-2 l-1 l l+1 l+2 l+3]];
                % [StartX EndX]
                ExC=[ExC;(i-1)*Span (i-1)*Span];
                % [Starty Endy]
                EyC=[EyC;(j-1)*H j*H];
            end
        end
    end
    %Establish beam elements, from bottom to top, then left to right
    for i = 1:Columns-1
        for j = 1:Stories
            if (i==1)&&(j==1)
                %Create array EdofC
                k = Columns*Stories+1;

```

```

    l = Stories*3+7;
    EdofB = [k 4 5 6 1 1+1 1+2];
    ExB=[0 Span];
    EyB=[H H];
else
    k = k + 1;
    l1 = (i-1)*(Stories*3+3)+(j*3+1);
    l2 = (i)*(Stories*3+3)+(j*3+1);
    % [Beam Element no, 1x 1y 1theta 2x 2y 2theta]
    EdofB = [EdofB; [k l1 l1+1 l1+2 l2 l2+1 l2+2]];
    % [StartX EndX]
    ExB=[ExB; (i-1)*Span i*Span];
    % [Starty Endy]
    EyB=[EyB; j*H j*H];
end
end
end

% Material properties, [El.modulus Area 2moment]
EPC=[EC AC IC]; % Columns
EPB=[EB AB IB]; % Beams

%Determine design loads acc. EC0.
alphaA=max(0.7,min(0.5+15/(D*(Span-BCol)),1)); %Reduction factor for beam
alphaN(Stories)=1; %Column reduction factor, top story
alphaN(Stories-1)=1; %Column reduction factor, top-1 story
%Determination of the rest of column reduction factors, for bottom stories:
if Stories > 2
    for j=1:(Stories-2)
        n=Stories-j+1;
        alphaN(j)=(2+(n-2)*psi0)/n;
    end
end
%Find the design permanent and imposed load for each story
for j=1:Stories
    alphamin=min(alphaA,alphaN(j));
    E610a=1.35*Gk+1.5*psi0*Qk; %Equation 6.10a
    E610b=1.2*Gk+1.5*alphamin*Qk; %Equation 6.10b
    if E610a>=E610b
        Gi(j)=1.35*Gk*D/1000;
        Qi(j)=1.5*psi0*Qk*D/1000;
    else
        Gi(j)=1.2*Gk*D/1000;
        Qi(j)=1.5*alphamin*Qk*D/1000;
    end
end
end

%Setup the beam line load
EQB=zeros(NoBeam,2);
for i=1:NoBeam
    j=mod(i-1,Stories)+1; %Find which floor the beam is on
    EQB(i,1)=0; %No horisontal loads
    if ismember(i,NoneImp)
        EQB(i,2)=-Gi(j); %If this beam has no imposed load, use only perm.
    else
        EQB(i,2)=- (Gi(j)+Qi(j)); %Else permanent + imposed
    end
end
end
%%* Line loads [qx qy]:
EQC=[0 0]; % Columns

```

```

% define the dimension of the load and stiffness matrices
Nodes=Columns*(Stories+1);
f=zeros(3*Nodes,1);
K=zeros(3*Nodes,3*Nodes);
% Establish column elements and assemble to system matrix
for i=1:NoCol
    Ke=beam2e(ExC(i,:),EyC(i,:),EPC);
    K=assem(EdofC(i,:),K,Ke);
end
% Establish beam elements + line loads and assemble to system matr.
for i=1:NoBeam
    [Ke,fe]=beam2e(ExB(i,:),EyB(i,:),EPB,EQB(i,:));
    [K,f]=assem(EdofB(i,:),K,Ke,f,fe);
end
%* Establish boundary conditions, bases either fixed or pinned

BC=[1 0;
    2 0];
if Rigidbases
    BC=[BC;3 0];
end
if Bracedleft
    for i=1:Stories
        BC=[BC;1+i*3 0];
    end
end
for i=1:Columns-1
    j=i*(Stories+1)*3+1;
    BC=[BC;j 0;j+1 0];
    if Rigidbases
        BC=[BC;j+2 0];
    end
end

% Solve unknown displacements (a) and reaction forces (r)
[a,r]=solveq(K,f,BC);
%get element displacements in global coordinates
Ed=extract([EdofC;EdofB],a);

%* Find section forces, columns
EsC=beam2s(ExC(1,:),EyC(1,:),EPC,Ed(1,:),EQC);
for i = 2:NoCol
    j=beam2s(ExC(i,:),EyC(i,:),EPC,Ed(i,:),EQC);
    EsC=[EsC;j];
end
%* Find section forces, beams
EsB=beam2s(ExB(1,:),EyB(1,:),EPB,Ed(NoCol+1,:),EQB(1,:),3);
for i = 2:NoBeam
    j=beam2s(ExB(i,:),EyB(i,:),EPB,Ed(NoCol+i,:),EQB(i,:),3);
    EsB=[EsB;j];
end
%Transfer column axial loads and end moments to result matrices of integers

%For easier check of one spec. member, one matrix for the member results
% row1:span; row2:N; row3:Ms; row4:Me
A2Result(1,ii)=Span;
A2Result(2,ii)=abs(int16(EsC(2*2-1,1)/1000)); %convert to positive
A2Result(3,ii)=int16(EsC(2*2-1,3)/1e6);
A2Result(4,ii)=int16(EsC(2*2,3)/1e6);

```

```

B1Result(1,ii)=Span;
B1Result(2,ii)=abs(int16(EsC(5*2-1,1)/1000)); %convert to positive
B1Result(3,ii)=int16(EsC(5*2-1,3)/1e6);
B1Result(4,ii)=int16(EsC(5*2,3)/1e6);

%Produce the full matrix of results if required; takes some more
%calculation time
if AllResults
    ResultNC(1,ii+1)=Span;
    ResultMCs(1,ii+1)=Span;
    ResultMCE(1,ii+1)=Span;
    for i = 1:NoCol
        ResultNC(i+1,ii+1)=int16(EsC(i*2-1,1)/1000);
        ResultMCs(i+1,ii+1)=int16(EsC(i*2-1,3)/1e6);
        ResultMCE(i+1,ii+1)=int16(EsC(i*2,3)/1e6);
    end
    %Transfer beam axial loads and end+mid moments to result matrices of
integers

    ResultNB(1,ii+1)=Span;
    ResultMBs(1,ii+1)=Span;
    ResultMBm(1,ii+1)=Span;
    ResultMBe(1,ii+1)=Span;
    for i = 1:NoBeam
        ResultNB(i+1,ii+1)=int16(EsB(i*3-1,1)/1000);
        ResultMBs(i+1,ii+1)=int16(EsB(i*3-2,3)/1e6);
        ResultMBm(i+1,ii+1)=int16(EsB(i*3-1,3)/1e6);
        ResultMBe(i+1,ii+1)=int16(EsB(i*3,3)/1e6);
    end
    if Span==CheckMSpan %Establish max moment, check all beams for
start,end,mid moment.
        for i=1:NoBeam
            CheckM
            =
max([abs(ResultMBs(i+1,ii+1)),abs(ResultMBm(i+1,ii+1)),abs(ResultMBe(i+1,ii
+1))]));
            if CheckM>MaxM
                MaxM=CheckM;
            end
        end
    end
end
end
end
MaxM

```

## Appendix J. MATLAB codes for ULS and fire verification of a CFT column

This appendix displays a MATLAB source code which can be used to verify a reinforced (or non-reinforced) CFT column for ULS and fire resistance in accordance to the EC4 rules [1,22].

### Key notes on the model:

- Only axial loads with the possibility for off-column centre application eccentricity and point moments (usually this means end moments) can be applied. Transverse loads has not been implemented since they are not relevant for the studies in the thesis but they would be easy to implement.
- CFT cross-sections are subject to a special rule in EC4, named the confinement effect. If the relative slenderness  $\bar{\lambda}$  is 0,5 or lower and the eccentricity ratio  $e/d$ :

$$\frac{e}{d} = \frac{M_{Ed}/N_{Ed}}{d}$$

*$M_{Ed}$  and  $N_{Ed}$  are design moment and axial force respectively,  $d$  is is the diameter of the cross-section*

is 0,1 or lower, then the characteristic strengths of the concrete and steel ( $f_{ck}$  and  $f_y$ ) may be changed in accordance to rules given by EC4, part 1-1 [3]. If so, the steel strength is lowered and the concrete strength increased, which gives an overall higher squash load resistance  $N_{pl,Rd}$ . The confinement effect is included in the model when the requirements are met. This includes calculating the squash load resistance  $N_{pl,Rd}$ , calculating the stress block axial force equilibrium for the MN interaction diagrams and for calculating the squash load resistance based on the partial material factor  $\gamma_{M1}$  (used for buckling resistance). The effect is not included when calculating the characteristic strength  $N_{Rk}$  required for the relative slenderness  $\bar{\lambda}$ . This approach is suggested by Dujmović et al. [39] in order to avoid iterative calculation, since the relative slenderness is an input parameter for determination of the confinement effect factors.

- Unlike the polygonal MN interaction diagram used for hand calculations shown in appendix B, an MN interaction diagram with a large/user selected number of points (200 for this thesis) is calculated. This is done in the fashion suggested by Johnson [25], by calculating the resultant moment and axial force for a large number of evenly spaced positions of the PNA. A difficulty with circular cross-sections when compared to orthogonal sections is to determine the more complex areas and section moduli of the concrete and steel sections. For a given position of the PNA, the area and plastic section modulus of the PNA to the centreline of the tubular mirrored about the centreline and inside the steel tube can be determined through calculations of the circular segment outside the area.

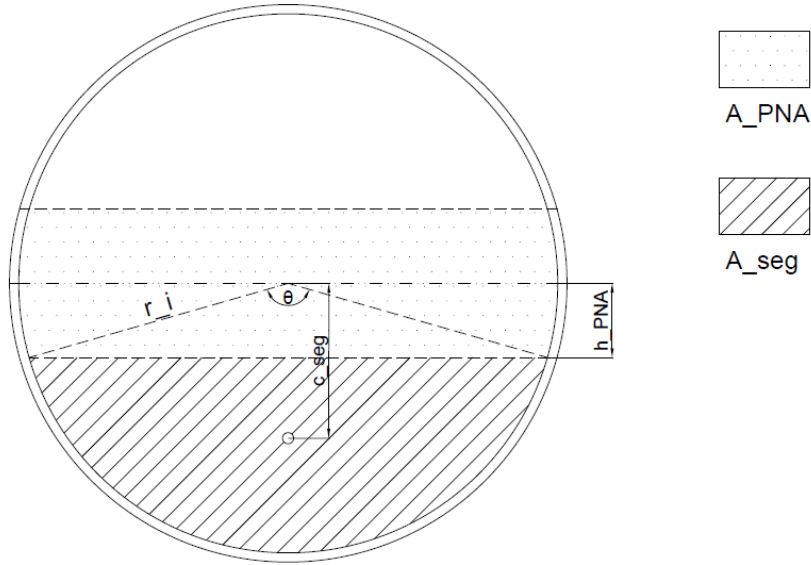


Figure J-1: CFT cross-section without rebars, area determination

A visualization of the relevant dimensions for the below calculations are given in Figure J-1. The angle between radii connecting the chord of the circular segment:

$$\theta = 2 * \arccos\left(\frac{h_{PNA}}{r}\right)$$

Area of circular segment outside the mirrored area:

$$A_{seg} = \frac{r^2}{2} (\theta - \sin\theta)$$

The mirrored area between PNA and centreline is that of a semicircle minus the circular segment previously calculated.

$$A_{PNA} = 2 * \text{abs}\left(\frac{\pi r^2}{2} - A_{seg}\right)$$

The first moments of the mirrored area can be calculated in steps accordingly:

Centroid of circular segment outside the mirrored area:

$$C_{seg} = \frac{4r}{3} \left( \frac{\sin^3\left(\frac{\theta}{2}\right)}{\theta - \sin\theta} \right)$$

The first moment of the circular segment outside the mirrored area:

$$S_{seg} = A_{seg} * C_{seg}$$

The first moment of a semi-circle:

$$S_{semi} = \frac{\pi r^2}{2} * \frac{4r}{3\pi} = \frac{2r^3}{3}$$

First moment of area for the mirrored area between PNA and midline:

$$S_{PNA} = 2 * (S_{semi} - S_{seg})$$

The plastic section modulus is then twice the first moment of area:

$$Z_{PNA} = 2 * S_{PNA}$$

The steel section has a slightly larger outer radius and thus an additional/similar set of calculations must be made for this radius.

- In difference to the example of the FEC cross-section shown in Appendix B, the position of the PNA ( $h_n$ ) at no design axial load is not easy to state with an algebraic expression of the force equilibrium. This is due to the expressions for circular segment area, which includes both  $\theta$  and  $\sin(\theta)$  terms. Due to this, the position of  $h_n$  is solved numerically by the bi-section method.
- The PNA for a CFT with 4 symmetrically located rebars in pure bending is assumed to be located between the rebars. For typical cross-sections this is the reasonable case, but a warning check is included to indicate if this assumption is wrong (if so, the model does not calculate the initial PNA correctly).

As the axial force increases and the PNA is gradually moved upwards, the calculations of areas and plastic section moduli changes pending on the material located inside the PNA to centreline area. By only having four longitudinal rebars, there are four principal positions of the PNA:

- Between the upper and lower rebar (PNA1)
- Inside the upper rebar (PNA2)
- Above the upper rebar, still within concrete (PNA3)
- Above the concrete, inside the steel tube (PNA4)

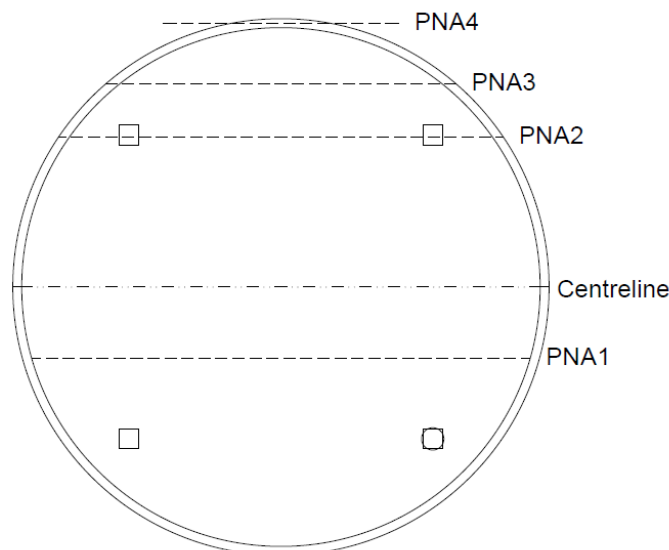


Figure J-2: PNA positions on CFT cross-section with 4 rebars

Each PNA position (see Figure J-2) requires a different set of calculations and each row of added rebars would add 2 new possible PNA positions/sets of equations. In addition, it becomes increasingly more difficult to determine the initial PNA position. Possibly there is an elegant way of stating the area and plastic section moduli for any PNA position and number of rebars, without having to explicitly write the equations for each PNA position, but that has not been investigated further. The model developed for this thesis uses a simple approach and only allows for either none or 4 rebars.



- For algebraic simplification, the rebars are assumed to be the square equivalent areas of the actual circular cross-sections. The side length of these idealized squares is used to determine whether the PNA is beneath, inside or above the reinforcement.  
This simplification only has a minute effect on the MN diagram, only noticeable when the PNA is inside the reinforcement. The square representation is shown in Figure J-2, with the actual circular area displayed in the lower right corner.
- The model does not consider the bending moment + axial force + shear force (M+N+V) case. This is due to the added complicity involved since the calculations would then have to consider where the PNA is located, with regards to the shear area of the steel section. No cases have been calculated in this thesis when shear has to be considered. A warning check is included which flags for situations when M+N+V should be considered.
- A fire verification mode is included, in which the fire load level  $\eta_{fi}$  is specified as a simple ratio (typically 0,65) and applied to all design loads and moments. The yield strength of the steel section is set to 235MPa and the longitudinal reinforcement is set to a diameter of  $0,17 * (\frac{D}{2} - t)$ , where D and t are the outer diameter and thickness of the steel section respectively. The reasons for these settings are given in Appendix F. If the fire verification mode is selected, the model calculates the maximum loadbearing fire resistance of the CFT cross-section, based on the loads and the steel section outer diameter. The user must manually remember to select a valid concrete cover according to the fire resistance class.

### Verification towards calculated examples:

The CFT MATLAB model has been used to calculate the MN interaction diagram of the worked example C2 by Dujmović et al. [39] with input as given in Table J-1.

*Table J-1: Calculation, worked example of column C2 from [39] - input data.*

<b>Input</b>	<b>Value</b>
Steel grade	S355
Concrete strength	C40/50
Concrete age at loading	28 days
Relative humidity	50%
Reinforcement strength	460 MPa
Diameter, steel tubular	406,4 mm
Thickness, steel tubular	10 mm
Reinforcement size	10xØ16 mm
Column length	4500mm, pinned ends

The reference example utilizes 10 radially evenly spaced longitudinal rebars, which is not an available amount in the developed MATLAB model. It is impossible to achieve the equivalent MN diagram with the 4 rebars setting available in the model, without significant changes to the code. Therefore, the reinforcement is set up to be as similar as possible.

For this verification, the plastic section moduli of the longitudinal reinforcement is set to equal that of the worked example, since reinforcement arguably has a larger influence on the bending resistance

than on the squash load resistance. This however results in a lower reinforcement cross-sectional area and subsequently, a lower squash load resistance.

The result of the verification is shown in Figure J-3 and it shows that the MN diagram calculated by the model looks as expected. It accurately predicts point D and undershoots point A. Point B and D differs slightly; the worked example for simplicity assumes a rectangular concrete section of width equal to the diameter of the circular concrete section thus achieving a slightly higher bending resistance. It is thus an inaccuracy of the worked example. It is also illustrated that usage of the simplified 4-point polynomial curve gives an unnecessary low yield resistance and thus an MN diagram with many calculation points may be economical in some cases.

Based on this verification and on undocumented trials/testing, the model is deemed fit to calculate the MN interaction diagram correctly according to the EC4 rules. The other ULS criteria has also been checked, but a verification of these has not been documented since they are based on simple algebraic expressions and are much easier to apply in code.

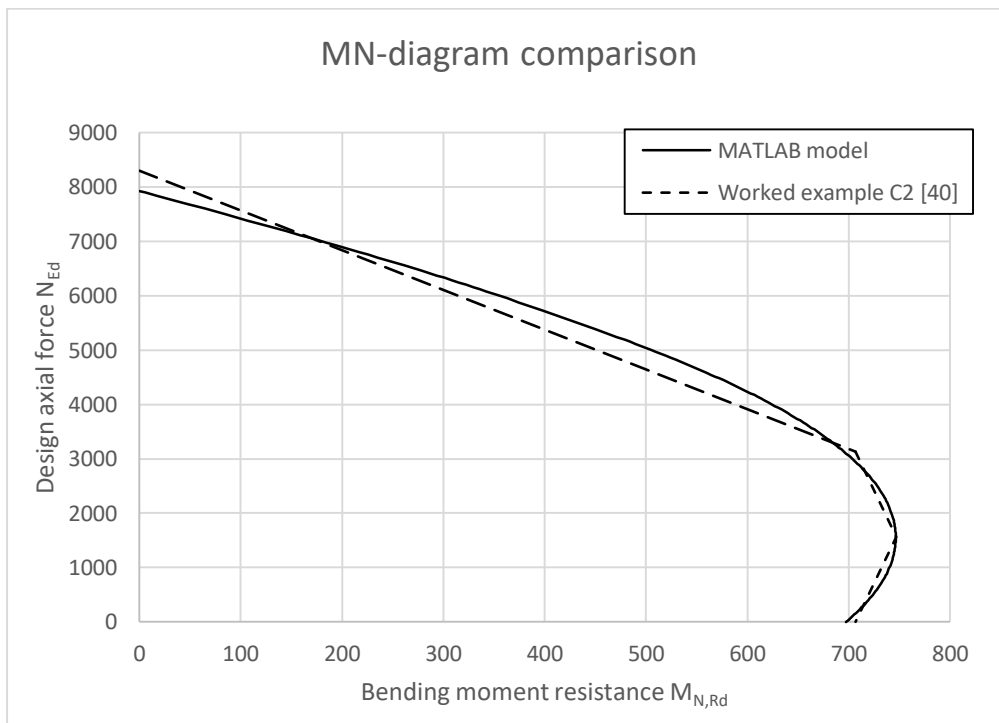


Figure J-3: Comparison of MN interaction diagrams, worked example C2 [39] and the developed MATLAB model

### Source code:

```
%This program verifies a concrete filled steel tubular, with/without
%reinforcement to ULS acc. EC4, part 1-1, simplified rules
%and loadbearing fire resistance acc. EC4, part 1-2 table 4.7.
%Note: there is no verification of the M+N+V case.
clear all;
close all;
clc;
%-----INPUT-----
%FIRE acc. table 4.7 EC4, part 1-2
Fire=false; %Use modified rules for fire loads?
eta_fi=0.65; %Fire load level (generic, does not consider imposed/perm)
k_bfi=0.5; %Fire buckling length factor (0.5 = intermediate; 0.7 =
top/bottom)
```

```

%MATERIAL
%material, steel
f_y=355;      %Yield strength, MPa
E_a=210000;  %Youngs Modulus, MPa
rho_a=7850;  %Density, kg/m3

%material, concrete
f_ck=40; %yield strength, cylinder, MPa
f_cm=48;  %yield strength, mean
E_cm=35000; %secant modulus elasticity, MPa
rho_c=2400; %density, kg/m3
RH=0.5;   %relative humidity
t0=28;    %age at loading (days)

%material, reinforcement
f_s=500;    %yield strength, MPa
E_s=210000; %Youngs Modulus, MPa
rho_s=7850; %Density, kg/m3

%partial factors
gamma_M0=1.05;
gamma_M1=1.05;
gamma_S=1.15;
gamma_C=1.5;
gamma_G=1.2;
gamma_Q=1.5;

%GEOMETRY
%dimensions, column
L=3000;      %Actual length, mm
k_b=1;       %Buckling length coefficient. 1=pin-pin, 0.5 = fix-fix etc.

%dimensions, steel
d_o=406.4;   %outer diameter,mm
t=12.5;     %thickness, mm

%dimensions, reinforcement
d_s=12;      %diameter, mm, changes to 3% ratio if fire is set to "true"
d_ts = 6;    %diameter, transverse reinforcement. At least 6 or d_s/4
no_s=4;      %number off (only 0 and 4 supported for now)
c_s=50;      %cover, mm (R30-;R60=30;R90=40;R120=50;R180=60)

%LOADS
%- All load matrices may be expanded.
%- Additional may be added (for instance transverse point and distributed),
% by modifying the calculations for M_Ed
%- Compressive force and counter-clockwise moments are positive.
%applied axial forces. [Force (kN), eccentricity y (mm), eccentricity z
%(mm),partial factor,perm_load?]
eta = 1.0; if Fire eta = eta_fi; end %Alter load factor if fire mode is
selected
N = [2500,0,0,gamma_G*eta,true;
     0,0,0,gamma_Q*eta,false];
Selfweight=false; %include self-weight?

%applied point moments. [Moment (kNm), distance (mm), partial factor]
M_y = [250,0,gamma_G*eta;
       0,0,gamma_G*eta];
M_z = [0,0,gamma_G*eta;
       0,0,gamma_G*eta];

```

```

%PROGRAM SETTINGS
%Points for determining MEd,VEd
Loadpoints=400;
%Points for MN diagram
MNpoints=400;
%Creep option (use h0 = max = 1600mm acc. EC2 fig 3.1). Else use perimeter
%of concrete to determine drying area.
creep_1600=true;
%Include 2nd order for NEd < 10% of Ncr,eff?
Always2nd=true;
%Include moment for imperfections?
Includeimp=true;
%Limit mu_d to 1?
mu_dLim = false;
%Tolerance for finding PNA
PNA_tol=0.00001;
Gravity=9.81;
%init string matrices for warning messages and verifications
warning=["Warnings:"];
verif=["Verifications:"];
%-----CALCULATIONS 1, cross-sectional geometrical properties-----
--
%steel
if Fire
    f_y=235;                %yield strength 235MPa if fire
    k_b=k_bfi*2;           %Calculate for double fire buckle length
end
r_o=d_o/2;                %outer radius, mm
r_i=r_o-t;                %inner radius, mm
A_a=pi()*(r_o^2-r_i^2);   %area, mm2
I_a=(pi()/4)*(r_o^4-r_i^4); %2nd moment of area, mm4
W_a=I_a/r_o;              %Elastic section modulus, mm3
Z_a=(4/3)*(r_o^3-r_i^3);  %Plastic section modulus, mm3
if f_y <= 355              %Material factor, steel
    alpha_M=0.9;
else
    alpha_M=0.8;
end

%reinforcement
if and(no_s~=0,no_s~=4)    %set reinforcement to 0 if not 4
    no_s=0;
end
if Fire
    d_s=0.17*(d_o/2-t);    %Use for fire calculations - gives the diameter for 3%
                           %reinf. ratio
end
r_s=d_s/2;                %radius,mm
A_rebar=pi()*r_s^2;       %rebar area, mm2
A_s=no_s*A_rebar;        %total area, mm2
y_s=(r_o-t-c_s-d_ts-d_s/2)/sqrt(2); %distance
                               %midline to center rebar
a_s=sqrt(A_rebar);        %side of equivalent rebar
                               %square
y_as=[-y_s+a_s/2,-y_s-a_s/2]; %coord [start end] rebar
                               %square
I_s=no_s*((pi()*r_s^4/4) + A_rebar*y_s^2); %2nd moment of area,mm4
W_s=I_s/y_s;              %Elastic section modulus, mm3
Z_s=no_s*(A_rebar*y_s);   %Plastic section modulus, mm3

```

```

%concrete, deducting reinforcement (if any)
A_c=pi()*r_i^2-A_s;           %area, mm2
I_c=pi()/4*r_i^4-I_s;       %2nd moment of area,mm4
W_c=pi()/4*r_i^3-W_s;       %Elastic section modulus, mm3
Z_c=(4/3)*r_i^3-Z_s;        %Plastic section modulus, mm3
rho_rebar=A_s/A_c;          %Reinforcement ratio

%-----CALCULATIONS 2, loads-----
%Reset design forces/moments
N_Ed=0;
N_GEd=0;
%Loop for all axial forces, find design axial force N_Ed and permanent
%part (N_GEd)
for i=1:size(N,1)
    N_Ed=N_Ed+N(i,1)*N(i,4);
    if N(i,5)
        N_GEd=N_GEd+N(i,1)*N(i,4);
    end
end
%add selfweight, if required
Mass=L*(A_a*rho_a+A_c*rho_c+A_s*rho_s)/1e9;      %Mass of column, kg
if Selfweight
    N_Ed=N_Ed+Mass*Gravity*gamma_G/1000;
    N_GEd=N_GEd+Mass*Gravity*gamma_G/1000;
end
%establish moment and shear force diagrams [M_Edy,M_Edz]
BMD=zeros(Loadpoints,3); % [x,My,Mz]
SFD=zeros(Loadpoints,3); % [x,Vy,Vz]
%add moments and shear forces for all sections
for i=1:Loadpoints+1 %add one, since data for x=0 is needed
    x=(i-1)*(L/Loadpoints);
    %Add distance
    BMD(i,1)=x; SFD(i,1)=x;
    %Add moments for axial load eccentricities
    for j=1:size(N,1)
        BMD(i,2)=BMD(i,2)-N_Ed*N(j,2); %y-axis
        BMD(i,3)=BMD(i,3)-N_Ed*N(j,3); %z-axis
    end
    %Add shear+moments for point moments y and z
    for j=1:size(M_y,1)
        SFD(i,2)=SFD(i,2) + M_y(j,1)*M_y(j,3)*1000/L;
        if x<=M_y(j,2)
            BMD(i,2)=BMD(i,2) + M_y(j,1)*M_y(j,3)*x/L;
        else
            BMD(i,2)=BMD(i,2) + (M_y(j,1)*x/L - M_y(j,1))*M_y(j,3);
        end
    end
    for j=1:size(M_z,1)
        SFD(i,3)=SFD(i,3) + M_z(j,1)*M_z(j,3)*1000/L;
        if x<=M_z(j,2)
            BMD(i,3)=BMD(i,3) + M_z(j,1)*M_z(j,3)*x/L;
        else
            BMD(i,3)=BMD(i,3) + (M_z(j,1)*x/L - M_z(j,1))*M_z(j,3);
        end
    end
end
end
%find design moment and shear
M_Ed=[0,0]; V_Ed=0; % [y-value, z-value]
for i=1:Loadpoints+1
    %check if it is max (absolute) moment
    if abs(BMD(i,2))>M_Ed(1,1)

```

```

        M_Ed(1,1)= abs(BMD(i,2));
    end
    if abs(BMD(i,3))>M_Ed(1,2)
        M_Ed(1,2)= abs(BMD(i,3));
    end
    %check if it is max (absolute) shear
    if abs(sqrt(SFD(i,2)^2+SFD(i,3)^2))>V_Ed
        V_Ed= sqrt(SFD(i,2)^2+SFD(i,3)^2);
    end
end
clear x;
%-----CALCULATIONS 3, creep-----
u=(2*r_i)*pi(); %perimeter, mm
if creep_1600
    h0=1600; %notional member size, mm
else
    h0=2*A_c/u;
end
if f_cm>35 %factors for fcm>35MPa
    alpha1=(35/f_cm)^0.7;
    alpha2=(35/f_cm)^0.2;
    alpha3=(35/f_cm)^0.5;
else
    alpha1=1;
    alpha2=1;
    alpha3=1;
end
phiRH=alpha2*(1+alpha1*(1-RH)/(0.1*h0^(1/3))); %RH factor
beta_fcm=16.8/sqrt(f_cm); %Strength factor
beta_t0=1/(0.1+t0^0.2); %age factor
phi0=phiRH*beta_fcm*beta_t0; %creep factor high age
E_ceff=E_cm/(1+(N_GEd/N_Ed)*phi0); %effective Emodulus
%clear intermediate variables
clear alpha1; clear alpha2; clear alpha3; clear phiRH;
clear beta_fcm; clear beta_t0;
%-----RESISTANCE 1 (N)-----
%Squash load res (kN)
N_Rd=((A_a*f_y/gamma_M0)+(A_c*f_ck/gamma_C)+(A_s*f_s/gamma_S))/1000;
%Steel squash load res (kN)
N_aRd=(A_a*f_y/gamma_M0)/1000;
%Steel contribution
delta=N_aRd/N_Rd;
%Calculate relative slenderness to determine whether confinement effect can
% be taken account for
%Flexural rigidity
EIeff=E_a*I_a+0.6*E_ceff*I_c+E_s*I_s;
%Critical force
N_cr=(pi()^2*EIeff/(k_b*L)^2)/1000;
%Characteristic strength, same as N_Rd but without partial factors
N_Rk=((A_a*f_y)+(A_c*f_ck)+(A_s*f_s))/1000;
%Relative slenderness
lambda=sqrt(N_Rk/N_cr);

%check whether confinement effect can be accounted for and determine
%strength factors, first setting to default (non-confinement) values
confine=false;
N_Rd2=N_Rd;
f_ck2=f_ck;
edivd=(1000*max(M_Ed)/N_Ed)/d_o;
if and(lambda<=0.5,edivd<0.1)
    confine=true;
end

```

```

eta_ao=0.25*(3+2*lambda);
eta_co=4.9-18.5*lambda+17*lambda^2;
if max(M_Ed)==0 %if there is no design moment
    eta_a=eta_ao;
    eta_c=eta_co;
else %if there is design moment
    eta_a=eta_ao+(1-eta_ao)*10*edivd;
    eta_c=eta_co*(1-10*edivd);
end
%check for limits of eta_a & eta_c
if eta_a>1
    eta_a=1;
end
if eta_c<0
    eta_c=0;
end
%calculate a new N_Rd according confinement
f_ck2=f_ck*(1 + eta_c*(t/d_o)*(f_y/f_ck)); %establish modified concrete
strength, due to confinement

N_Rd2=((eta_a*A_a*f_y/gamma_M0)+(A_c*f_ck2/gamma_C)+(A_s*f_s/gamma_S))/1000
;
end
%use the new N_Rd, if it is larger (not sure whether it is possible that its
smaller).
if N_Rd2>N_Rd
    N_Rd=N_Rd2;
else
    N_Rd2=N_Rd; %if the confinement N_Rd is smaller than the original,
revert to default
    confine=false; %don't use confinement rules further on
end

%-----RESISTANCE 2 (V)-----
%Shear area steel (mm2)
A_v=2*A_a/pi();
%Shear resistance steel
V_aRd=A_v*f_y/(sqrt(3)*gamma_M0*1000);
%Shear resistance concrete (NOT IMPLEMENTED)
V_cRd=0;
%Shear resistance (CONCRETE NOT IMPLEMENTED)
V_Rd=V_aRd;
%-----RESISTANCE 3 (N+V)-----
%Check whether the shear ratio is large enough to consider.
%If so, reduce acc. EC3
f_yV=f_y;
if V_Ed/V_Rd > 0.5
    warning=[warning;"shear must be considered for M+N+V"]
    rhoV=(2*V_Ed/V_Rd-1)^2;
    f_yV=(1-rhoV)*f_y;
end
%Resistance due to N+V
N_VRd=((A_v*f_yV/gamma_M0)+((A_a-
A_v)*f_y/gamma_M0)+(A_c*f_ck/gamma_C)+(A_s*f_s/gamma_S))/1000;
if confine %recalculate if confinement effect kicks in
    N_VRd=((eta_a*A_v*f_yV/gamma_M0)+(eta_a*(A_a-
A_v)*f_y/gamma_M0)+(A_c*f_ck2/gamma_C)+(A_s*f_s/gamma_S))/1000;
end
%-----RESISTANCE 4 (N+M)-----
%finding PNA numerically, bi-sectional method, assume PNA is in concrete
guess_hn=0; max_hn=r_i; min_hn=-r_i;

```

```

while l==1 %No repeat function available in MATLAB?, use while+break instead
    %Concrete in compression
    c_ccom=2*r_i*sqrt(1-(guess_hn/r_i)^2); %cord of circle segment
    if guess_hn==0 %avoid error for arctan(0)
        theta_ccom=pi();
    else
        theta_ccom=2*atan(c_ccom/(2*guess_hn)); %angle of cord towards
midline
    end
    A_ccom=(r_i^2/2)*(theta_ccom-sin(theta_ccom))-(no_s*A_rebar/2); %area,
concrete in compression

    %Steel in compression
    c_acom=2*r_o*sqrt(1-(guess_hn/r_o)^2); %cord of circle segment
    if guess_hn==0 %avoid error for arctan(0)
        theta_acom=pi();
    else
        theta_acom=2*atan(c_acom/(2*guess_hn)); %angle of cord towards
midline
    end
    A_acom=(r_o^2/2)*(theta_acom-sin(theta_acom)) - A_ccom - no_s*A_rebar/2;
%area, steel in compression

    %Steel in tension
    A_aten=A_a-A_acom;

    %Check force equilibrium
    PNA_eq=(f_y*(A_acom-A_aten)/gamma_M0)+(f_ck*A_ccom/gamma_C);
    if confine %recalculate if confinement effect kicks in
        PNA_eq=(eta_a*f_y*(A_acom-A_aten)/gamma_M0)+(f_ck2*A_ccom/gamma_C);
    end
    if abs(PNA_eq)<PNA_tol
        break %if in force equilibrium, then exit the while loop.
    end
    %bi-section method to make new guess
    if PNA_eq>0
        min_hn=guess_hn;
    else
        max_hn=guess_hn;
    end
    guess_hn=(max_hn-min_hn)/2 + min_hn;
end
hn=guess_hn;
if hn > y_s-(r_s/2)
    warning=[warning;"PNA beyond reinforcement"]
end
%Clear temp variables
clear A_acom; clear c_acom; clear theta_acom; clear A_aten;
clear A_ccom; clear c_ccom; clear theta_ccom;
clear guess_hn; clear max_hn; clear min_hn; clear PNA_eq;

%geometry for semi-circle
A_semii=pi()*r_i^2/2; %inner semicircle
A_semio=pi()*r_o^2/2; %outer semicircle
S_semii=A_semii*(4*r_i)/(3*pi()); %1st moment of area inner semicircle
S_semio=A_semio*(4*r_o)/(3*pi()); %1st moment of area outer semicircle

for i=1:MNpoints+1
    %change PNA

```



```

MN(i,1)=hn-(i-1)*(r_o+hn)/(MNpoints);
%"force" one PNA value to be 0, in order to calculate point D
if and(i>1,MN(i,1)<0)
    if MN(i-1,1)>0
        MN(i,1)=0;
        Point(4,1)=i;    %save location of point D
    end
end
%"force" one PNA value to be -hn, in order to calculate point C
if and(i>1,MN(i,1)<-hn)
    if MN(i-1,1)>-hn
        MN(i,1)=-hn;
        Point(3,1)=i;    %save location of point C
    end
end
end
Point(1,1)=Loadpoints+1; %location of point A
Point(2,1)=1;           %location of point B
%check whether the location is in steel section only
PNAinC=true;
if MN(i,1)<-r_i
    PNAinC=false;
end
%check where the location is, in relation to the idealized rebar square
PNArebar=0;           %PNA between rebars
if MN(i,1)<=y_as(1,1) %PNA within upper rebar
    PNArebar=1;
end
if MN(i,1)<=y_as(1,2) %PNA past upper rebar
    PNArebar=2;
end
end

%geometry for inner circle segment outside hn
%required for calculation of concrete in compression
if PNAinC %check if PNA is still inside the concrete
    theta_iseg=2*acos(MN(i,1)/r_i);
else
    theta_iseg=2*pi();
end
end

A_iseg=(r_i^2/2)*(theta_iseg-sin(theta_iseg)); %area, inner circle
segment
C_iseg=(4*r_i/3)*((sin(theta_iseg/2)^3)/(theta_iseg-sin(theta_iseg)));
%centroid, inner circle segment
S_iseg=A_iseg*C_iseg; %1st moment of area,
circle segment

%areas and centroids of rebar in circle segment outside hn (A_isq &
%C_isq)
%areas and plastic section moduli of rebar within 2hn (A_ishn & Z_ishn)
if PNArebar == 0 %before upper rebar
    A_sseg = no_s*0.5*A_rebar; %area
    C_sseg=y_s; %centroid
    A_s2hn = 0; %area, rebar within 2hn. Assumed PNA is between
lower rebar and midline
    Z_s2hn = 0; %pl.section mod., rebar within 2hn
elseif PNArebar ==1 %inside upper rebar
    A_sseg = no_s*0.5*A_rebar*(1 + (y_as(1,1) - MN(i,1))/a_s); %area
    C_sseg=y_s*((MN(i,1)-y_as(1,2))/a_s); %centroid, gradually tuned from
y_s to 0
    A_s2hn = no_s*A_rebar*((y_as(1,1) - MN(i,1))/a_s); %area, rebar
within 2hn.

```

```

        Z_s2hn = A_s2hn*-(MN(i,1)+y_as(1,1))/2;           %pl.section mod.,
rebar within 2hn
    elseif PNArebar ==2           %past upper rebar
        A_sseg = no_s*A_rebar;   %area
        C_sseg=0;                %centroid
        A_s2hn = no_s*A_rebar;   %area, rebar within 2hn.
        Z_s2hn = A_s2hn*y_s;     %pl.section mod., rebar within 2hn
    end
    %Remove rebar (if any) from concrete areas and centroids
    A_co2hn=A_iseg-A_sseg;       %Total area
    C_co2hn=(A_iseg*C_iseg-A_sseg*C_sseg)/A_co2hn; %Total centroid
    S_co2hn=A_co2hn*C_co2hn;    %1st moment of area

    %geometry for concrete, mirrored area from hn to midline
    S_cs2hn=S_semii-S_iseg;    %1MOA for concrete + rebar, relevant for steel
section
    A_c2hn=2*abs(A_semii - A_iseg)-A_s2hn;
    S_c2hn=S_semii-S_co2hn;
    Z_c2hn=2*S_c2hn-Z_s2hn;

    %geometry for outer circle segment outside hn
    theta_oseg=2*acos(MN(i,1)/r_o);
    A_oseg=(r_o^2/2)*(theta_oseg-sin(theta_oseg)); %area
    C_oseg=(4*r_o/3)*((sin(theta_oseg/2)^3)/(theta_oseg-sin(theta_oseg)));
%centroid
    S_oseg=A_oseg*C_oseg; %1st moment of area

    %geometry for steel, mirrored area from hn to midline
    A_a2hn=2*abs(A_semio - A_oseg)-2*abs(A_semii - A_iseg);
    S_a2hn=S_semio-S_oseg-S_cs2hn;
    Z_a2hn=2*S_a2hn;

    %Calculate NEd from stress blocks difference

    if MN(i,1)>0
        %PNA beneath midline - concrete in compression, steel in tension
        MN(i,2)=((f_ck*A_co2hn/gamma_C)-(f_y*A_a2hn/gamma_M0)-
(f_s*A_s2hn/gamma_S))/1000;
        if confine
            MN(i,2)=((f_ck2*A_co2hn/gamma_C)-(f_y*eta_a*A_a2hn/gamma_M0)-
(f_s*A_s2hn/gamma_S))/1000;
        end
    else
        %PNA above midline - concrete, steel & rebar in compression
MN(i,2)=((f_ck*A_co2hn/gamma_C)+(f_y*A_a2hn/gamma_M0)+(f_s*A_s2hn/gamma_S))
/1000;
        if confine

MN(i,2)=((f_ck2*A_co2hn/gamma_C)+(f_y*eta_a*A_a2hn/gamma_M0)+(f_s*A_s2hn/ga
mma_S))/1000;
        end
    end
    %Calculate M,NRd from plastic section moduli
    MN(i,3)=((0.5*f_ck*(Z_c-Z_c2hn)/gamma_C)+(f_y*(Z_a-
Z_a2hn)/gamma_M0)+(f_s*(Z_s-Z_s2hn)))/1e6;

    if confine
        MN(i,3)=((0.5*f_ck2*(Z_c-Z_c2hn)/gamma_C)+(f_y*eta_a*(Z_a-
Z_a2hn)/gamma_M0)+(f_s*(Z_s-Z_s2hn)/gamma_S))/1e6;
    end
end

```

```

end
%Where on MN diagram is N_Ed?
MN_x=0;
for i=1:MNpoints
    if and(MN(i,2)<=N_Ed,MN(i+1,2)>N_Ed)
        MN_x=i;
    end
end
%Get M resistance due to N from linear interpolation of MN curve
if MN_x>0
    M_NRd=MN(MN_x,3)+(N_Ed-MN(MN_x,2))*(MN(MN_x+1,3)-
MN(MN_x,3))/(MN(MN_x+1,2)-MN(MN_x,2));
else
    M_NRd=0;
end
%Find contribution factor
mu_d=M_NRd/MN(1,3);
if and(mu_dLim, mu_d>1) %limit mu_d to 1? (If moments arent due to axial
force)
    mu_d=1;
    M_NRd=MN(1,3)*mu_d;
end
%get point values for N and M
for i=1:4
    Point(i,2)=MN(Point(i,1),2); %N value
    Point(i,3)=MN(Point(i,1),3); %M value
end
%Clearing temp variables
clear A_a2hn; clear A_c2hn; clear A_co2hn; clear A_cseg; clear A_oseg;
clear A_s2hn; clear A_semii; clear A_semio; clear A_sseg;
clear C_co2hn; clear C_cseg; clear C_oseg; clear C_sseg;
clear S_a2hn; clear S_c2hn; clear S_co2hn; clear S_co2hn; clear S_cs2hn;
clear S_cseg; clear S_oseg; clear S_semii; clear S_semio;
clear theta_cseg; clear theta_oseg;
clear Z_a2hn; clear Z_c2hn; clear Z_s2hn;
clear PNArebar; clear PNAinC;

%-----RESISTANCE 5 (N buckling)-----

%Choosing imperfection factor "alpha" and member imperfection length "e_0"
%based on reinforcement ratio
if rho_rebar > 0.03
    alpha=0.34;
    e_0=L/200;
else
    alpha=0.21;
    e_0=L/300;
end
%phi-factor
phi_b=0.5*(1+alpha*(lambda-0.2)+lambda^2);
%chi-factor
chi_b=1/(phi_b+sqrt(phi_b^2-lambda^2));
if chi_b > 1
    chi_b = 1;
end
N_RdM1 = ((A_a*f_y/gamma_M1)+(A_c*f_ck/gamma_C)+(A_s*f_s/gamma_S))/1000;
if confine
    N_RdM1
    =
    ((A_a*f_y*eta_a/gamma_M1)+(A_c*f_ck2/gamma_C)+(A_s*f_s/gamma_S))/1000;
end
N_bRd = chi_b*N_RdM1;

```

```

%-----RESISTANCE 6 (M+N 2nd order)-----
%Note: This is no actual resistance, rather a re-evaluation of
%the design moments used for MN verification adding amplified moments for
%2nd order
%Flexural rigidity (ii) and reduced critical force
EIEffii=0.9*(E_a*I_a+0.5*E_oeff*I_c+E_s*I_s);
N_creff=pi()^2*EIEffii/(1000*(k_b*L)^2);
%check whether to include 2nd order effects
Include2nd=true;
if and(N_Ed*10<=N_creff,Always2nd==false)
    Include2nd=false;
end
%determine size of end moments, y-axis
if and(BMD(1,2)==0,BMD(Loadpoints+1,2)==0) %zero end moments
    beta_y=1;
elseif abs(BMD(1,2))>=abs(BMD(Loadpoints+1,2)) %divide smallest by largest
    beta_y=0.66+0.44*(BMD(Loadpoints+1,2)/BMD(1,2));
elseif abs(BMD(1,2))<abs(BMD(Loadpoints+1,2))
    beta_y=0.66+0.44*(BMD(1,2)/BMD(Loadpoints+1,2));
end
if beta_y<0.44 %minimum beta
    beta_y=0.44;
end
%determine size of end moments, z-axis
if and(BMD(1,3)==0,BMD(Loadpoints+1,3)==0) %zero end moments
    beta_z=1;
elseif abs(BMD(1,3))>=abs(BMD(Loadpoints+1,3)) %divide smallest by largest
    beta_z=0.66+0.44*(BMD(Loadpoints+1,3)/BMD(1,3));
elseif abs(BMD(1,3))<abs(BMD(Loadpoints+1,3))
    beta_z=0.66+0.44*(BMD(1,3)/BMD(Loadpoints+1,3));
end
if beta_z<0.44 %minimum beta
    beta_z=0.44;
end
%k-factors, y&z axis and imperfection moments
k_y=beta_y/(1-N_Ed/N_creff);
if k_y<1
    k_y = 1;
end
k_z=beta_z/(1-N_Ed/N_creff);
if k_z<1
    k_z = 1;
end
k_imp=1/(1-N_Ed/N_creff);
%include 2nd order factor if relevant
M_Ed2nd(1,1)=M_Ed(1,1)*(1+(k_y-1)*Include2nd);
M_Ed2nd(1,2)=M_Ed(1,2)*(1+(k_z-1)*Include2nd);
%include member imperfection (if selected) on the axis with the largest
design moment
%(no weak axis due to both axis being equal)
M_imp=Includeimp*N_Ed*e_0*k_imp/1000;
if M_Ed2nd(1,1)>=M_Ed2nd(1,2) %M largest on y axis
    M_Ed2nd(1,1)=M_Ed2nd(1,1)+M_imp;
else
    M_Ed2nd(1,2)=M_Ed2nd(1,2)+M_imp;
end
%-----FIRE DESIGN LOAD LEVEL-----
%Assuming either buckling due to N, NM or NMM
etafi1=N_Ed/N_bRd; %Load level, Buckling due to compression
etafi2=M_Ed(1,1)/(M_NRd*alpha_M); %Load level, Buckling due to NMy
etafi3=M_Ed(1,2)/(M_NRd*alpha_M); %Load level, Buckling due to NMz

```

```

etafi4=(M_Ed2nd(1,1)+M_Ed2nd(1,2))/M_NRd; %Load level, Buckling due to NMyMz
eta_fit=max([etafi1,etafi2,etafi3,etafi4]);
%-----VERIFICATIONS-----
%Print verification results at the end.
%!" sign indicates a failure, followed by which type
isok=true; %assume ok until proven wrong
%Steel grade
if and(f_y>=235,f_y<=460)
    verif=[verif;"Steel grade: S"+num2str(f_y)+" is ok"];
else
    verif=[verif;"! Steel grade: S"+num2str(f_y)+" must be between S235 and
S460"];
    isok=false;
end
%Concrete class
if and(f_ck>=20,f_ck<=50)
    verif=[verif;"Concrete class: C"+num2str(f_ck)+" is ok"];
else
    verif=[verif;"! Concrete class: C"+num2str(f_ck)+" must be between
C20/25 and C50/60"];
    isok=false;
end
%Steel contribution
if and(delta>=0.2,delta<=0.9)
    verif=[verif;"Steel contribution ratio "+num2str(delta)+" is ok"];
else
    verif=[verif;"! Steel contribution ratio "+num2str(f_y)+" must be
between 0.2 and 0.9"];
    isok=false;
end
%Local buckling
if d_o/t <= 90*(235/f_y)
    verif=[verif;"Local buckling max d/t is ok"];
else
    verif=[verif;"! Local buckling, d/t: "+num2str(r_o/t)+"; max value is "+
num2str(90*(235/f_y))];
    isok=false;
end
%Relative slenderness
if lambda <= 2
    verif=[verif;"Relative slenderness: "+num2str(lambda)+" is ok"];
else
    verif=[verif;"! Relative slenderness: "+num2str(lambda)+"; max value is
2.0"];
    isok=false;
end
%Reinforcement ratio
if rho_rebar <= 0.06
    verif=[verif;"Reinforcement ratio: "+num2str(rho_rebar*100)+"% is ok"];
else
    verif=[verif;"! Reinforcement ratio: "+num2str(rho_rebar*100)+"%; max
value is 6%"];
    isok=false;
end
%Compression (N)
if N_Ed<=N_Rd
    verif=[verif;"C/s yield resistance from (N); N_Ed/N_Rd:
"+num2str(N_Ed/N_Rd)+" is ok"];
else
    verif=[verif;"! C/s yield resistance from (N); N_Ed/N_Rd:
"+num2str(N_Ed/N_Rd)+" is above 1"];

```

```

        isok=false;
end
%Shear (V)
if V_Ed<=V_Rd
    verif=[verif;"C/s yield resistance from (V); V_Ed/V_Rd:
"+num2str(V_Ed/V_Rd)+" is ok"];
else
    verif=[verif;"! C/s yield resistance from (V); V_Ed/V_Rd:
"+num2str(V_Ed/V_Rd)+" is above 1"];
    isok=false;
end
%Compression + Shear (N+V)
if N_Ed<=N_VRd
    verif=[verif;"C/s yield resistance from (N+V); N_Ed/N_V,Rd:
"+num2str(N_Ed/N_VRd)+" is ok"];
else
    verif=[verif;"! C/s yield resistance from (N+V); N_Ed/N_V,Rd:
"+num2str(N_Ed/N_VRd)+" is above 1"];
    isok=false;
end
%Compression + uniaxial bending (N+M), y-axis
if M_Ed(1,1)<=M_NRd*alpha_M
    verif=[verif;"C/s y-axis yield resistance from (N+My); M_Ed,y/M_NRd:
"+num2str(M_Ed(1,1)/M_NRd)+" is ok"];
else
    verif=[verif;"! C/s y-axis yield resistance from (N+My); M_Ed,y/M_NRd:
"+num2str(M_Ed(1,1)/M_NRd)+" is above alphaM: "+num2str(alpha_M)];
    isok=false;
end
%Compression + uniaxial bending (N+M), z-axis
if M_Ed(1,2)<=M_NRd*alpha_M
    verif=[verif;"C/s z-axis yield resistance from (N+Mz); M_Ed,z/M_NRd:
"+num2str(M_Ed(1,2)/M_NRd)+" is ok"];
else
    verif=[verif;"! C/s z-axis yield resistance from (N+Mz); M_Ed,z/M_NRd:
"+num2str(M_Ed(1,2)/M_NRd)+" is above alphaM: "+num2str(alpha_M)];
    isok=false;
end
%Compression + biaxial bending (N+My+Mz)
if (M_Ed(1,1)+M_Ed(1,2))<=M_NRd
    verif=[verif;"C/s yield resistance from (N+My+Mz);
(M_Ed,y+M_Ed,z)/M_NRd: "+num2str((M_Ed(1,1)+M_Ed(1,2))/M_NRd)+" is ok"];
else
    verif=[verif;"! C/s yield resistance from (N+My+Mz);
(M_Ed,y+M_Ed,z)/M_NRd: "+num2str((M_Ed(1,1)+M_Ed(1,2))/M_NRd)+" is above
1"];
    isok=false;
end
%Buckling due compression
if N_Ed<=N_bRd
    verif=[verif;"Buckling resistance from (N); N_Ed/N_bRd:
"+num2str(N_Ed/N_bRd)+" is ok"];
else
    verif=[verif;"! Buckling resistance from (N); N_Ed/N_bRd:
"+num2str(N_Ed/N_bRd)+" is above 1"];
    isok=false;
end
%2nd order check due to compression + uniaxial bending (N+M), y-axis
if M_Ed2nd(1,1)<=M_NRd*alpha_M
    verif=[verif;"2nd order c/s y-axis yield resistance from (N+My);
M_Ed2,y/M_NRd: "+num2str(M_Ed2nd(1,1)/M_NRd)+" is ok"];

```

```

else
    verif=[verif;"! 2nd order c/s y-axis yield resistance from (N+My);
M_Ed2,y/M_NRd: "+num2str(M_Ed2nd(1,1)/M_NRd)+" is above alphaM:
"+num2str(alpha_M)];
    isok=false;
end
%2nd order check due to compression + uniaxial bending (N+M), z-axis
if M_Ed2nd(1,2)<=M_NRd*alpha_M
    verif=[verif;"2nd order c/s z-axis yield resistance from (N+Mz);
M_Ed2,z/M_NRd: "+num2str(M_Ed2nd(1,2)/M_NRd)+" is ok"];
else
    verif=[verif;"! 2nd order c/s z-axis yield resistance from (N+Mz);
M_Ed2,z/M_NRd: "+num2str(M_Ed2nd(1,2)/M_NRd)+" is above alphaM:
"+num2str(alpha_M)];
    isok=false;
end
%2nd order check due compression + bi-axial bending
if (M_Ed2nd(1,1)+M_Ed2nd(1,2))<=M_NRd
    verif=[verif;"2nd order c/s yield resistance from (N+My+Mz);
(M_Ed2,y+M_Ed2,z)/M_NRd: "+num2str((M_Ed2nd(1,1)+M_Ed2nd(1,2))/M_NRd)+" is
ok"];
else
    verif=[verif;"! 2nd order c/s yield resistance from (N+My+Mz);
(M_Ed2,y+M_Ed2,z)/M_NRd: "+num2str((M_Ed2nd(1,1)+M_Ed2nd(1,2))/M_NRd)+" is
above 1"];
    isok=false;
end
if Fire %only show fire verifications if relevant
    verif=[verif;"Fire Verifications:"];
    %Column length
    if d_o*30>=L
        verif=[verif;"Column L/D "+num2str(L/d_o)+" is ok"];
    else
        verif=[verif;"! Column L/D "+num2str(L/d_o)+" must be equal or
smaller than 30"];
        isok=false;
    end
    if eta_fit<=0.66
        verif=[verif;"Fire design load level "+num2str(eta_fit)+" is ok"];
    else
        verif=[verif;"! Fire design load level "+num2str(eta_fit)+" must be
equal or smaller than 0.66"];
        isok=false;
    end
    %Checks for fire resistance. Only column diameter is checked,
reinforcement must be designed per the table.
    FiRes="No fire resistance, d_o must be larger"; %Unless a fire res is
found..
    if eta_fit<=0.28 %Resistance level 1
        verif=[verif;"Fire design load level <= 0.28 - Case 1"];
        if d_o >= 400 FiRes="R180";
            elseif d_o >= 260 FiRes="R120";
            elseif d_o >= 220 FiRes="R90";
            elseif d_o >= 200 FiRes="R60";
            elseif d_o >= 160 FiRes="R30";
        end
    elseif eta_fit <=0.47 %Resistance level 2
        verif=[verif;"Fire design load level <= 0.47 - Case 2"];
        if d_o >= 500 FiRes="R180";
            elseif d_o >= 450 FiRes="R120";
            elseif d_o >= 400 FiRes="R90";

```

```
        elseif d_o >= 260 FiRes="R60";
    end
elseif eta_fit <=0.66 %Resistance level 3
    verif=[verif;"Fire design load level <= 0.66 - Case 3"];
    if d_o >= 550 FiRes="R90";
        elseif d_o >= 450 FiRes="R60";
        elseif d_o >= 260 FiRes="R30";
    end
end
verif=[verif;"Fire load bearing resistance: "+FiRes];
end
verif
```



## Appendix K. Calculations for the case study

This appendix includes:

- Snow and wind load calculations for the case study (in Norwegian)
- Self-weight estimation for the case study lattice girders
- Calculation of the column design loads
- Investigative R30 and R60 fire calculation of the columns, in accordance to Annex G of EC4, part 1-2 [4].

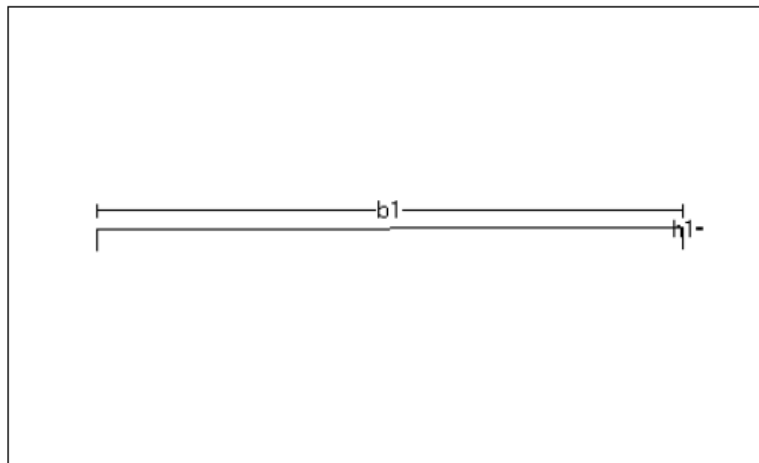
### Snow load

#### Masteroppgave

Titel Idrettshall 30 x 45			Side 1
Prosjekt Snølast	Ordre	Sign	Dato 05-04-2019

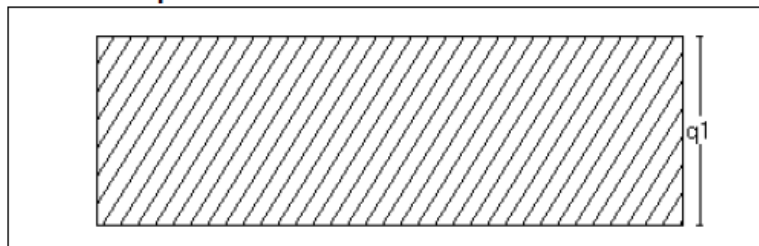
Dataprogram: LastBeregning versjon 6.2.5 Laget av Sletten Byggdata AS  
Standard NS-EN 1991-1-3: Snølaster

#### 1. Geometri



$b_1$  30000 mm  
 $h_1$  100 mm

#### 2. Snølast på tak



Last nr.:1  
 $q_1$  3.20 kN/m<sup>2</sup>

#### 3. Snølastdata

Fylke	Vest-Agder
Kommune	Kristiansand
Sted	
Byggets plassering (moh)	10 moh
Eksponeeringskoeffisient $C_e$	1
Termisk koeffisient $C_t$	1
Snølast, $S$ :	4 kN/m <sup>2</sup>

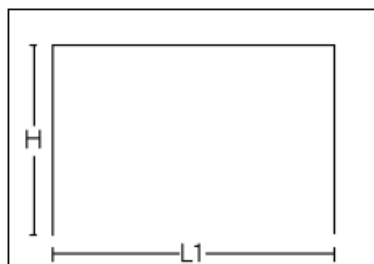
## Wind loads

### Masteroppgave

Tittel Idrettshall 30 x 45			Side 1
Prosjekt Snølast	Ordre	Sign	Dato 05-04-2019

Dataprogram: LastBeregning versjon 6.2.5 Laget av Sletten Byggdata AS  
Standard NS-EN 1991-1-4: Vindlaster

### 1. Geometri



H 10000 mm  
L1 30000 mm

Byggets lengde, L2: 45000 mm  
Takvinkel : 0.00 (grader)

Vertikalsnitt

### 2. Vindhastighet

Fylke: Vest-Agder Kommune: Kristiansand Referansevindhastighet: 26 m/s

Byggested, høyde over havet (m): 10 Calt: 1

Returperiode (år):50 Cprob: 1

Årstidsfaktoren, Cseason: 1 hele året

Vindretning (region):Bruker retningsfaktoren C-ret: 1

Basisvindhastighet: 26 m/s

Høyde Z over grunnivået: 10 m

#### BYGGSTEDETS TERRENGDATA

Terrenghetskategori 0: Åpent opprørt hav.

Terrenghetsfaktoren  $K_t$ : 0.16 Ruhetslengden  $Z_0$  (m): 0.003  $Z_{min}$  (m): 2  $V_m$  (m/s): 33.74  $C_r$ : 1.30

TOPOGRAFI: Ingen topografisk påvirkning.

Terrengeformfaktor  $C_o(z)$ : 1 Turbulensfaktor  $K_i$ : 1

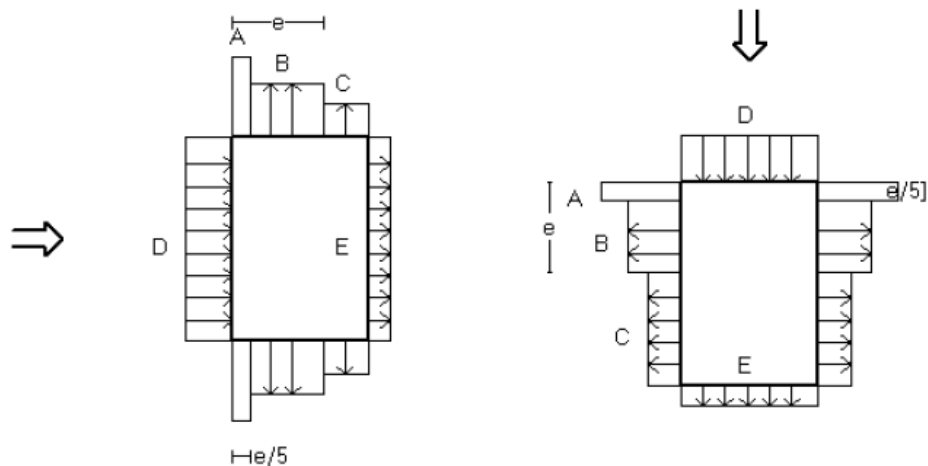
Vkast: 46.06 m/s

Qkast: 1.326 kN/m<sup>2</sup>

Titel Idrettshall 30 x 45			Side 2
Prosjekt Snølast	Ordre	Sign	Dato 05-04-2019

### 3. Yttervegger

#### 3.1 Utvendig vindlast



Vindretning 0 grader.  $e=20000$  mm

Vindretning 90 grader.  $e=20000$  mm

Vindinnfallsretning på 0 grader.

	A	B	C	D	E
Formfaktor $C_{pe,10}$	-1.20	-0.80	-0.50	0.71	-0.32
Utvendig last (kN/m <sup>2</sup> )	-1.59	-1.06	-0.66	0.94	-0.43
Formfaktor $C_{pe,1}$	-1.40	-1.10	-0.50	1.00	-0.32
Utvendig last (kN/m <sup>2</sup> )	-1.86	-1.46	-0.66	1.33	-0.43
Utstrekning (mm)	4000	16000	10000	45000	45000

Vindinnfallsretning på 90 grader.

	A	B	C	D	E
Formfaktor $C_{pe,10}$	-1.20	-0.80	-0.50	0.70	-0.30
Utvendig last (kN/m <sup>2</sup> )	-1.59	-1.06	-0.66	0.93	-0.40
Formfaktor $C_{pe,1}$	-1.40	-1.10	-0.50	1.00	-0.30
Utvendig last (kN/m <sup>2</sup> )	-1.86	-1.46	-0.66	1.33	-0.40
Utstrekning (mm)	4000	16000	25000	30000	30000

Positiv verdi for last gir trykk. Negativ verdi hvis last er sug.

#### 3.2 Innvendig vindlast

Bygning uten dominerende vindfasade

Beregn innvendig vindlast for  $u=0.2$  overtrykk og  $u=-0.3$  (undertrykk)

	Undertrykk	Overtrykk
Formfaktor	-0.30	0.20
Innvendig last (kN/m <sup>2</sup> )	-0.40	0.27

Titel Idrettshall 30 x 45		Side 3
Prosjekt Snølast	Ordre	Sign Date 05-04-2019

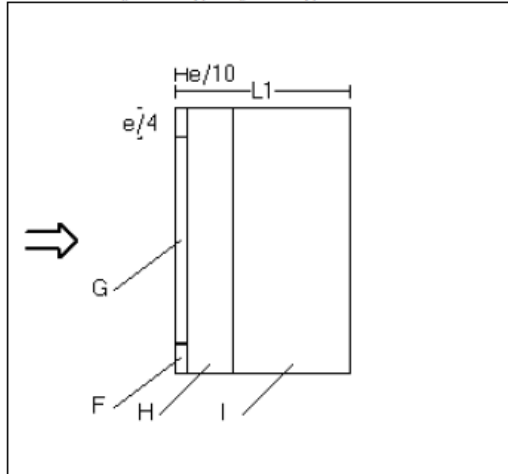
#### 4 Overside av tak

Taktype: Flatt tak

L1=30000 mm L2=45000 mm

Cpe,10 Gjelder for hele bygget. (>=10m2)

Positiv verdi for last gir trykk. Negativ verdi hvis last er sug.



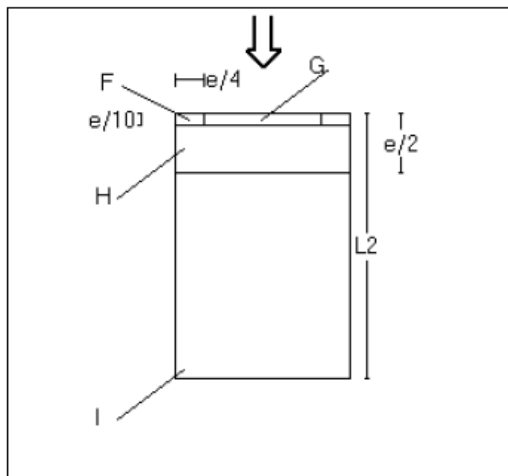
Utstrekning (mm)

e=20000

e/4=5000

e/10=2000

	Cpe,10	Last (kN/m2)	Hor.prosjeksjon (mm)
F	-1.80	-2.39	5000x2000
G	-1.20	-1.59	35000x2000
H	-0.70	-0.93	45000x8000
I	+/-0.20	+/-0.27	45000x20000



Utstrekning (mm)

e=20000

e/4=5000

e/10=2000

	Cpe,10	Last (kN/m2)	Hor.prosjeksjon (mm)
F	-1.80	-2.39	5000x2000
G	-1.20	-1.59	20000x2000
H	-0.70	-0.93	30000x8000
I	+/-0.20	+/-0.27	30000x35000

## Self-weight, lattice girders

The typical mass of a lattice girder is estimated from an online calculation tool of Maku, a supplier of lattice girders as per Figure K-1. Due to limitations in the calculation tool, the girder mass for the actual girder spacing of 7,2m cannot be determined. The mass of the lattice girder required for half the spacing (3,75m) is equal to ~5000 kg. The mass of a girder required for the double spacing is assumed to be doubled = 10000kg →  $g_{truss} = 100\text{kN}$ . The error margin in this estimate is high, but the contribution of the lattice girder to the total axial column load is relatively small, when compared to the self-weight (which also is assumed) and snow load of the roof. It is therefore determined that the error margin is acceptable.

**Taklutning**

0-15°

**Spännvidd**

30,0 m

**Dimensionerad last**

Beräkning av dimensionerad löpmeterlast

Land: Norge

Säkerhetsklass: Säkerhetsklass 3

Snözon: 4 Kristiansand (Vest -)

Avstånd mellan sekundärbalkar: 3,75 m

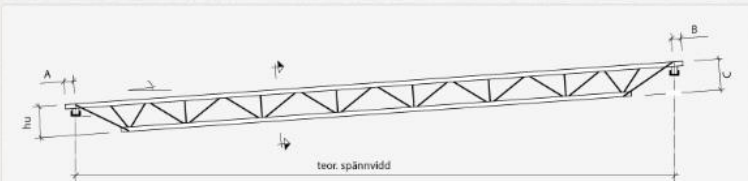
Kontinuitetsfaktor: 1,1

Egenvikt (tak): 1 kN/m<sup>2</sup>

Installationslast: 0 kN/m<sup>2</sup>

### Parallellfackverk

För att undvika felaktigheter vid val av parametrar eller feltolkning av resultat så kommer alltid Maku Stål AB att dimensionera och konstruera det slutgiltiga fackverket. Detta är också ett villkor för att uppfylla vårt SBS-godkännande. Denna dimensionering ligger sedan till grund för slutgiltig offert och order.



Taklutning: 0-15°      Spännvidd: 30,0 m      Dim. last: 24,8 kN/m

Visa 10 rader      Sök:

Lutning	Hu (mm)	Q dim. (kN/m)	Beteckning	Vikt (kg)	Nedb. koeff	
0-15°	1250	30	U 160-160-140-1250	5460	8,9	Offert
0-15°	1350	26,3	U 160-150-140-1350	4970	8,6	Offert
0-15°	1350	32,6	U 160-160-160-1350	5660	7,5	Offert
0-15°	1450	28,5	U 160-150-140-1450	5050	7,5	Offert
0-15°	1450	26,2	U 150-150-140-1450	4450	8,4	Offert

Visar 1 till 5 av 5 rader (filtrerad ifrån 23 rader totalt)

← Föreg. 1 Nästa →

Figure K-1: Self-weight of lattice girders, calculation [76]

## Design loads on columns

### Determination of loads:

Permanent axial load onto a column, due to self-weight of roof, trusses and wall construction:

$$N_{g,G} = \frac{g_{roof} * W_{roof} * d_{side} * k_c + g_{truss}}{2} + g_{wall} = \frac{1,0 * 30,6 * 7,55 * 1,1 + 100}{2} + 30 \text{ kN} = 212,1 \text{ kN}$$

Imposed axial load onto a column, due to snow:

$$N_{q,S} = \frac{q_{snow} * W_{roof} * d_{side} * k_c}{2} = \frac{3,2 * 30,6 * 7,55 * 1,1}{2} \text{ kN} = 406,6 \text{ kN}$$

Imposed horizontal distributed load, due to wind:

$$Q_{q,W} = q_{wind} * d_{side} * k_c = 1,34 * 7,55 * 1,1 \text{ kN/m} = 11,13 \text{ kN/m}$$

Load combination S (snow is the leading imposed load):

Axial load on column, permanent:

$$N_{Ed,G,S} = \xi \gamma_G * N_{g,S} = 1,2 * 212,1 = 254,5 \text{ kN}$$

Axial load on column, total:

$$N_{Ed,S} = N_{Ed,G,S} + \gamma_Q * N_{q,S} = 254,5 + 1,5 * 406,6 = 864,4 \text{ kN}$$

Transverse distributed load on column:

$$Q_{Ed,S} = \gamma_Q * \psi_{0,W} * Q_{q,W} = 1,5 * 0,6 * 11,13 = 10,0 \text{ kN/m}$$

Load combination W (wind is the leading imposed load):

Axial load on column, permanent:

$$N_{Ed,G,W} = N_{Ed,G,S} = 254,5 \text{ kN}$$

Axial load on column, total:

$$N_{Ed,W} = N_{Ed,G,W} + \gamma_Q * \psi_{0,S} * N_{q,S} = 254,5 + 1,5 * 0,7 * 406,6 = 681,4 \text{ kN}$$

Transverse distributed load on column:

$$Q_{Ed,W} = \gamma_Q * Q_{q,W} = 1,5 * 11,13 = 16,70 \text{ kN/m}$$

Load combination Fi (Fire scenario with snow as the leading imposed load):

Axial load on column, permanent:

$$N_{Ed,G,Fi} = N_{g,S} = 212,1 \text{ kN}$$

Axial load on column, total:

$$N_{Ed,Fi} = N_{Ed,G,Fi} + \psi_{1,S} * N_{q,S} = 212,1 + 0,5 * 406,6 = 415,4 \text{ kN}$$

Transverse distributed load on column:

$$Q_{Ed,Fi} = \psi_{1,W} * Q_{q,W} = 0,2 * 11,13 = 2,2 \text{ kN/m}$$

Second order effects due to sway:

Sway imperfection:

Basic value for sway imperfection:

$$\phi_0 = 1/200$$

Reduction factor for column height h:

$$\alpha_h = \frac{2}{\sqrt{h}} = \frac{2}{\sqrt{9}} = \frac{2}{3} \text{ (within bounds } \frac{2}{3} \text{ to } 1)$$

Reduction factor for columns in a row (m=2):

$$\alpha_m = \sqrt{0,5(1 + \frac{1}{m})} = \sqrt{0,5(1 + \frac{1}{2})} = 0,866$$

Sway imperfection angle:

$$\phi = \phi_0 \alpha_h \alpha_m = \frac{1}{200} * \frac{2}{3} * 0,866 \text{ rad} = 0,00289 \text{ rad}$$

It is assumed that there is little axial compression in the lattice girder, meaning the frame buckling factor  $\alpha_{cr}$  can be calculated accordingly:

$$\alpha_{cr} = \frac{H_{Ed,i}}{V_{Ed,i}} * \frac{h}{\delta_{H,Ed,i}}$$

Without a global elastic analysis of the structure, the deflection of the top of the building  $\delta_{H,Ed,i}$  cannot be determined, neither  $\alpha_{cr}$  for the load combination "i". No reference values of  $\alpha_{cr}$  for similar types of structures was found.

A control check is made for the snow load combination, which will have the lowest  $\alpha_{cr}$  due to having higher vertical reaction force.

EHF due to sway (pinned ends, bow imperfections are considered in member checks and disregarded here):

$$H_{EFG,S} = \phi * N_{Ed,S} = 0,00289 * 864,4 \text{ kN} = 2,5 \text{ kN}$$

Horizontal reaction force at the base of the column, including half the side wall wind load:

$$H_{Ed,S} = \frac{Q_{Ed,S} * h_b}{2} + H_{EFG,S} = \frac{10,02 * 10}{2} + 2,5 \text{ kN} = 52,6 \text{ kN}$$

Vertical reaction force at the base of the column:

$$V_{Ed,S} = N_{Ed,S} = 864,4 \text{ kN}$$

Maximum allowable deflection at top of building, before considering 2<sup>nd</sup> order effects:

$$\alpha_{cr} = 10 = \frac{H_{Ed,S}}{V_{Ed,S}} * \frac{h}{\delta_{H,Ed,S}} \rightarrow \delta_{H,Ed,S} = \frac{52,6}{864,4} * \frac{9000}{10} = 55 \text{ mm}$$

It is deemed reasonable that the top of the building would deflect less than 55mm during the snow load scenario, thus the assumption is ok.

## Fire calculations, PEC columns

The columns are calculated for buckling in a fire scenario about the minor axis to EC4, 1-2 Annex G [4], and for buckling about the major axis with the method suggested by Vassart et al. [47], which basically is the same method, only compensating for the change of the second moments of inertia. The wind loads giving bending moments on the major axis are represented as an equivalent load eccentricity. The R30 and R60 load bearing resistances are considered as the method is not available for R15 resistance.

A PEC cross-section with HE-240B/S355 grade steel section, concrete grade of C40/50, reinforcement consisting of  $\phi_L = 4 \times \phi 25 \text{ mm}$  rebars in the longitudinal direction and  $\phi_T = \phi 8 \text{ mm}$  stirrups for transverse reinforcement of B500NC grade is considered. The reinforcement has a concrete cover of  $c_z = 30 \text{ mm}$  in the z-axis and  $c_y = 20 \text{ mm}$  in the y-axis. In order to calculate the cross-section, it is divided into flanges, reduced web, reduced concrete and reinforcement as per Annex G. The divided cross-section is shown in Figure K-2.

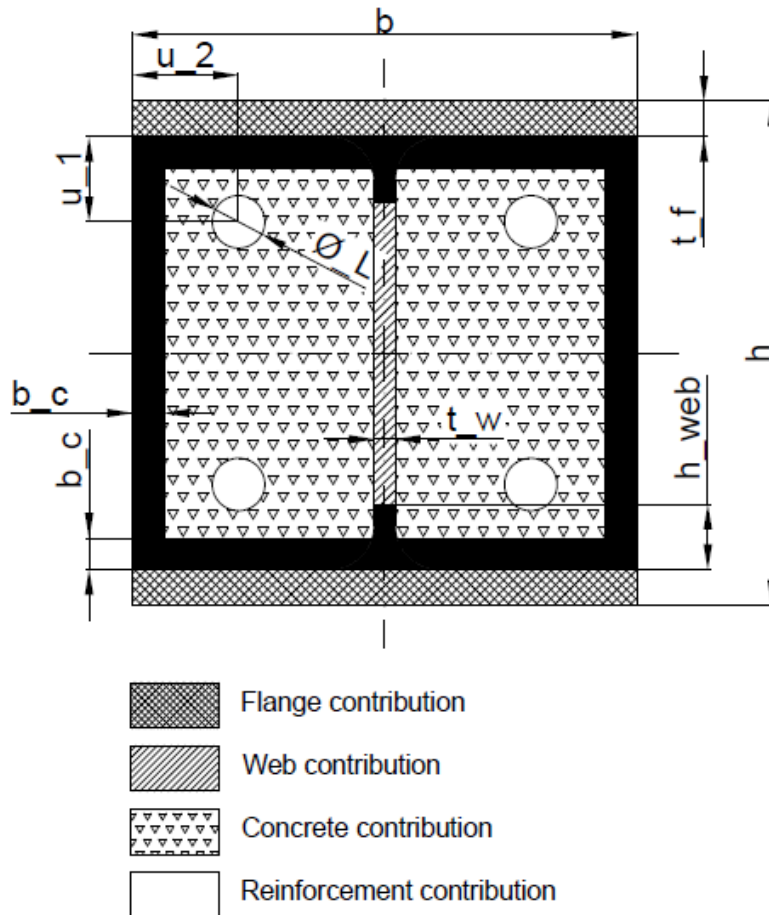


Figure K-2: PEC HE-240B cross-section according EC4, part 1-2 Annex G [4].

Cross-sectional geometry (taken from A3C where not calculated):

$$\text{Steel area: } A_a = 10599\text{mm}^2$$

$$\text{Reinforcement area: } A_s = 1963\text{mm}^2$$

$$\text{Concrete area: } A_c = 45749\text{mm}^2$$

First the field of application according EC4, part 1-2 Annex G [4] is checked:

Buckling length in a fire scenario:

$$L_{fi} = 0,7 * L = 0,7 * 9000\text{mm} = 6300\text{mm}$$

$$L_{fi} > 13,5 * b = 13,5 * 240\text{mm} = 3240\text{mm} \text{ (Not ok!)}$$

Cross-section dimensions:

$$b = 240 \geq 230\text{mm} \text{ (Ok!)}$$

$$h = 240 \geq 230\text{mm} \text{ (Ok!)}$$

Reinforcement ratio for fire calculations:

$$\rho_{s,fi} = \frac{A_s}{A_c + A_s} = \frac{1963}{45749 + 1963} = 4,11\% \text{ (In between 1\% and 6\%; ok!)}$$



As a conclusion, the PEC column is not suitable to calculate according to Annex G due to the large buckling length in a fire scenario. However, this was already known and the subsequent calculations are done anyways to provide an indication of what results would be achieved by using advanced fire calculations.

The contribution of the steel flanges in a fire scenario:

Section factor:

$$\frac{A_m}{V} = \frac{2(h+b)}{hb} = \frac{2(0,24+0,24)}{0,24*0,24} m^{-1} = 16,67 m^{-1}$$

Factors from Annex G, table G.1:

$$R30: \theta_{o,R30} = 550^\circ\text{C}; k_{R30} = 9,65 m^\circ\text{C}$$

$$R60: \theta_{o,R60} = 680^\circ\text{C}; k_{R60} = 9,55 m^\circ\text{C}$$

Average temperatures of the flanges for R30 and R60 duration:

$$\theta_{f,R30} = \theta_{o,R30} + k_{R30} * \frac{A_m}{V} = 550 + 9,65 * 16,67 = 711^\circ\text{C}$$

$$\theta_{f,R60} = \theta_{o,R60} + k_{R60} * \frac{A_m}{V} = 680 + 9,55 * 16,67 = 839^\circ\text{C}$$

Reduction factors of the flanges in the average temperatures, linearly interpolated from table 3.2 of EC4, 1-2 [4]:

$$k_{y,fl,R30} = 0,217$$

$$k_{y,fl,R60} = 0,091$$

$$k_{E,fl,R30} = 0,126$$

$$k_{E,fl,R60} = 0,081$$

Plastic resistances to axial compression of flanges in fire:

$$N_{pl,fl,R30,Rd} = \frac{2 * b * t_f * f_y * k_{y,fl,R30}}{\gamma_{M0,fi}} = \frac{2 * 240 * 17 * 355 * 0,217}{1,0} N = 628 kN$$

$$N_{pl,fl,R60,Rd} = \frac{2 * b * t_f * f_y * k_{y,fl,R60}}{\gamma_{M0,fi}} = \frac{2 * 240 * 17 * 355 * 0,091}{1,0} N = 264 kN$$

Flexural rigidities of flanges in fire, buckling about the minor axis:

$$(EI)_{fl,R30,z} = \frac{E_a * k_{E,fl,R30} * t_f * b^3}{6} = \frac{210000 * 0,126 * 17 * 240^3}{6} Nmm^2 = 1036 kNm^2$$

$$(EI)_{fl,R60,z} = \frac{E_a * k_{E,fl,R60} * t_f * b^3}{6} = \frac{210000 * 0,081 * 17 * 240^3}{6} Nmm^2 = 666 kNm^2$$

Second moment of area of flanges about major axis, Steiners theorem:

$$I_{fl,y} = 2 * \left( \frac{b * t_f^3}{12} + b * t_f * \left( \frac{h - t_f}{2} \right)^2 \right) = 2 * \left( \frac{240 * 17^3}{12} + 240 * 17 * \left( \frac{240 - 17}{2} \right)^2 \right) mm^4$$

$$= 1,02 * 10^8 mm^4$$

Flexural rigidities of flanges in fire, buckling about the major axis:

$$(EI)_{fl,R30,y} = E_a * k_{E,fl,R30} * I_{fl,y} = 210000 * 0,126 * 1,02 * 10^8 Nmm^2 = 2699 kNm^2$$

$$(EI)_{fl,R60,y} = E_a * k_{E,fl,R60} * I_{fl,y} = 210000 * 0,081 * 1,02 * 10^8 \text{ Nmm}^2 = 1735 \text{ kNm}^2$$

The contribution of the steel web in a fire scenario:

Web reduction factors from Annex G, table G.2:

$$H_{R30} = 350 \text{ mm}$$

$$H_{R60} = 770 \text{ mm}$$

Reductions in web height:

$$\begin{aligned} h_{web,R30} &= 0,5 * (h - 2 * t_f) * \left( 1 - \sqrt{1 - 0,16 \left( \frac{H_{R30}}{h} \right)} \right) \text{ mm} \\ &= 0,5 * (240 - 2 * 17) * \left( 1 - \sqrt{1 - 0,16 \left( \frac{350}{240} \right)} \right) \text{ mm} = 12,8 \text{ mm} \end{aligned}$$

$$\begin{aligned} h_{web,R60} &= 0,5 * (h - 2 * t_f) * \left( 1 - \sqrt{1 - 0,16 \left( \frac{H_{R60}}{h} \right)} \right) \text{ mm} \\ &= 0,5 * (240 - 2 * 17) * \left( 1 - \sqrt{1 - 0,16 \left( \frac{770}{240} \right)} \right) \text{ mm} = 31,1 \text{ mm} \end{aligned}$$

Yield stresses in the remaining part of the web:

$$f_{y,web,R30} = f_y \sqrt{1 - \left( 0,16 \frac{H_{R30}}{h} \right)} = 355 \sqrt{1 - \left( 0,16 \frac{350}{240} \right)} \text{ MPa} = 310,8 \text{ MPa}$$

$$f_{y,web,R60} = f_y \sqrt{1 - \left( 0,16 \frac{H_{R60}}{h} \right)} = 355 \sqrt{1 - \left( 0,16 \frac{770}{240} \right)} \text{ MPa} = 247,7 \text{ MPa}$$

Plastic resistances to axial compression of web in fire:

$$\begin{aligned} N_{pl,web,R30,Rd} &= \frac{t_w * (h - 2(t_f + h_{web,R30})) * f_{y,web,R30}}{\gamma_{M0,fi}} = \frac{10 * (240 - 2(17 + 12,8)) * 310,8}{1,0} \text{ N} \\ &= 561 \text{ kN} \end{aligned}$$

$$\begin{aligned} N_{pl,web,R60,Rd} &= \frac{t_w * (h - 2(t_f + h_{web,R60})) * f_{y,web,R60}}{\gamma_{M0,fi}} = \frac{10 * (240 - 2(17 + 31,1)) * 247,7}{1,0} \text{ N} \\ &= 356 \text{ kN} \end{aligned}$$

Flexural rigidities of web in fire, buckling about the minor axis:

$$\begin{aligned} (EI)_{web,R30,z} &= \frac{E_a * (h - 2(t_f + h_{web,R30})) * t_w^3}{12} = \frac{210000 * (240 - 2(17 + 12,8)) * 10^3}{12} \text{ Nmm}^2 \\ &= 3 \text{ kNm}^2 \end{aligned}$$

$$\begin{aligned} (EI)_{web,R60,z} &= \frac{E_a * (h - 2(t_f + h_{web,R60})) * t_w^3}{12} = \frac{210000 * (240 - 2(17 + 31,1)) * 10^3}{12} \text{ Nmm}^2 \\ &= 3 \text{ kNm}^2 \end{aligned}$$

Flexural rigidities of web in fire, buckling about the major axis:

$$(EI)_{web,R30,y} = \frac{E_a * t_w * (h - 2(t_f + h_{web,R30}))^3}{12} = \frac{210000 * 10 * (240 - 2(17 + 12,8))^3}{12} Nmm^2$$

$$= 1027kNm^2$$

$$(EI)_{web,R60,y} = \frac{E_a * t_w * (h - 2(t_f + h_{web,R60}))^3}{12} = \frac{210000 * 10 * (240 - 2(17 + 31,1))^3}{12} Nmm^2$$

$$= 520kNm^2$$

The contribution of the reinforcement in a fire scenario:

Mean concrete cover of longitudinal bar centre, u:

$$u_1 = \left( c_y + \emptyset_t + \frac{\emptyset_L}{2} \right) = \left( 30 + 8 + \frac{25}{2} \right) mm = 50,5mm$$

$$u_2 = \left( c_z + \emptyset_t + \frac{\emptyset_L}{2} \right) = \left( 20 + 8 + \frac{25}{2} \right) mm = 40,5mm$$

$$abs(u_1 - u_2) \leq 10mm \rightarrow u = \sqrt{u_1 * u_2} = \sqrt{50,5 * 40,5} mm = 45,5mm$$

By conservatively assuming u = 45mm, we get the temperature dependent material factors directly from Table G.5 of EC4, part 1-2 [4]:

$$k_{y,s,R30} = 1$$

$$k_{y,s,R60} = 0,883$$

$$k_{E,s,R30} = 0,865$$

$$k_{E,s,R60} = 0,647$$

Plastic resistances to axial compression of reinforcement in fire:

$$N_{pl,s,R30,Rd} = \frac{A_s * k_{y,s,R30} * f_s}{\gamma_{s,fi}} = \frac{1963 * 1 * 500}{1,0} N = 982kN$$

$$N_{pl,s,R60,Rd} = \frac{A_s * k_{y,s,R60} * f_s}{\gamma_{s,fi}} = \frac{1963 * 0,883 * 500}{1,0} N = 867kN$$

Second moment of area, reinforcement, minor axis:

$$I_{s,z} = 4 * \left( \frac{\pi}{4} * \left( \frac{\emptyset_L}{2} \right)^4 + \pi * \left( \frac{\emptyset_L}{2} \right)^2 * \left( \frac{b}{2} - \emptyset_T - \frac{\emptyset_L}{2} - c_z \right)^2 \right) =$$

$$= 4 * \left( \frac{\pi}{4} * \left( \frac{25}{2} \right)^4 + \pi * \left( \frac{25}{2} \right)^2 * \left( \frac{240}{2} - 8 - \frac{25}{2} - 30 \right)^2 \right) mm^4 = 9,56 * 10^6 mm^4$$

Second moment of area, reinforcement, major axis:

$$I_{s,y} = 4 * \left( \frac{\pi}{4} * \left( \frac{\emptyset_L}{2} \right)^4 + \pi * \left( \frac{\emptyset_L}{2} \right)^2 * \left( \frac{h}{2} - t_f - \emptyset_T - \frac{\emptyset_L}{2} - c_y \right)^2 \right) =$$

$$= 4 * \left( \frac{\pi}{4} * \left( \frac{25}{2} \right)^4 + \pi * \left( \frac{25}{2} \right)^2 * \left( \frac{240}{2} - 17 - 8 - \frac{25}{2} - 20 \right)^2 \right) mm^4 = 7,75 * 10^6 mm^4$$

Flexural rigidities of reinforcement in fire, buckling about the minor axis:

$$(EI)_{fl,R30,z} = E_s * k_{E,s,R30} * I_{s,z} = 210000 * 0,865 * 9,56 * 10^6 Nmm^2 = 1737kNm^2$$

$$(EI)_{fL,R60,z} = E_s * k_{E,s,R30} * I_{s,z} = 210000 * 0,647 * 9,56 * 10^6 Nmm^2 = 1299kNm^2$$

Flexural rigidities of reinforcement in fire, buckling about the major axis:

$$(EI)_{fL,R30,y} = E_s * k_{E,s,R30} * I_{s,y} = 210000 * 0,865 * 7,75 * 10^6 Nmm^2 = 1407kNm^2$$

$$(EI)_{fL,R60,y} = E_s * k_{E,s,R30} * I_{s,y} = 210000 * 0,647 * 7,75 * 10^6 Nmm^2 = 1053kNm^2$$

The contribution of the concrete in a fire scenario:

The outer layer of concrete is neglected, with thicknesses according to EC4, part 1-2 [4] Table G.3:

$$b_{c,R30} = 4mm$$

$$b_{c,R60} = 15mm$$

The average temperatures in the remaining concrete are calculated according to EC4, part 1-2 [4] Table G.4, based on the earlier calculated section factor  $A_m/V$  and derived through linear interpolation:

$$\theta_{c,R30} = 245^\circ C$$

$$\theta_{c,R60} = 364^\circ C$$

The temperature reduction factors for concrete are linearly interpolated from EC4, part 1-2[4] Table 3.3, based on calculated average temperatures:

$$k_{c,R30} = 0,905$$

$$k_{c,R60} = 0,786$$

$$\varepsilon_{cu,R30} = 6,175 * 10^{-3}$$

$$\varepsilon_{cu,R60} = 8,920 * 10^{-3}$$

The secant moduli of concrete in a fire scenario are calculated:

$$E_{c,sec,R30} = \frac{f_c * k_{c,R30}}{\varepsilon_{cu,R30}} = \frac{40 * 0,905}{6,175 * 10^{-3}} MPa = 5862MPa$$

$$E_{c,sec,R60} = \frac{f_c * k_{c,R60}}{\varepsilon_{cu,R60}} = \frac{40 * 0,786}{8,920 * 10^{-3}} MPa = 3525MPa$$

The design yield strengths of the concrete in a fire scenario is calculated:

$$f_{c,R30} = \frac{0,85 * f_{ck} * k_{c,R30}}{\gamma_{c,fi}} = \frac{0,85 * 40 * 0,905}{1,0} = 30,8MPa$$

$$f_{c,R60} = \frac{0,85 * f_{ck} * k_{c,R60}}{\gamma_{c,fi}} = \frac{0,85 * 40 * 0,786}{1,0} = 26,7MPa$$

Plastic resistances to axial compression of reinforcement in fire:

$$\begin{aligned} N_{pl,c,R30,Rd} &= 0,86 \left( (h - 2t_f - 2b_{c,R30})(b - t_w - 2b_{c,R30}) - A_s \right) * f_{c,R30} \\ &= 0,86 \left( (240 - 2 * 17 - 2 * 4)(240 - 10 - 2 * 4) - 1963 \right) * 30,8N = 1112kN \end{aligned}$$

$$\begin{aligned} N_{pl,c,R60,Rd} &= 0,86 \left( (h - 2t_f - 2b_{c,R60})(b - t_w - 2b_{c,R60}) - A_s \right) * f_{c,R60} \\ &= 0,86 \left( (240 - 2 * 17 - 2 * 15)(240 - 10 - 2 * 15) - 1963 \right) * 26,7N = 763kN \end{aligned}$$

Flexural rigidities of concrete in fire, buckling about the minor axis:

$$\begin{aligned}
(EI)_{c,R30,z} &= E_{c,sec,R30} \left( \left( \frac{(h - 2t_f - 2b_{c,R30})((b - 2b_{c,R30})^3 - t_w^3)}{12} \right) - I_{s,z} \right) \\
&= 5862 \left( \left( \frac{(240 - 2 * 17 - 2 * 4)((240 - 2 * 4)^3 - 10^3)}{12} \right) - 9,56 * 10^6 \right) Nmm^2 \\
&= 1152kNm^2
\end{aligned}$$

$$\begin{aligned}
(EI)_{c,R60,z} &= E_{c,sec,R60} \left( \left( \frac{(h - 2t_f - 2b_{c,R60})((b - 2b_{c,R60})^3 - t_w^3)}{12} \right) - I_{s,z} \right) \\
&= 3525 \left( \left( \frac{(240 - 2 * 17 - 2 * 15)((240 - 2 * 15)^3 - 10^3)}{12} \right) - 9,56 \right. \\
&\quad \left. * 10^6 \right) Nmm^2 = 445kNm^2
\end{aligned}$$

Flexural rigidities of concrete in fire, buckling about the major axis:

$$\begin{aligned}
(EI)_{c,R30,y} &= E_{c,sec,R30} \left( \left( \frac{(b - t_w - 2b_{c,R30})(h - 2t_f - 2b_{c,R30})^3}{12} \right) - I_{s,y} \right) \\
&= 5862 \left( \left( \frac{(240 - 10 - 2 * 4)(240 - 2 * 17 - 2 * 4)^3}{12} \right) - 7,75 * 10^6 \right) Nmm^2 \\
&= 796kNm^2
\end{aligned}$$

$$\begin{aligned}
(EI)_{c,R60,y} &= E_{c,sec,R60} \left( \left( \frac{(b - t_w - 2b_{c,R60})(h - 2t_f - 2b_{c,R60})^3}{12} \right) - I_{s,y} \right) \\
&= 3525 \left( \left( \frac{(240 - 10 - 2 * 15)(240 - 2 * 17 - 2 * 15)^3}{12} \right) - 7,75 * 10^6 \right) Nmm^2 \\
&= 293kNm^2
\end{aligned}$$

The plastic resistances of the cross-section in a fire scenario, adding up all contributions of the constituent parts:

$$\begin{aligned}
N_{pl,R30,Rd} &= N_{pl,web,R30,Rd} + N_{pl,fl,R30,Rd} + N_{pl,s,R30,Rd} + N_{pl,c,R30,Rd} = 628 + 561 + 981 + 1112kN \\
&= 3283kN
\end{aligned}$$

$$\begin{aligned}
N_{pl,R60,Rd} &= N_{pl,web,R60,Rd} + N_{pl,fl,R60,Rd} + N_{pl,s,R60,Rd} + N_{pl,c,R60,Rd} = 264 + 356 + 867 + 763kN \\
&= 2250kN
\end{aligned}$$

The effective flexural rigidities of the cross-section in a fire scenario, adding up all contributions of the constituent parts, with reduction coefficients:

Reduction coefficients, from EC4, part 1-2 [4], table G.7:

$$\begin{aligned}
\text{Flange: } \varphi_{fl,R30} &= 1,0 \\
\varphi_{fl,R60} &= 0,9
\end{aligned}$$

$$\begin{aligned}
\text{Web: } \varphi_{web,R30} &= 1,0 \\
\varphi_{web,R60} &= 1,0
\end{aligned}$$

$$\begin{aligned}
\text{Reinforcement: } \varphi_{s,R30} &= 1,0 \\
\varphi_{s,R60} &= 0,9
\end{aligned}$$

$$\begin{aligned}
\text{Concrete: } \varphi_{c,R30} &= 0,8 \\
\varphi_{c,R60} &= 0,8
\end{aligned}$$

Flexural rigidities of the cross-section in fire, buckling about the minor axis:

$$(EI)_{R30,z} = \varphi_{fl,R30}(EI)_{fl,R30,z} + \varphi_{web,R30}(EI)_{web,R30,z} + \varphi_{s,R30}(EI)_{s,R30,z} + \varphi_{c,R30}(EI)_{c,R30,z} =$$

$$= 1,0 * 1036 + 1,0 * 3 + 1,0 * 1737 + 0,8 * 1152 kNm^2 = 3697 kNm^2$$

$$(EI)_{R60,z} = \varphi_{fl,R60}(EI)_{fl,R60,z} + \varphi_{web,R60}(EI)_{web,R60,z} + \varphi_{s,R60}(EI)_{s,R60,z} + \varphi_{c,R60}(EI)_{c,R60,z} =$$

$$= 0,9 * 666 + 1,0 * 3 + 0,9 * 1299 + 0,8 * 445 kNm^2 = 2127 kNm^2$$

Flexural rigidities of the cross-section in fire, buckling about the major axis:

$$(EI)_{R30,y} = \varphi_{fl,R30}(EI)_{fl,R30,y} + \varphi_{web,R30}(EI)_{web,R30,y} + \varphi_{s,R30}(EI)_{s,R30,y} + \varphi_{c,R30}(EI)_{c,R30,y} =$$

$$= 1,0 * 2699 + 1,0 * 1027 + 1,0 * 1407 + 0,8 * 796 kNm^2 = 5769 kNm^2$$

$$(EI)_{R60,y} = \varphi_{fl,R60}(EI)_{fl,R60,y} + \varphi_{web,R60}(EI)_{web,R60,y} + \varphi_{s,R60}(EI)_{s,R60,y} + \varphi_{c,R60}(EI)_{c,R60,y} =$$

$$= 0,9 * 1735 + 1,0 * 520 + 0,9 * 1053 + 0,8 * 203 kNm^2 = 3264 kNm^2$$

Axial buckling resistances about the minor axis in a fire scenario:

Critical axial forces in a fire scenario:

$$N_{cr,R30,z} = \frac{\pi^2 * (EI)_{R30,z}}{L_{fi}^2} = \frac{\pi^2 * 3697}{(0,7 * 9)^2} kN = 919 kN$$

$$N_{cr,R60,z} = \frac{\pi^2 * (EI)_{R60,z}}{L_{fi}^2} = \frac{\pi^2 * 2127}{(0,7 * 9)^2} kN = 529 kN$$

Relative slendernesses in a fire scenario (the characteristic resistance equals the design resistance, due to the fire material partial factors equalling 1,0).

$$\bar{\lambda}_{R30,z} = \sqrt{\frac{N_{pl,R30,Rd}}{N_{cr,R30,z}}} = \sqrt{\frac{3283}{919}} = 1,890$$

$$\bar{\lambda}_{R60,z} = \sqrt{\frac{N_{pl,R60,Rd}}{N_{cr,R60,z}}} = \sqrt{\frac{2127}{529}} = 2,005$$

Buckling curve c is used -> imperfection factor  $\alpha = 0,49$

$\phi$ -factors in a fire scenario

$$\phi_{R30,z} = 0,5 \left( 1 + \alpha(\bar{\lambda}_{R30,z} - 0,2) + \bar{\lambda}_{R30,z}^2 \right) = 2,700$$

$$\phi_{R60,z} = 0,5 \left( 1 + \alpha(\bar{\lambda}_{R60,z} - 0,2) + \bar{\lambda}_{R60,z}^2 \right) = 2,94$$

$\chi$ -factors in a fire scenario:

$$\chi_{R30,z} = \frac{1}{\phi_{R30,z} + \sqrt{\phi_{R30,z}^2 - \bar{\lambda}_{R30,z}^2}} = 0,216$$

$$\chi_{R60,z} = \frac{1}{\phi_{R60,z} + \sqrt{\phi_{R60,z}^2 - \bar{\lambda}_{R60,z}^2}} = 0,195$$

Axial buckling resistances in a fire scenario, buckling about the minor axis:

$$N_{b,R30,z,Rd} = \chi_{R30,z} * N_{pl,R30,Rd} = 0,216 * 3283 = 709kN$$

$$N_{b,R60,z,Rd} = \chi_{R60,z} * N_{pl,R60,Rd} = 0,195 * 2127 = 415kN$$

Axial buckling resistances about the major axis in a fire scenario:

Critical axial forces in a fire scenario:

$$N_{cr,R30,y} = \frac{\pi^2 * (EI)_{R30,y}}{L_{fi}^2} = \frac{\pi^2 * 5769}{(0,7 * 9)^2} kN = 1435 kN$$

$$N_{cr,R60,y} = \frac{\pi^2 * (EI)_{R60,y}}{L_{fi}^2} = \frac{\pi^2 * 3264}{(0,7 * 9)^2} kN = 812 kN$$

Relative slendernesses in a fire scenario (the characteristic resistance equals the design resistance, due to the fire material partial factors equalling 1,0).

$$\bar{\lambda}_{R30,z} = \sqrt{\frac{N_{pl,R30,Rd}}{N_{cr,R30,z}}} = \sqrt{\frac{3283}{1435}} = 1,513$$

$$\bar{\lambda}_{R60,z} = \sqrt{\frac{N_{pl,R60,Rd}}{N_{cr,R60,z}}} = \sqrt{\frac{2127}{812}} = 1,618$$

Buckling curve c is used -> imperfection factor  $\alpha = 0,49$

$\phi$ -factors in a fire scenario

$$\phi_{R30,y} = 0,5 \left( 1 + \alpha (\bar{\lambda}_{R30,y} - 0,2) + \bar{\lambda}_{R30,y}^2 \right) = 1,966$$

$$\phi_{R60,y} = 0,5 \left( 1 + \alpha (\bar{\lambda}_{R60,y} - 0,2) + \bar{\lambda}_{R60,y}^2 \right) = 2,156$$

$\chi$ -factors in a fire scenario:

$$\chi_{R30,y} = \frac{1}{\phi_{R30,y} + \sqrt{\phi_{R30,y}^2 - \bar{\lambda}_{R30,y}^2}} = 0,310$$

$$\chi_{R60,y} = \frac{1}{\phi_{R60,y} + \sqrt{\phi_{R60,y}^2 - \bar{\lambda}_{R60,y}^2}} = 0,279$$

Axial buckling resistances in a fire scenario, buckling about the major axis:

$$N_{b,R30,y,Rd} = \chi_{R30,y} * N_{pl,R30,Rd} = 0,310 * 3283 = 1017kN$$

$$N_{b,R60,y,Rd} = \chi_{R60,y} * N_{pl,R60,Rd} = 0,279 * 2127 = 593kN$$

Buckling resistance about the major axis due to load eccentricity:

About the major axis, there is a bending moment in a fire scenario due to wind load. The design wind load action in a fire scenario was calculated earlier to  $Q_{Ed,Fi} = 2,2 kN/m$  as a distributed transverse load. This gives a parabolic BMD, with a peak moment of:

$$M_{Ed,fi} = \frac{Q_{Ed,Fi} * L^2}{8} kNm = \frac{2,2 * 9^2}{8} = 22,8kNm$$

The EC4, part 1-2 [4] Annex G does not provide calculation rules for parabolic BMD, but allows for load eccentricity to be used in the calculations. The load eccentricity  $e$  which results in a constant BMD of  $M_{Ed,fi}$  for the fire design load  $N_{Ed,fi} = 415,4$  kN is determined. This is conservative, since the

$$e = \frac{M_{Ed,fi}}{N_{Ed,fi}} = \frac{22,8}{415,4} m = 55 mm$$

The buckling resistance in a fire situation, with axial load eccentricity  $e$  is modified by a factor equivalent to the ratio of axial buckling load with/without the eccentricity when the column is calculated for normal temperature.

How the axial buckling load should be calculated with a load eccentricity is however not given by EC4, part 1-1 [3]. A method suggested by Arezki and Said [74] is to use the Campus-Massonet criteria, where a modified buckling  $\chi$ -coefficient for load eccentricity is determined. The relative slenderness  $\bar{\lambda}_y$  and the buckling factor  $\chi_y$  for bending about the major axis for normal temperature is calculated for the axial load of  $N_{Ed,fi}$  in A3C to equal:

$$\bar{\lambda}_y = 1,372; \chi_y = 0,394$$

Using the Campus-Massonet criteria to find the buckling factor for load eccentricity:

$$\chi_{e,y} = \frac{\chi}{1 + \frac{4 * e}{h(\frac{1}{\chi} - 0,3\bar{\lambda})}} = \frac{0,394}{1 + \frac{4 * 55}{240(\frac{1}{0,394} - 0,3 * 1,372)}} = 0,275$$

The reduced buckling resistances about the major axis can now be determined:

$$N_{b,e,R30,y,Rd} = N_{b,R30,y,Rd} * \frac{\chi_{e,y}}{\chi_y} = 1017 * \frac{0,275}{0,394} = 710 kN$$

$$N_{b,e,R60,y,Rd} = N_{b,R60,y,Rd} * \frac{\chi_{e,y}}{\chi_y} = 593 * \frac{0,275}{0,394} = 414 kN$$

### Verification of fire loads

Verification of cross-sectional yield due to axial loads:

$$\frac{N_{Ed,Fi}}{N_{pl,R30,Rd}} = \frac{415,4}{3283} = 0,13 < 1,0 \text{ (ok!)}$$

$$\frac{N_{Ed,Fi}}{N_{pl,R60,Rd}} = \frac{415,4}{2127} = 0,2 < 1,0 \text{ (ok!)}$$

Buckling resistance about the minor axis:

$$\frac{N_{Ed,Fi}}{N_{b,R30,z,Rd}} = \frac{415,4}{709} = 0,59 < 1,0 \text{ (ok!)}$$

$$\frac{N_{Ed,Fi}}{N_{b,R60,z,Rd}} = \frac{415,4}{415} > 1,0 \text{ (not ok!)}$$

Buckling resistance about the major axis:

$$\frac{N_{Ed,Fi}}{N_{b,e,R30,y,Rd}} = \frac{415,4}{710} = 0,58 < 1,0 \text{ (ok!)}$$

$$\frac{N_{Ed,Fi}}{N_{b,e,R60,y,Rd}} = \frac{415,4}{414} > 1,0 \text{ (not ok!)}$$